

**Towards Understanding Synergic s-Block Chemistry: New
Insights from Zincate and Magnesiate Reactions**

by

Liam Balloch

A thesis submitted to the Department of Pure and Applied Chemistry, University of Strathclyde, in part
fulfilment of the requirements for the degree of Doctor of Philosophy.

February 2012

The copyright of this thesis belongs to the author under the terms of the United Kingdom Copyright Acts as qualified by the University of Strathclyde Regulation 3.49. Due acknowledgements must always be made to the use of any material contained in, or derived from this thesis.

Acknowledgements

Over the past few months in anticipation of this thesis, I went back to the results I had achieved two or three years ago. It was like revisiting old friends who had been awaiting your return to relive the excitement of the original experiments and to close the circle on an important experience that had been interrupted in quest of the next discovery.

In the spring of 2008, the world was a different place; it was Celtic who were completing three consecutive championships and a young man who was coming off the back of a topsy-turvy undergraduate relationship with chemistry was considering his options, believing the world was his oyster. At 21, I was still held in thrall by the exhilaration of my early research experience in the form of my final year project and hoping that my next step would match that fervour and continue to fill me with a purpose that would stand me in good stead for the years to come. As I page through this thesis and survey the body of work, the last three years have done that for me.

My career path was chosen when the offer of PhD came along and for that I must acknowledge my supervisor Prof Robert Mulvey for not only masterminding and creating the project but for giving me the opportunity to work in his laboratory and the encouragement he has provided along the way. A special thank you to Dr Charlie O'Hara who has laboured in the shadows with me these last few years but whose inspiration and excellence have been essential in helping me bring you my best work. Additionally, I would like to extend thanks to Dr Stuart Robertson, a talented chemist who did a terrific job with the poor quality crystalline samples I often presented.

Foremost, I want to acknowledge the unending support of my friends and family, principally, my parents. I now recognise the sacrifices they have made to provide opportunities that they never had for both me and my brother Nial, and how they are the principal reason for the privileged position we find ourselves in today. Throughout my years at university they have shown tremendous patience with me as I battled with my own conscience and their humility and work ethic has been the cornerstone of my PhD studies and will continue to shape my entire life.

Finally thanks to all members and collaborators of the extended Mulvey group, including Dr Eva Hevia, Dr Alan Kennedy and Dr David Armstrong for assistance in their field of expertise and to my many lab colleagues over the years, Pablo, Jan, Joaquin, Thomas, Lorna,

Ben C, Vicki, Gemma, Matt, Ross, Ben F, Sharon, Zoe, Elaine, Jenni, Donna, Sarah and Emma, thank you for the laughs on the journey we made together. I owe the choices and the slightly younger man who made them back in 2008 my respect and gratitude.

Abstract

Metallation, in which an inert carbon-hydrogen bond is transformed into a labile carbon-metal bond, is a useful tool for constructing substituted aromatic compounds. Routinely, highly polar organolithium reagents are employed for this purpose; however, there are limitations to their use. This project was based on further developing an alternative metallation strategy, namely Alkali-Metal-Mediated Metallation (AMMM), with emphasis on zincation by exploiting the synergic chemistry that can be generated when pairing a group 1 metal amide with a low polarity dialkyl zinc reagent.

AMMM reactions of the sodium TMP-zincate [(TMEDA)Na(μ -TMP)(μ -*t*Bu)Zn(*t*Bu)] (**1**) were explored leading to the development of a new concept within Directed-*ortho*-Metallation (DoM) chemistry with three electron-rich aromatic substrates cleanly zincated *ortho* to the directing metallation group (DMG) under ambient temperatures; while reaction with benzyl methyl ether produced an *ortho*-zincated intermediate instead of the thermodynamic α -metallated product. Additionally, a remarkable structural variety was observed when investigating the competition between a DMG and a heteroatom in the *N*, *N*-diethyl thiophene-2-carboxamide ring for the site of metallation. Through structurally mapping these reactions and subsequent electrophilic quenches, these studies established reagent **1** as a powerful metallating agent. A case study of the metallation of *N*, *N*-dimethylaniline offers complementary insight into the selectivity and mechanism of the base underlining how the cooperative action of the bi-metal partnership promotes special reactions beyond the scope of homometallic reagents.

Outwith metallation, some unexpected highlights were the product of this research. Courtesy of a novel four-step domino sequence, a series of unique zwitterionic zincabicyclic complexes were prepared from the reaction of synergic reagents and chlorobenzene. Complementing its Brønsted basicity, zincate **1** underwent single electron transfer with the radical TEMPO; while, treating TEMPO with sodium metal and crystallisation from a hexane/TMEDA mixture produced a ladder structure which represents a rare example of elemental-metal single electron reduction of the radical.

Publications

Peer-reviewed papers arising from work carried out in this project

1. *Single Electron Transfer (SET) Activity of the Dialkyl-Amido Sodium Zincate [(TMEDA)Na(μ -TMP)(μ -tBu)Zn(tBu)] towards TEMPO and Chalcone.* D. R. Armstrong, L. Balloch, J. J. Crawford, B. J. Fleming, L. M. Hogg, A. R. Kennedy, J. Klett, R. E. Mulvey, C. T. O'Hara, S. A. Orr and S. D. Robertson. *Chem. Commun.* **2012**, 48, 1541 - 1543.
2. *Meta-Metallation of N, N-dimethylaniline: Contrasting Direct Sodium-Mediated Zincation with Indirect Sodiation-Dialkylzinc Co-complexation.* D. R. Armstrong, L. Balloch, E. Hevia, A. R. Kennedy, R. E. Mulvey, C. T. O'Hara, S. D. Robertson. *Beilstein J. Org. Chem.* **2011**, 7, 1234 - 1248.
3. *Concerning the Structures of Alkali-Metal-Mediated ortho Zincation of Benzamides and Phenyl O-Carbamate.* L. Balloch, A. R. Kennedy, R. E. Mulvey, T. Rantanen, S. D. Robertson, V. Snieckus. *Organometallics.* **2011**, 30, 145 - 152.
4. *Structural Elaboration of the Surprising ortho-Zincation of Benzyl Methyl Ether.* L. Balloch, A. R. Kennedy, J. Klett, R. E. Mulvey, C. T. O'Hara. *Chem. Commun.* **2010**, 46, 2319 - 2321.
5. *Synergic Synthesis of Benzannulated Zincabicyclic Complexes, alpha-Zincated N Ylides, through Sodium-TMEDA-Mediated Zincation of a Haloarene.* D. R. Armstrong, L. Balloch, W. Clegg, S. H. Dale, P. García-Álvarez, E. Hevia, L. M. Hogg, A. R. Kennedy, R. E. Mulvey, C. T. O'Hara. *Angew. Chem. Int. Ed.* **2009**, 48, 8675 - 8678.
6. *Structural Variations within Group 1 (Li-Cs)⁺ (2,2,6,6-Tetramethyl-1-piperidinyloxy)⁻ Complexes Made via Metallic Reduction of the Nitroxyl Radical.* L. Balloch, A. M. Drummond, P. García-Álvarez, D. V. Graham, A. R. Kennedy, J. Klett, R. E. Mulvey, C. T. O'Hara, P. J. A. Rodger, I. D. Rushworth. *Inorg. Chem.* **2009**, 48, 6934 - 6944.

Other peer-reviewed papers from the author

7. *A μ_4 -Oxide-Containing a Dimeric Variant of a Sodium Dialkyl(Amido)-Zincate Reagent.* L. Balloch, A. R. Kennedy, R. E. Mulvey, S. D. Robertson. *Acta Crystallogr., Sect. C: Cryst. Struct. Commun.* **2011**, 67, m252-m254.
8. *Metalation of 2,4,6-Trimethylacetophenone Using Organozinc Reagents: The Role of the Base in Determining Composition and Structure of the Developing Enolate.* D. R. Armstrong, A. M. Drummond, L. Balloch, D. V. Graham, E. Hevia, A. R. Kennedy. *Organometallics.* **2008**, 27, 5860 - 5866.

Conference Presentations

1. *Synergic Synthesis and Structures of Zincated Aromatic Substrates*, Poster Presentation, USIC, July 2011, University of Glasgow.
2. *Synergistic Synthesis and Structures of Zincated Aromatic Substrates*, Poster Presentation, 2010 International Chemical Congress of Pacific Basin Societies, December 2010, Honolulu, Hawaii. Abstract INOR-499.
3. *Synergic Synthesis and Structures of Zincated Aromatic Substrates*, Oral Presentation, USIC, July 2010, University of Durham.
4. *Transforming TMEDA to an α -Zincated Nitrogen Ylide*, Poster Presentation, USIC, September 2009, Heriot-Watt University.
5. *New Directions for Alkali-Metal-Mediated Zincation*, Oral Presentation, University of Strathclyde Inorganic Section Meeting, June 2009, West Brewery.

Abbreviations

AMMM	Alkali-Metal-Mediated Metallation
AMMZ n	Alkali-Metal-Mediated Zincation
n Bu	n -butyl
s Bu	s -butyl
t Bu	t -butyl
CIPE	Complex Induced Proximity Effect
COSY	Correlation Spectroscopy
DA	Diisopropylamide
DA(H)	Diisopropylamine
DFT	Density Functional Theory
DMG	Directed Metallating Group
DoM	Directed- <i>ortho</i> -Metallation
Et	Ethyl
HMDS	1,1,1,3,3,3-hexamethyldisilazide
HMDS(H)	1,1,1,3,3,3-hexamethyldisilazane
HSQC	Heteronuclear Single Quantum Correlation Spectroscopy
LDA	Lithium Diisopropylamide
LICKOR	Alkyl lithium/Potassium Alkoxide Superbase
Me	Methyl
NOESY	Nuclear Overhauser Effect Spectroscopy
NMR	Nuclear Magnetic Resonance
Ph	Phenyl
PMDETA	N,N,N',N'',N'' -pentamethylethylenediamine
ppm	Part per million
i Pr	<i>iso</i> -propyl
R	Generic Alkyl Group
TEMPO	2,2,6,6-tetramethyl-1-piperidinyloxy
THF	Tetrahydrofuran
TMCDA	N,N,N',N' -tetramethylcyclohexane-1,2-diamine
TMEDA	N,N,N',N' -tetramethylethylenediamine
TMP	2,2,6,6-tetramethylpiperidide
TMP(H)	2,2,6,6-tetramethylpiperidine

Table of Contents

Acknowledgements	i
Abstract	iii
Publications	iv
Conference Presentations	vi
Abbreviations	vii
Table of Contents	viii

Chapter 1: General Introduction to Organometallic and Metallation Chemistry

1.1	Organolithiums: Structure and Reactivity	1
1.2	Organozinc Reagents in Synthesis	11
1.3	Second Generation Metallation	20
1.4	Aims of the PhD Research Project	41
	Chapter 1 - References	42

Chapter 2: Regioselective Deprotonation and the Use of Synergic Reagents

2.1	Directed- <i>ortho</i> -Metallation	49
2.2	AMMZn of Benzamides and Phenyl <i>O</i> -Carbamate	52
2.3	The Surprising <i>ortho</i> -Zincation of Benzyl Methyl Ether	65
2.4	Structural Complexity of the Zincation of a Thiophene Derivative	71
2.5	Experimental Section	88
	Chapter 2 - References	98

Chapter 3: Case Study - The Metallation of *N,N*-dimethylaniline

3.1	Uncovering Synergic Surprises	102
3.2	The Original Direct <i>meta</i> -Zincation Reaction	105
3.3	The Direct <i>meta</i> -Zincation Reaction: A Closer Look	106
3.4	The Indirect Sequential Sodiation-Dialkylzinc Co-complexation Approach	107
3.5	DFT Calculations	120
3.6	Attempted Thermal Isomerisation	125
3.7	Concluding Remarks on Direct AMMZn versus Indirect Sodiation-Zinc Co-complexation Approaches	126

3.8	Experimental Section	129
	Chapter 3 - References	133
Chapter 4: Synergic Synthesis of Benzannulated Metallacyclic Complexes		
4.1	Multicomponent Reactions	135
4.2	Background to Arynes	140
4.3	The Unexpected Synthesis of Zincabicyclic Complexes	141
4.4	The Quest for Molecular Diversity	150
4.5	Experimental Section	155
	Chapter 4 - References	159
Chapter 5: Redox Reactions in Sodium-Zinc Chemistry		
5.1	Nitroxides: Applications in Synthesis	162
5.2	Single Electron Transfer Activity of the Sodium TMP-Zincate	167
5.3	Elemental Metal Reduction	178
5.4	Experimental Section	186
	Chapter 5 - References	191
Chapter 6: Structural Variations of Bis(bis(trimethylsilyl)methyl)magnesium		
6.1	The Quest for Direct-remote-Metallation	195
6.2	A Potential New Precursor to Heterobimetallic Complexes	202
6.3	Experimental Section	209
	Chapter 6 - References	212
Chapter 7: General Experimental Techniques		
7.1	Schlenk Techniques	214
7.2	Use of a Dry Box with a Gas Recirculation and Purification System	215
7.3	Solvent and Liquid Purification	216
7.4	Standardisation of Reagents	217
7.5	Preparation of Common Starting Materials	218
7.6	Analytical Procedures	219
	Chapter 7 - References	221

Chapter 8: Conclusions and Future Work

8.1	Conclusions	222
8.2	Future Work	226
	Chapter 8 - References	234

Chapter 1: General Introduction to Organometallic and Metallation Chemistry

This chapter endeavours to introduce two significant but distinctive classes of organometallic reagent, namely organolithium and organozinc compounds. By looking back in time and considering the distinctive architecture of the classic aforementioned reagents we can appreciate the unique reactivity that has positioned organometallics as a forerunner in modern organic synthesis.

This section will evolve and tell the story of the burgeoning theme of mixed-metal chemistry both outwith and within the Mulvey group, where we have developed new alternative metallation reagents which can be interpreted as composite molecules, made up of an alkali-metal amide and a low polarity metal reagent [Zn, Mg or Mn(II) alkyls].

The development of these reagents as excellent chemo- and regioselective metallators (ability to deprotonate C-H and X-H bonds to turn them into more labile C-metal and X-metal bonds) form the basis of this PhD research programme, while it sets out to offer a complementary insight into the selectivities and mechanisms of bimetallic bases underlining how the cooperative action of the bi-metal partnership can promote reactions beyond the scope of traditional homometallic reagents.

1.1) Organolithiums: Structure and Reactivity

The illustrious German chemist Wilhelm Schlenk engaged in one of the great experimental challenges of all time. Ambitious and enterprising, Schlenk along with Holtz reported the first preparation of neutral organosodium compounds and also the first organolithium compounds methyllithium, ethyllithium and phenyllithium,^[1] imparting expressive depictions of the properties of these compounds with methyllithium said to burn in air forming a brilliant red flame with a shower of golden

sparks. Earning a Nobel Prize nomination for his chemistry, his handling of challenging air and moisture sensitive compounds is remembered to this day with the techniques and glassware commonly employed in inert atmosphere synthesis carrying his name.

The deprotonative metallation reaction (most simply represented as $R-H + R'-M \rightarrow R-M + R'-H$) is widely regarded as the preeminent path for the generation of reactive carbonucleophiles; entailing of displacement of a hydrogen atom by a metal, the efficiency of the conversion is dependent upon two criteria being met. To be considered synthetically useful it is a pre-requisite for the reaction mechanism to be selective, discriminating between various types of C-H bond resulting in the abstraction of one specific proton. The second hurdle to clear is the requirement for a strong base to convince the hydrocarbon to partake in the metal-hydrogen exchange. Consequently, the ideal candidates ought to exhibit a high reactivity potential. Organometallic species unite strongly electropositive metals and organic reagents to form highly polar and as a result, highly reactive carbon-metal bonds; thus the metallation reaction has become synonymous with organolithium reagents.

The importance of organolithium-mediated reactions in organic synthesis cannot be downplayed. Metallation followed by electrophilic quench is one of the world's most practiced synthetic transformations and has found numerous applications in total synthesis.^[2] For example, the simple alkylation of Mevacor, a hypolipidemic drug used to control elevated cholesterol, to prepare Zocor results in bioactivity some six times that of the starting material (Scheme 1.1).^[3]

solution,^[4] and with the advent of sophisticated NMR spectroscopic and X-ray crystallography techniques many of these structures have now been inferred.

Dietrich reported the first solvent-free organometallic crystal structure, when he deduced the tetrameric arrangement, built up of two strongly associated $(C_2H_5Li)_2$ dimers, of ethyllithium in 1963.^[5] One year later, Weiss contributed the landmark structure of the simplest organolithium, methyllithium (Figure 1.1).^[6]

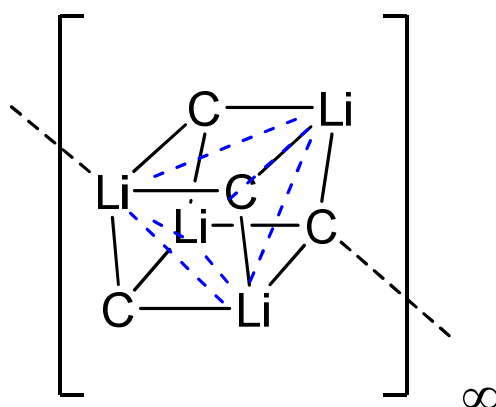
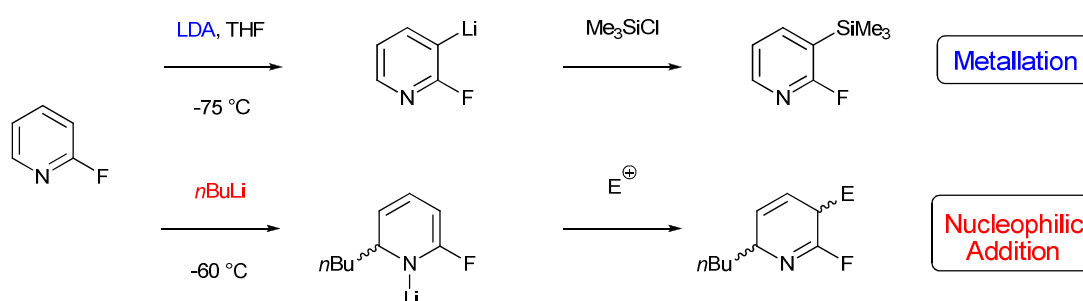


Figure 1.1: Distorted cubane substructure of methyllithium illustrating intermolecular interactions which create a polymeric network.

Analogous to that of ethyllithium, the lattice of methyllithium consists of tetrameric subunits, where the carbon atom of a methyl group forms three short contacts to three lithium atoms constructing a distorted cubane with lithium and carbon at alternate corners. Methyllithium, along with phenyllithium are anomalies in organolithium reagent chemistry in that they are insoluble in hydrocarbon solvent in the absence of donor additives. The insolubility and low volatility of methyllithium are a direct result of the cubane clusters interacting with each other via intermolecular agostic interactions creating a three-dimensional polymeric network. The aggregation state and strength of inter-cluster interactions prevalent in organolithiums can generally be related to steric properties. For example, in reagents bearing bulkier, more space-consuming organic

fragments such as hexameric *n*BuLi (*n*-butyllithium) or tetrameric *t*BuLi (*t*-butyllithium), intermolecular interactions are precluded by steric effects.^[7]

Alkylolithiums are considered cornerstone reagents of modern synthesis; however they are also the gateway to another important class of organolithium compound through deprotonation of more acidic amines such as DA(H) (diisopropylamine) and TMP(H) (2,2,6,6-tetramethylpiperidine) generating bulky lithium amide bases. Sterically hindered lithium amides combination of low nucleophilicity and high kinetic basicity ensured these derivatives emerged as valuable competitors to alkylolithiums and in many instances the favoured reagent for deprotonative metallation of sensitive heterocycles where the high nucleophilicity of alkylolithiums can be problematic. For example, treatment of 2-fluoropyridine with *n*BuLi results in the product of addition; nonetheless the selectivity pendulum can be swung in favour of metallation when deploying LDA (lithium diisopropylamide) in THF at -75 °C (Scheme 1.2).^[8]



Scheme 1.2: Contrasting reactivity of LDA (top) and *n*BuLi (bottom) towards 2-fluoropyridine.

Illustrated by the above example, LDA is widely regarded as a supreme player in the art of proton abstraction, regioselectively deprotonating organic substrates bearing sensitive functional groups such as esters,^[9] nitriles^[10] and nitrosamines.^[11] Reflecting the prominent role it plays in synthetic chemistry, LDA has been the subject of various structural studies. Collum has studied the hydrocarbon solution-state structures of LDA

using isotopically labelled [^6Li]LDA and [$^6\text{Li},^{15}\text{N}$]LDA.^[12] The ^6Li NMR spectrum intimates the presence of a number of cyclic oligomers with five discrete resonances, while the corresponding ^6Li and ^{15}N NMR spectra of [$^6\text{Li},^{15}\text{N}$]LDA show overlapping triplets and quintets. The severe overlap rendered precise identification difficult; however, such resonances typically correspond to cyclic dimers, trimers and higher oligomers. LDA displays appreciable solubility in hexane solution at ambient temperature allowing the isolation of donor-solvent free crystals and an X-ray crystallographic analysis of uncomplexed LDA (Figure 1.2).^[13]

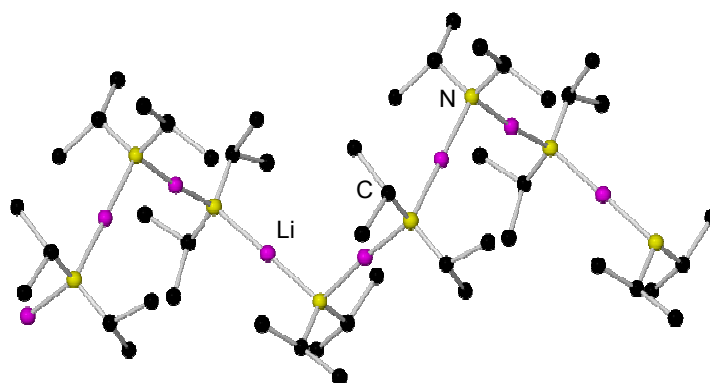


Figure 1.2: Helical chain structure of unsolvated, polymeric LDA.

The crystal structure depicts LDA adopting a unique helical, polymeric arrangement in the solid state. Consistent with their alkyl relatives, lithium amides can participate in extensive aggregation as a direct consequence of the highly polar bond between the electropositive lithium and electronegative nitrogen, coupled with the presence of the lone pair of electrons on the nitrogen. Two factors which can influence the extent of aggregation of metal amides in general are the nature of the metal and the steric bulk of the organic attachments on the amido nitrogen atoms. The steric argument can be supported by considering two other widely utilised amides. LiHMDS (lithium hexamethyldisilazane) was the first amidolithium to be structurally characterised and

was found to form a cyclic trimer in the solid state,^[14] whereas moving to the bulkier, cyclic amine TMP(H) results in an eight-membered tetrameric ring arrangement (Figure 1.3).^[15]

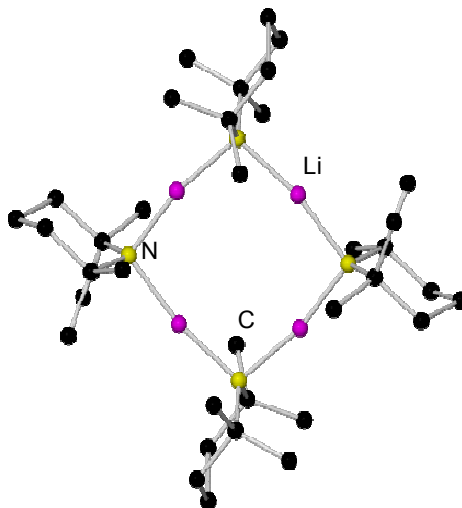


Figure 1.3: The cyclic tetrameric molecular structure of LiTMP.

A third dynamic that can affect the degree of aggregation is donor ligands, with Lewis bases such as amines or ethers posing as an alternative source of electron-density for the Lewis acidic lithium atoms. By offering up electron density they can not only stabilise the electron-deficient alkali-metal centre, such ligands can encourage a shift in aggregation to an entropically favoured lower oligomer, while enhancing solubility in non-polar solvents. In the context of this PhD research programme, the chelating diamine TMEDA (*N,N,N',N'*-tetramethylethylenediamine) provides a pertinent example, for Collum and Williard have shown when LDA is crystallised from a neat TMEDA solution, the aforementioned helical polymer is broken down to dimers, albeit still interlinked by TMEDA bridges to form an infinite chain (Figure 1.4).^[16]

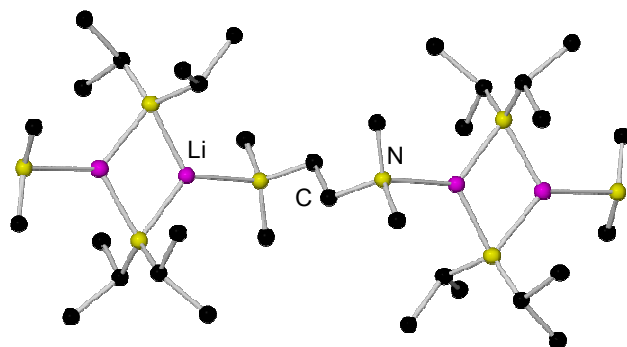


Figure 1.4: Section of the infinite chain of $[(\text{LDA})_2\text{TMEDA}]_\infty$.

In contrast, the addition of TMEDA to tetrameric LiTMP provided an ionic structure within alkali-metal amide chemistry with TMEDA-solvated LiTMP adopting a distinctive hemi-solvated “open-dimer” arrangement (Figure 1.5).^[17] This structural motif was considered to be an integral component in permitting the enolisation step of the aldol reaction to take place and it provided structural evidence to authenticate Collum’s observation of open dimers of LiTMP in solution.^[18] In 2011, the Mulvey group extended structural studies to hetero (alkali-metal) TMP chemistry, reporting an array of diverse structural motifs including open dimers and trimers through a co-complexation synthetic protocol by using polydentate N-donors, TMEDA and PMDETA (*N,N,N',N'',N'''*-pentamethylethylenediamine), in a non-polar medium.^[19]

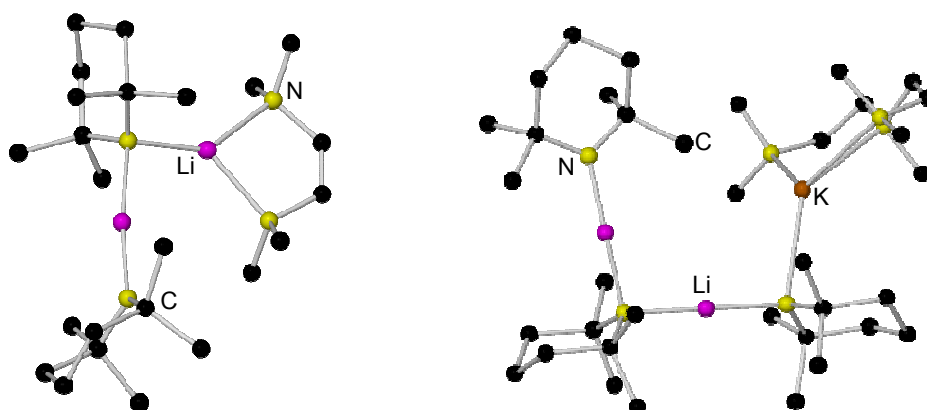
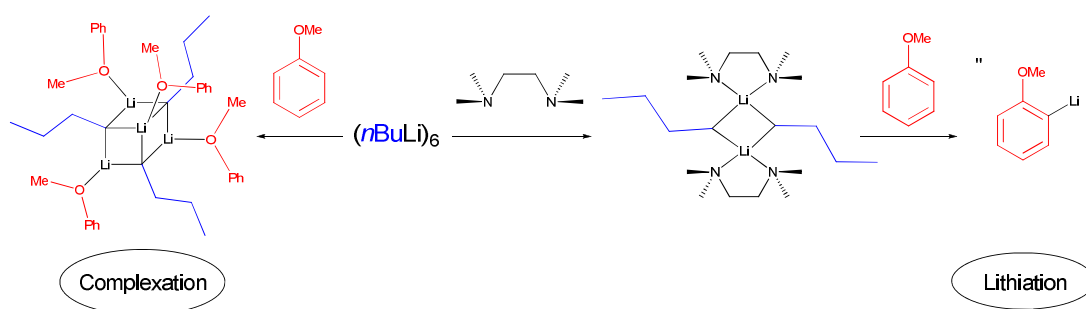


Figure 1.5: Crystal structures of the TMEDA-solvated, open dimer of LiTMP (L.H.S) and the trinuclear open arrangement of $[(\text{PMDETA})\text{K}(\mu\text{-TMP})\text{Li}(\mu\text{-TMP})\text{Li}(\text{TMP})]$ (R.H.S).

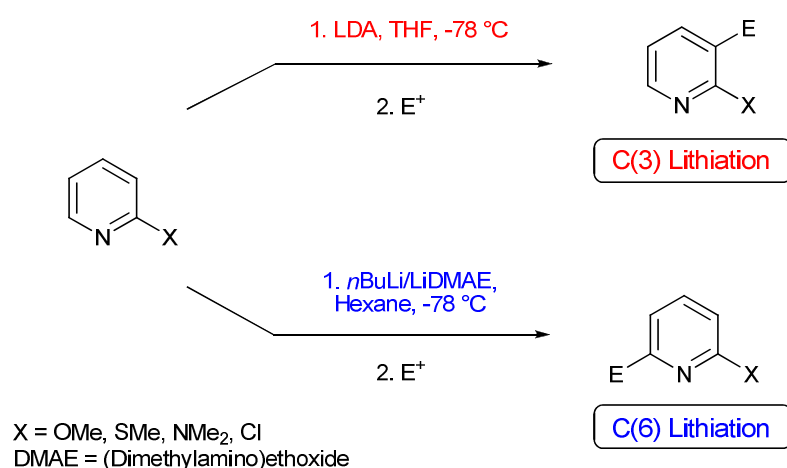
By transforming the structural make-up and solubility, donor solvents also significantly augment the reactivity profile of organolithiums, to such an extent that an ether or amine solvent is deemed essential for scores of popular organolithium reactions. The upshot is exemplified in treatment of the alkyl aryl ether anisole with $n\text{BuLi}$.^[20] In the absence of TMEDA, the methoxy oxygen doubles as a pseudo coordinating ligand deaggregating the $n\text{BuLi}$ hexamer into a tetrameric $n\text{BuLi}$ -anisole complex. However, in the presence of TMEDA, a mechanism entailing $n\text{BuLi}\cdot\text{TMEDA}$ dimers can be proposed for successful deprotonation at the *ortho*-position with metallation directed by the acidifying effect of the methoxy group on neighbouring protons (Scheme 1.3).



Scheme 1.3: Proposed reaction pathway for anisole and $n\text{BuLi}$, with and without the addition of TMEDA. The fourth n -butyl group of the tetrameric $n\text{BuLi}$ -anisole complex is omitted for clarity.

Nonetheless, in a thought provoking review Collum addresses many of the widespread misconceptions related to TMEDA and the mechanisms by which it governs organolithium structure and reactivity.^[21] The notion that TMEDA promoted deaggregation can be exercised to explain differences in reactivity can only hold true in hydrocarbon solution in the absence of strong donors such as THF or ethers, with evidence suggesting THF is a superior ligand for lithium and that organolithiums are deaggregated just as much by commonly utilised bulk THF as by stoichiometric TMEDA in THF.

Lithiation by selective deprotonation of a C-H bond is central to so many aspects of synthetic chemistry but the outcome and viability of the reaction is dependent on an assortment of experimental parameters coming together. Many years of intensive research has been devoted to the optimisation of organolithium methodology and this passage aspired to summarise some of the vital considerations, including the reaction medium and choice of base. Of course, these key parameters are interrelated and the objective of the reaction must be taken into account when devising the synthetic protocol. For example, upon altering the lithiating reagent and its Lewis base co-solvent, the position of metallation can be tuned for a series of 2-substituted pyridines (Scheme 1.4).^[22]



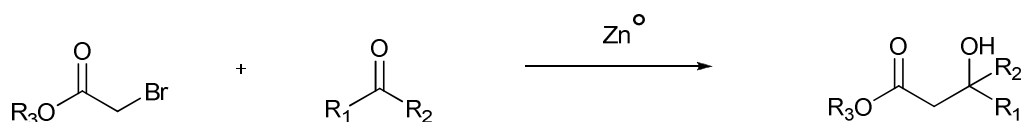
Scheme 1.4: Different metallation regioselectivities obtained for 2-substituted pyridines when varying base and reaction medium.

In reality, it can be difficult to envisage which course an organolithium-mediated reaction will follow without accounting for each of these subtle intricacies, particularly when managing multi-hydrogen containing substrates. The dawn of Directed-*ortho*-Metallation (DoM) was a revolutionary breakthrough in the creation of regiospecifically substituted aromatic rings but the nature of the most widely used directing groups leaves them susceptible to unwelcome side reactions such as nucleophilic addition. The

generic faults and limitations associated with organolithiums, and the improvements that have been sought on the performance of existing methodology will be addressed in the coming pages.

1.2) *Organozinc Reagents in Synthesis*

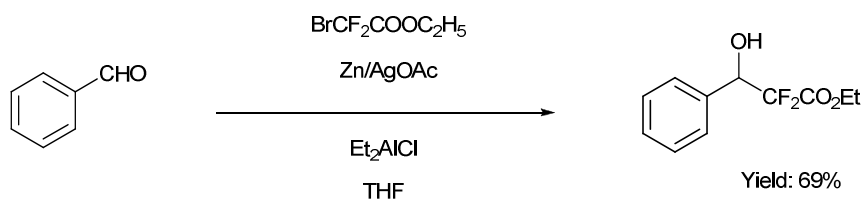
Initiating over a century of ensuing exploration, the discovery of organozinc compounds carries distinction as the naissance of organometallic chemistry. Working in his laboratory in 1849, Frankland fabricated the first class of compounds to boast a metal-carbon σ -bond; treating methyl or ethyl iodide with metallic zinc he produced the related dialkyl zinc reagents.^[23] Although, often kept in the shade by their more polar lithium and magnesium counterparts, organozinc reagents cooperate in many elementary organic reactions finding particular prowess in addition to carbonyl groups. The Reformatsky reaction, which utilises a zinc reagent prepared by reduction of an α -haloester with metallic zinc to create β -hydroxy esters, represents a pertinent example (Scheme 1.5).^[24]



Scheme 1.5: Generic example of the Reformatsky reaction.

With the evolution of organolithium chemistry, the Reformatsky reaction gradually faded out of the spotlight as expedient methods exploiting lithium enolates, prepared by direct deprotonation of the ester, were sought. However, in recent years the Reformatsky reaction, complete with a few adaptations, has re-emerged to once again find synthetic value. In one instance, the inclusion of organoaluminium additives as Lewis acids enhances the reactivity of the Reformatsky reagent in the reaction of ethyl

bromodifluoroacetate with aliphatic or aromatic ketones, aldehydes and *N*-protected- α -amino aldehydes, permitting the preparation of α,α -difluoro- β -hydroxy esters at 0 °C to room temperature (Scheme 1.6),^[25] where previously the presence of the aldehyde function prohibited the use of lithium reagents and the archetypal Reformatsky reagents required sonicating conditions to produce good yields.^[26]



Scheme 1.6: The Et₂AlCl-AgOAc modified Reformatsky reaction, producing α,α -difluoro- β -hydroxy esters in good yield.

Although the reaction has attracted widespread appreciation, the make-up and characteristics of the genuine Reformatsky reagent have remained ill defined. In preparing β -hydroxy esters, the Reformatsky reagent adds to carbonyl groups in a manner reminiscent of a Grignard reagent leading to a formulation of the type “ROC(O)CH₂ZnBr” being proposed. As part of a far reaching research programme probing the coordination chemistry of substituted organozinc compounds, Boersma and co-workers investigated the nature of the Reformatsky reagent derived from the *tert*-butyl ester of bromoacetic acid in both solution and the solid-state.^[27] In solution dimeric association was found to be the preferred state of the reagent in all but the most polar of solvents, and the dimeric structure persists in the solid-state (Figure 1.6).

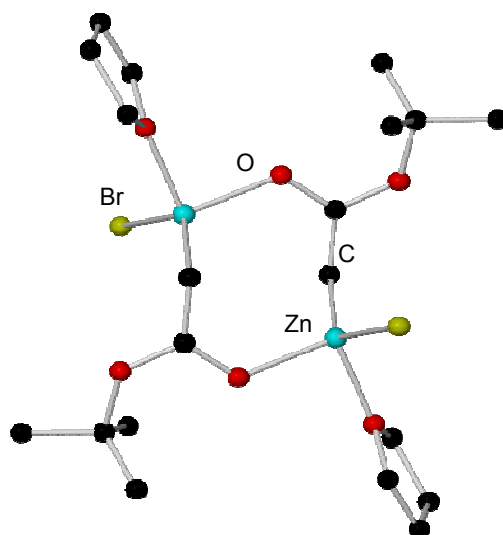


Figure 1.6: Crystal structure of the $[\text{THF}\cdot t\text{BuOC}(\text{O})\text{CH}_2\text{ZnBr}]_2$ dimer.

A previous report by Vaughan *et al.* had implied that Reformatsky reagents exhibit enolate character with the absence of an $\text{C}=\text{O}$ absorption at 1700 cm^{-1} in IR studies,^[28] while on the contrary, complementary NMR studies highlighted a paucity of vinylic resonances in the ^1H NMR spectra lending weight to the proposed carbon-metallated structure.^[29] However, the nature of a reagent in solution and its subsequent spectroscopic properties are defined by the polarity of the solvent, thus an equilibrium between the two species was put forward to explain the data observed in IR and NMR spectra with alternative solvents (Figure 1.7).

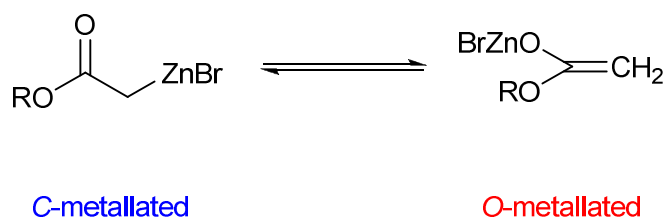
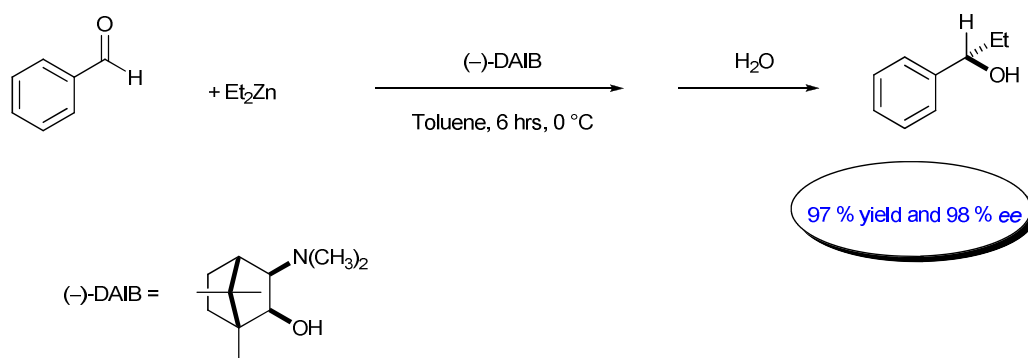


Figure 1.7: Proposed equilibrium between the potential carbon and oxygen metallated structures of Reformatsky reagents.

The crystal structure determined by Boersma, indicates that at least in the solid-state, the Reformatsky reagent cannot be assigned as either carbon or oxygen metallated with

the zinc-carbon and zinc-oxygen distances in the dimer all in the range of normal single bonds. THF solvation of the zinc centre and the steric bulk of the two *tert*-butyl groups may be key factors in preventing association to a higher aggregate. As a product of this structural study, the dimeric nature of the reagents in common solvents could then be factored into mechanistic discussions of the Reformatsky reaction.

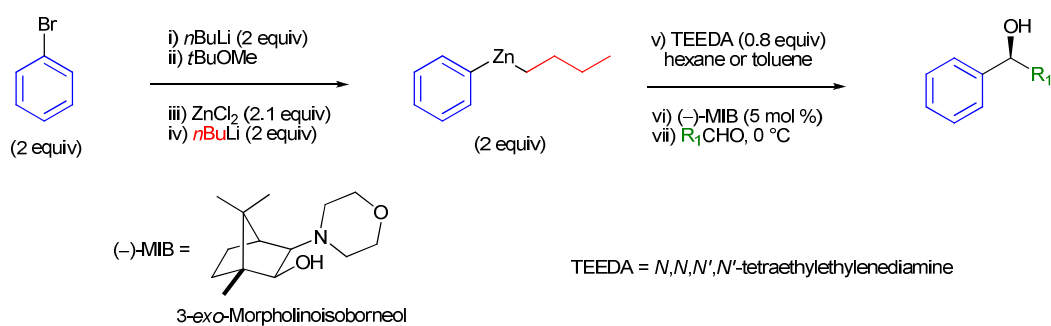
Nucleophilic addition of organometallic reagents to carbonyl substrates and the ensuing carbon-carbon bond formation constitutes a fundamental reaction in organic synthesis. In an extension of the Reformatsky reaction, enantioselective alkylation of carbonyl compounds presents a passage to the synthesis of optically active alcohols, and amidst the multitude of existing organometallic reagents available, diorganozinc compounds retain prestige as alkyl donors in asymmetric alkylation.^[30] In a fully optimised procedure, only 2 mol % of the optically active amino alcohol (–)-DAIB [(–)-3-*exo*-dimethylaminoisoborneol] is required to effect highly enantioselective addition of diethylzinc to the carbonyl group of benzaldehyde providing near maximum synthetic efficiency (Scheme 1.7).^[31]



Scheme 1.7: DAIB-promoted enantioselective addition of diethylzinc to benzaldehyde.

Furthermore, the addition of aryl groups has also drawn considerable interest with diarylmethanols central components in a number of biologically active compounds.^[32]

The obvious synthetic strategy would nominate diphenylzinc as the aryl transfer reagent; while this route has found applicability, issues with low enantioselectivity^[33] and the expensive nature of diphenylzinc (£91.50 for 1g from Sigma-Aldrich)^[34] have led to the development of more cost-effective methodologies. Walsh has reported a method that is instigated by the *in situ* generation of aryl zinc intermediates from readily available and inexpensive aryl bromides with subsequent asymmetric addition transpiring to afford highly enantioselective diarylmethanols and benzylic alcohols (Scheme 1.8).^[35]

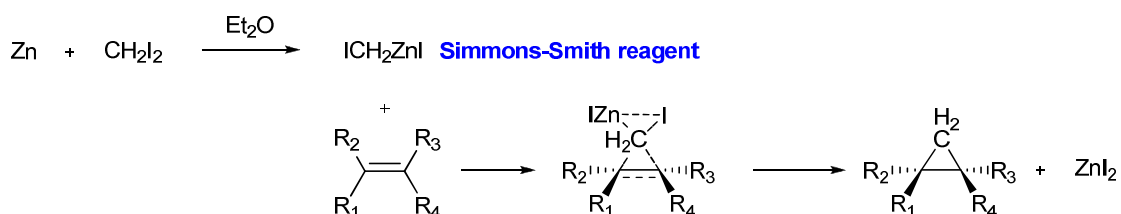


Scheme 1.8: Generic example of the one-pot arylation of aldehydes starting from aryl bromides.

To circumvent the low enantioselectivity that has been noted with diphenylzinc, mixed alkyl-aryl zinc intermediates were prepared by metal-halogen exchange between PhBr and *n*BuLi, followed by a transmetallation reaction with ZnCl₂ producing PhZnCl. A second equivalent of the alkyllithium and ensuing metathesis reaction generated the aryl zinc intermediate PhZnBu which was used *in situ* in the asymmetric addition reaction delivering an enantioselectivity higher than that of diphenylzinc and a versatile method for the synthesis of enantioenriched benzylic alcohols.

Arguably, the Simmons-Smith reagent which delivers cyclopropane rings from olefins equates to the benchmark for organozinc reagents in organic synthesis. There are a

variety of individual techniques for the production of Simmons-Smith reagents, however, the original preparation reported in 1958,^[36] encompassing oxidative addition of a dihalomethane to zinc metal remains the preferred route to the (iodomethyl) zinc reagent (Scheme 1.9).



Scheme 1.9: Preparation of Simmons-Smith reagent and its subsequent utilisation in the synthesis of a cyclopropane ring.

For a prolonged period of time after its discovery and vast usage, the structure of the cyclopropanating species remained ambiguous. Meticulous studies by Simmons and his co-workers surmised that the presence of the Schlenk-type equilibrium engenders (ICH₂)₂Zn/ZnI₂ the active reagent;^[37] while in a separate study probing the bromo analogue, NMR spectroscopic experiments conducted by Fabisch and Mitchell corroborate the initial formation of BrCH₂ZnBr and ensuing equilibration to (BrCH₂)₂Zn/ZnBr₂.^[38] In recent years, experimental and theoretical studies have made headway in clarifying the structure of (halomethyl) zinc reagents, none more so than those of the group of Denmark who scrutinised their constitution by the collaborative NMR and X-ray crystallographic approach.^[39] The NMR spectroscopic studies authenticate the suspicion that bis(halomethyl) zinc species are formed on addition of either CH₂I₂ or ClCH₂I to Et₂Zn, and that the resultant heteroleptic species are stabilised by the presence of coordinating ligands; with hexane solutions of a variety of glycol ether [(1,7,7-trimethyl)(2,3-dimethoxy)bicycloheptane] complexes readily producing

crystals upon cooling. The first X-ray crystallographic analysis of a bis(iodomethyl) zinc complex could be performed and was reported in 1992 (Figure 1.8).

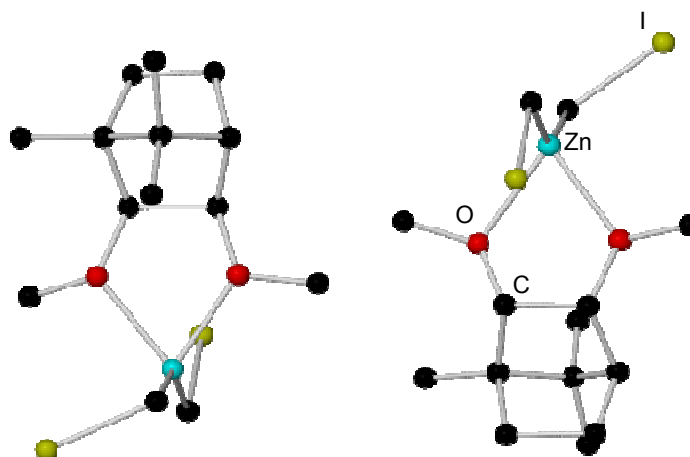
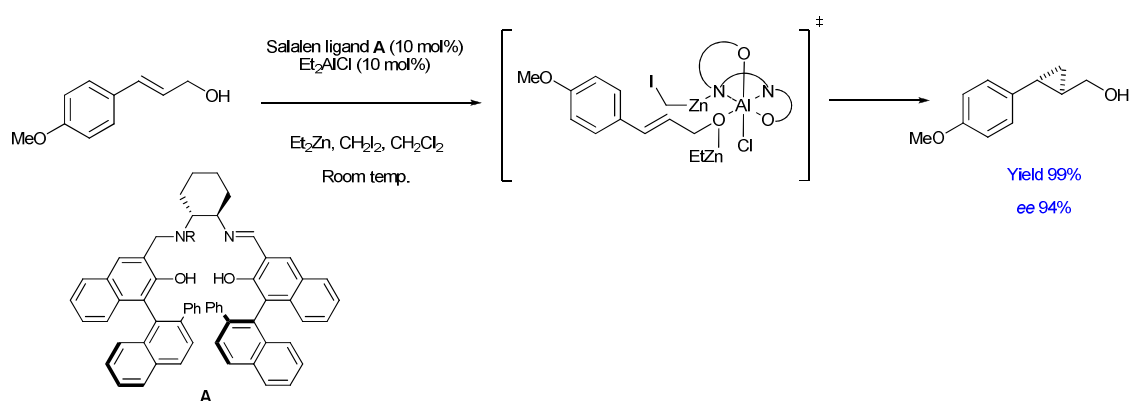


Figure 1.8: The two independent molecules within the crystal structure of a glycol ether solvated bis(iodomethyl) Simmons-Smith reagent.

The bis(iodomethyl) zinc complex crystallised as a monomer with two independent molecules in the unit cell. The glycol ether ligand regulates the orientation of the iodomethyl groups. *Endo* iodomethyl groups sit directly underneath the five-membered chelate rings but as a consequence of steric constraints with the bridgehead methyl groups, the *exo* iodomethyl groups cannot adopt this conformation thus it is anticlinal to one of the Zn-O bonds. In hatching a mechanism for the cyclopropanation reaction, Simmons proposed internal activation of the methylene by formation of a bond between the iodine and zinc atoms. The relatively close contacts between zinc and the *exo* iodine atoms [3.350(3) and 3.329(2) Å] in the aforesaid structure lend weight to his interpretation.

Remarkable progress has been made in the Simmons-Smith reaction and polished mechanistic profiles are continually forthcoming. Cyclopropanation of alkenes carrying an alcohol occurs much faster than those without such functionality.^[40] Upon introducing a chiral auxiliary into the mix, asymmetric Simmons-Smith reactions can be

conducted in a catalytic and enantioselective manner at room temperature, with the alcohol or resulting alkoxyzinc species forming an aggregate (or co-complex) with the (iodomethyl) zinc species and chiral auxiliary. In one procedure an Al(salalen) complex [salalen = salen/salan hybrid; salen = *N,N'* bis(salicylidene)ethylenediamine; salan=*N,N'*-bis(*o*-hydroxybenzyl)-1,2-diaminoethane], an aluminium Lewis acid/*N* Lewis base bifunctional catalyst, duly enables interaction with the (iodomethyl) zinc and hydroxyl sites delivering high enantioselectivities and quantitative yields at ambient temperatures (Scheme 1.10).^[41]



Scheme 1.10: Asymmetric Simmons-Smith reaction of allylic alcohols, illustrating the proposed intermediate.

Despite their covetable combination of exceptional functional group tolerance and soft nucleophilicity, organozinc reagents have found limited efficacy in deprotonative metallation. The metallation of comparatively inert C-H bonds solicits the use of a robust, highly polar base whereas with a propensity to form strong σ -bonds to carbon, dialkyl zinc reagents are afflicted by slow kinetics. Circumnavigating the kinetic inertness of common organozincs, catalytic amounts of secondary amines were shown to increase the rate of Zn-H exchange between Ph₂Zn and a collection of carbon acids,^[42] initiating exploration of the metallating capabilities of amidozinc reagents.

The structure of the homoleptic zinc bis(amide) $\text{Zn}(\text{TMP})_2$ (Figure 1.9) was reported by Rees in 1998, made from the reaction of two molar equivalents of LiTMP with ZnCl_2 in diethyl ether,^[43] however, almost a decade would pass before its potential in metallation chemistry was unlocked. Hagadorn examined the reactivity of four zinc amide bases for stoichiometric deprotonation; ethylzinc diphenylamide (EtZnNPh_2), ethylzinc diisopropylamide (EtZnNiPr_2) and $\text{Zn}(\text{HMDS})_2$ as well as $\text{Zn}(\text{TMP})_2$.^[44] Complications with side reactions and the low basicity of the diphenylamido anion resulted in an unsuccessful trial for both alkyl-amido zinc reagents, while poor kinetics plagued the reactivity of $\text{Zn}(\text{HMDS})_2$. However, $\text{Zn}(\text{TMP})_2$ showcased its capacity as an effective base, comfortably deprotonating an assortment of functionalised substrates bearing ketones, esters, sulfones or sulfoxides under mild conditions.

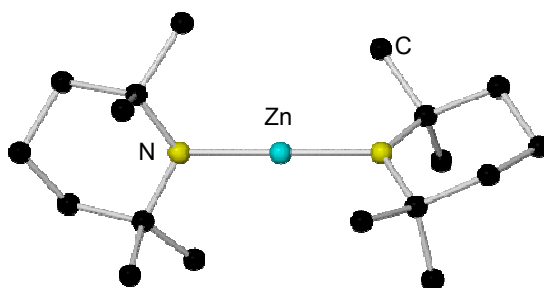


Figure 1.9: The molecular structure of $\text{Zn}(\text{TMP})_2$.

Notwithstanding their pivotal role in organic synthesis outlined in this section, organozinc compounds have long remained in the shadow of organolithium and Grignard reagents. However, an alkylzinc compound discovered over 150 years ago once again has zinc reagents basking in the limelight. In 1858, Wanklyn prepared sodium triethylzincate “ NaZnEt_3 ” via direct reaction of sodium metal and diethylzinc;^[45] subsequently termed “ates” in the realisation that classes of such metal complexes with anionic formulations could be developed, Wittig was first to appreciate the unique reactivity exhibited by such compounds. Extending Wanklyn’s pioneering studies, he synthesised the first magnesiate “ LiMgPh_3 ” prepared by reaction of the

homometallic components and noted that reaction with benzalacetophenone yielded a product of mainly 1,4-addition, in contrast to the 1,2-addition product obtained with PhLi.^[46]

This research programme builds upon the foundations laid by Wanklyn and Wittig, and the special reactivity profile that has established alkali-metal zincates as contemporary reagents in synthetic chemistry will be considered in the next section.

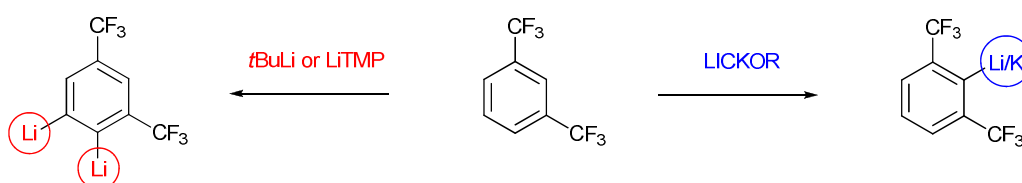
1.3) Second Generation Metallation

The underlying importance of the metallation reaction has inspired chemists to pursue novel, progressive reagents capable of selectively abstracting hydrogen from organic substrates. Although, alkyllithium or lithium amide reagents are viewed as the favoured metallating tools for countless synthetic renovations,^[47] there are constraints allied to their use. Prominent among these are poor functional group tolerance and low stability of the developing lithio-intermediates, therefore imposing the use of subambient temperatures to effect the desired reactions and avoid decomposition or side reactions. The necessity for energy input to maintain low temperatures creates cost implications when performing reactions on a larger scale with statistics from Chemical Development at GlaxoSmithKline suggesting that effecting reactions at temperatures less than -40 °C encounters an extra cost of at least £250 000 per annum per batch process.^[48] In light of this disadvantage, research groups all over the globe have been initiating innovative bimetallic alternatives to the customary homometallic reagents.

The ultimate proton abstractor would exhibit good functional group tolerance, high reactivity (preferably at ambient temperature) and high selectivity, particularly ability to deprotonate at positions inaccessible with previous incarnations. New reagents designed for this purpose can be considered composite molecules or concoctions constituting of

two or more compound types. Organolithium compounds can interact with alkali-metal alkoxides in two distinct ways. Whilst lithium alkoxides and organolithium compounds form adducts displaying comparable reactivity to the parent organolithium, a transmetallation (or part transmetallation) often transpires with heavier alkali-metal alkoxides, furnishing heavy alkali-metal organic compounds and lithium alkoxides. This exchange is accompanied by an extraordinary increase in reactivity compared to that of the starting organolithium compound, and the increased basicity of the *in situ* mixtures led to the coining of the name “superbase”.

The leading Lochmann-Schlosser reagent (LICKOR), prepared by combining *n*BuLi and *t*BuOK, has been commonly employed in deprotonation reactions, exhibiting enhanced reactivity over organolithium reagents. The trifluoromethyl group exerts only a small acidifying effect on adjacent protons and as a result a superbasic reagent is obligatory for the *ortho*-metallation of trifluoromethylbenzene to proceed satisfactorily,^[49] with *n*BuLi on its own in refluxing diethyl ether affording poor yields and imperfect regioselectivity.^[50] Advantageously, the LICKOR superbase opens up new reactivity on introducing a second trifluoromethyl group on the aromatic ring. Scheme 1.11 illustrates the contrasting metallation regioselectivities observed for 1,3-(trifluoromethyl)benzene using LICKOR and organolithium reagents.^[51]



Scheme 1.11: Complementary regioselectivities obtained for the metallation of 1,3-(trifluoromethyl)benzene utilising LICKOR and homometallic organolithiums.

On a comparative, qualitative scale of basicity the LICKOR reagent occupies an intermediate position higher than *n*BuLi but lower than *n*BuK, tentatively implying that complete transmetallation to the heavy alkali-metal organic compound does not come to pass or if it does, it does so in the form of a co-complex (see below) with the lithium alkoxide and possibly donor ligands. Benzene with a pK_a of around 40 is not easy to deprotonate due to its lack of activating electron-withdrawing substituents. For metallation to ensue utilising *n*BuLi, the presence of an electron-donating Lewis base such as TMEDA is required.^[52] Contrarily, upon employing the LICKOR superbases deprotonation of benzene proceeds quantitatively in the absence of such a donor.^[53] Schlosser surmised that the enhanced reactivity of *n*BuLi in the presence of *t*BuOK could be interpreted in terms of solvation of the *n*BuLi by the oxygen atom of the alkoxide,^[54] analogous to the solvation of organometallics by ethers, nevertheless categorical structural detail of the LICKOR reagent remains evasive. Revisiting a reaction surveyed by Lochmann in 1979,^[55] Mulvey and co-workers have elucidated the structure of the lithium primary amide - potassium alkoxide composite $[(t\text{BuNH})_4(t\text{BuO})_4\text{Li}_4\text{K}_4 \cdot (\text{C}_6\text{H}_6)_n]$, which contains dimeric (LiN)₂ and (KO)₂ rings fused together in a carousel arrangement (Figure 1.10).^[56] Although its superbases character was endorsed by its ability to abstract a proton from toluene, synthetic use of this complex is extremely limited as its constituent homometallic compounds, are weak bases themselves.

In 2011, O'Shea described a method for benzylic metallation of *ortho*, *meta* and *para*-substituted toluenes using a mixed-metal amide base generated from a *n*BuLi/*t*BuOK/TMP(H) mixture at -78 °C in THF (Scheme 1.12). The OMOM (methoxymethoxy) group is a strong *ortho*-directing substituent, therefore *ortho*-metallation proceeds satisfactorily with the superbasic mixture but overcoming the

ortho-directing influence, the excellent level of benzylic selectivity achieved is attributed to the mixed-metal amide bases ability to facilitate an aryl migration from the kinetic *ortho*-metallation site to the benzylic position. Notably, this controlled anion migration is attainable with catalytic quantities of TMP.^[57] It is worth mentioning that O'Shea's variant of the Lochmann/Schlosser superbases mixture has only ever been generated *in situ* and the precise identity of its active base ingredients have not yet been established.

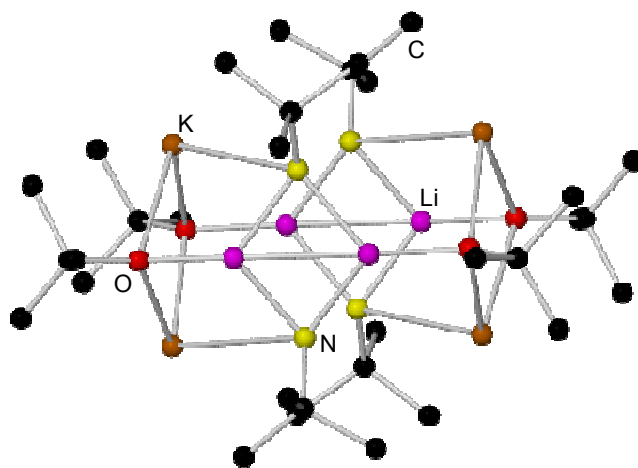
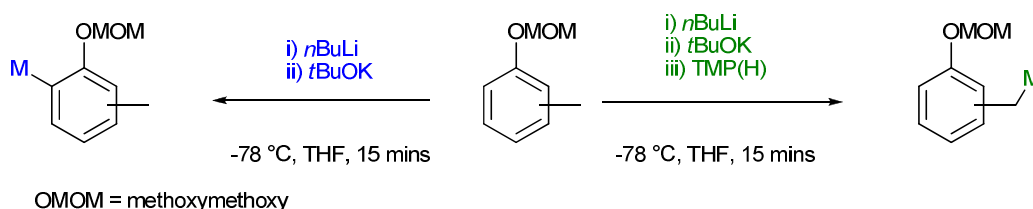
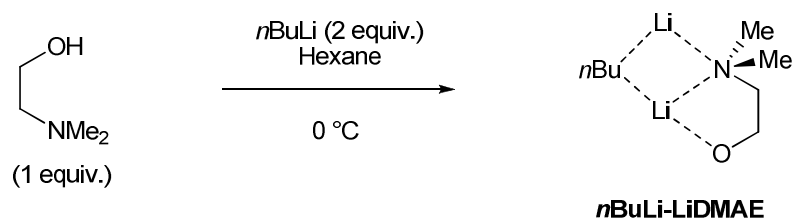


Figure 1.10: Molecular structure of the mixed lithium-potassium amide alkoxide “superbase” $[(t\text{BuNH})_4(t\text{BuO})_4\text{Li}_4\text{K}_4 \cdot (\text{C}_6\text{H}_6)_n]$.



Scheme 1.12: Selective *ortho* and benzylic metallations of OMOM-substituted toluenes using variants of the superbasic mixture.

Supplementing the mixed-metal LICKOR reagent, a new class of unimetal superbases derived from co-complexation of alkyllithiums and lithium aminoalkoxides have emerged. Engineered with the desire of amplifying basicity by association and arresting nucleophilicity through the formation of sterically hindered aggregates, renowned amongst these is Caubère's reagent, *n*BuLi-LiDMAE [where DMAE is (dimethylamino)ethoxide],^[58] the formulation of which suggests the metallating reagent is prepared by mixing an alkyllithium with an amino alcohol in an apolar, non-coordinating solvent (Scheme 1.13). The RLi/ROLi reagents have been promoted in metallation chemistry by Gros and Fort with notable reactivity and selectivity in the deprotonation of pyridines.^[59]



Scheme 1.13: Preparation and empirical structure of *n*BuLi-LiDMAE reagent.

The pyridine substructure is an important motif for pharmaceuticals^[60] and optoelectronic^[61] or luminescent materials.^[62] Accordingly, chemists have endeavoured to formulate efficient and selective protocols to perform chemical manipulations on the pyridine ring. In this context, regioselective lithiation procedures are highly sought after; however, the π -deficiency of pyridine has proven detrimental to the execution of this reaction with alkyllithiums, resulting in nucleophilic attack on the azomethine (N=C) bond.^[63] Attention turned to the sterically hindered non-nucleophilic lithium dialkylamides, typically LDA and LiTMP, and despite their lower basicities these reagents can initiate metallation of common pyridines.^[64] Nonetheless, their preparation commences with expensive amines and typically they are deployed in excess (2 - 4

equiv.), hence diligence has been re-directed to turning nucleophilic alkyllithiums into basic reagents by virtue of co-complexation. The marked reactivity of *n*BuLi/aminoalkoxide reagents was first noted during the lithiation of 2-methoxypyridine (Table 1.1).^[65]

Table 1.1: Treatment of 2-methoxypyridine with *n*BuLi-TMEDA/DMAE combinations.

1) *n*BuLi (1 equiv.)
chelating agent
hexane, 0 °C

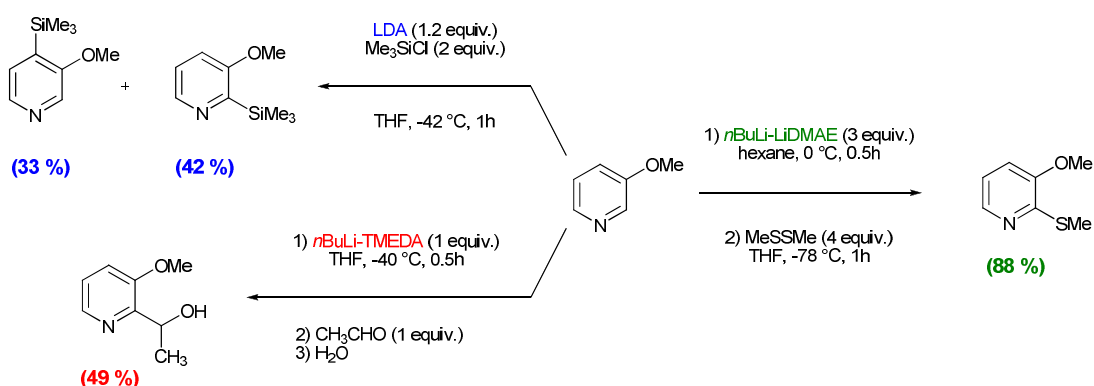
2) Me₃SiCl, 0 °C

A **B** **C**

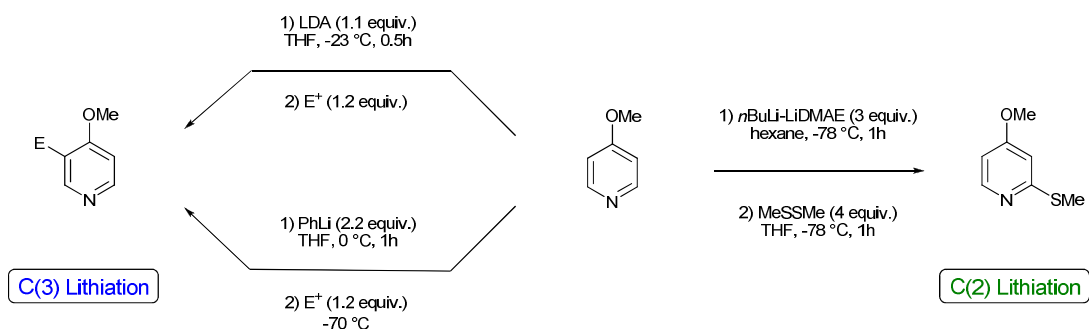
Chelating Agent	A (%)	B (%)	C (%)
TMEDA	31	16	-
DMAE	28	-	42

2-methoxypyridine was treated with assorted *n*BuLi-chelating agent combinations and the resultant lithiated species were quenched with an excess of chlorotrimethylsilane. GC analysis revealed the TMEDA solvated complex principally afforded the 6-addition product **A**, while the *n*BuLi-LiDMAE reagent afforded the best metallation/addition ratio producing **C** in 42% yield. Granted the extent of lithium-hydrogen exchange is not striking, this study nonetheless unveiled the capability of these aminoalkoxide aggregates and set in motion investigations into the application of these reagents. The lithiation of 3-methoxypyridine is extensively documented in the literature with efficiency and selectivity dependent upon the metallating agent and reaction conditions (Scheme 1.14).

Conventional reagents LDA^[66] and *n*BuLi/TMEDA^[67] in THF predominantly delivered the C-2 substituted product in moderate yields, but with *n*BuLi-LiDMAE in hexane this selectivity was achieved in an excellent 88% yield after 30 minutes at 0 °C.^[59a] Metallation of regioisomeric 4-methoxypyridine conceived a new selectivity, enriching the scope of the *n*BuLi-LiDMAE partnership.^[59a] Whereas exclusive C-3 lithiation was observed with LDA^[68] and PhLi,^[69] a complete reversal of selectivity to the C-2 position was witnessed with Caubère's reagent at -78 °C launching *n*BuLi/lithium aminoalkoxide aggregates as attractive selective reagents (Scheme 1.15).

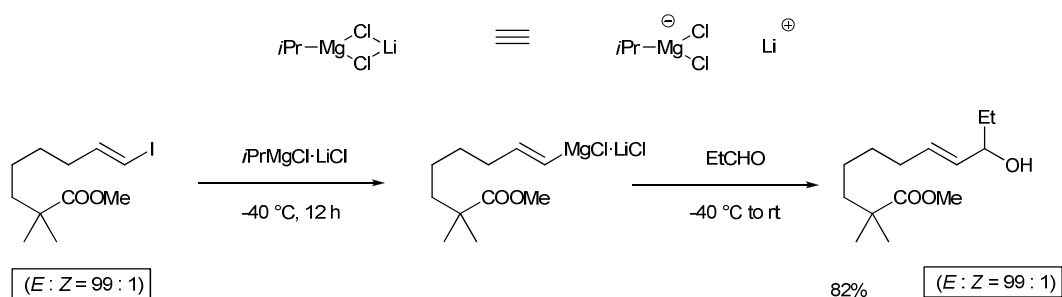


Scheme 1.14: Treatment of 3-methoxypyridine with *n*BuLi-LiDMAE and customary lithiating agents.



Scheme 1.15: Contrasting metallation regioselectivities towards 4-methoxypyridine with conventional organolithium reagents or *n*BuLi-LiDMAE.

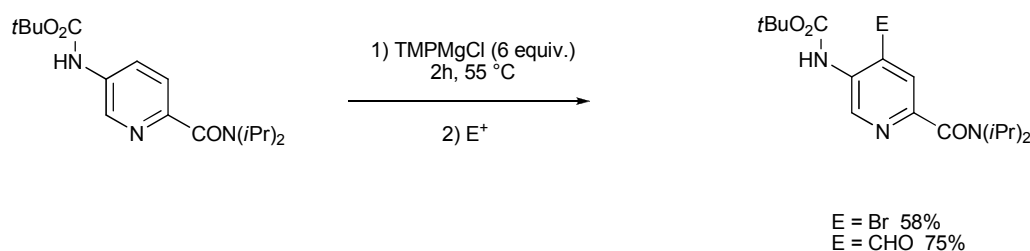
Nowadays, there is increasing realisations that direct metallation with low polarity metals such as magnesium, zinc or manganese(II) is attainable with imaginatively composed bases. The work of Knochel has unmasked a special reactivity that can be realised with a mixed lithium halide - alkylmagnesium complex, labelled a “turbo-Grignard” reagent. While exploring the synthesis of organomagnesium compounds, it was shown that addition of LiCl to the Grignard reagent $i\text{PrMgCl}$ bestows a significant boost in reactivity for magnesium-halogen exchange reactions.^[70] This augmented reactivity is credited in part to an additional negative charge at the magnesium centre (*i.e.* “ate” formation) which swells the nucleophilic properties of the $i\text{Pr}$ group. Supplementing its high reactivity and regioselectivity, this reagent displays a wide functional group tolerance, with nitriles, halides and esters all tolerated as functionalised alkenyl iodides were converted to the subsequent alkenylmagnesium derivatives (Scheme 1.16).^[71]



Scheme 1.16: Synthesis of functionalised alkenylmagnesium reagents using the “turbo-Grignard” $i\text{PrMgCl}\cdot\text{LiCl}$.

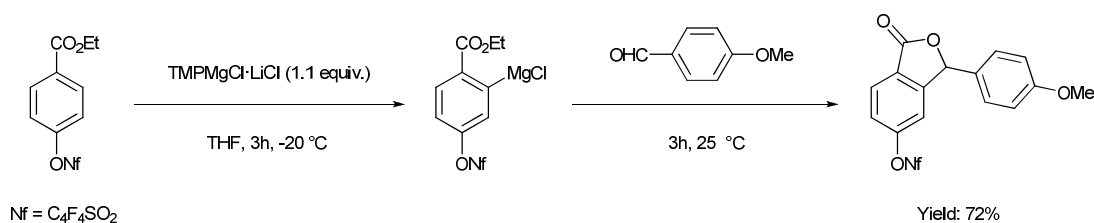
In 1947, Hauser described magnesium amide bases of the general formula R_2NMgX or $(\text{R}_2\text{N})_2\text{Mg}$.^[72] Possessing a more covalent metal-nitrogen bond in comparison to those in lithium amides, these reagents were found to be tolerant towards various commonly encountered organic functionalities, consequently alleviating the energetic burden of cryogenic temperatures. Amidst important contributions from Eaton^[73] and Kondo,^[74]

Mulzer reported the regioselective magnesiation of pyridine carboxamides and carbamates deploying TMPMgCl (Scheme 1.17).^[75] Unfortunately, as a consequence of their low solubility in common organic solvents a large excess of magnesium amide can be mandatory for high conversions and reaction rates.



Scheme 1.17: Magnesiation of a pyridine carboxamide derivative using TMPMgCl.

Embracing the turbo-Grignard methodology, the combination of sterically hindered magnesium amides with LiCl generates kinetically highly reactive and THF soluble bases.^[76] Reacting *i*PrMgCl·LiCl with an equivalent of TMP(H) for 24 hours, quantitatively produces TMPMgCl·LiCl which can be stored under the obligatory inert atmosphere in a stable THF solution. Illustrating tolerance towards sensitive, more reactive substituents, a highly electrophilic nonaflate is compatible with an equimolar quantity of base under mild conditions and addition of an aromatic aldehyde provides the expected lactone in 72% yield (Scheme 1.18).^[77]



Scheme 1.18: Preparation of a highly functionalised aromatic using TMPMgCl·LiCl.

The high solubility and reactivity of the $\text{TMPMgCl}\cdot\text{LiCl}$ reagent would imply a non-polymeric structure, with LiCl potentially forming a mixed-aggregate with the bulky magnesium amide. This interpretation was ratified by the Mulvey group when the monomeric turbo-Hauser base was structurally characterised in the solid-state for the first time in 2008 (Figure 1.11).^[78] Revealing the molecular halide composition provided structural justification for the reagent's impressive magnesiating ability. The TMP is bound to magnesium and its terminal fixation signifies only one bond needs to be broken to release the active base, and with a potentially labile THF ligand geminal to TMP, a vacant site could facilitate pre-coordination of the functionalised aromatic prior to its magnesiation.

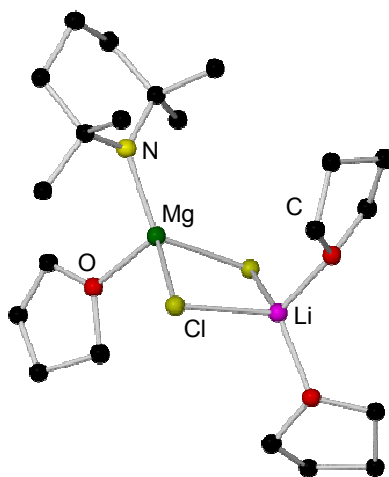
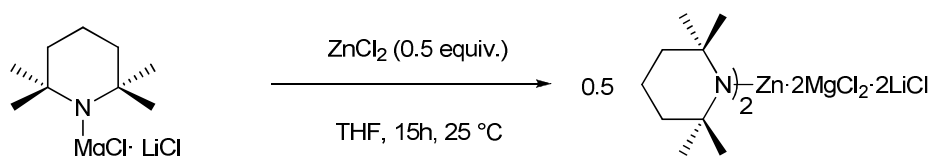


Figure 1.11: Molecular structure of turbo-Hauser $\text{TMPMgCl}\cdot\text{LiCl}$ reagent.

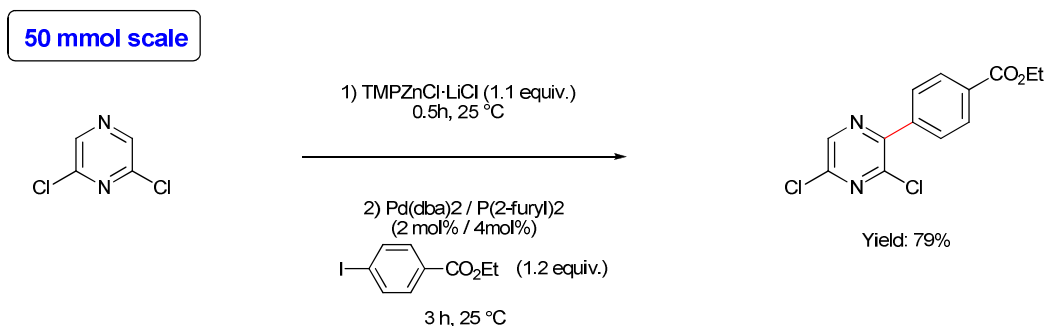
Despite the fact TMP-magnesium bases like $\text{TMPMgCl}\cdot\text{LiCl}$ showcase a high functional group tolerance towards nitriles, esters and aryl ketones, there are still a number of important but more reactive functional groups like nitros and aldehydes that are not compatible with the use of a magnesium base. Recent communications have seen Knochel blend his magnesium reagents with zinc chloride to fashion a chemoselective base for direct zincation of arenes and heteroarenes (Scheme 1.19).^[79] Formation of the composite base $(\text{TMP})_2\text{Zn}\cdot 2\text{MgCl}_2\cdot 2\text{LiCl}$ transpires in high yield with

the presence of both MgCl_2 and LiCl essential for the solubility and high reactivity of the base.



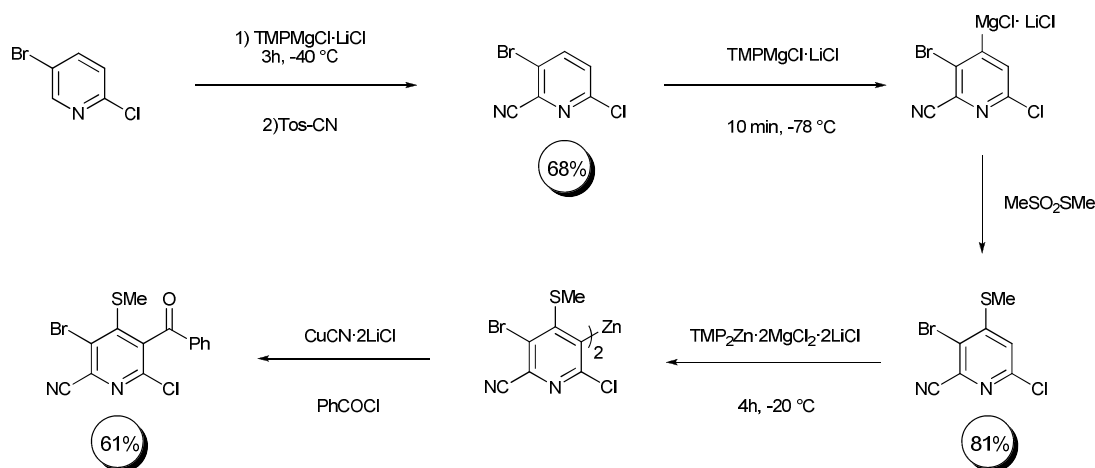
Scheme 1.19: Preparation of the base $(\text{TMP})_2\text{Zn}\cdot 2\text{MgCl}_2\cdot 2\text{LiCl}$.

Direct zincation of sensitive aromatics and heteroaromatics was achievable, nonetheless with this reagent some electron-poor functionalised arenes and heteroarenes still give unsatisfactory results in terms of yields and reaction selectivity. Furthermore, various activated aromatics or heteroaromatics such as nitro derivatives or pyridazines compel metallations below $-50\text{ }^\circ\text{C}$, which is not convenient for reaction upscaling.^[80] These problems can be circumvented by the use of the commercially available, more selective zinc base $\text{TMPZnCl}\cdot\text{LiCl}$ that executes chemo- and regioselective zincation of aryl and heteroaryl substrates containing sensitive groups typically at ambient temperature^[81] and on the multigram scale with metallation rates comparable to those obtained for small scale processes.^[82] The synthesis of functional aryl and heteroaryl zinc reagents via direct zincation facilitates accelerated Negishi cross coupling,^[83] whereas lithiated or magnesiated substrates typically require preceding transmetallation with zinc chloride, opening up the efficient construction of a myriad of organic skeletons. For instance, the zinc intermediates manufactured on a 50 mmol scale exhibit excellent reactivity in Pd-catalysed Negishi cross coupling reactions with substituted aryl iodides (Scheme 1.20).^[82]



Scheme 1.20: Zincation of 2,6-dichloropyrazine using $\text{TMPZnCl}\cdot\text{LiCl}$ and subsequent Negishi cross-coupling.

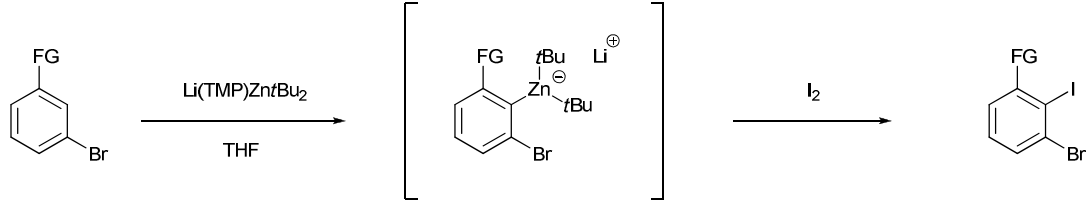
The new LiCl-solubilised TMP bases have recently been the subject of two comprehensive review articles and for that reason a line will be drawn under their discussion.^[84] Their discovery has written a whole new chapter in the metallation story, with exceptionally good functional group tolerance and mild reaction conditions desirably complementing the high kinetic basicity of the new TMP-bases. Whether deployed independently or synchronically (Scheme 1.21),^[85] the resulting organometallics are readily functionalised by electrophiles conveying broad application in organic synthesis.



Scheme 1.21: Full functionalisation of the pyridine core using sequential LiCl solubilised TMP base/electrophilic interception protocols.

In general, alkali-metal zincates demonstrate greater selectivity and functional group tolerance than many more established reagents. As briefly touched upon in Section 1.2, they also exhibit enhanced reactivity in comparison to kinetically retarded, neutral dialkyl zinc compounds R_2Zn .^[86] Pioneering work of Kondo and Uchiyama provided inspiration for the theme of this PhD programme. In the late 1990's, their research focused on the development of ate complexes, particularly zincates and exploiting the unique characteristics of these reagents in synthesis. Initial investigations chronicled that lithium trialkylzincates could be used as chemoselective reagents in metal-halogen exchange reactions.^[87]

Amongst this family of bimetallic compounds, dialkyl-amido zincates, $MZn(NR_2)R'_2$ have been given more consideration due to the high degree of selectivity expressed in their aromatic deprotonation reactions. The novel deprotonative zincation of functionalised aromatic and heteroaromatics was realised using a TMP-zincate. The *ortho*-metallation of arenes harbouring directing metallating groups was smoothly accomplished engaging “ $LiZn(TMP)tBu_2$ ” at room temperature, with ensuing electrophilic quench with iodine producing the iodobenzoates in excellent yields.^[88] Significantly, stepwise treatment of the alkyl benzoates with $LiTMP$ and tBu_2Zn was found to be ineffectual for the formation of the arylzincates, and as a consequence pre-complexation of $LiTMP$ and tBu_2Zn was deemed an intrinsic facet of the metallation. Zincation with “ $LiZn(TMP)tBu_2$ ” also proved a powerful tool for the preparation of 1,2,3-trisubstituted aromatic compounds (Table 1.2),^[89] where the use of alkyllithium bases is limited by the presence of a bromine atom on the arene due to competing metal-halogen exchange^[90] and *ortho*-metallation with hindered lithium dialkylamides partly eliminates lithium bromide generating a benzyne intermediate that can be intercepted *in situ* with the base.^[91]

Table 1.2: Chemoselective metallation of functionalised bromobenzenes and subsequent iodination.


The reaction scheme shows a functionalised bromobenzene (with FG and Br substituents) reacting with Li(TMP)Zn(tBu)_2 in THF to form a zincate intermediate. The intermediate is shown in brackets as a benzene ring with FG and Br substituents, coordinated to a zinc atom which is also bonded to two tBu groups and a lithium ion (Li^+). This intermediate then reacts with I_2 to produce the iodinated product.

FG	Time (h)	Temperature ($^{\circ}\text{C}$)	Yield (%)
CN	3	0	96
OMe	12	-30	95
$\text{CON}i\text{Pr}_2$	3	0	84
Cl	24	-30	77
F	24	-30	93

Additionally, Uchiyama has studied the mechanism and origins of chemoselectivity in the *ortho*-metallation of functionalised arenes with TMP-zincate bases revealing the high substrate compatibility they exhibit.^[92] Employing $\text{LiZn(NMe}_2)_2$ as the chemical model of their bases, computational/theoretical studies focused on the reaction pathway of TMP-zincates with benzonitrile and methyl benzoate both of which react forcibly with alkyllithiums to afford the 1,2-addition adducts. The results not only illustrate the lower barrier to *ortho*-metallation over 1,2-addition; overall, the broad substrate compatibility in these metallations with zincates is beautifully portrayed. In the reaction with benzonitrile, the lithium atom tweaks its position so that the Me_2N ligand can interact with the *ortho*-hydrogen atom; while the “closed-form” of the zincate is preserved in the reaction of methyl benzoate suggesting the zincate bases can adapt their transition state structures flexibly to suit the specific substrate (Figure 1.12).

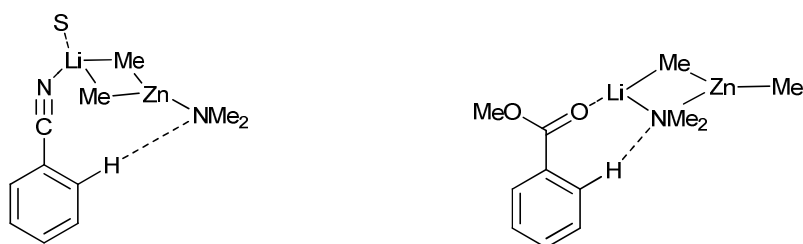
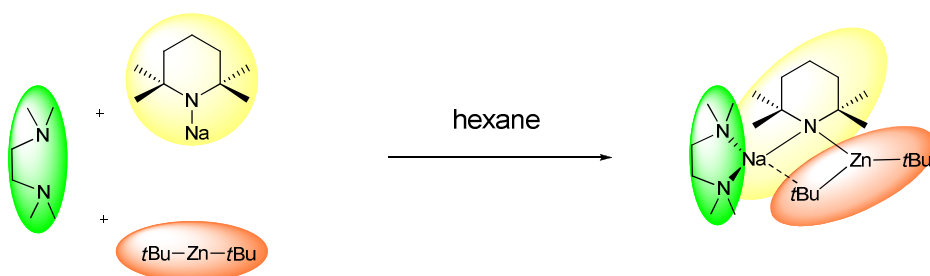


Figure 1.12: Transition states in the reactions of $\text{Li}(\text{NMe}_2)\text{ZnMe}_2$ with benzonitrile or methylbenzoate.

Complementing this theoretical study, a measure of regiocontrol can be implemented in the deprotonative metallation of bromopyridines by choosing one of two tuneable amidozincates.^[93] This cooperative or synergic behaviour is a feature of heterobimetallic ate compounds where the alkali-metals are associated with another metal, creating unique chemistries that cannot be replicated by either of the homometallic components from which they are comprised. Acknowledging that structure and reactivity are often intertwined, the Mulvey group have successfully created a structural template that is primed for executing deprotonative metallation.^[94] Conceptually, the avenue leading to this class of metallating agent can be deemed a “co-complexation” reaction with the three distinct components of the reaction interlinking to produce the composite molecule (Scheme 1.22).



Scheme 1.22: Co-complexation synthesis of a sodium TMP-zincate.

Thus far this section has aspired to herald the deprotonative power of the new generation of complex metallators, but nowhere has this increased reactivity been so

apparent than with the sodium dialkyl-amidozincate [(TMEDA)Na(μ -TMP)(μ -*t*Bu)Zn(*t*Bu)] (**1**). Introduced by the Mulvey group in 2005,^[95] the structure of **1** embodies the first crystallographically characterised sodium diorgano-amidozincate. Sodium and zinc centres are linked by a bridging TMP which bonds to each metal via its nitrogen atom. The bidentate TMEDA ligand chelates to sodium, while zinc carries a terminal *t*Bu ligand. Completing a central 5-membered (NaNZnCC) ring is an unusual asymmetric *t*Bu bridge, bonding directly to zinc and additionally engaging in a medium-long Na \cdots Me agostic contact [2.75(10) Å] denoted by the dashed line in Figure 1.13.

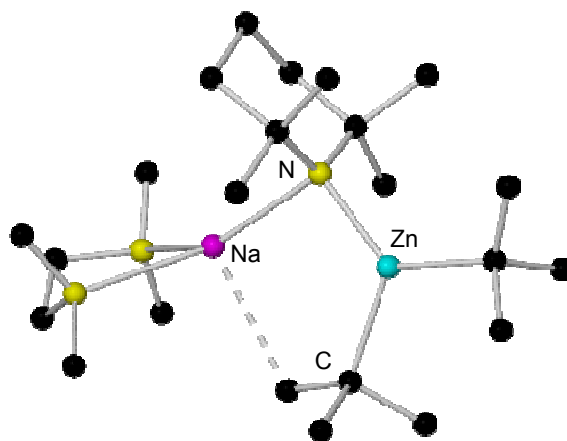


Figure 1.13: Molecular structure of [(TMEDA)Na(μ -TMP)(μ -*t*Bu)Zn(*t*Bu)] (**1**).

This complex has been proven to be a powerful and effective regioselective base towards various arenes; displaying high functional group tolerance, reactions can be carried out under mild conditions, generally at room temperature. Particularly impressive is the ease at which metallation of unactivated aromatics progresses. The fused ring aromatic hydrocarbon naphthalene was reacted with **1** under benign experimental conditions (namely in hexane, at room temperature and stirred for 2 hours) furnishing crystalline 2-monometallated naphthalene [(TMEDA)Na(μ -TMP)(μ -2-C₁₀H₇)Zn(*t*Bu)] in typical isolated yields of 50% (Figure 1.14).^[96]

Erstwhile applications of **1** had been confined to mono-deprotonation reactions; however, when naphthalene was subjected to an excess of **1**, di-zincation was effortlessly accomplished. Exploiting two equivalents of base at reflux conditions for 5 hours harvests a crop of di-zincated 2,6-dinaphthalenediide [(TMEDA)₂Na₂(TMP)₂(2,6-C₁₀H₆)Zn₂(*t*Bu)₂], the mono-zincated product and unaffected naphthalene in 7:1:1 ratio as validated by NMR spectroscopic analysis. Emphasising the revolutionary essence of this study, dimetallation of polycyclic naphthalene utilising the superbasic LICKOR reagent churns out a mixture of 10 different di-substituted isomers all in poor yields.^[53]

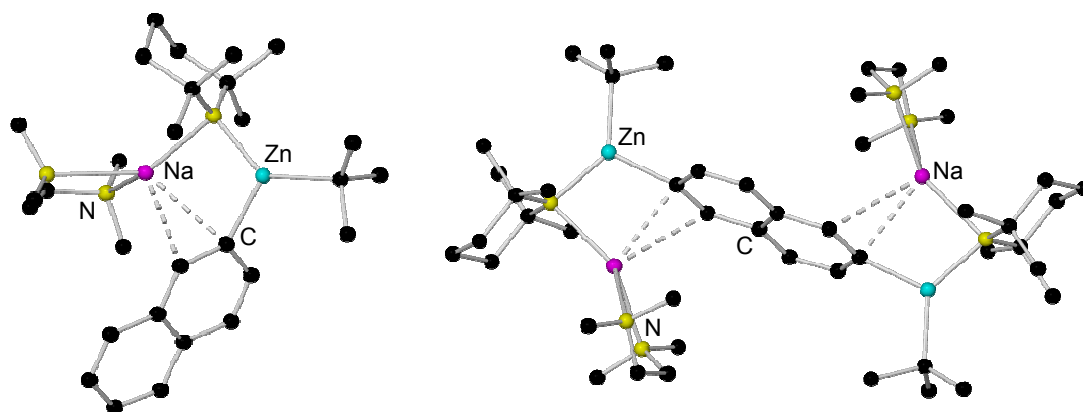
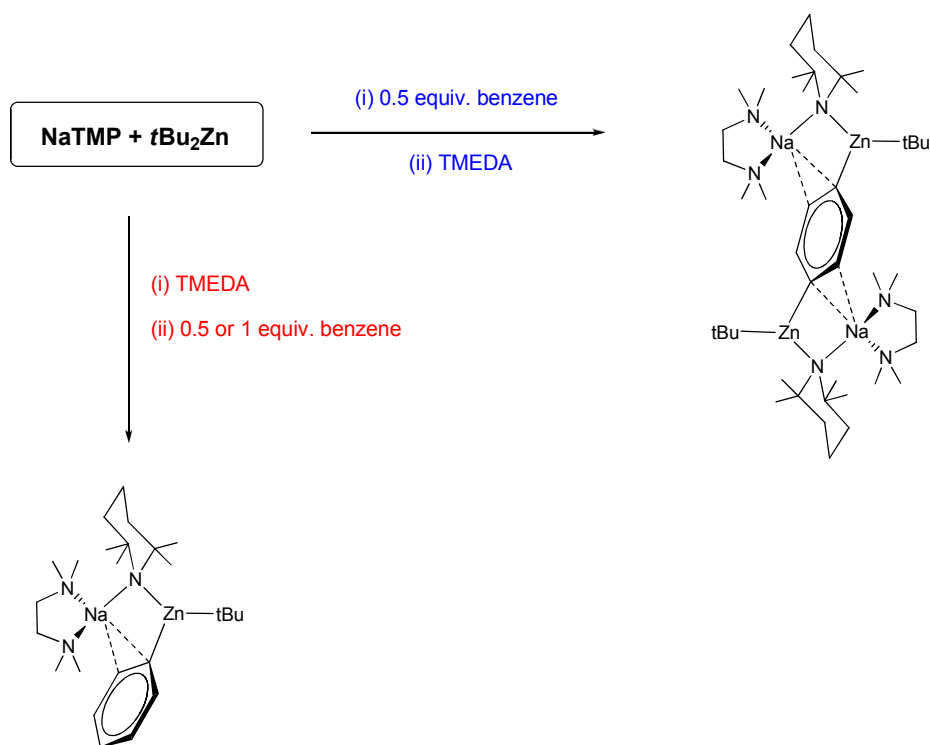


Figure 1.14: Molecular structures of mono- and di-zincated naphthalene.

The simplest aromatic molecule benzene is also stoichiometrically 1,4-dideprotonated on reaction with two equivalents of **1**.^[97] Close inspection revealed that the reaction is dependent on the order of reagent addition. In the absence of TMEDA, the combination of NaTMP and *t*Bu₂Zn is insoluble in hydrocarbon media; yet dissolution and complex formation could be accomplished upon addition of 0.5 molar equivalents of benzene. Stirring this reaction mixture for 48 hours before introducing TMEDA encourages crystallisation of the product, namely the 1,4-dizincated complex

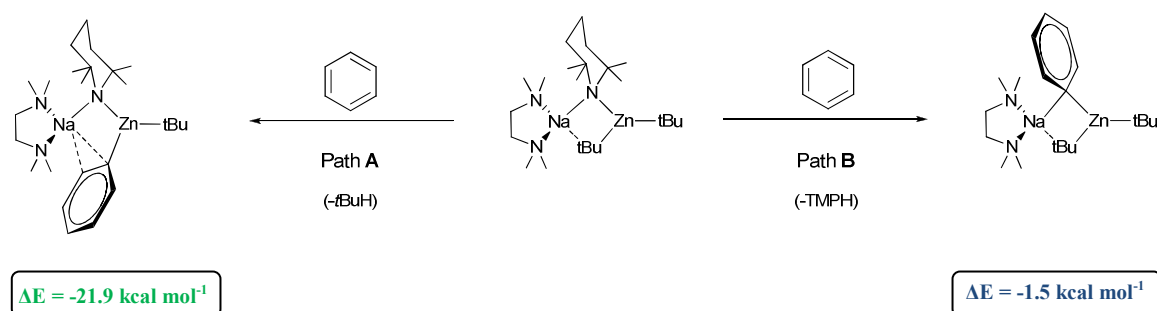
$[(\text{TMEDA})_2\text{Na}(\text{TMP})_2(1,4\text{-C}_6\text{H}_4)\text{Zn}_2(\text{tBu})_2]$. Interestingly, TMEDA exerts a debilitating effect on the ability of **1** to di-deprotonate benzene; for if it is implanted at an earlier juncture only the mono-deprotonated benzene complex $[(\text{TMEDA})\text{Na}(\mu\text{-TMP})(\mu\text{-C}_6\text{H}_5)\text{Zn}(\text{tBu})]$ is formed (Scheme 1.23), implying TMEDA acts only as a crystallisation aid in the formation of **1** and appears not to be involved in the transition structures of the deprotonation steps.



Scheme 1.23: Importance of the order of reagent addition in the synergic mono- and di-zincation of benzene.

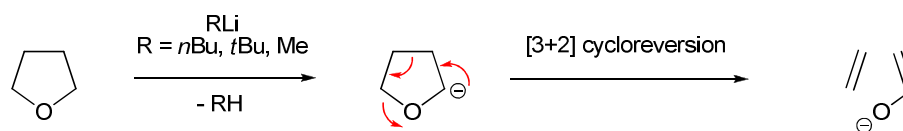
In each of the preceding studies, X-ray crystallographic and NMR spectroscopic analyses have been utilised to decree whether TMP-zincate **1** behaves as an alkyl or amido base. ^1H NMR spectra recorded passively in deuterated benzene solution show integration ratios consistent with a 1:1 $\text{tBu}:\text{TMP}$ stoichiometry, whilst tandem X-ray crystallography studies substantiate alkyl basicity with the TMP ligand retaining its indigenous bridging position. In an effort to rationalise the alkyl basicity, DFT

calculations were used to gauge the energetics of the reaction of **1** with an equimolar measure of benzene.^[95] Scheme 1.24 illustrates route **A**, which appears to mimic the experimental reaction, and route **B**, a putative reaction where TMP acts as the base. Both are exothermic processes. Reassuringly, the energy released for path **A** is far greater intimating that the preference for *t*Bu ligand transfer is, at least in part, thermodynamically driven. However, in the intervening years complementary experimental and theoretical studies have come forth filling in the gaps and inferring a twist in the reactivity profiles of TMP-zincates. This dual basicity will be elaborated upon in the forthcoming pages.



Scheme 1.24: DFT modelled reactions of **1 with benzene, illustrating calculated heats of formation for alkyl basicity (L.H.S) versus amido basicity (R.H.S.).**

The highlight for the Mulvey group came in the form of synthetically useful THF metallation. For generations of chemists, the controlled metallation of ethers has presented the ultimate challenge; highly unstable, metallated ethers readily cleave via one of a number of possible pathways.^[98] Pointedly, metallation at the α -position of THF localises a large degree of negative character on the α -C adjacent to the electron-rich O atom, kindling a grave destabilisation that solicits a spontaneous ring opening. The identity of the final decomposition products depends upon the reaction conditions, but a mixture of ethene and the enolate of acetaldehyde is most common (Scheme 1.25).^[99]



Scheme 1.25: Common mechanism for the cleavage of THF with alkyllithium reagents.

However, refining the synergic mixed-metal approach it was not only possible to directly zincate the cyclic ether (Figure 1.15) but also it can be effected with the vulnerable α -metallated THF fragment staying intact at ambient temperature without any ring opening or cleavage entertaining interception by the common electrophile benzoyl chloride.^[100] To meet the challenge of a delicate zincation, the highly basic *t*Bu carbanions were substituted for the gentler trimethylsilylmethyl ligand. The analogous potassium zinc reagent [(PMDETA)K(μ -TMP)(μ -CH₂SiMe₃)Zn(CH₂SiMe₃)] also trapped the elusive CH₂=CH⁻ anion via deprotonation of ethene, with Zn forming a σ -bond to the deprotonated C atom and K engaging the π -system of the unsaturated C₂ unit. This one report had far-reaching implications for metallation and organometallic chemistry in general.

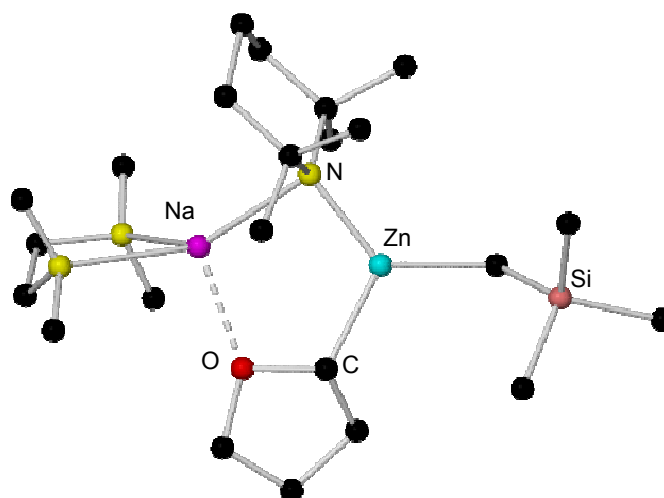


Figure 1.15: Molecular structure of the α -zincated THF complex.

It is worth re-emphasising that on their own, dialkyl zinc compounds are feeble deprotonating agents unable to perform any of the aforementioned zincations. Marrying this less electropositive metal with an alkali-metal partner stimulates a special synergy that augments the zincation. While the alkali-metal component is essential for the synergic metallation to follow its course, it takes on more of a secondary, supporting role prompting reactions of this type to be best regarded as “Alkali-Metal-Mediated Zincations (AMMZn)”

1.4) *Aims of the PhD research project*

The primary aim of this research project was to perform a comprehensive study of the reaction chemistry of the synergic sodium-zinc mixed alkyl-amido reagent [(TMEDA)Na(μ -TMP)(μ -*t*Bu)Zn(*t*Bu)] (**1**). Focusing on zinc-hydrogen exchange processes, reactions of **1** towards a series of organic substrates were investigated. Specific objectives within this remit are now outlined:

- To study the reactions of the synergic base with a series of functionalised electron-rich aromatics to compare and contrast with previous literature metallations (generally lithiations). Additionally haloaromatics were studied, probing the effect of benzyne formation.
- To attempt to isolate and crystallise, where possible, the zinc-aryl products of these reactions. In appropriate cases electrophilic interception reactions were subsequently performed on these compounds to generate the metal-free products.
- To fully characterise these reactive metallo products by a complementary combination of NMR spectroscopic (solution) and X-ray crystallographic (solid-state) studies.
- To shed more light on the mechanism of these so called Alkali-Metal-Mediated Zincation reactions.
- To explore the redox chemistry of **1** by studying its behaviour towards the free radical TEMPO, attempting to grow crystalline samples of metal-TEMPO products for X-ray crystallographic study.

Chapter 1 - References

- [1] W. Schlenk, J. Holtz, *Ber. Dtsch. Chem. Ges.* **1917**, *50*, 262 - 274.
- [2] (a) K. C. Nicolaou, J. S. Chen, D. J. Edmonds, A. A. Estrada, *Angew. Chem. Int. Ed.* **2009**, *121*, 670 - 732; (b) K. C. Nicolaou, E. J. Sorenson, in *Classics in Total Synthesis*, WILEY-VCH: Weinheim, Germany, **1996**; (c) K. C. Nicolaou, S. A. Snyder, in *Classics in Total Synthesis II*, WILEY-VCH: Weinheim, Germany, **2003**.
- [3] T. R. Verhoeven, D. Askin, in *Process for α -C-alkylation of the δ -acyl group on mevinolin and analogs thereof. (Merck & Co., Inc.)*. U.S. Pat. 4,820,850, **1989**.
- [4] T. L. Brown, *Acc. Chem. Res.* **1968**, *1*, 23 - 32.
- [5] (a) H. Dietrich, *Acta Cryst.* **1963**, *16*, 681 - 689; (b) H. Dietrich, *J. Organomet. Chem.* **1981**, *205*, 291 - 299.
- [6] E. Weiss, E. A. C. Lucken, *J. Organomet. Chem.* **1964**, *2*, 197 - 205.
- [7] C. Elschenbroich, in *Organometallics*, WILEY-VCH: Weinheim, Germany, **2006**.
- [8] (a) F. Marsais, P. Granger, G. Quéguiner, *J. Org. Chem.* **1981**, *46*, 4494 - 4497; (b) T. GÜngör, F. Marsais, G. Quéguiner, *J. Organomet. Chem.* **1981**, *215*, 139 - 150.
- [9] M. Hammell, R. Levine, *J. Org. Chem.* **1950**, *15*, 162 - 168.
- [10] G. Stork, L. Maldonado, *J. Am. Chem. Soc.* **1971**, *93*, 5286 - 5287.
- [11] (a) D. Seebach, D. Enders, *Angew. Chem. Int. Ed.* **1972**, *11*, 301 - 302; (b) D. Seebach, D. Enders, *Angew. Chem. Int. Ed.* **1975**, *14*, 15 - 32.
- [12] Y. J. Kim, M. P. Bernstein, A. S. Galiano Roth, F. E. Romesberg, P. G. Williard, D. J. Fuller, A. T. Harrison, D. B. Collum, *J. Org. Chem.* **1991**, *56*, 4435 - 4439.
- [13] N. D. R. Barnett, R. E. Mulvey, W. Clegg, P. A. O'Neil, *J. Am. Chem. Soc.* **1991**, *113*, 8187 - 8188.
- [14] A. Mootz, A. Zinnius, B. Bottcher, *Angew. Chem. Int. Ed.* **1969**, *8*, 378 - 379.
- [15] M. F. Lappert, M. J. Slade, A. Singh, J. L. Atwood, R. D. Rogers, R. Shakir, *J. Am. Chem. Soc.* **1983**, *105*, 302 - 304.
- [16] M. P. Bernstein, F. E. Romesberg, D. J. Fuller, A. T. Harrison, D. B. Collum, Q. Y. Liu, P. G. Williard, *J. Am. Chem. Soc.* **1992**, *114*, 5100 - 5110.
- [17] P. G. Williard, Q. Y. Liu, *J. Am. Chem. Soc.* **1993**, *115*, 3380 - 3381.

- [18] J. F. Remenar, B. L. Lucht, D. Kruglyak, F. E. Romesberg, J. H. Gilchrist, D. B. Collum, *J. Org. Chem.* **1997**, *62*, 5748 - 5754.
- [19] D. R. Armstrong, A. R. Kennedy, R. E. Mulvey, S. D. Robertson, *Chem. Eur. J.* **2011**, *17*, 8820 - 8831.
- [20] (a) R. A. Rennels, A. S. Maliakal, D. B. Collum, *J. Am. Chem. Soc.* **1998**, *120*, 421 - 422; (b) S. T. Chadwick, R. A. Rennels, J. L. Rutherford, D. B. Collum, *J. Am. Chem. Soc.* **2000**, *122*, 8640 - 8647.
- [21] D. B. Collum, *Acc. Chem. Res.* **1995**, *25*, 448 - 454.
- [22] P. Gros, S. Choppin, J. Mathieu, Y. Fort, *J. Org. Chem.* **2002**, *67*, 234 - 237.
- [23] E. Frankland, *Liebigs. Ann. Chem.* **1849**, *71*, 171 - 213.
- [24] S. Reformatsky, *Ber. Dtsch. Chem. Ges.* **1887**, *20*, 1210 - 1211.
- [25] T. T. Curran, *J. Org. Chem.* **1993**, *58*, 6360 - 6363.
- [26] (a) R. W. Lang, B. Schaub, *Tetrahedron Lett.* **1988**, *29*, 2943 - 2946; (b) R. P. Robinson, K. M. Donahue, *J. Org. Chem.* **1992**, *57*, 7309 - 7314.
- [27] J. Dekker, P. H. M. Budzelaar, J. Boersma, G. J. M. Van Der Kerk, A. L. Spek, *Organometallics* **1984**, *3*, 1403 - 1407.
- [28] W. R. Vaughan, S. C. Bernstein, M. E. Lorber, *J. Org. Chem.* **1965**, *30*, 1790 - 1795.
- [29] F. Orsini, F. Pelizzoni, G. Ricca, *Tetrahedron Lett.* **1982**, *23*, 3945 - 3948.
- [30] (a) R. Noyori, M. Kitamura, *Angew. Chem. Int. Ed.* **1991**, *30*, 49 - 69; (b) K. Soai, S. Niwa, *Chem. Rev.* **1992**, *92*, 833 - 856.
- [31] M. Kitamura, S. Suga, K. Kawai, R. Noyori, *J. Am. Chem. Soc.* **1986**, *108*, 6071 - 6072.
- [32] (a) A. Shafi'ee, G. Hite, *J. Med. Chem.* **1969**, *12*, 266 - 270; (b) G. Hite, V. Barouh, H. Dall, D. Patel, *J. Med. Chem.* **1971**, *14*, 834 - 836; (c) P. Müller, P. Nury, G. Bernardinelli, *Eur. J. Org. Chem.* **2001**, 4137 - 4147.
- [33] (a) P. I. Dosa, J. C. Ruble, G. C. Fu, *J. Org. Chem.* **1997**, *62*, 444 - 445; (b) W. S. Huang, L. Pu, *J. Org. Chem.* **1999**, *64*, 4222 - 4223; (c) J. Rudolph, C. Bolm, P. O. Norrby, *J. Am. Chem. Soc.* **2005**, *127*, 1548 - 1552.
- [34] www.sigmaaldrich.com, November 2011.
- [35] J. G. Kim, P. Walsh, *Angew. Chem. Int. Ed.* **2006**, *45*, 4175 - 4178.
- [36] (a) H. E. Simmons, R. D. Smith, *J. Am. Chem. Soc.* **1958**, *80*, 5323 - 5324; (b) H. E. Simmons, R. D. Smith, *J. Am. Chem. Soc.* **1959**, *81*, 4256 - 4264.

- [37] (a) E. P. Blanchard, H. E. Simmons, *J. Am. Chem. Soc.* **1964**, *86*, 1337 - 1347; (b) H. E. Simmons, E. P. Blanchard, R. D. Smith, *J. Am. Chem. Soc.* **1964**, *86*, 1347 - 1356.
- [38] B. Fabisch, T. N. Mitchell, *J. Organomet. Chem.* **1984**, *269*, 219 - 221.
- [39] S. E. Denmark, J. P. Edwards, S. R. Wilson, *J. Am. Chem. Soc.* **1992**, *114*, 2592 - 2602.
- [40] (a) J. H. H. Chan, B. Rickborn, *J. Am. Chem. Soc.* **1968**, *90*, 6406 - 6411; (b) J. A. Staroscik, B. Rickborn, *J. Org. Chem.* **1972**, *37*, 738 - 740.
- [41] H. Shitama, T. Katsuki, *Angew. Chem. Int. Ed.* **2008**, *47*, 2450 - 2453.
- [42] M. L. Hlavinka, J. F. Greco, J. R. Hagadorn, *Chem. Commun.* **2005**, 5304 - 5306.
- [43] W. S. Rees, O. Just, H. Schumann, R. Weimann, *Polyhedron* **1998**, *17*, 1001 - 1004.
- [44] M. L. Hlavinka, J. R. Hagadorn, *Organometallics* **2007**, 4105 - 4108.
- [45] J. A. Wanklyn, *Liebigs. Ann. Chem.* **1858**, *108*, 67 - 79.
- [46] G. Wittig, F. J. Meyer, G. Lange, *Liebigs. Ann. Chem.* **1951**, *571*, 167 - 201.
- [47] (a) M. Schlosser, in *Organometallics in Synthesis, 2nd Ed.*, Wiley: Chichester, U.K., **2002**; (b) J. Clayden, in *Organolithiums: Selectivity for Synthesis, Vol. 23*, Tetrahedron Organic Chemistry Series; Pergamon, Elsevier Science: Oxford, U.K., **2002**.
- [48] L. S. Bennie, W. J. Kerr, M. Middleditch, A. J. B. Watson, *Chem. Commun.* **2011**, *47*, 2264 - 2266.
- [49] M. Schlosser, G. Katsoulos, S. Takagishi, *Synlett* **1990**, 747 - 748.
- [50] (a) J. D. Roberts, D. Y. Curtin, *J. Am. Chem. Soc.* **1946**, *68*, 1658 - 1660; (b) D. A. Shirley, J. R. Johnson, J. P. Hendrix, *J. Organomet. Chem.* **1968**, *11*, 209 - 216.
- [51] M. Schlosser, J. Porwisiak, F. Mongin, *Tetrahedron* **1998**, *54*, 895 - 900.
- [52] M. D. Rausch, D. J. Ciappenelli, *J. Organomet. Chem.* **1967**, *10*, 127 - 136.
- [53] M. Schlosser, H. C. Jung, S. Takagishi, *Tetrahedron* **1990**, *46*, 5633 - 5648.
- [54] M. Schlosser, *J. Organomet. Chem.* **1967**, *8*, 9 - 16.
- [55] L. Lochmann, J. Trekoval, *J. Organomet. Chem.* **1979**, *179*, 123 - 132.
- [56] A. R. Kennedy, J. G. MacLellan, R. E. Mulvey, *Angew. Chem. Int. Ed.* **2001**, *40*, 3245 - 3247.
- [57] P. Fleming, D. F. O'Shea, *J. Am. Chem. Soc.* **2011**, *133*, 1698 - 1701.

- [58] P. Caubère, *Chem. Rev.* **1993**, *93*, 2317 - 2334.
- [59] (a) P. Gros, Y. Fort, *Eur. J. Org. Chem.* **2002**, 3375 - 3383; (b) P. Gros, Y. Fort, *Eur. J. Org. Chem.* **2009**, 4199 - 4209.
- [60] (a) A. Thurkauf, J. Yuan, X. Chen, X. S. He, J. W. F. Wasley, A. Hutchison, K. H. Woodruff, R. Meade, D. C. Hoffman, H. Donovan, D. K. Jones-Hertzog, *J. Med. Chem.* **1997**, *40*, 1 - 3; (b) M. W. Holladay, J. T. Wasicak, N. H. Lin, Y. He, K. B. Ryther, A. W. Bannon, M. J. Buckley, D. J. B. Kim, M. W. Decker, D. J. Anderson, J. E. Campbell, T. A. Kuntzweiler, D. L. Donnelly-Roberts, M. Piattoni-Kaplan, C. A. Briggs, M. Williams, S. P. Arneric, *J. Med. Chem.* **1998**, *41*, 407 - 412.
- [61] (a) T. Kambara, T. Koshida, N. Saito, I. Kuwajima, K. Kubata, T. Yamamoto, *Chem. Lett.* **1992**, 583 - 586; (b) H. Le Bozec, T. Renouard, *Eur. J. Inorg. Chem.* **2000**, 229 - 239.
- [62] (a) M. J. Cook, A. P. Lewis, G. S. C. McAuliffe, V. Skarda, A. J. Thomson, J. L. Glasper, D. J. Robbins, *J. Chem. Soc., Perkin. Trans. 2* **1984**, 1293 - 1301; (b) B. O'Regan, M. Grätzel, *Nature* **1991**, *353*, 737 - 740.
- [63] (a) C. S. Giam, J. L. Stout, *J. Chem. Soc., Chem. Commun.* **1969**, 142 - 144; (b) C. S. Giam, E. E. Knaus, F. M. Pasutto, *J. Org. Chem.* **1974**, *39*, 3565 - 3568.
- [64] (a) F. Marsais, G. Quéguiner, *Tetrahedron* **1983**, *39*, 2009 - 2021; (b) A. S. Galiano Roth, Y. J. Kim, J. H. Gilchrist, A. T. Harrison, D. J. Fuller, D. B. Collum, *J. Am. Chem. Soc.* **1991**, *113*, 5053 - 5055; (c) F. E. Romesberg, D. B. Collum, *J. Am. Chem. Soc.* **1994**, *116*, 9187 - 9197; (d) P. L. Hall, J. H. Gilchrist, D. B. Collum, *J. Am. Chem. Soc.* **1991**, *113*, 9571 - 9574; (e) N. Plé, A. Turck, P. Martin, S. Barbey, G. Quéguiner, *Tetrahedron Lett.* **1993**, *34*, 1605 - 1608.
- [65] P. Gros, Y. Fort, G. Quéguiner, P. Caubère, *Tetrahedron Lett.* **1995**, *36*, 4791 - 4794.
- [66] D. L. Comins, D. H. La Munyon, *Tetrahedron Lett.* **1988**, *29*, 773 - 776.
- [67] F. Marsais, G. Le Nard, G. Quéguiner, *Synthesis* **1982**, 235 - 237.
- [68] D. L. Comins, S. P. Joseph, R. R. Goerhing, *J. Am. Chem. Soc.* **1994**, *116*, 4719 - 4728.
- [69] F. Trécourt, M. Mallet, O. Mongin, B. Gervais, G. Quéguiner, *Tetrahedron* **1993**, *49*, 8373 - 8380.
- [70] A. Krasovskiy, P. Knochel, *Angew. Chem. Int. Ed.* **2004**, *43*, 3333 - 3336.

- [71] H. Ren, A. Krasovskiy, P. Knochel, *Org. Lett.*, **2004**, *6*, 4215 - 4217.
- [72] C. R. Hauser, H. J. Walker, *J. Am. Chem. Soc.* **1947**, *69*, 295 - 297.
- [73] (a) P. E. Eaton, C. H. Lee, Y. Xiong, *J. Am. Chem. Soc.* **1989**, *111*, 8016 - 8018; (b) P. E. Eaton, Y. Xiong, R. Gilardi, *J. Am. Chem. Soc.* **1993**, *115*, 10195 - 10202.
- [74] (a) Y. Kondo, A. Yoshida, T. Sakamoto, *J. Chem. Soc., Perkin. Trans. 1* **1996**, 2331 - 2332; (b) M. Shilai, Y. Kondo, T. Sakamoto, *J. Chem. Soc., Perkin. Trans. 1* **2001**, 442 - 444.
- [75] W. Schlecker, A. Huth, E. Ottow, J. Mulzer, *Synthesis* **1995**, 1225 - 1227.
- [76] (a) A. Krasovskiy, V. Krasovskaya, P. Knochel, *Angew. Chem. Int. Ed.* **2006**, *45*, 2958 - 2961; (b) W. Lin, O. Baron, P. Knochel, *Org. Lett.*, **2006**, *8*, 5673 - 5676; (c) M. Mosrin, P. Knochel, *Org. Lett.*, **2008**, *10*, 2497 - 2500; (d) M. Mosrin, N. Boudet, P. Knochel, *Org. Biomol. Chem.*, **2008**, *6*, 3237 - 3239.
- [77] G. Monzon, P. Knochel, *Synlett* **2010**, 304 - 308.
- [78] P. García-Álvarez, D. V. Graham, E. Hevia, A. R. Kennedy, J. Klett, R. E. Mulvey, C. T. O'Hara, S. Weatherstone, *Angew. Chem. Int. Ed.* **2008**, *47*, 8079 - 8081.
- [79] (a) S. H. Wunderlich, P. Knochel, *Angew. Chem. Int. Ed.* **2007**, *46*, 7685 - 7688; (b) S. H. Wunderlich, P. Knochel, *Org. Lett.*, **2008**, *10*, 4705 - 4707; (c) Z. Dong, G. C. Clososki, S. H. Wunderlich, A. Unsinn, J. Li, P. Knochel, *Chem. Eur. J.* **2009**, *15*, 457 - 468; (d) M. Mosrin, P. Knochel, *Chem. Eur. J.* **2009**, *15*, 1468 - 1477; (e) S. H. Wunderlich, C. J. Rohbogner, A. Unsinn, P. Knochel, *Org. Process Res. Dev.*, **2010**, *14*, 339 - 345.
- [80] S. H. Wunderlich, P. Knochel, *Chem. Commun.* **2008**, 6387 - 6389.
- [81] (a) M. Mosrin, P. Knochel, *Org. Lett.*, **2009**, *11*, 1837 - 1840; (b) M. Mosrin, G. Monzon, T. Bresser, P. Knochel, *Chem. Commun.* **2009**, 5615 - 5617; (c) T. Bresser, M. Mosrin, G. Monzon, P. Knochel, *J. Org. Chem.* **2010**, *75*, 4686 - 4695; (d) T. Bresser, P. Knochel, *Angew. Chem. Int. Ed.* **2011**, *50*, 1914 - 1917.
- [82] T. Bresser, G. Monzon, M. Mosrin, P. Knochel, *Org. Process Res. Dev.*, **2010**, *14*, 1299 - 1303.
- [83] (a) E. Negishi, *Acc. Chem. Res.* **1982**, *15*, 340 - 348; (b) E. Negishi, *Bull. Chem. Soc. Jpn.* **2007**, *80*, 233 - 257; (c) E. Negishi, *Angew. Chem. Int. Ed.* **2011**, *50*, 6738 - 6764.

- [84] (a) C. T. O'Hara, in *Organometallic Chemistry, Vol. 37*, Royal Society of Chemistry: Specialist Periodical Reports, **2011**, pp. 1 - 26; (b) B. Haag, M. Mosrin, H. Ila, V. Malakhov, P. Knochel, *Angew. Chem. Int. Ed.* **2011**, *50*, 9794 - 9824.
- [85] M. Jaric, B. M. Haag, S. M. Manolikakes, P. Knochel, *Org. Lett.*, **2011**, *13*, 2306 - 2309.
- [86] P. Knochel, P. Jones, in *Organozinc Reagents: A Practical Approach*, Oxford University Press, **1999**.
- [87] (a) Y. Kondo, N. Takazawa, C. Yamazaki, T. Sakamoto, *J. Org. Chem.* **1994**, *59*, 4717 - 4718; (b) Y. Kondo, N. Fujinami, M. Uchiyama, T. Sakamoto, *J. Chem. Soc., Perkin. Trans. 1* **1997**, 799 - 800; (c) M. Uchiyama, M. Koike, M. Kameda, Y. Kondo, T. Sakamoto, *J. Am. Chem. Soc.* **1996**, *118*, 8733 - 8734; (d) M. Uchiyama, M. Kameda, O. Mishima, N. Yokoyama, M. Koike, Y. Kondo, T. Sakamoto, *J. Am. Chem. Soc.* **1998**, *120*, 4934 - 4946.
- [88] Y. Kondo, M. Shilai, M. Uchiyama, T. Sakamoto, *J. Am. Chem. Soc.* **1999**, *121*, 3539 - 3540.
- [89] (a) M. Uchiyama, T. Miyoshi, Y. Kajihara, T. Sakamoto, Y. Otani, T. Ohwada, Y. Kondo, *J. Am. Chem. Soc.* **2002**, *124*, 8514 - 8515; (b) M. Uchiyama, Y. Kobayashi, T. Furuyama, S. Nakamura, Y. Kajihara, T. Miyoshi, T. Sakamoto, Y. Kondo, K. Morokuma, *J. Am. Chem. Soc.* **2008**, *130*, 472 - 480.
- [90] W. E. Parham, C. E. Bradcher, *Acc. Chem. Res.* **1982**, *15*, 300 - 305.
- [91] F. Gohier, J. Mortier, *J. Org. Chem.* **2003**, *68*, 2030 - 2033.
- [92] M. Uchiyama, Y. Matsumoto, S. Usui, Y. Hashimoto, K. Morokuma, *Angew. Chem. Int. Ed.* **2007**, *46*, 926 - 929.
- [93] T. Imahori, M. Uchiyama, T. Sakamoto, Y. Kondo, *Chem. Commun.* **2001**, 2450 - 2451.
- [94] (a) R. E. Mulvey, *Organometallics* **2006**, *25*, 1060 - 1075; (b) R. E. Mulvey, F. Mongin, M. Uchiyama, Y. Kondo, *Angew. Chem. Int. Ed.* **2007**, *46*, 3802 - 3824; (c) R. E. Mulvey, *Acc. Chem. Res.* **2009**, *42*, 743 - 755.
- [95] P. C. Andrikopoulos, D. R. Armstrong, H. R. L. Barley, W. Clegg, S. H. Dale, E. Hevia, G. W. Honeyman, A. R. Kennedy, R. E. Mulvey, *J. Am. Chem. Soc.* **2005**, *127*, 6184 - 6185.
- [96] W. Clegg, S. H. Dale, E. Hevia, L. M. Hogg, G. W. Honeyman, R. E. Mulvey, C. T. O'Hara, *Angew. Chem. Int. Ed.* **2006**, *45*, 6548 - 6550.

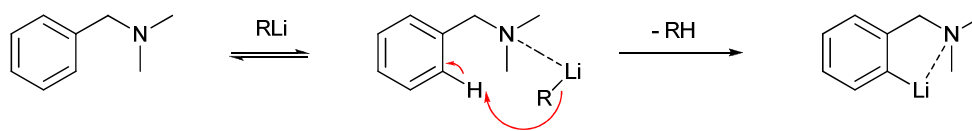
- [97] D. R. Armstrong, W. Clegg, S. H. Dale, D. V. Graham, E. Hevia, L. M. Hogg, G. W. Honeyman, A. R. Kennedy, R. E. Mulvey, *Chem. Commun.* **2007**, 598 - 600.
- [98] (a) J. Clayden, S. A. Yasin, *New J. Chem.* **2002**, 26, 191 - 192; (b) A. Maercker, *Angew. Chem. Int. Ed.* **1987**, 26, 972 - 989.
- [99] R. B. Bates, L. M. Kroposki, D. E. Potter, *J. Org. Chem.* **1972**, 37, 560 - 562.
- [100] A. R. Kennedy, J. Klett, R. E. Mulvey, D. S. Wright, *Science* **2009**, 326, 706 - 708.

Chapter 2: Regioselective Deprotonation and the Use of Synergic Reagents

2.1) Directed-ortho-Metallation

Organic synthesis and the production of fine chemicals rely heavily on the controlled functionalisation of aromatic molecules.^[1] Acknowledging, the abundance of C-H bonds in many common aromatic substrates, selective manipulation of one C-H bond which does not impinge upon the residing infrastructure of the molecule would represent an enticing synthetic blueprint. Directed-*ortho*-Metallation (DoM) is a special sub-category of deprotonative metallation. Defined as a metallation (nearly always lithiation) of an aromatic ring directed towards a position adjacent (*ortho*) to an activating heteroatom containing functional group, it is widely regarded as a rival if not superior methodology to electrophilic aromatic substitution for constructing regiospecifically substituted aromatic rings.^[2] On the back of the landmark *ortho*-lithiation of anisole,^[3] the number of accessible directed metallating groups (DMG) has multiplied and DoM chemistry has been the topic of exhaustive research.^[4]

The mechanisms involved in the deprotonation of a substituted aromatic ring by an organolithium reagent are the subject of much conjecture but for the most part, there are two contributory factors behind the success of the directed deprotonation. DoM is reliant on the substituent, in the main the heteroatom, welcoming the alkyllithium with a coordination point thus enhancing reactivity around the coordination site and directing the regioselectivity. For example, in the case of *N,N*-dimethylbenzylamine, the aromatic protons are no more acidic than those of benzene, yet the amine is deprotonated rapidly and regioselectively at the 2-position, closest to the DMG (Scheme 2.1).^[5]



Scheme 2.1: Coordination driven *ortho*-lithiation of *N,N*-dimethylbenzylamine.

For strong DMGs, it is surmised that coordination between substrate and the alkyllithium, feasibly evoking deaggregation of the alkyllithium, heralds the first step en route to lithiation; albeit, the capacity of the DMG to acidify protons through the inductive effect is also a key contributory feature. Where coordination to the heteroatom is electronically or geometrically impossible, it is the effects of acidity which direct the lithiation. The base utilised in the lithiation can influence the balance of coordination and acidity. Illustrating the point in a general sense, coordination to a basic solvent depresses the Lewis acidity of the alkyllithium, thus the inclination to be driven by coordination is reduced and acidity prospers as the assertive factor (Figure 2.1).^[6]

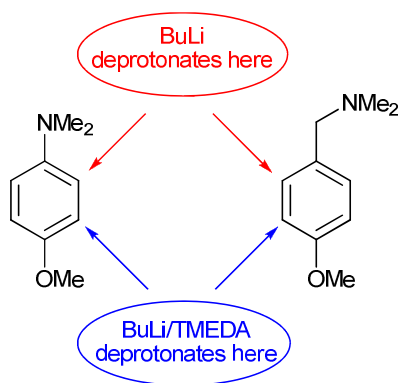
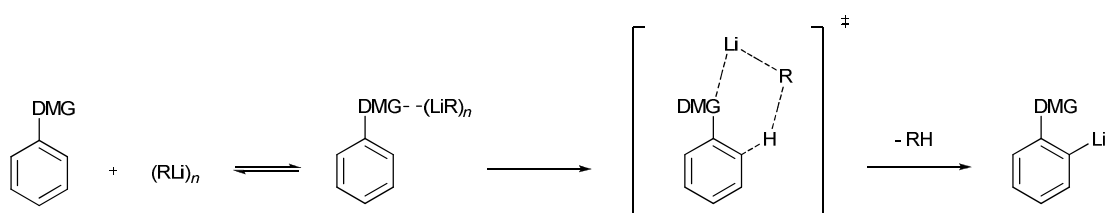


Figure 2.1: Preference of the lithiating reagent in the coordination versus acidity competition within DoM chemistry.

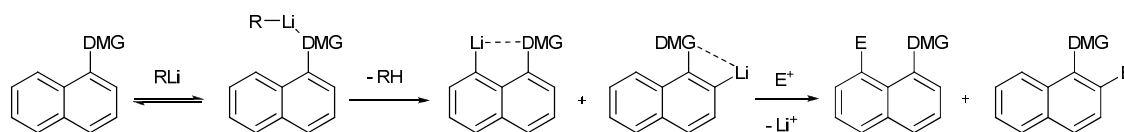
The interpretation of a two-step process, in which the formation of a pre-lithiation complex brings reactive groups into proximity for directed deprotonation, was addressed by Snieckus and Beak in an illuminating review in 2004.^[7] Termed the

“Complex-Induced Proximity Effect (CIPE)” the concept can be adopted to account for prevalent classical reactions where strong analogies exist for complex formation (Scheme 2.2); however, particularly exciting is the potential application of CIPE in synthetic design and in thinking beyond thermodynamic acidity whether pre-complexation could lead to synthetic methodologies for more remote functionalisation on the same or even alternative aryl rings.



Scheme 2.2: Deprotonation of an organic substrate with an organolithium reagent, illustrating the Complex-Induced Proximity Effect.

As far as DoM and synthetic utility goes, it is evident that aromatics carrying electron-withdrawing substituents are more readily lithiated than those which acidify proximate protons weakly or not at all. Admittedly, while steric considerations will play a role, the increased emphasis on acidity is portrayed in the different regioselectivities encountered in a series of *peri*- and *ortho*-lithiations of 1-substituted naphthalenes (Table 2.1).^[8] A DMG that advocates coordination can champion lithiation at either the *peri* or the *ortho* position; whereas on the contrary, a DMG that facilitates lithiation by acidifying neighbouring protons can only promote lithiation at the *ortho* position. En masse, the efficacious DMGs tend to blend the basic properties desired for good coordination to lithium and the acidic properties required for fast, efficient and selective deprotonation.

Table 2.1: Comparison of isomeric *ortho*- and *peri*-products, following lithiation of 1-substituted naphthalenes and reaction with electrophiles.

DMG	Conditions	E ⁺	Yield <i>peri</i> (%)	Yield <i>ortho</i> (%)
CH ₂ NMe ₂	BuLi, Et ₂ O, hexane, -78 °C	Ph ₂ CO	58	0
NMe ₂	BuLi, Et ₂ O, 20 °C	DMF	76	0
CH(OMe) ₂	<i>t</i> BuLi, Et ₂ O	MeI	27	13
OCONR ₂	<i>s</i> BuLi, TMEDA, THF, -78 °C	MeI	0	90
CONR ₂	<i>s</i> BuLi, TMEDA, THF, -78 °C	various	0	76-93

A primary aim of this PhD research project was to further develop and extend a new concept within DoM chemistry. The DoM process is extremely pertinent in organolithium chemistry with lithiation of scores of aromatic substrates well documented; however, the numbers are understandably considerably less in terms of zincations. Conventionally, zinc reagents fail in DoM chemistry as a consequence of their weak kinetic basicity but efforts to extend the Alkali-Metal Mediated Zincation (AMMZn) methodology to *ortho*-deprotonation are addressed in the ensuing pages.

2.2) AMMZn of Benzamides and Phenyl O-Carbamate

The DoM reaction hinges on a heteroatom substituent with proficient DMG capability, for blending the basic properties required for proficient metal coordination and the acidic properties imperative for C-H deprotonation. Foremost in their efficiency are

tertiary amide and *O*-carbamate DMGs (Figure 2.2),^[4d, 9] their qualitative DMG power derives from the complementary acid-base virtues of a highly basic heteroatom and an electron-withdrawing acidifying effect. For all that, a major complication with such DMGs is their inherent electrophilicity which leaves them susceptible to hostile nucleophilic attacks from metallating agents inducing undesired side reactions and complicating synthetic utility.

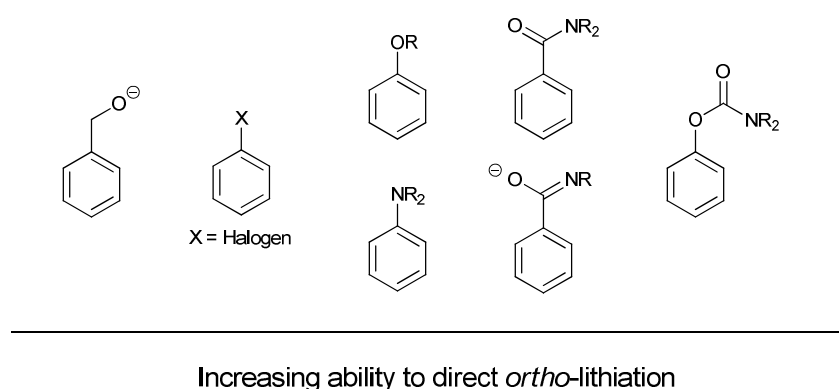
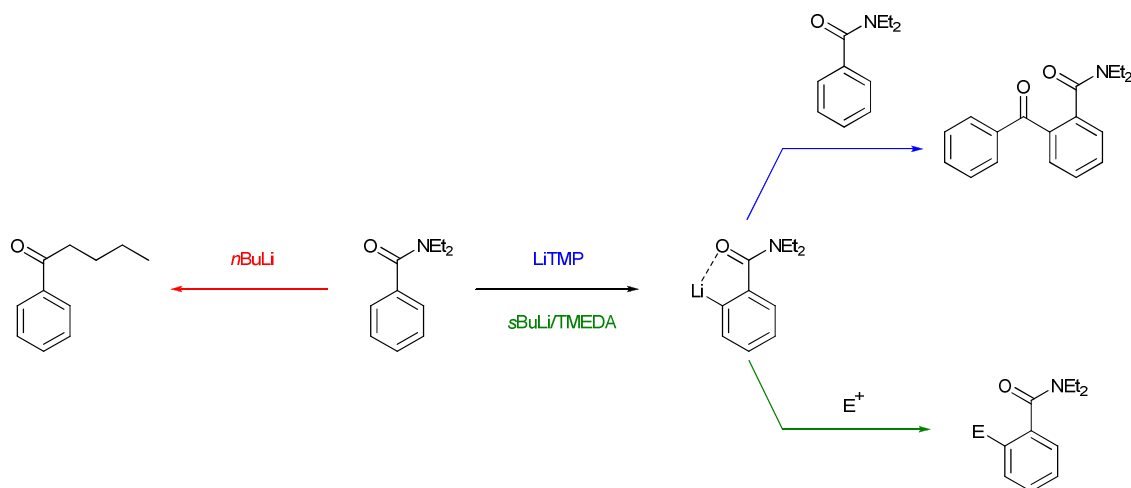


Figure 2.2: Common metallation directors and their relative directing ability.

Having previously accomplished chemo- and regioselective zincation of several aromatic and heteroaromatic substrates, the sodium TMP-zincate [(TMEDA)Na(μ -TMP)(μ -*t*Bu)Zn(*t*Bu)] (**1**) was the AMMZn reagent of choice for the reactions reported herein. Under ambient temperature conditions three different electron-rich aromatic substrates, *N,N*-diethylbenzamide, *N,N*-diethyl-3-methoxybenzamide and *N,N*-diethyl phenyl *O*-carbamate were cleanly zincated *ortho* to the DMG (in between both substituents in the second case) in a non-polar hexane medium.

The metallation chemistry of *N,N*-diethylbenzamide has been painstakingly explored in pursuit of the optimal procedure for *ortho*-deprotonation (Scheme 2.3).^[4c] As a prelude, Hauser disclosed that employing *n*BuLi led to attack at the carbonyl group of a dialkyl amide to give ketone products by reference to previous work and showed that by charge

deactivation *N*-methylbenzamide undergoes the DoM reaction with excess *n*BuLi.^[10] Resultant studies by Beak acknowledged that *N,N*-diethylbenzamide may be metallated by engaging the hindered, non-nucleophilic reagent LiTMP but only incomplete deprotonation is achieved and undesirably the *ortho*-lithio intermediate spontaneously attacks another molecule of starting material to give a benzophenone product.^[11] However, in salient experiments that triggered extensive synthetic application,^[2a, 2b, 12] Beak discovered that by adopting the *s*BuLi/TMEDA combination, the diethylbenzamide can be efficiently *ortho*-metallated in THF.^[13] Although this reaction necessitates subambient temperature conditions (-78 °C), it has found application in industrial practice on a very large scale.^[2a, 2b] In contrast, and a harbinger of potential future application, sodium TMP-zincate **1** with special synergic chemistry may be harnessed to perform DoM of *N,N*-diethylbenzamide at room temperature to produce the heterotri-anion zincate [(TMEDA)Na(μ-TMP){μ-2-(1-C(O)NEt₂)-C₆H₄}Zn(*t*Bu)] (**2**) in a yield of 54% of isolated crystalline material.



Scheme 2.3: Treatment of *N,N*-diethylbenzamide with common organolithium reagents.

Successful crystal growth bestows a precious insight into the skeletal architecture of the metallated intermediates. The molecular structure of **2** (Figure 2.3) conserves the

“{(TMEDA)Na(μ -TMP)Zn(*t*Bu)}” infrastructure of reactant zincate **1** with the *ortho*-metallated benzamide furnishing a central seven-membered, five-element (NaZnCCCO) ring by bridging asymmetrically through its carbonyl oxygen and *ortho*-carbon atoms. Encapsulated as a contact ion-pair, **2** can be compared to the cognate *ortho*-zincated *N,N*-diisopropylbenzamide complex [(TMEDA)Na(μ -TMP){ μ -2-(1-C(O)N*i*Pr₂)-C₆H₄}Zn(*t*Bu)] previously reported by the Mulvey group.^[14]

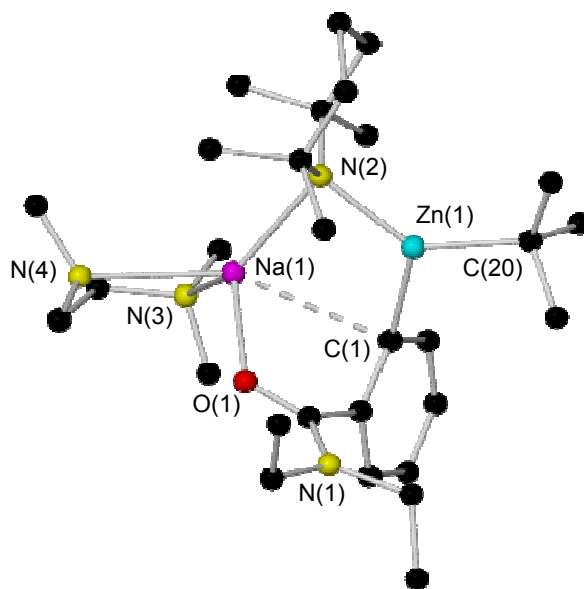
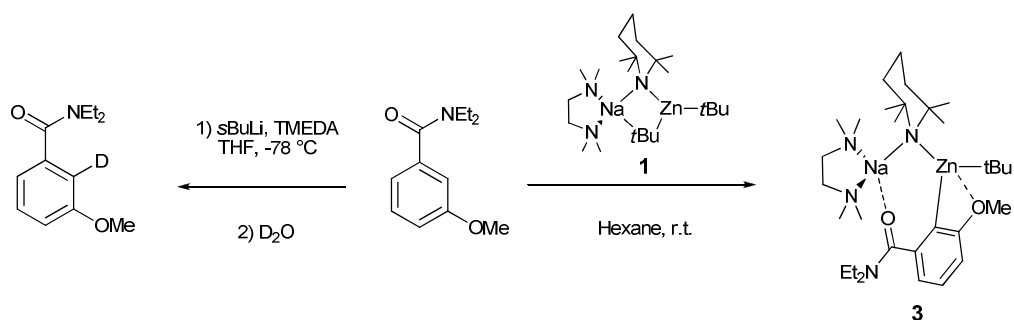


Figure 2.3: Molecular structure of **2** with selective atom labelling. Hydrogen atoms omitted for clarity. The long Na \cdots C_{ortho} contact is highlighted by a dashed line. Selected bond lengths (Å) and angles (deg): Zn(1)-N(2) 2.0047(12), Zn(1)-C(1) 2.0637(17), Zn(1)-C(20) 2.0434(16), Na(1) \cdots C(1) 2.9250(16), Na(1)-O(1) 2.2855(12), Na(1)-N(2) 2.4445(14); N(2)-Zn(1)-C(20) 132.11(6), N(2)-Zn(1)-C(1) 116.07(6), C(20)-Zn(1)-C(1) 111.59(6), Na(1)-N(2)-Zn(1) 88.08(5), O(1)-Na(1)-N(2) 110.20(5).

Perhaps, unsurprisingly the bond lengths and angles at the hub of each structure are immune to the change in alkyl group from ethyl to isopropyl. For example, the Zn-C_{aryl} and Na-O bond lengths in the foregoing isopropyl substituted benzamide complex [2.077(3) and 2.258(2) Å, respectively] are in good agreement with the Zn(1)-C(1) [2.0637(17) Å] and Na(1)-O(1) [2.2855(12) Å] values found for **2**. Significantly, defining the metallation as a zincation, zinc fashions a short, strong σ -bond with the

deprotonated carbon while the alkali-metal is remote from the carbanion [Na(1)···C(1) 2.9250(16) Å]. This distance is longer than that found for PMDETA-solvated phenylsodium [(PMDETA)NaPh]₂^[15] (mean Na···C bond length of 2.669 Å) but within the range of π -arene···Na contacts present in the sodium phosphanide [(TMEDA)Na[P(C₆H₄-2-NMe₂){CH(SiMe₃)₂}] of 2.8792(14) and 3.0072(14) Å.^[16]

Following the accomplishment of direct zincation of the benzamide, the metallation ability of the synergic base towards substituted benzamides was tested. In lithiation DoM chemistry, the electron-donating methoxy substituent can direct the deprotonation through a combined coordination-inductive effect of the oxygen atom. Upon treatment with the synergic but bulkier base **1**, direct zincation of *N*, *N*-diethyl-3-methoxybenzamide proceeds in between the methoxy and tertiary amide substituents akin to when an organolithium reagent is administered (Scheme 2.4);^[13] intimating that the metallation regioselectivity is not overly sensitive to appended substituents.



Scheme 2.4: *Ortho*-metallation of *N*, *N*-diethyl-3-methoxybenzamide employing *s*BuLi/TMEDA or sodium TMP-zincate **1.**

Adopting the synthetic protocol which led to the preparation of **2**, *N*, *N*-diethyl-3-methoxybenzamide was subjected to an equimolar quantity of bimetallic base **1** in hexane solution. The successful growth of crystalline material granted an X-ray crystallographic analysis, elucidating the new triheteroleptic alkyl-aryl-amido zincate

[(TMEDA)Na(μ -TMP){ μ -2-(1-C(O)NEt₂)(3-OMe)-C₆H₃}Zn(*t*Bu)] (**3**) with the position of zincation between the two activating aryl substituents (Figure 2.4).

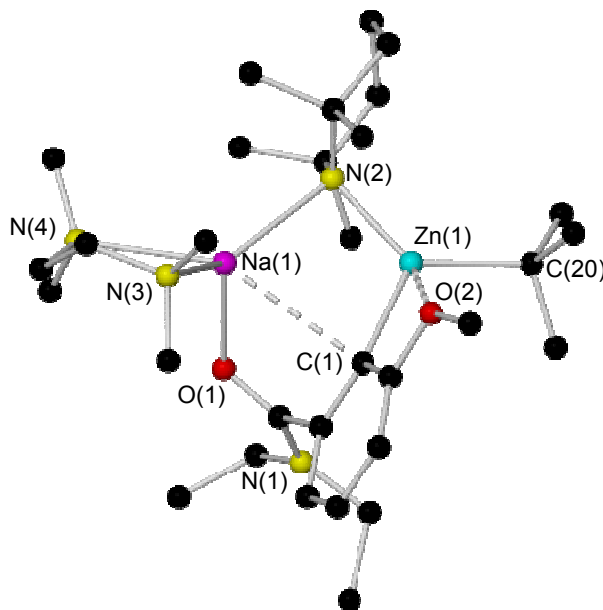
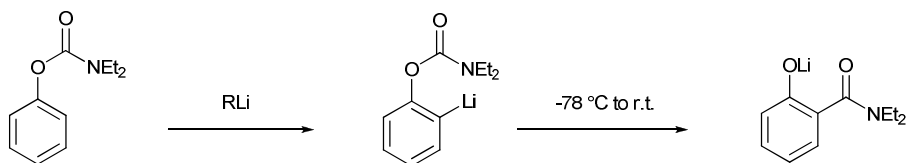


Figure 2.4: Molecular structure of **3** with selective atom labelling. Hydrogen atoms are omitted for clarity. The long Na \cdots C_{ortho} and Zn \cdots OMe contacts are highlighted by dashed lines. Selected bond lengths (Å) and angles (deg): Zn(1)-N(2) 2.0170(11), Zn(1)-C(1) 2.0827(14), Zn(1)-C(20) 2.0531(15), Zn(1) \cdots O(2) 2.8625(10), Na(1) \cdots C(1) 2.9548(14), Na(1)-O(1) 2.2722(11), Na(1)-N(2) 2.4370(13); N(2)-Zn(1)-C(20) 129.86(6), N(2)-Zn(1)-C(1) 114.35(5), C(20)-Zn(1)-C(1) 115.80(6), Na(1)-N(2)-Zn(1) 90.68(5), O(2)-Na(1)-N(2) 105.72(4).

Reminiscent of **2**, the molecular structure of **3** resides a highly puckered seven-membered ring at its core; with its component Na-N_{TMP} and Na-O bond lengths [2.4370(13) and 2.2722(11) Å, respectively] concurrent with those in the diethylamide complex **2** [2.4445(14) and 2.2855(12) Å]. The distorted trigonal-planar geometry of Zn apparent in **2** is also evident in **3**. However, the introduction of the ancillary methoxy substituent delivers the distinguishing feature of **3** for it charts a long Zn \cdots O interaction [2.8625(10) Å]; acutely elongated in comparison to a series of alkylzinc fencholates^[17] (bond distances ranging from 2.15 to 2.40 Å) and in calixarene complexes prepared by Raston^[18] and Vigalok^[19] [2.222(7); and 2.1944(16); 2.391(2);

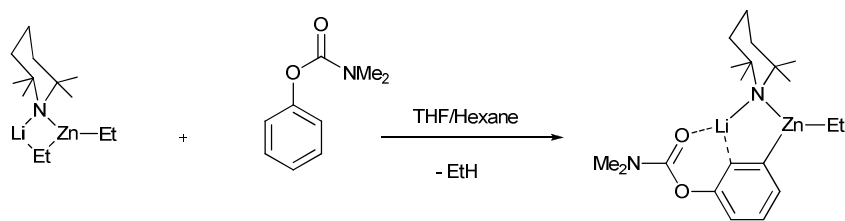
2.406(2) Å]. These comparisons suggest the long Zn \cdots O bond is an artefact of the proximity of the OMe group to the zincated C(1) centre and is not significant to the stability of the complex.

Aryl dialkylcarbamates can lay a claim to the title of virtuoso metallation director; all the same, to guarantee maximum efficacy, reaction conditions have to be stringently controlled for it to perform. Once *ortho*-lithiated, *N,N*-dimethyl phenyl *O*-carbamates are habitually unstable and undergo facile rearrangement by a carbamoyl transfer mechanism known as the “anionic *ortho*-Fries rearrangement”.^[4d, 9] While this may be suppressed by employing the more sterically hindered diethylcarbamates at -78 °C, carbamoyl rearrangement to salicylamides materialises slowly upon warming to higher temperatures (Scheme 2.5).^[20]



Scheme 2.5: Spontaneous anionic Fries rearrangement of the *ortho*-lithio aryl dialkylcarbamate.

In 2008, Uchiyama and Wheatley reported the first structural evidence for the *ortho*-metallation of aryl dialkyl *O*-carbamates that resist anionic Fries rearrangement at room temperature.^[21] Treatment of *N,N*-dimethyl phenyl *O*-carbamate with an *in situ* mixture of *n*BuLi, TMP(H) and Et₂Zn afforded dimeric, *ortho*-zincated [(C₆H₄{OC(O)NMe₂}-{Zn(μ-TMP)Et}-2)Li]₂ (Scheme 2.6). Simultaneously, the resistance of the intermediate zincate to rearrangement was mirrored by the near-quantitative conversion of the *N,N*-diethyl counterpart, upon iodination to the 2-iodophenyl derivative; although no metallated intermediates were isolated prior to electrophilic quench with iodine and an excess of zincate reagent was deployed to encourage higher yields.



Scheme 2.6: The clean directed *ortho*-metallation of *N, N*-dimethyl phenyl *O*-carbamate utilising a lithium TMP-zincate.

Coming back to our own studies with sodium as the alkali-metal, *N, N*-diethyl phenyl *O*-carbamate was treated with heterobimetallic base **1** at ambient temperature to scrutinise the propensity for Fries rearrangement. Storage of the reaction vessel in a refrigerator at 5 °C deposited colourless crystals with X-ray analysis affirming *ortho*-deprotonation of the aryl carbamate manifested in the formation of another triheteroleptic complex [(TMEDA)Na(μ -TMP){ μ -2-(1-OC(O)NEt₂)-C₆H₄}Zn(*t*Bu)] (**4**) (Figure 2.5).

Emanating from the inclusion of the additional oxygen atom; structure **4** embodies a larger eight-membered (NaNZnCCOCO) interior ring system. A feature of the mono-zincated benzene complex [(TMEDA)Na(μ -TMP)(μ -Ph)Zn(*t*Bu)]^[22] and the *meta*- and *para*-deprotonated toluene regioisomers [(TMEDA)Na(μ -TMP)(μ -C₆H₄Me)Zn(*t*Bu)]^[23] is the manner in which the Zn centre lies almost coplanar to the arene ring [deviation from arene plane of 0.213(4), 0.19(3) and 0.18(2) Å, respectively], while in contrast the Na atom adopts a more perpendicular disposition [correspondingly deviations of 2.6604(14), 2.6830(14) and 2.7006(14) Å] engaging more with the π -system of the aromatic ring. In the series of complexes **2**, **3** and **4**, the increased functionality of the organic substrate, with respect to benzene and toluene, compels the alkali-metal to pursue the oxygen heteroatom (as opposed to the more sterically shielded π -system) to satisfy its coordinative/electronic unsaturation. Henceforth, complexes **2** and **3** take

possession of a highly strained seven-membered interior ring and with it comes a minor divergence away from the plane of the aryl ring for the Zn atom [0.5165(2) and 0.3913(2) Å for **2** and **3**, respectively]. However, increasing the size of the internal ring, as in **4** with the inclusion of the additional oxygen atom, reduces the strain involved and the Zn atom re-aligns closer to coplanarity with the arene ring [deviation of only 0.2800(2) Å], while Na still bonds to the oxygen atom of the carbonyl group.

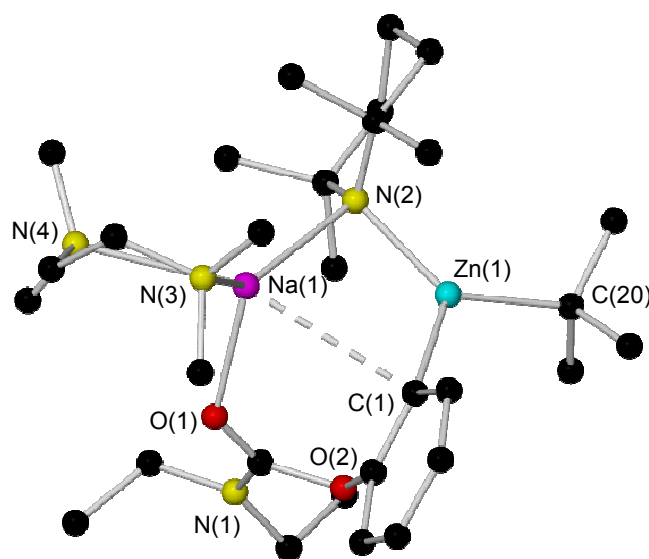


Figure 2.5: Molecular structure of **4** with selective atom labelling. Hydrogen atoms and minor disordered component of TMEDA are omitted for clarity. The long Na \cdots C_{ortho} contact is highlighted by a dashed line. Selected bond lengths (Å) and angles (deg): Zn(1)-N(2) 2.0112(11), Zn(1)-C(1) 2.0581(13), Zn(1)-C(20) 2.0426(13), Na(1) \cdots C(1) 3.0438(14), Na(1)-O(1) 2.2728(10), Na(1)-N(2) 2.4741(11); N(2)-Zn(1)-C(20) 132.26(5), N(2)-Zn(1)-C(1) 113.56(5), C(20)-Zn(1)-C(1) 113.99(5), Na(1)-N(2)-Zn(1) 92.98(4), O(1)-Na(1)-N(2) 111.69(4).

A consequential search of the Cambridge Structural Database,^[24] declared that **4** represents the first example of a crystallographically characterised monomeric *ortho*-zincated (or indeed *ortho*-metallated) phenyl dialkyl *O*-carbamate to be prepared by direct metallation.^[25] Accordingly, Uchiyama's aforementioned dimer

$[(C_6H_4\{OC(O)NMe_2\}-\{Zn(\mu-TMP)Et\}-2)Li]_2$ bears the most striking resemblance to complex **4** and emphasises the offshoot of heightened sterics on the constitution of the resulting structure. Supplementing the aggregation state change (due to no donor uptake in the Li reaction), the effect of moving from Li to the larger Na is a protracted Na(1)-N(2)-Zn(1) bond angle of $92.98(4)^\circ$ (in contrast to a Li-N-Zn angle of 88.6°) and this fact is duly reflected in the bond distance between the alkali-metal and the carbamoyl O-centre [Li-O 2.003(8) and Na(1)-O(1) 2.2728(10) Å]. Moreover, the bulkier *t*Bu group in **4** induces a longer terminal zinc-alkyl bond [2.0426(13) Å] when matched to the related Zn-Et bond [2.008(5) Å]. Finally, as may be forecast the transannular Na(1)⋯C(1) distance in **4** [3.0438(14) Å] is longer than the reciprocal interaction in complexes **2** and **3** [2.9250(16) and 2.9548(14) Å] as a result of the inflated ring size.

Through the medium of preliminary reactivity studies, the potential utility of complexes **2**, **3** and **4** was explored. Observing a standard electrophilic quenching procedure, *in situ* mixtures of **2**, **3** and **4** were exposed to three molar equivalents of iodine in THF solution, delivering the envisaged *ortho*-iodo products. For *N, N*-diethylbenzamide, the yield was essentially quantitative; while admirable yields were also obtained for the iodination of *N, N*-diethyl-3-methoxybenzamide and *N, N*-diethyl phenyl *O*-carbamate (yields of 71% and 75%, respectively) as determined by NMR spectroscopy.

Complexes **2**, **3** and **4** are soluble in *d*₆-benzene solution, allowing a parallel solution analysis by NMR spectroscopy. Tables 2.2 and 2.3 detail the key diagnostic chemical shifts in the ¹H and ¹³C NMR spectra, respectively, for the three zincate compounds. Highlighting the restricted, rigid structural make-up of complexes **2** and **3** (Spectrum 2.1), the ¹H NMR spectra reveal all four TMP CH₃ groups to be chemically distinct; thus endorsing the solid-state structures obtained from the X-ray data. Additionally, the sterically cluttered nature in all three complexes is conveyed in the resonances depicting

the ethyl arms of the carboxamide. In the free, uncomplexed substrate both the CH₂ and CH₃ units are evident as solitary signals, encompassing the region 3.08-3.13 and 0.89-0.94 ppm, respectively. Upon *ortho*-zincation and incorporation as part of a bulky, heterotri-anionic zincate, these resonances split and appear inequivalent. The discrete CH₃ resonances are represented in Table 2.2. The CH₂ groups decoalesce into a series of multiplets to underline the inflexible conformation of the aromatic fragment in these complexes.

Table 2.2: Comparison of selected ¹H NMR (400.13 MHz, 300 K) chemical shifts (δ in ppm) for zincates 2, 3 and 4 in *d*₆-benzene solution.

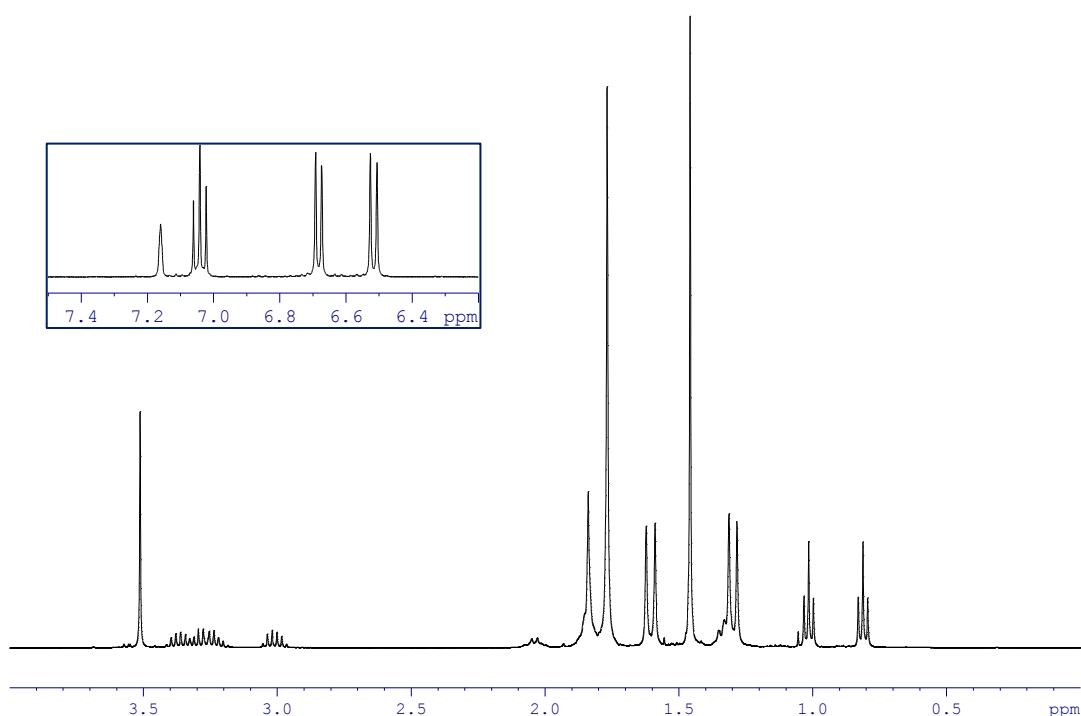
Compound	δ(TMP-CH ₃)	δ(β-TMP)	δ(γ-TMP)	δ(Ethyl-CH ₃)
2	1.52, 1.50, 1.32, 1.21	1.88, 1.57	1.96	1.02, 0.79
3	1.62, 1.59, 1.34, 1.31	1.82 ^a , 1.34	2.04, 1.84	1.02, 0.81
4	1.38-1.26 (br)	1.60	1.96	1.00, 0.89

^a See Experimental Section for full analysis

Table 2.3: Comparison of selected ¹³C NMR (100.62 MHz, 300 K) chemical shifts (δ in ppm) for zincates 2, 3 and 4 in *d*₆-benzene solution.

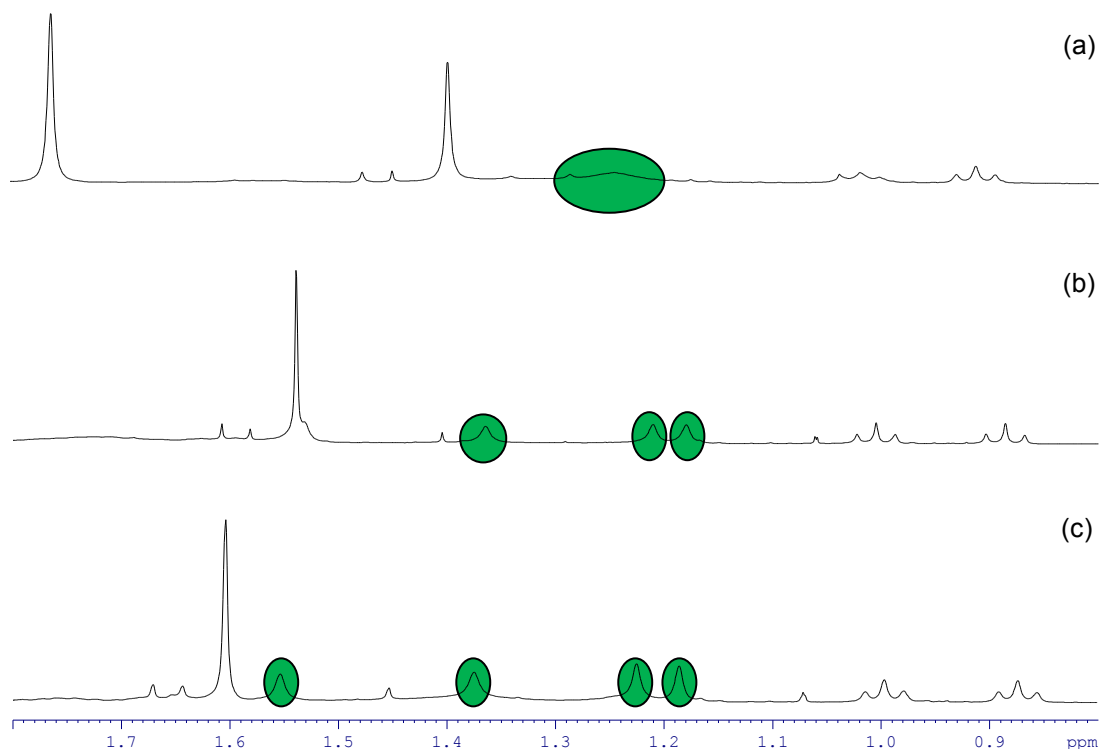
Compound	δ(TMP-CH ₃)	δ(β-TMP)	δ(γ-TMP)	δ(α-TMP)	δ(Ethyl-CH ₃)
2	37.4, 35.2, 34.6, 34.4	40.7, 39.7	20.4	52.8	13.9, 12.9
3	36.6, 35.6, 35.5, 33.0	41.8, 41.2	20.4	53.2	13.9, 12.9
4	35.0	40.1	20.4	52.6	14.0, 13.3


The ¹³C NMR spectra, which were assigned by implementing 2D ¹H-¹³C HSQC experiments, also substantiate these data, while the chemical shift of the *ortho*-carbon atom reiterates the site of metallation. As a product of zincation, the *ortho*-carbon resonances in complexes **2**, **3**, and **4** are noted at 168.9, 167.9, and 159.4 ppm; a telling manoeuvre downfield from those of unbound, non-metallated substrate (126.8, 112.4, and 122.1 ppm, respectively).



Spectrum 2.1: Aliphatic region of the ^1H NMR (400.13 MHz, 300 K) spectrum of **3 obtained in d_6 -benzene solution and inset, the aromatic region.**

The ^1H NMR spectrum of complex **4** resembles that of **2** and **3** with the exception of the resonances denoting the TMP ligand; a broad signal (spanning 1.26-1.38 ppm) is observed for the TMP CH_3 groups, intimating that a dynamic process must be occurring in solution at room temperature. Variable temperature NMR spectroscopic studies of a d_8 -toluene solution of **4** validate this scenario (Spectrum 2.2). At low temperature (250 K), the broad resonance observed at room temperature diverges into three distinct signals (at 1.18, 1.21, and 1.36 ppm, each with an integration of three hydrogen atoms) and upon further cooling to 230 K, the fourth and final CH_3 entity emerges at 1.55 ppm from beneath the *t*Bu group to complete the full complement of CH_3 signals.



Spectrum 2.2: Selected aliphatic region of the ^1H NMR spectrum of **4** in d_8 -toluene solution, showing the methyl resonances of the TMP ligand  at various temperatures [(a) 300 K; (b) 250 K; (c) 220 K)].

The AMMZn portfolio has thus been developed to include some of the functional groups frequently encountered in DoM-mediated aromatic synthesis. Treatment of *N,N*-diethylbenzamide, *N,N*-diethyl-3-methoxybenzamide, and *N,N*-diethyl phenyl *O*-carbamate with the sodium TMP-zincate base $[(\text{TMEDA})\text{Na}(\mu\text{-TMP})(\mu\text{-}t\text{Bu})\text{Zn}(t\text{Bu})]$ (**1**) produced the three new selectively *ortho*-zincated crystalline complexes $[(\text{TMEDA})\text{Na}(\mu\text{-TMP})\{\mu\text{-}2\text{-}[1\text{-C}(\text{O})\text{NEt}_2]\text{C}_6\text{H}_4\}\text{Zn}(t\text{Bu})]$ (**2**), $[(\text{TMEDA})\text{Na}(\mu\text{-TMP})\{\mu\text{-}2\text{-}(1\text{-C}(\text{O})\text{NEt}_2)(3\text{-OMe})\text{C}_6\text{H}_3\}\text{Zn}(t\text{Bu})]$ (**3**), and $[(\text{TMEDA})\text{Na}(\mu\text{-TMP})\{\mu\text{-}2\text{-}(1\text{-OC}(\text{O})\text{NEt}_2)\text{C}_6\text{H}_4\}\text{Zn}(t\text{Bu})]$ (**4**). Although the metallation regioselectivities realised in these reactions are not new, it is worth stressing that these highly chemo- and regioselective reactions are executed at ambient temperatures with no suggestion of complications in the form of side reactions that would plague the use of organolithium reagents under the same conditions. Collectively, these results emphasise the efficiency

of the synergic bimetallic bases and lay the foundations on which some of the highlights of this PhD research programme were built.

2.3) *The Surprising ortho-Zincation of Benzyl Methyl Ether*

Alkyl aryl ethers are classic and frequent lithiation substrates with varied reports communicating the mechanism and efficiency of the lithiation of anisole and its derivatives.^[6] Assessing the relative heats of protonation of lithiated anisole derivatives reveals that the *ortho*-isomer is most stable.^[26] Although not particularly basic, they typically direct lithiation at higher temperatures by inductively acidifying nearby protons. Consequently, the best oxygen based DMGs are those in which the oxygen is attached to the aromatic ring exerting a significant inductive effect on the *ortho*-protons and those which bear a second oxygen atom (*i.e.* an acetal) primed for lithium coordination.

Previous work in our laboratory established that anisole could be *ortho*-metallated by the synergic base **1**, manifested in the isolated intermediate [(TMEDA)Na(μ -TMP){ μ -2-(1-OMe)-C₆H₄}Zn(*t*Bu)] (Figure 2.6). Ensuing studies probed the strength of the methoxy groups directing capability and the effect of additional substituents on the ring with 2-, 3- and 4-methylanisole treated with an equimolar quantity of bimetallic base **1**.^[27] X-ray crystallographic analysis confirmed each methylanisole substrate had been zincated *ortho* to the methoxy group, implying the position of the methyl substituent does not affect the regioselectivity (at least its final outcome) and reinforcing the long history of the methoxy group in DoM.

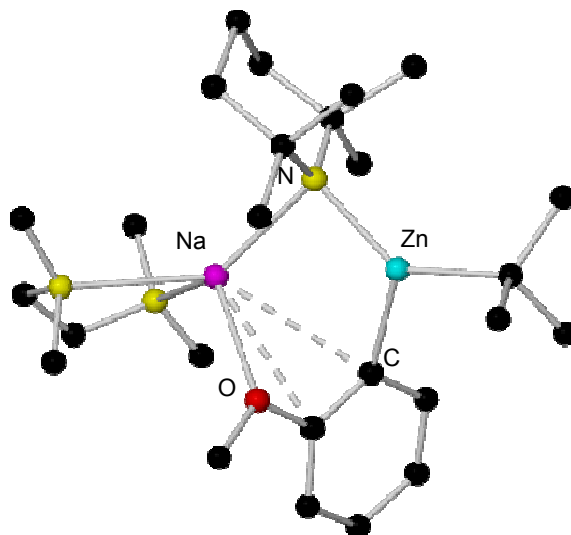
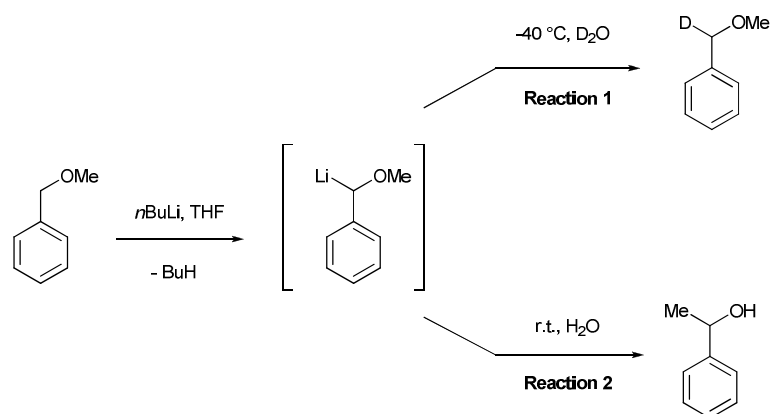


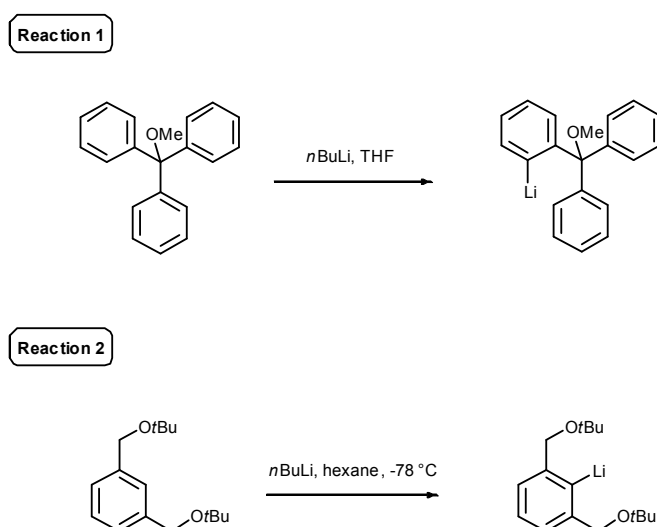
Figure 2.6: Molecular structure of the *ortho*-zincated anisole [(TMEDA)Na(μ -TMP){ μ -2-(1-OMe)-C₆H₄}Zn(*t*Bu)].

An eminent class of organic molecule which have proven to be exceedingly poor *ortho*-directing molecules is the benzylic ethers (both primary and secondary).^[2c, 28] These compounds harbour highly acidic hydrogen atoms on the α -carbon by virtue of being directly adjacent to an electronegative oxygen atom and an electron-withdrawing phenyl group. Azzena and co-workers have comprehensively explored the lithiation chemistry of benzylic ethers.^[29] Foremost, their experiments revealed that ethers such as benzyl methyl ether are exclusively metallated at the α -position (benzylic) when an excess of *n*BuLi in THF is employed.^[29a] The ultimate fate of the lithium containing intermediate depends on the reaction temperature. At low temperature (-40 °C), lithiation followed by a D₂O quench delivered the desired α -deuterated ether in high yield (Scheme 2.7, reaction 1). However, at ambient temperature the aqueous work-up revealed that the lithio-intermediate had completely rearranged to 1-phenylethanol – a product of the Wittig rearrangement process (Scheme 2.7, reaction 2).



Scheme 2.7: Benzylic lithiation of benzyl methyl ether and the product dependency on reaction temperature.

A key point to note from Azzena's studies and a related contribution from Toshimitsu^[30] is that the phenyl group preserves its integrity. To date, the only methylbenzylic ether which has been shown to undergo *ortho*-lithiation is the benzylic hydrogen atom-free (tertiary) ether Ph_3COMe (Scheme 2.8, reaction 1) where no competitive proton abstraction is possible (*meta/para* not realistic);^[31] while *ortho*-metallation to form an O,C,O-pincer organolithium compound is possible when two ether functional groups are bound to a phenyl ring *meta* to one another (Scheme 2.8, reaction 2).^[32]



Scheme 2.8: *Ortho*-lithiation of a pair of benzylic ethers.

Breaking with convention, the reaction of sodium zincate **1** with benzyl methyl ether produces exclusively an *ortho*-zincated intermediate [(TMEDA)Na(μ -TMP){ μ -2-(1-CH₂OMe)-C₆H₄}Zn(*t*Bu)] (**5**) (Figure 2.7) in lieu of the envisaged “thermodynamic” α -metallated product. Complex **5** is prepared by reacting an *in situ* hexane solution of sodium TMP-zincate **1** with one molar equivalent of benzyl methyl ether at ambient temperature. After 12 hours, colourless crystalline *ortho*-zincated product **5** deposited from the hydrocarbon solution in a crystalline yield of 49%. As the TMP anion is preserved in **5**, thermodynamically, zincate **1** serves as an alkyl base ultimately towards the ethereal substrate in accordance with the reactivity precedent observed for complexes **2-4**.

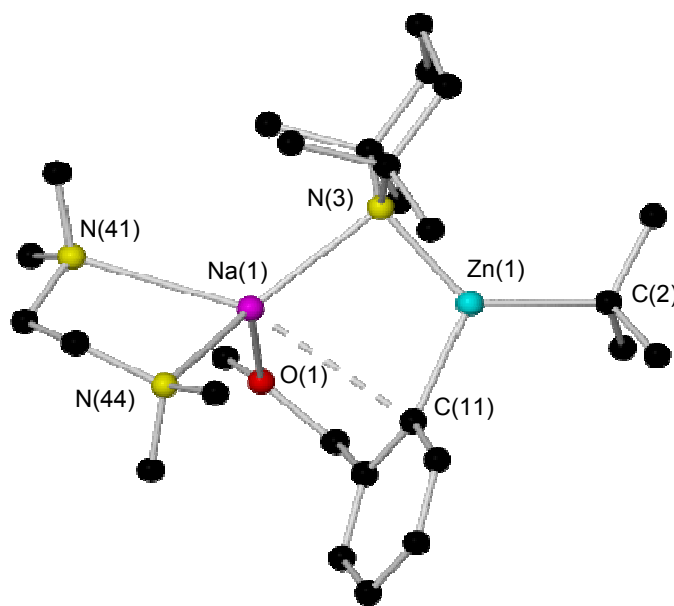


Figure 2.7: Molecular structure of **5** with selective atom labelling. Hydrogen atoms are omitted for clarity. The long Na \cdots C_{ortho} contact is highlighted by a dashed line. Selected bond lengths (Å) and angles (deg): Na(1)-O(1) 2.3705(15), Na(1)-N(3) 2.4675(19), Na(1)-N(41) 2.7043(19), Na(1)-N(44) 2.4983(17), Na(1)-C(11) 2.9597(19), Zn(1)-N(3) 2.0109(15), Zn(1)-C(2) 2.038(2), Zn(1)-C(11) 2.0652(18); O(1)-Na(1)-N(3) 104.72(6), O(1)-Na(1)-N(41) 101.34(6), O(1)-Na(1)-N(44) 114.95(6), N(3)-Na(1)-N(41) 121.87(6), N(3)-Na(1)-N(44) 134.48(6), N(41)-Na(1)-N(44) 72.07(6), N(3)-Zn(1)-C(2) 130.48(7), N(3)-Zn(1)-C(11) 114.38(6), C(2)-Zn(1)-C(11) 114.94(8).

From a solid-state perspective, this means that the main structural backbone [*i.e.* {(TMEDA)Na(μ -TMP)Zn(*t*Bu)}] in **1** is retained and captures the *ortho*-zincated benzyl methyl ether molecule to complete the molecular structure of **5** fashioning a seven-membered (five-element) NaOCCCZnN ring. The availability of structure **5** and the similarities in their key structural parameters enables comparison with the aforementioned *ortho*-zincated anisole relative. Due to its terminal coordination to the bidentate TMEDA ligand, the Na centre in **5** is formally four-coordinate and adopts a distorted tetrahedral geometry (mean angle subtended at Na 108.24°); while the Zn atom maintains a trigonal planar geometry made up of a terminal *t*Bu and two bridging ligands (TMP and the deprotonated substrate). The Na(1)-O(1) distance in **5** [2.3705(15) Å] is noticeably shorter than that in the related anisole complex [2.456(13) Å], while the O(1)-Na(1)-N(3) bond angle in **5** [104.72(6)°] is relatively larger than in the zincated anisole species [101.1(4)°]; both presumably a consequence of the extra atom accommodated in **5** to deliver the seven-membered ring.

As in the previous section, *in situ* hexane solutions of the zincated intermediate, here **5**, were intercepted by iodine to determine the potential utility in electrophilic substitution reactions. When the active zincate base to ether ratio was 1:1, 59% of 1-iodo-2-(methoxymethyl)benzene was prepared following standard electrophilic quenching protocols. Increasing the base:ether ratio to 2:1 resulted in isolation of the *ortho*-iodo product in an improved 88% yield. The pre-requisite for an excess of base in zincate metallations to achieve enhanced reaction yields has been commented on previously during the metallation of alkylbenzoate and π -deficient heteroaromatic compounds by an analogous lithium-containing zincate base.^[33] To further emphasise the highly regioselective, clean nature of the zincation, the ¹H NMR spectrum of a *d*₆-benzene

solution of the crude organic mixture showed no signs of any other iodinated products (*i.e.* Wittig rearrangement product, benzylic metallation or *meta/para* metallation).

Complex **5** is soluble in a variety of common organic solvents (including cyclohexane, benzene, toluene and THF) which allowed a full solution-state analysis by NMR spectroscopy in both polar and non-polar media (Table 2.4). ^1H NMR spectroscopic analysis of a d_{12} -cyclohexane solution of **5** revealed that the complex stays intact in alkane solution. Indeed, highlighting the rigidity of the molecule all four TMP CH_3 groups are chemically distinct and are observed at different chemical shifts, acquiescing with the solid-state structure acquired from the X-ray data. Variable temperature NMR spectroscopic studies of a d_8 -toluene solution of **5** show the four methyl resonances at low temperature (210 K); however, on warming to ambient temperature (300 K) these coalesced to one broad resonance.

Table 2.4: Comparison of selected ^1H NMR (400.13 MHz) chemical shifts (δ in ppm) for zincate **5 in deuterated cyclohexane and THF solution.**

Solvent	$\delta(\text{TMP-CH}_3)$	$\delta(\beta\text{-TMP})$	$\delta(\gamma\text{-TMP})$	$\delta(\text{CH}_2\text{-OMe})$
d_8 -cyclohexane	1.34, 1.29, 1.16, 1.14	1.38	1.75	4.48, 4.07
d_8 -THF	1.24	1.42	1.74	4.29

^1H NMR (400.13 MHz, 300 K) chemical shifts (δ in ppm) for TMP(H) in deuterated cyclohexane and THF solution.

Solvent	$\delta(\text{TMP-CH}_3)$	$\delta(\beta\text{-TMP})$	$\delta(\gamma\text{-TMP})$
d_8 -cyclohexane	1.06	1.29	1.62
d_8 -THF	1.06	1.29	1.63

In d_8 -THF, a much simplified ^1H NMR spectrum is obtained which implies that TMEDA is no longer bound to the Na centre. All the resonances are considerably sharper than those observed in the hydrocarbon solutions intimating the framework of **5**

undergoes a structural change in d_8 -THF, most likely adopting one of two possible scenarios. Firstly, the complex could remain as a contacted ion-pair whereby the Na centre is solvated by d_8 -THF molecules precluding the need for the Na-O_{benzyl} interaction. Subsequently the reduced sterics around TMP, could allow possible ring flipping resulting in the noted sharp resonances. Secondly a solvent-separated species such as $[\text{Na}(\text{THF})_x]^+ [\text{Zn}(\text{TMP})(t\text{Bu})(\text{C}_6\text{H}_4\text{CH}_2\text{OMe})]^-$ could give rise to the observed spectrum. While a combination of both processes could be possible, evidence from the existing literature seems to suggest that the latter scenario is more plausible.^[34]

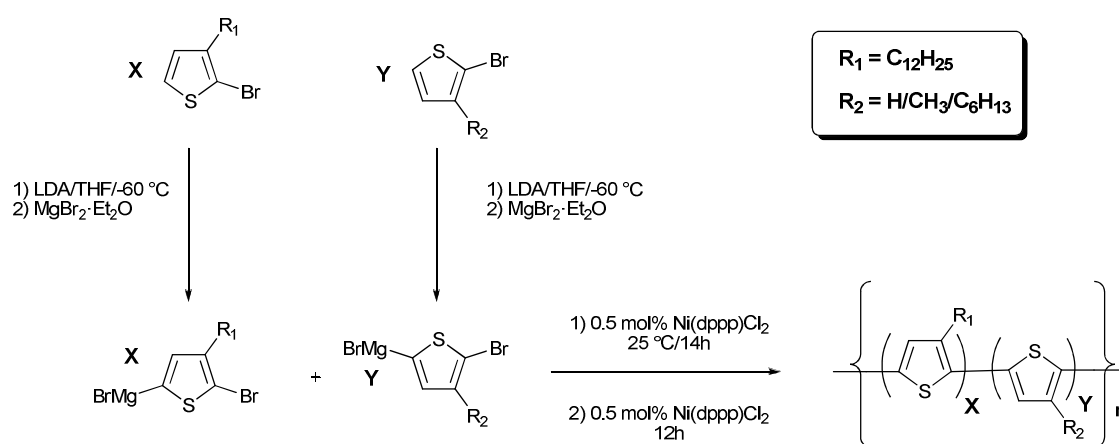
The successful isolation and characterisation of **5** has shown that AMMZn can be utilised to achieve previously unobtainable metallation regioselectivities using highly favourable reaction conditions and should instigate further studies with key aromatic substrates, including a range of primary and secondary alkyl ethers, which have so far shown little or no promise in the classical DoM reaction.

2.4) Structural Complexity of the Zincation of a Thiophene Derivative

Running parallel to DoM is the concept of α -lithiation (lithiation adjacent to a heteroatom), in which acidifying groups continue to play a prominent role. Acidity is increased and α -lithiation can be directed accordingly, if the proton abstracted is benzylic, allylic, vinylic or a constituent of an aromatic or small-ring saturated heterocycle.^[35] An example of an aromatic heterocycle, the thiophene motif is a valuable scaffold in synthetic chemistry and the construction of many useful materials are the product of its lithiation.

For example, polythiophenes are among the archetypal class of conjugated polymers that produce some of the myriad of environmentally and thermally stable materials that can be engaged as electrical conductors, polymer LEDs, batteries or solar cells to name

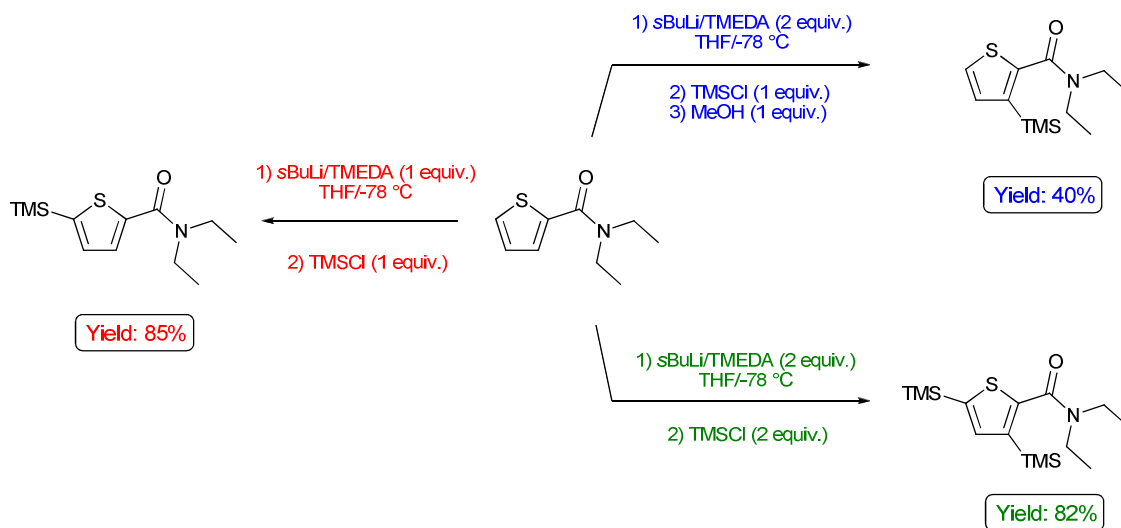
but a few.^[36] The polythiophenes illustrated in Scheme 2.9 exhibit good solubility in common organic solvents and possess excellent film-forming-abilities; while this methodology has very recently been extended to utilise Knochel's turbo-Hauser base (TMPMgCl·LiCl) for regioselective metallation of the 3-substituted thiophenes at ambient temperature, precluding the need for the transmetallation step.^[37] Additionally, substituted thiophenes have also received considerable attention in contemporary medicinal chemistry^[38] exemplified by the fact that as recently as 2007, five of the top 100 selling drugs in the US accommodate a thiophene component.^[39]



Scheme 2.9: Synthesis of random polyalkylthiophenes, embracing lithiation methodology.

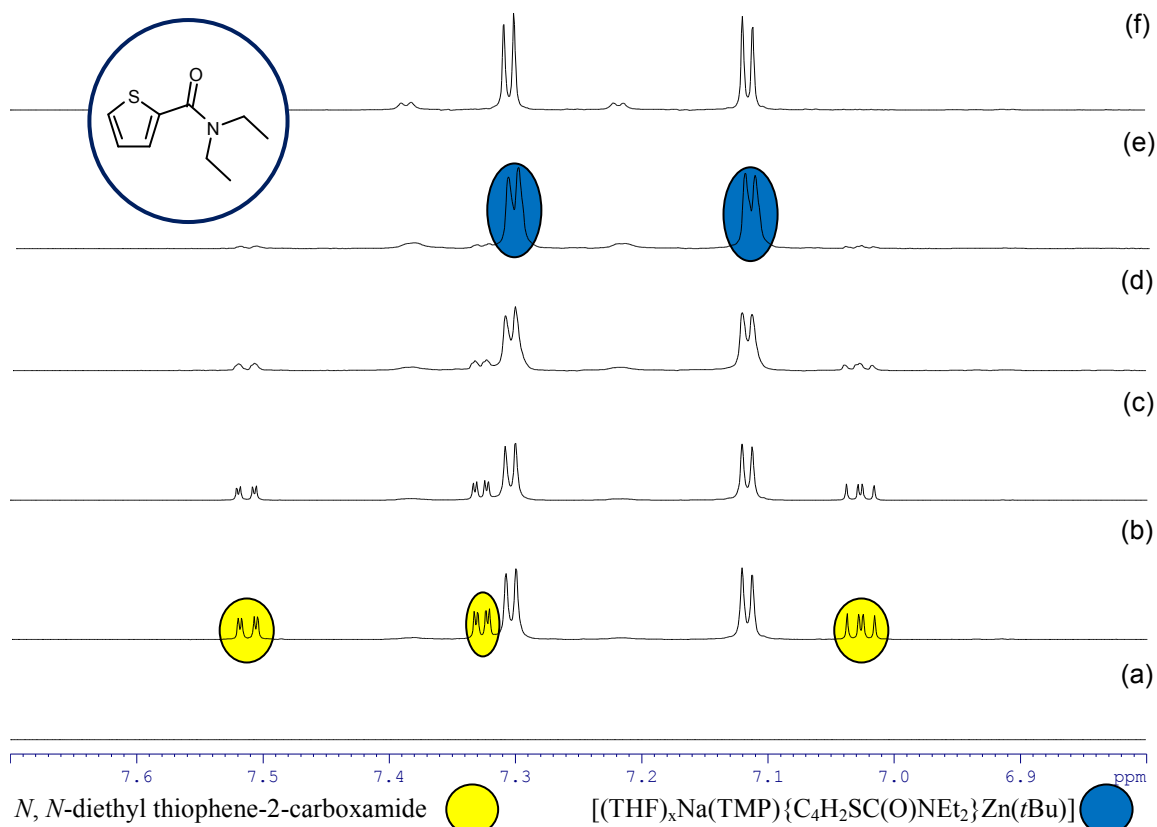
The mono-deprotonation of thiophene and its derivatives at ambient temperature has been performed in recent years utilising the original Hauser base (*i*Pr₂N)MgCl^[40] and Knochel's "turbo" variant TMPMgCl·LiCl.^[41] In relation to the theme of this section, of particular interest is the often unpredictable competition between a DMG and a heteroatom in the aromatic ring for the site of metallation. The lithiation of 3-substituted thiophenes and furans presents a gateway to 2,3-disubstituted products,^[42] however, with notable exceptions,^[43] the readily prepared 2-substituted congeners suffer exclusive C(5) metallation thereby tendering 2,5-disubstituted products.

Supplementing his work on di-metallated aromatics, Snieckus reported the direct preparation of the 3,5-dilithiated thiophene-2-carboxamide and illustrated its potential for the assembly of individual 2,3-, 2,5- and 2,3,5-functionalised thiophene derivatives by manipulation of the chosen electrophiles and their stoichiometries (Scheme 2.10).^[44]



Scheme 2.10: Organolithium-mediated synthesis of di- and tri-substituted thiophenes.

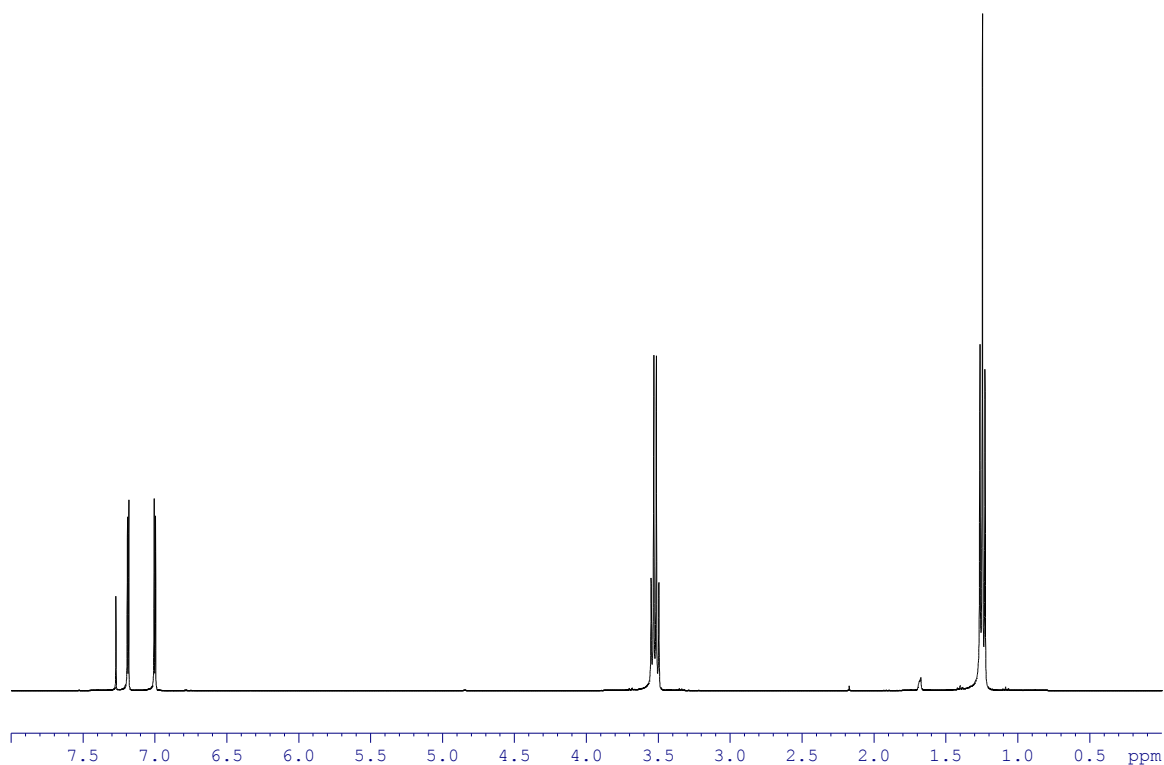
Subsequent offerings from Chadwick^[45] and Pujol^[46] have endorsed the tertiary carboxamido functions inability to direct β -metallation of thiophene. Intrigued by the designated regioselectivity, we studied the zincation of *N,N*-diethyl thiophene-2-carboxamide, scrutinising what effect the identity of the solvent has on the outcome. Initially, the reaction of synergic base **1** and the thiophene derivative was performed in THF solution ensuring consistency with each of the aforesaid literature investigations. However, with the increased polarity of the solution rendering crystal growth difficult, the reaction pathway was monitored by ¹H NMR spectroscopy in *d*₈-THF solution at room temperature (Spectrum 2.3).



Spectrum 2.3: Aromatic region of ^1H NMR spectra in d_8 -THF solution monitoring the reaction of synergic base 1 and N, N -diethyl thiophene-2-carboxamide (shown in inset) at various time intervals [(a) base alone; (b) 2 hrs; (c) 4 hrs; (d) 9 hrs; (e) 24 hrs; (f) 72 hrs].

As exhibited in Spectrum 2.3, the emergence of two doublets is indicative of successful ring metallation but with the position of the carboxamide substituent, this multiplicity pattern alone does not grant unambiguous identification of the site of deprotonation/zincation [C(3) or C(5)]. An additional complication is the presence of a minor product of metallation visible in the reaction after 48 hours. In total the reaction was surveyed for 12 days to explore and definitively rule out the possibility of a rearrangement in the site of metallation. Encouraged by the efficient deprotonation of the thiophene subunit, the reaction was transported to the bench where electrophilic quenching of the *in situ* mixture would facilitate product isolation and therefore confirmation of the metallation regioselectivity. Following column chromatography and

^1H - ^1H NOESY NMR experiments, *N,N*-diethyl-5-iodothiophene-2-carboxamide (Spectrum 2.4) was isolated in a 79% yield; thus sodium TMP-zincate **1** executes C(5) deprotonation in THF solution concurring with the previously reported, but low temperature regime, organolithium-mediated transformations.



Spectrum 2.4: The ^1H NMR (400.13 MHz, 300 K) spectrum of *N,N*-diethyl-5-iodothiophene-2-carboxamide in *d*-chloroform.

Previous, important new discoveries within the Mulvey group, in the context of synergic zincation have principally been unearthed in bulk, non-polar hexane solution. Consequently, the equimolar reaction of the bimetallic base **1** and the substituted thiophene was undertaken in this medium, but upon addition of the organic substrate an insoluble, waxy material was deposited. Increasing the polarity of the solution and ensuring its homogeneity the deprotonation was pursued in benzene, conserving the hydrocarbon nature of the reaction medium. Within 3-4 days a crop of yellow crystals were produced at ambient temperature in a yield of 47%; the structure and composition

of which was elucidated using a combination of NMR spectroscopy and preliminary X-ray data which due to its poor quality will not be discussed herein. However, recrystallisation of this crystalline material from a THF/hexane mixture revealed the surprising complex $[(D)Na\{\mu\text{-}3,5\text{-}(2\text{-C(O)NEt}_2\text{-C}_4\text{H}_1\text{S}\}Zn(t\text{Bu})\}_4]$ (where D represents the donor sites which are a mixture of bidentate TMEDA or two monodentate THF molecules and were modelled as such) (**6**) (Figure 2.8). The thiophene ring has been dizincated; unlike most of the previous organozincate intermediates discussed this one is tetrameric (*c.f.* monomeric) and octanuclear (containing four Zn and four Na atoms).

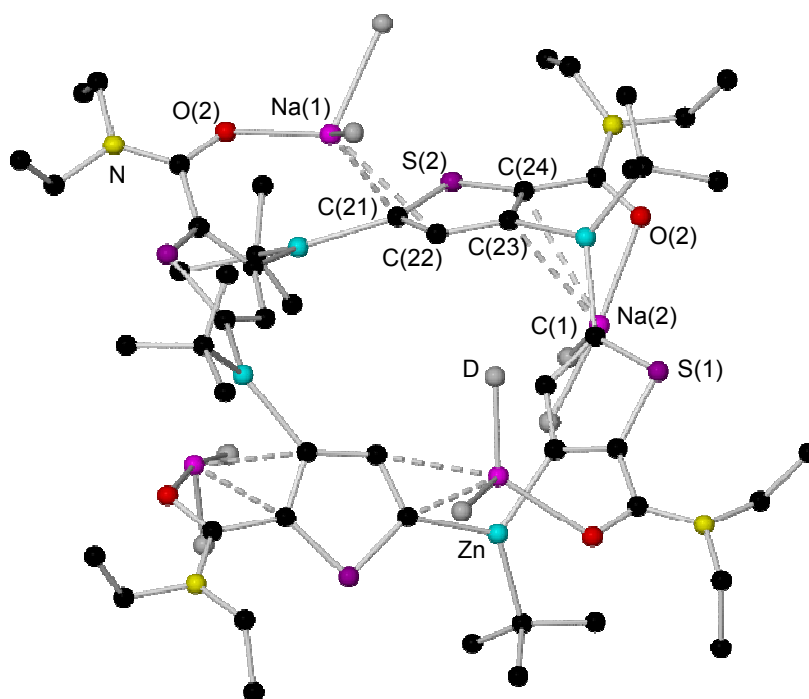
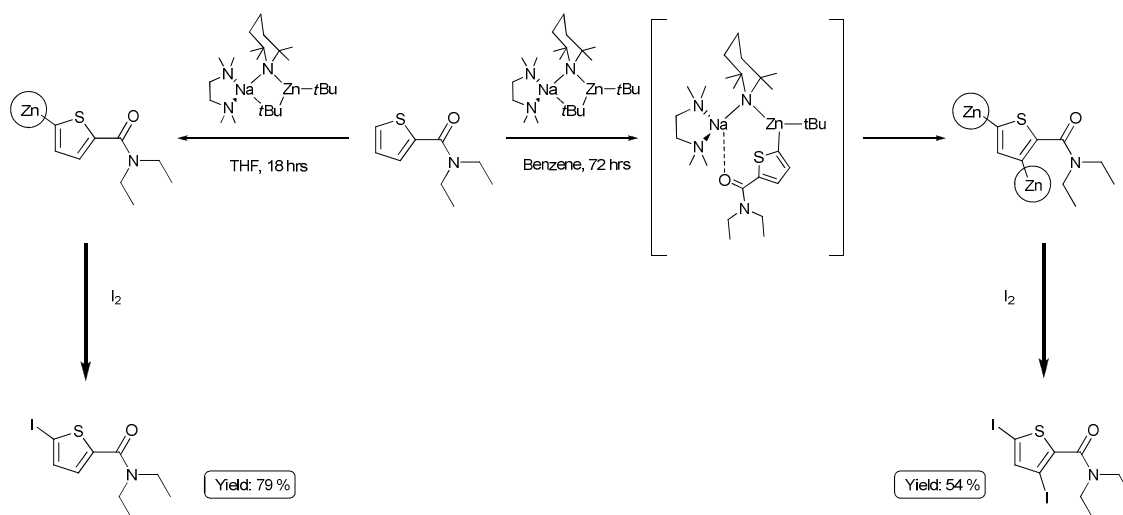


Figure 2.8: Molecular structure of **6** with selective atom labelling. Hydrogen atoms and donor solvent backbone are omitted for clarity. The long $\text{Na}\cdots\text{C}_{\text{aryl}}$ contacts are highlighted by dashed lines. Selected bond lengths (Å): $\text{Na}(1)\cdots\text{C}(3)$ 3.050(4), $\text{Na}(1)\cdots\text{C}(21)$ 2.647(5), $\text{Na}(1)\cdots\text{C}(22)$ 2.923(4), $\text{Na}(1)\text{-O}(1)$ 2.276(3), $\text{Na}(2)\cdots\text{C}(1)$ 3.027(4), $\text{Na}(2)\cdots\text{C}(23)$ 2.999(4), $\text{Na}(2)\cdots\text{C}(24)$ 3.053(4), $\text{Na}(2)\text{-O}(2)$ 2.311(4).



Scheme 2.11: Synergic metallation of *N,N*-diethyl thiophene-2-carboxamide using sodium TMP-zincate 1 in THF and benzene, and subsequent quenching with I_2 to produce mono- and di-iodinated derivatives, respectively.

The sodium atoms in **6** are three-coordinate, primarily bound to two donor solvent atoms and the carbonyl oxygen atom but to satisfy its coordinative/electronic unsaturation it also engages the π -system of the thiophene rings. Bearing similarities in functionality to complexes **2-4**, the $Na \cdots C_{aryl}$ contacts in **6** are generally in good agreement with the related distances in the aforementioned monomers [for **2-4** $Na \cdots C_{aryl}$ contacts range from 2.9250(16) to 3.0438(14) Å] but steric effects result in the $Na(1) \cdots C(21)$ distance [2.647(5) Å] deviating from the norm; while the Na-O bond distances also reflected this effect with the $Na(2)-O(2)$ distance [2.311(4) Å] slightly longer than those found in the monozincated complexes **2-4** [range from 2.2722(11) to 2.2855(12) Å]. The thiophene rings are tilted $46.1(1)^\circ$ and $51.7(1)^\circ$ relative to each other [$S(1)-S(2')$ and $S(1)-S(2)$, respectively] and with distances in the range of 16-17 Å from diagonally opposite ethyl arms, **6** can be classed a nanomolecule.

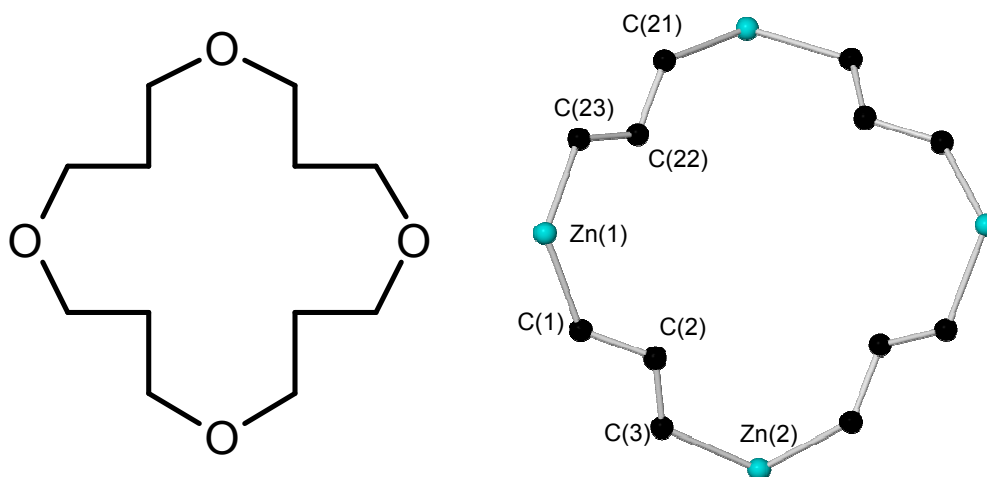


Figure 2.9: The [16]crown-4 ether architecture (L.H.S) and the “anti-crown” core of **6** from top face view (R.H.S) with selective atom labelling. Selected bond lengths (Å) and angles (deg): Zn(1)-C(1) 2.036(4), Zn(1)-C(23) 2.023(4), Zn(2)-C(3) 2.021(4), Zn(2)-C(21) 2.047(4); C(1)-Zn(1)-C(23') 111.85(15), C(3)-Zn(2)-C(21) 109.36(15).

Complex **6** can be considered a charge-reversed analogue of the [16]crown-4 macrocycle (Figure 2.9). The framework of this “anti-crown” consists of four di-deprotonated thiophene subunits linked by their carbanionic C atoms to four zinc atoms in a cyclic tetramer with crystallographically imposed C_2 symmetry. The four zinc atoms in two distinct sets form a distorted tetrahedron, giving the core metallacycle an overall cradle/bowl appearance (Figure 2.10) with the endocyclic C-Zn-C bond angles heavily distorted from 120° [C(23')-Zn(1)-C(1) $111.85(15)^\circ$ and C(3)-Zn(2)-C(21) $109.36(15)^\circ$]. In addition to carrying a terminal *t*Bu ligand, each zinc links carbon atoms of two individual thiophene molecules with Zn-C bond distances of 2.036(4), 2.023(4), 2.021(4) and 2.047(4) Å [for Zn(1)-C(1), Zn(1)-C(23), Zn(2)-C(3) and Zn(2)-C(21), respectively]. The distances between adjacent zinc atoms are 6.2218(8) and 6.2254(6) Å; while the transannular Zn \cdots Zn distances are 7.7644(8) and 7.7990(6) Å [Zn(1) \cdots Zn(1') and Zn(2) \cdots Zn(2'), respectively], hinting at a larger cavity than that in a 16-MC-4 [MC is an abbreviation for metallacrown] zinc metallacycle [Zn₄(picoline-

tetrazolyamide)₈] where the Zn ions are connected via N-C-N bridges with diagonal and adjacent distances of 7.349 and 5.658 Å, respectively.^[47]

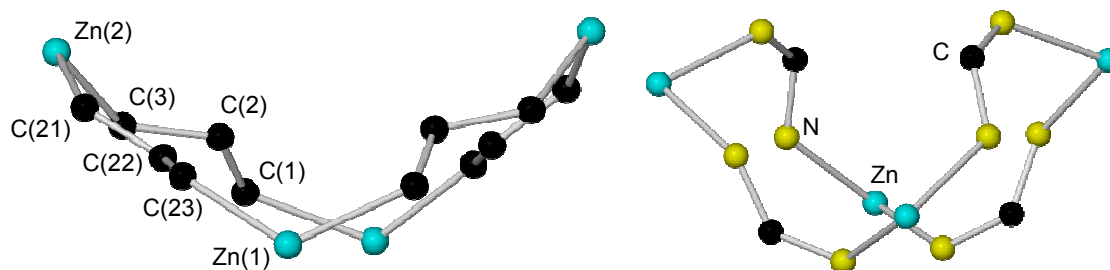
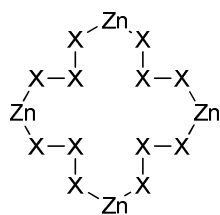


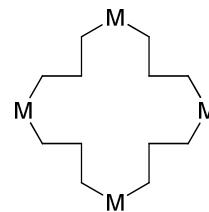
Figure 2.10: Side edge view of the core of **6** with selective atom labelling, illustrating its bowl conformation (L.H.S) and the less open structure of the previously reported 16-MC-4 zinc metallacycle with N-C-N bridges (R.H.S).

Closely related to this study, the sodium-mediated magnesiation of furan has previously been studied in the Mulvey group.^[48] Treating furan with the heteroleptic alkyl-amido reagent [(TMEDA)Na(μ -CH₂SiMe₃)(μ -TMP)Mg(TMP)] produced the unexpected dodecasodium-hexamagnesium complex [{(TMEDA)₃Na₆Mg₃-(CH₂SiMe₃)(2,5-C₄H₂O)₃(2-C₄H₃O)₅}₂] engendered from 10 α -monodeprotonated furyl anions and 6 α,α' -twofold-deprotonated furyl dianions, meaning an astonishing 22 deprotonations in total. Coupled with the synthesis of **6**, the combination of synergic bimetallic bases and the right substrate could provide a fresh approach to creating potential building blocks for supramolecular systems. In that regard, Saalfrank's aforementioned complex is a very rare example of a 16-MC-4 zinc metallacycle; while to the best of our knowledge, complex **6** represents the first crystallographically characterised 16-MC-4 complex of any metal where the organic constituents of the hexadecanuclear ring are all carbon atoms (Figure 2.11).



Where X is any atom

Only true zinc 16-MC-4 is
Saalfrank's with N-C-N links



Where M is any metal

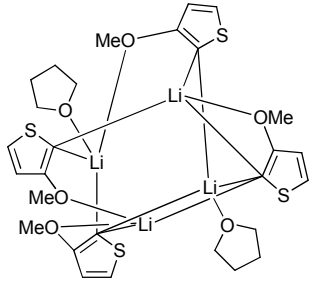
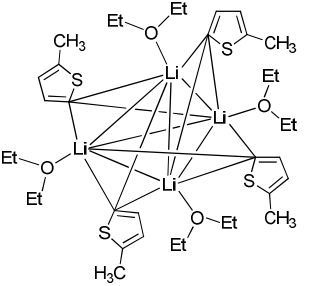
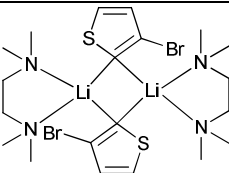
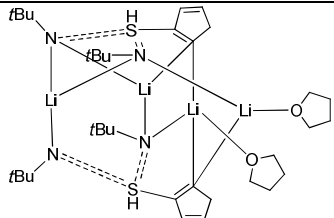
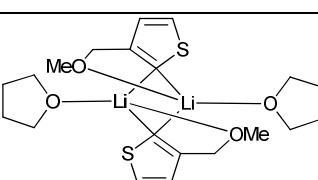
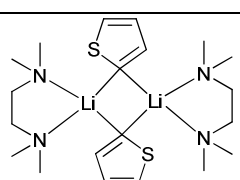
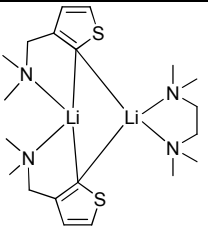
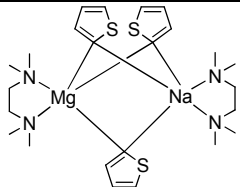
No hits

Figure 2.11: Queries entered into the Cambridge Crystallographic Database and the results returned (Date of search November 2011).

From a metallation point of view and as outlined in Section 1.3, synergic base **1** has previously been successfully employed in the di-deprotonation of benzene and naphthalene. However, these poly-metallations necessitated two equivalents of base, whereas the di-metallation manifested in complex **6** was performed utilising an equimolar quantity of reagent **1** with the basic TMP and bridging *t*Bu executing the deprotonations offering an energy efficient di-metallation at ambient temperature. While this ambibasic behaviour has precedent in lithium TMP-zincate chemistry with other types of organic substrate,^[14, 49] the synthesis of **6** provides an infrequent example of **1** exhibiting this dual basicity.

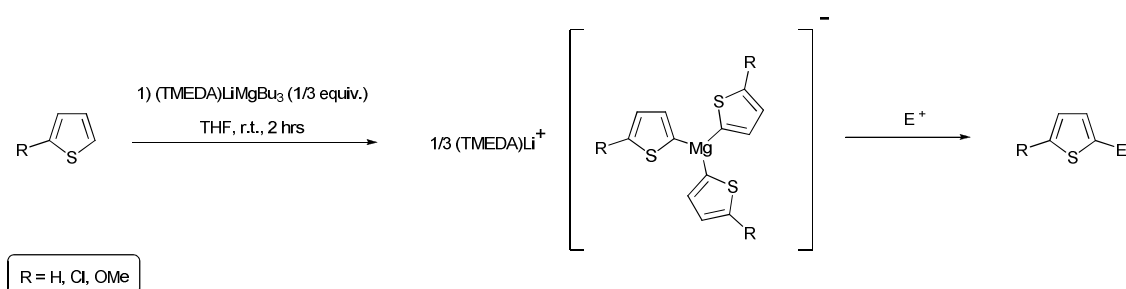
Furthermore there would appear to be no precedent for a zincated (mono- or di-deprotonated) thiophene structure in the literature. Table 2.5 details the α -metallated thiophene complexes listed on the Cambridge Crystallographic Database at the time of writing that have been prepared by direct deprotonative metallation.^[24] There are seven lithium examples and only one non-lithium example. Significantly, they are all mono-deprotonated examples.

Table 2.5: Crystallographically characterised α -metallated thiophene molecules prepared by direct metallation, detailing metal-carbon bond distances.

	[50]		[51]
<p>Li-C: 2.129; 2.195; 2.250; 2.141 Å</p>		<p>Li-C: 2.260 Å</p>	
	[52]		[53]
<p>Li-C: 2.298; 2.218; 2.237; 2.258 Å</p>		<p>Li-C: 2.191; 2.190; 2.325; 2.228 Å</p>	
	[54]		[55]
<p>Li-C: 2.158; 2.223 Å</p>		<p>Li-C: 2.209; 2.179; 2.205; 2.250 Å</p>	
	[56]		[57]
<p>Li-C: 2.179; 2.159; 2.200; 2.215 Å</p>		<p>Mg-C: 2.217; 2.236; 2.263 Å</p>	

Of particular interest is the *tris*-(α -magnesiated) product, previously reported by the Mulvey group. Prepared rationally by reacting $n\text{BuNa}$, $\text{Mg}(\text{CH}_2\text{SiMe}_3)_2$, TMEDA and thiophene in a 1:1:2:3 ratio in hexane, all three alkyl arms have been engaged in the deprotonation of a thiophene molecule. This tri-basicity has also been observed by

Mongin and co-workers who revealed that thiophene is regioselectively deprotonated at the α -carbon using 1/3 equivalent of LiMgBu_3 in THF (Scheme 2.12), although this earlier report does not provide any structural information or indeed any information at all on the nature of the metallated intermediate prior to electrophilic interception.^[58]



Scheme 2.12: Sub-stoichiometric (with respect to magnesiate) deprotonation of thiophenes using a lithium trialkylmagnesiate and subsequent trapping with electrophiles.

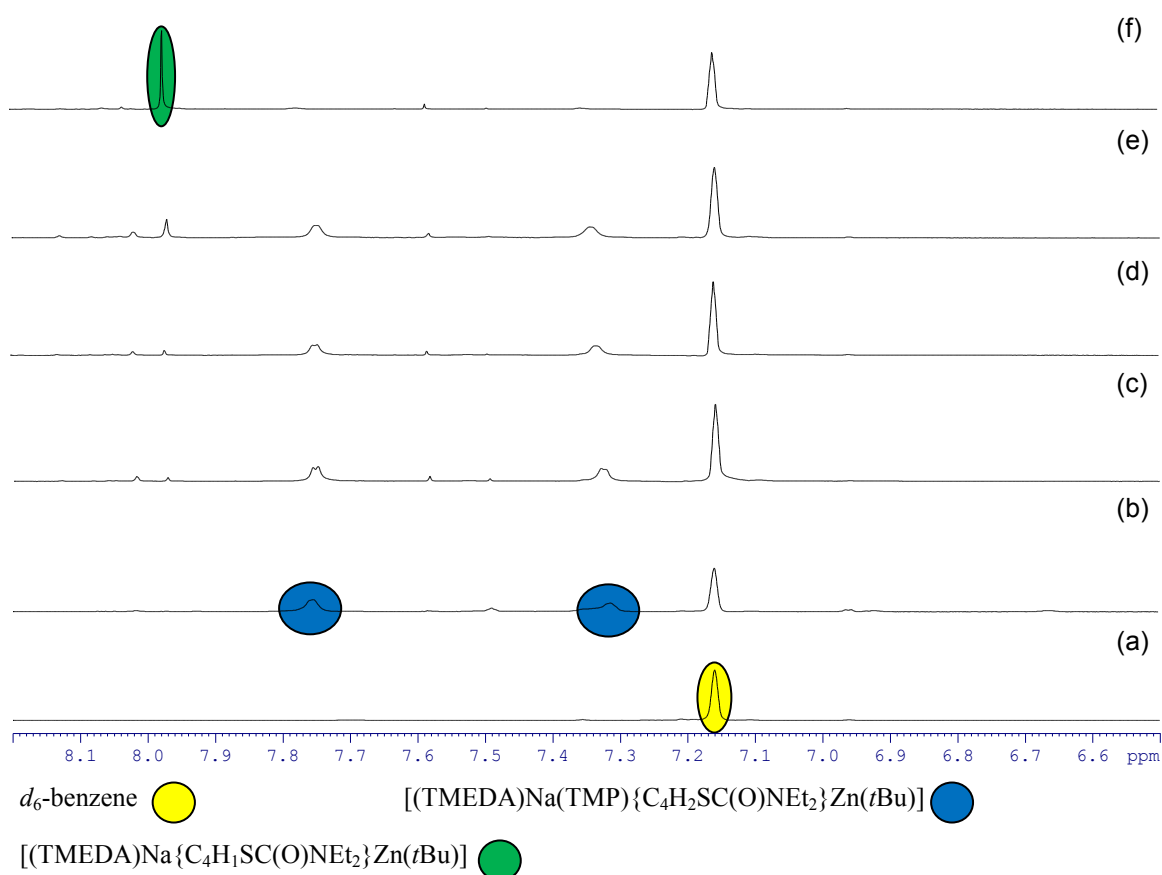
The solution integrity of complex **6** was studied by NMR spectroscopy. The ^1H NMR spectral analysis of isolated crystalline **6** in d_8 -toluene solution shows unequivocally that the material is pure. Most informative is the single aromatic signal at 7.85 ppm providing a diagnostic marker for the di-metallation and its position between two zincated carbons is reflected in its downfield shift from the thiophene starting material (7.08, 6.90 and 6.65 ppm). Table 2.6 details the major ^1H and ^{13}C NMR chemical shifts of **6**. An interesting comparison is provided by the aforesaid tris-(α -magnesiated) complex, with its NMR spectroscopic data collected in d_6 -benzene solution. It is evident that the identity of the metal makes little difference to the chemical shift of the α -metallated carbon atom (Zn-C 164.8 ppm versus Mg-C 169.1/167.4 ppm), however the presence of the adjacent electron-withdrawing carboxamide and its β -position sees zincated C(3) appear at a more upfield shift of 137.5 ppm [however, still downfield from C(3) in the starting thiophene at 126.6 ppm in d_8 -toluene solution].

Table 2.6: Selected ^1H NMR (400.13 MHz, 300 K) and ^{13}C NMR (100.62 MHz, 300 K) chemical shifts (δ in ppm) for zincate **6 in d_8 -toluene solution.**

$\delta(t\text{Bu-CH}_3)$	$\delta(\text{Ethyl-CH}_3)$	$\delta(\text{Ethyl-CH}_2)$	$\delta(\text{Aromatic-CH})$	
1.57	1.24	3.92 (1H), 3.59-3.46 (3H, br)	7.85	
$(t\text{Bu-CH}_3)$	$\delta(\text{Ethyl-CH}_3)$	$\delta(\text{Ethyl-CH}_2)$	$\delta(\text{Aromatic})$	$\delta(\text{C=O})$
35.1	14.9, 13.2	44.1, 40.7	173.1(C2), 164.8(C5), 145.9(C4), 137.5(C3)	176.3

In an attempt to gain greater insight into the mechanism of the unexpected non-stoichiometric di-deprotonation, the reaction was monitored *in situ* in d_6 -benzene solution by ^1H NMR spectroscopy. As illustrated in Spectrum 2.5, the mono-deprotonation of the thiophene substrate proceeds essentially quantitatively after 2 hours at room temperature (depicted by the two signals emerging at 7.78 and 7.31 ppm). During this period, formation of isobutane and TMP(H) are noted by the indicative doublet at 0.86 ppm and amine proton at 0.33 ppm, respectively (these are not shown in Spectrum 2.5). While the isobutane continues to evolve and its integral steadily increases, the relative ratio of the N-H resonance in TMP(H) peaks at 1-2 hours before falling off, gradually decreasing in the time frame 4-24 hours suggesting the generation of the putative intermediate [(TMEDA)Na(μ -TMP){ μ -5-(2-C(O)NEt₂)-C₄H₂S}Zn(*t*Bu)], consistent with the concept of an initial stepwise deprotonation which will be discussed in detail in the next chapter. From here, the first definite signs of the second deprotonation are apparent after 24 hours; however, much slower than the preceding metallation, the reaction needs approximately 72 hours to go to completion with the one remaining ring proton portrayed by the sole singlet at 7.97 ppm. Emphasising the deprotonative capability of zincate **1**, the small signal at 7.60 ppm

corresponds to di-metallated benzene (*i.e.*, di-deprotonation of the deuterated NMR solvent).^[59]



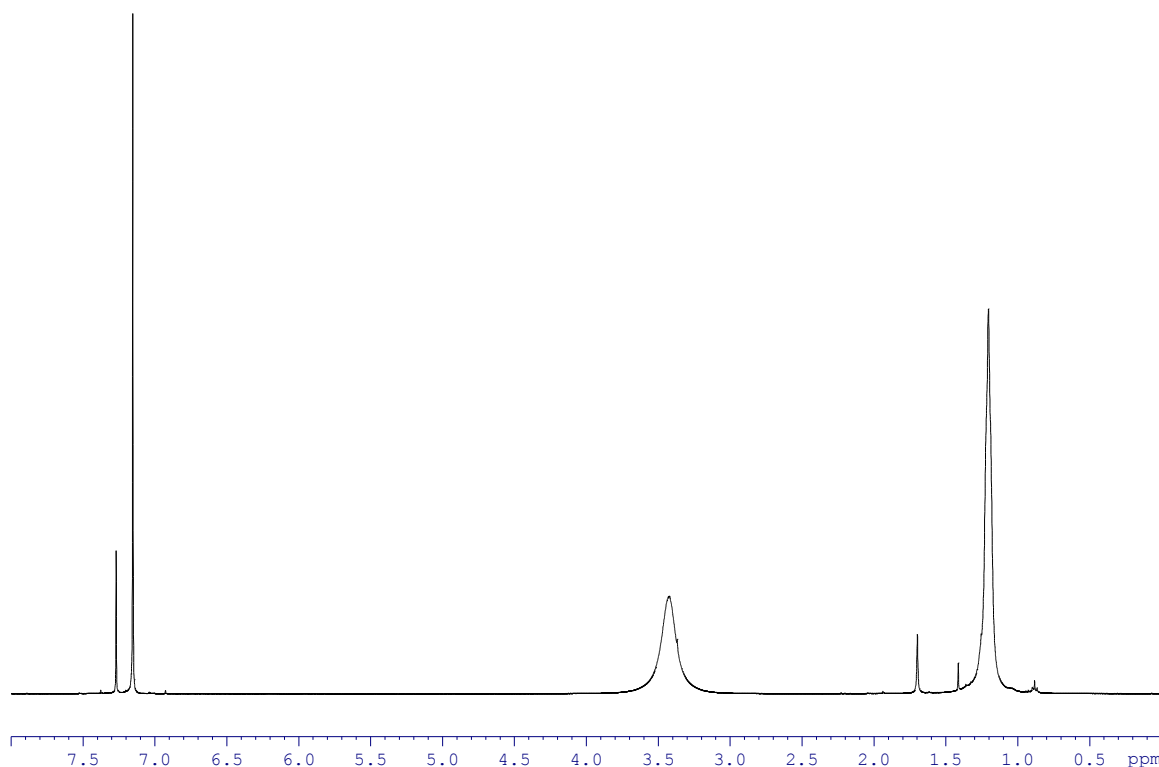
Spectrum 2.5: Aromatic region of the ^1H NMR spectrum in d_6 -benzene solution following the reaction of synergic base **1 with *N,N*-diethyl thiophene-2-carboxamide at various time intervals [(a) base alone; (b) 2 hrs; (c) 4 hrs; (d) 9 hrs; (e) 24 hrs; (f) 72 hrs].**

The stark difference in reactivity noted in the two different solvent mediums can be rationalised by considering the structural make-up of bimetallic base **1** in each. In hydrocarbon solvent, it has been established that the contact ion-pair nature of these zincates is retained; assuring intimate contact between sodium and zinc through the TMP bridge that delivers the second, unforeseen deprotonation. As illustrated when discussing the solution structure of complex **5** in the previous section (Section 2.3), dissolution in polar THF typically results in the formation of solvent separated species such as $[\text{Na}(\text{THF})_x]^+ [\text{Zn}(\text{TMP})(t\text{Bu})\{\mu\text{-}5\text{-(1-C}(\text{O})\text{NEt}_2\text{)-C}_4\text{H}_2\text{S}\}]^-$ with the sodium

atom completely sequestered by donor THF molecules inhibiting any communication between the two metals. Highlighting the significance of this interaction, Uchiyama and Kondo's hitherto discussed studies on a related lithium TMP-zincate routinely employ a polar THF solvent medium with all published results thus far ordinarily obeying the established principles of DoM or α -lithiation.^[21, 33, 60]

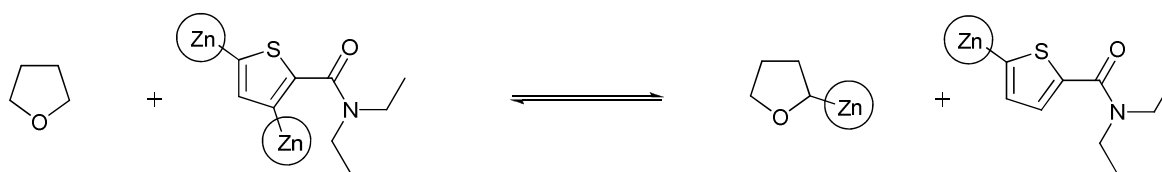
Schlosser has previously assessed the practicality of dimetallations, studying alkyl substituted benzenes and *N, N*-crowded anilines.^[61] Dimetallation was found to only occur with an excess of a highly concentrated *n*BuLi/*t*BuOK superbasic mixture in hydrocarbon media, and even then it only occurred incompletely with the best yield detailed a moderate 41%. Dimetallation was considered kinetically, but not thermodynamically favoured over monometallation and was recognised to proceed by an aggregation phenomenon with evidence suggesting the second deprotonation is accomplished within a tightly packed mixed aggregate, the formation of which requires high reagent concentrations and non-coordinating solvents. Coincidentally, in THF no trace of dimetalled species was found, although such species are stable in this solvent at -75 °C by generating a specific monometallated intermediate and then introducing the second metal separately.

In order to determine the stability of di-zincated **6**, an *in situ* equimolar mixture of synergic base **1** and *N, N*-diethylthiophene-2-carboxamide was treated with a THF solution of iodine. Following work-up and column chromatography, *N, N*-diethyl-3,5-diiodothiophene-2-carboxamide (Spectrum 2.6) was isolated in an optimum yield of 54%; while 31% of the previously prepared di-substituted product (arising from a mono-metallated intermediate) *N, N*-diethyl-5-iodothiophene-2-carboxamide was also recovered.

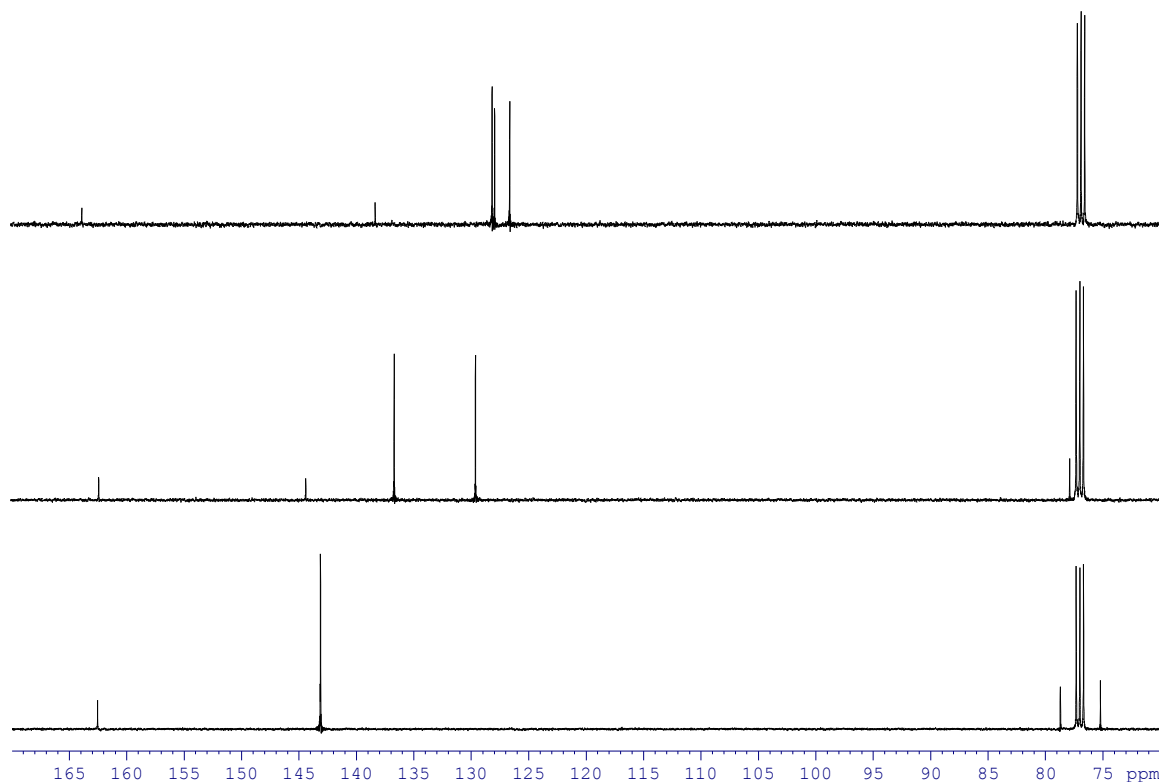


Spectrum 2.6: The ^1H NMR (400.13 MHz, 300 K) spectrum of *N,N*-diethyl-3,5-diiodothiophene-2-carboxamide in *d*-chloroform.

Based on the high conversion noted in ^1H NMR monitoring experiments, one could not rule out destruction of the dimetalled species by solvent attack with the THF necessary for the dissolution of iodine (Scheme 2.13). Indeed, when quenching an NMR sample of pure, crystalline **6** in d_8 -toluene with excess iodine dissolved in freeze-pump-thaw dried d_8 -THF, 12% of *N,N*-diethyl-5-iodothiophene-2-carboxamide is detected by ^1H NMR spectroscopy. Assessing the ^{13}C NMR data of the thiophene starting material and resulting quenched products in *d*-chloroform solution, confirms the level of iodo-substitution with iodo-bonded carbon atoms experiencing a considerable shift upfield, typically to around 75 - 80 ppm (Spectrum 2.7).



Scheme 2.13: Possible equilibrium leading to α -metallation of THF and concomitant degradation of di-zincated **6**.



Spectrum 2.7: Selected aromatic region of the ^{13}C NMR (100.62 MHz, 300 K) spectrum of (a) *N,N*-diethyl thiophene-2-carboxamide, (b) *N,N*-diethyl-5-iodothiophene-2-carboxamide and (c) *N,N*-diethyl-3,5-diiodothiophene-2-carboxamide.

Surveying the findings of this section it is clear the reaction medium and therefore the molecular structure of the base can be tuned to effect special metallations in different ways. The unique synergic chemistry that brought about the remarkable di-deprotonation and exquisite structure **6** will be explored in the next chapter underlining the influence of the TMP bridge interlinking the two metals.

2.5) Experimental section

Synthesis of [(TMEDA)Na(μ -TMP)(μ -*t*Bu)Zn(*t*Bu)] **1**

NaTMP was prepared *in situ* by reaction of *n*BuNa (0.16 g, 2 mmol) with TMPH (0.34 mL, 2 mmol) in 10 mL of dry hexane. The yellow suspension was allowed to stir for 2 hours. In a separate Schlenk tube, *t*Bu₂Zn (0.36 g, 2 mmol) was dissolved in hexane (10 mL), before being transferred to the already prepared NaTMP by cannula. TMEDA (0.3 mL, 2 mmol) was then added and the contents of the Schlenk tube were stirred for 30 minutes with gentle heating affording a clear, yellow solution. This solution was allowed to cool to ambient temperature before being moved to the freezer (at -28 °C) to aid crystallisation. A crop of colourless crystals formed in solution (Typical yield: 0.53 g, 58%). ¹H NMR (400.13 MHz, 300 K, *d*₁₂-cyclohexane): δ 2.36 [s, 4H, NCH₂ (TMEDA)], 2.25 [s, 12H, NCH₃ (TMEDA)], 1.72 [m, br, 6H, γ -CH₂ and β -CH₂ (TMP)], 1.29 [s, 12H, CH₃ (TMP)], 1.19-0.95 [m, br, 18H, distinct singlet at 1.00, CH₃ (*t*Bu)]. ¹³C {¹H} NMR (100.62 MHz, 300 K, *d*₁₂-cyclohexane): δ 58.3 [NCH₂ (TMEDA)], 52.7 [α -C (TMP)], 46.9 [NCH₃ (TMEDA)], 40.1 [β -CH₂ (TMP)], 35.7 [br, CH₃ (TMP)], 30.6 [C(CH₃)₃ (*t*Bu)], 23.5 [C(CH₃)₃ (*t*Bu)], 20.4 [γ -CH₂ (TMP)].

Synthesis of [(TMEDA)Na(μ -TMP){ μ -2-(1-C(O)NEt₂)-C₆H₄}Zn(*t*Bu)] **2**

X-ray quality crystalline material was prepared by treating the aforementioned hexane *in situ* solution of **1** with *N,N*-diethylbenzamide (0.354 g, 2 mmol), and the reaction mixture was allowed to stir at ambient temperature for 18 hours. Following gentle heating, the orange solution was concentrated *in vacuo* and transferred to a freezer for storage (at -28 °C), where colourless crystals of **2** were deposited overnight (0.63 g, 54%). Mp: 123-125 °C. ¹H NMR (400.13 MHz, 300 K, *d*₆-benzene): δ 7.94 [d {³J(H,H) 7.00 Hz}, 1H, *H*_{meta}], 7.21 (t, 1H, *H*_{para}), 6.99 (m, 2H, *H*_{meta'} and *H*_{ortho'}), 3.46-3.20 [m,

3H, CH₂ (Ethyl)], 2.93 [m, 1H, CH₂ (Ethyl)], 1.99-1.88 [m, 4H, β-CH₂ and γ-CH₂ (TMP)], 1.78 [s, 4H, NCH₂ (TMEDA)], 1.71 [s, 12H, NCH₃ (TMEDA)], 1.57 [m, 2H, β-CH₂ (TMP)], 1.52 [s, 3H, CH₃ (TMP)], 1.50 [s, 12H, C(CH₃)₃ (*t*Bu) and CH₃ (TMP)], 1.32 [s, 3H, CH₃ (TMP)], 1.21 [s, 3H, CH₃ (TMP)], 1.02 [t {³J(H,H) 7.14 Hz}, 3H, CH₃ (Ethyl)], 0.79 [t {³J(H,H) 7.13 Hz}, 3H, CH₃ (Ethyl)]. ¹³C {¹H} NMR (100.62 MHz, 300 K, *d*₆-benzene): δ 177.9 (C=O), 168.9 (*C*_{ortho}-Zn), 145.8 (*C*_{ipso}), 141.3 (*C*_{meta}), 126.8 (*C*_{para}), 123.3 and 123.1 (*C*_{meta'} and *C*_{ortho'}), 57.3 [NCH₂ (TMEDA)], 52.8 [2 x α-C (TMP)], 45.6 [NCH₃ (TMEDA)], 43.6 [CH₂ (Ethyl)], 40.7 [β-CH₂ (TMP)], 39.7 [β-CH₂ (TMP)], 38.3 [CH₂ (Ethyl)], 37.4 [CH₃ (TMP)], 35.8 [C(CH₃)₃ (*t*Bu)], 35.2 [CH₃ (TMP)], 34.6 [CH₃ (TMP)], 34.4 [CH₃ (TMP)], 20.4 [γ-CH₂ (TMP)], 20.2 [C(CH₃)₃ (*t*Bu)], 13.9 [CH₃(Ethyl)], 12.9 [CH₃ (Ethyl)].

Crystal data for **2**: C₃₀H₅₇N₄NaOZn, *M* = 578.16, monoclinic, *P*2₁/*n*, *a* = 10.4215(3) Å, *b* = 16.4560(3) Å, *c* = 19.5649(4) Å, β = 94.868(2)°, *V* = 3343.20(13) Å³, *Z* = 4; 28026 reflections collected, 9698 were unique, *R*_{int} = 0.0450, *R* = 0.0348, *R*_w = 0.0637, GOF = 0.841, 347 refined parameters, max. and min. residual electron density = 0.512 and -0.412 e·Å⁻³.

Synthesis of [(TMEDA)Na(μ-TMP){μ-2-(1-C(O)NEt₂)(3-OMe)-C₆H₃}Zn(*t*Bu)] **3**

N,N-diethyl-3-methoxybenzamide (0.415 g, 2 mmol) was introduced to the aforementioned hexane solution of **1**. To obtain a homogeneous solution, THF (2 mL) was added, and the resulting reaction mixture was allowed to stir at room temperature overnight. The dark orange solution was concentrated *in vacuo* and stored in a refrigerator (at 5 °C) preceding the growth of small, colourless block crystals of **3** (0.54 g, 44%). Mp: 120-122 °C. ¹H NMR (400.13 MHz, 300 K, *d*₆-benzene): δ 7.04 [t {³J(H,H) 7.70 Hz}, 1H, *H*_{meta'}], 6.68 [d {³J(H,H) 7.38 Hz}, 1H, *H*_{ortho'}], 6.51 [d {³J(H,H)

7.94 Hz}, 1H, H_{para}], 3.51 (s, 3H, OCH₃), 3.41-3.18 [m, 3H, CH₂ (Ethyl)], 3.01 [m, 1H, CH₂ (Ethyl)], 2.04 [m, 1H, γ -CH₂ (TMP)], 1.84 [s, 5H, γ -CH₂ (TMP) and NCH₂ (TMEDA)], 1.77 [s, 12H, NCH₃ (TMEDA)], 1.62 [s, 3H, CH₃ (TMP)], 1.59 [s, 3H, CH₃ (TMP)], 1.46 [s, 9H, C(CH₃)₃ (*t*Bu)], 1.34 [m, 2H, β -CH₂ (TMP)] 1.31 [s, 3H, CH₃ (TMP)], 1.28 [s, 3H, CH₃ (TMP)], 1.02 [t {³J(H,H) 7.13 Hz}, 3H, CH₃ (Ethyl)], 0.81 [t {³J(H,H) 7.13 Hz}, 3H, CH₃ (Ethyl)]. *From 2D HSQC and COSY experiments, the second β -CH₂ (TMP) resonance appears to be masked by the TMEDA signals around 1.82 ppm. ¹³C {¹H} NMR (100.62 MHz, 300 K, *d*₆-benzene): δ 177.4 (C=O), 167.9 (*C*_{ortho}-Zn), 155.3 and 146.3 (*C*_{ipso} and *C*_{meta}), 125.6 (*C*_{meta}), 117.1 (*C*_{ortho}), 107.1 (*C*_{para}), 57.4 [NCH₂ (TMEDA)], 53.9 (OCH₃), 53.2 [2 x α -C (TMP)], 45.7 [NCH₃ (TMEDA)], 43.6 [CH₂ (Ethyl)], 41.8 [β -CH₂ (TMP)], 41.2 [β -CH₂ (TMP)], 38.3 [CH₂ (Ethyl)], 36.6 [CH₃ (TMP)], 35.8 [C(CH₃)₃ (*t*Bu)], 35.6 [CH₃ (TMP)], 35.5 [CH₃ (TMP)], 33.0 [CH₃ (TMP)], 20.4 [γ -CH₂ (TMP)], 19.6 [C(CH₃)₃ (*t*Bu)], 13.9 [CH₃ (Ethyl)], 12.9 [CH₃ (Ethyl)].

Crystal data for **3**: C₃₁H₅₉N₄NaO₂Zn, *M* = 608.18, monoclinic, *P*2₁/*c*, *a* = 16.3094(2) Å, *b* = 10.3360(2) Å, *c* = 20.8204(4) Å, β = 98.105(2)°, *V* = 3474.72(10) Å³, *Z* = 4. 34313 reflections collected, 10077 were unique, *R*_{int} = 0.0345, *R* = 0.0326, *R*_w = 0.0723, GOF = 0.923, 366 refined parameters, max. and min. Residual electron density = 0.505 and -0.392 e·Å⁻³.

Synthesis of [(TMEDA)Na(μ -TMP){ μ -2-(1-OC(O)NEt₂)-C₆H₄}-Zn(*t*Bu)] **4**

To a hexane solution of **1** was introduced *N,N*-diethyl phenyl *O*-carbamate (0.386 g, 2 mmol), and the reaction mixture was allowed to stir at ambient temperature for 18 hours. The yellow solution was concentrated by the removal of solvent *in vacuo* and then subsequently transferred to a refrigerator (at 5 °C), where colourless crystals were

deposited (0.45 g, 38%). Mp: 126-128 °C. ^1H NMR (400.13 MHz, 300 K, d_6 -benzene): δ 7.73 (d, 1H, H_{meta}), 7.13 (m, 1H, H_{para}), 7.05 (t, 1H, $H_{meta'}$), 6.78 [d { $^3\text{J}(\text{H,H})$ 7.68 Hz}, 1H, $H_{ortho'}$], 3.29-2.98 [m, 3H, CH_2 (Ethyl)], 2.89 [m, 1H, CH_2 (Ethyl)], 1.96 [m, 2H, $\gamma\text{-CH}_2$ (TMP)], 1.85 [s, 4H, NCH_2 (TMEDA)], 1.78 [s, 12H, NCH_3 (TMEDA)], 1.60 [br, 4H, $\beta\text{-CH}_2$ (TMP)], 1.53 [s, 9H, $\text{C}(\text{CH}_3)_3$ (*t*Bu)], 1.38-1.26 [br, 9H, CH_3 (TMP)], 1.00 [t { $^3\text{J}(\text{H,H})$ 7.13 Hz}, 3H, CH_3 (Ethyl)], 0.89 [t { $^3\text{J}(\text{H,H})$ 7.13 Hz}, 3H, CH_3 (Ethyl)]. ^{13}C { ^1H } NMR (100.62 MHz, 300 K, d_6 -benzene): δ 159.9 (C=O), 159.4 ($C_{ortho}\text{-Zn}$), 158.5 (C_{ipso}), 140.4 (C_{meta}), 126.3 ($C_{meta'}$), 125.1 (C_{para}), 119.6 ($C_{ortho'}$), 57.5 [NCH_2 (TMEDA)], 52.6 [$\alpha\text{-C}$ (TMP)], 45.6 [NCH_3 (TMEDA)], 41.9 [2 x CH_2 (Ethyl)], 40.1 [$\beta\text{-CH}_2$ (TMP)], 35.1 [$\text{C}(\text{CH}_3)_3$ (*t*Bu)], 35.0 [CH_3 (TMP)], 20.4 [$\gamma\text{-CH}_2$ (TMP)], 20.0 [$\text{C}(\text{CH}_3)_3$ (*t*Bu)], 14.0 [CH_3 (Ethyl)], 13.3 [CH_3 (Ethyl)].

Crystal data for **4**: $\text{C}_{30}\text{H}_{57}\text{N}_4\text{NaO}_2\text{Zn}$, $M = 594.16$, monoclinic, $P2_1/c$, $a = 18.2070(4)$ Å, $b = 10.3460(2)$ Å, $c = 19.9460(4)$ Å, $\beta = 116.629(3)^\circ$, $V = 3358.68(12)$ Å³, $Z = 4$; 27340 reflections collected, 8907 were unique, $R_{\text{int}} = 0.0304$, $R = 0.0287$, $R_w = 0.0602$, GOF = 0.894, 393 refined parameters, max. and min. residual electron density = 0.389 and -0.271 e \cdot Å⁻³.

Electrophilic Quenching Reactions

An *in situ* hexane solution of the previously reported zincate **1** (2 mmol) was prepared as described above. The organic substrate (2 mmol) was then added to the base, and the reaction mixtures were allowed to stir at ambient temperature for 18 hours. The resultant solutions were treated with a freshly prepared solution of 1 M iodine in THF (6 mL, 6 mmol) and allowed to stir for 2 hours. A 5 mL amount of NH_4Cl was added along with the addition of saturated $\text{Na}_2\text{S}_2\text{O}_3$ until bleaching occurred (5 mL). The organic layer was separated from the aqueous layer and dried over magnesium sulfate

for 1 hour. After filtration, the solvent was removed under vacuum to give a light yellow oil. The NMR spectrum of the crude material was obtained to determine the yield of the iodo-product relative to unreacted starting material.

***N, N*-diethyl-2-iodobenzamide**: Yield: >99%. ^1H NMR (400.13 MHz, 300 K, d_6 -benzene): δ 7.52 (d, 1H, H_{meta}), 6.90 (m, 2H, H_{para} and $H_{ortho'}$), 6.54 (t, 1H, $H_{meta'}$), 3.70 [br, 1H, CH_2 (Ethyl)], 3.04 [br, 1H, CH_2 (Ethyl)], 2.75 [m, 2H, CH_2 (Ethyl)], 1.14 [t $\{^3\text{J}(\text{H,H})$ 7.13 Hz}, 3H, CH_3 (Ethyl)], 0.65 [t $\{^3\text{J}(\text{H,H})$ 7.13 Hz}, 3H, CH_3 (Ethyl)].

***N, N*-diethyl-2-iodo-3-methoxybenzamide**: Yield: 70.8%. ^1H NMR (400.13 MHz, 300 K, d_6 -benzene): δ 6.89 [t $\{^3\text{J}(\text{H,H})$ 7.78 Hz, 1H, H_{meta}], 6.69 (d, 1H, $H_{ortho'}$), 6.15 (d, 1H, H_{para}), 3.77 [m, 1H, CH_2 (Ethyl)], 3.18 [s, 3H, OCH_3], 3.03 [m, 1H, CH_2 (Ethyl)], 2.86 [m, 1H, CH_2 (Ethyl)], 2.75 [m, 1H, CH_2 (Ethyl)], 1.17 [t $\{^3\text{J}(\text{H,H})$ 7.14 Hz}, 3H, CH_3 (Ethyl)], 0.68 [t $\{^3\text{J}(\text{H,H})$ 7.14 Hz}, 3H, CH_3 (Ethyl)].

***N, N*-diethyl-2-iodophenyl-*O*-carbamate**: Yield: 74.9%. ^1H NMR (400.13 MHz, 300 K, d_6 -benzene): δ 7.54 (d, 1H, H_{meta}), 7.06 (d, 1H, $H_{ortho'}$), 6.92 (t, 1H, H_{para}), 6.45 (t, 1H, $H_{meta'}$), 3.17 [m, 4H, CH_2 (Ethyl)], 1.07 [t $\{^3\text{J}(\text{H,H})$ 7.13 Hz}, 3H, CH_3 (Ethyl)], 0.97 [t $\{^3\text{J}(\text{H,H})$ 7.13 Hz}, 3H, CH_3 (Ethyl)].

Synthesis of [(TMEDA)Na(μ -TMP){ μ -2-(1- CH_2OMe)- C_6H_4] $\text{Zn}(t\text{Bu})$] **5**

To a hexane solution of **1** benzyl methyl ether (0.24 mL, 2 mmol) was added and the reaction mixture was allowed to stir at ambient temperature for 12 hours. The resulting orange solution was concentrated *in vacuo*, preceding the growth of large colourless crystals of **5** (0.51 g, 49%). Anal: actual C 61.99, H 10.02, N 8.03; found C 61.04, H 10.00, N 7.74%. ^1H NMR (400.13 MHz, 300 K, d_{12} -cyclohexane): δ 7.59 [d $\{^3\text{J}(\text{H,H})$ 7.01 Hz}, 1H, H_{meta}], 7.01 (m, 2H, H_{para} and $H_{meta'}$), 6.90 (m, 1H, $H_{ortho'}$), 4.48 [d

$\{^3J(\text{H,H})\ 8.60\ \text{Hz}\}$, 1H, PhCH], 4.07 [d $\{^3J(\text{H,H})\ 8.54\ \text{Hz}\}$, 1H, PhCH], 3.43 (s, 3H, OCH₃), 2.10 [br s, 4H, NCH₂ (TMEDA)], 1.83 [br s, 12H, NCH₃ (TMEDA)], 1.75 [m, 2H, γ -CH₂ (TMP)], 1.38 [m, 4H, β -CH₂ (TMP) (observed by COSY NMR spectroscopy)], 1.34 [s, 3H, CH₃ (TMP)], 1.29 [s, 3H, CH₃ (TMP)], 1.16 [s, 3H, CH₃ (TMP)], 1.14 [s, 3H, CH₃ (TMP)], 0.84 [s, 9H, CH₃ (*t*Bu)]. ¹³C $\{^1\text{H}\}$ NMR (100.62 MHz, 300 K, *d*₁₂-cyclohexane): δ 172.0 (*C*_{ortho}-Zn), 145.3 (*C*_{ipso}), 140.8 (*C*_{meta}), 129.0 (*C*_{para} or *C*_{meta'}), 126.8 (*C*_{para} or *C*_{meta'}), 125.2 (*C*_{ortho'}), 84.2 (PhCH₂), 59.1 (OCH₃), 58.3 [NCH₂ (TMEDA)], 53.4 [α -C (TMP)], 52.9 [α -C (TMP)], 46.2 [NCH₃ (TMEDA)], 41.0 [β -CH₂ (TMP)], 40.0 [β -CH₂ (TMP)], 37.4 [CH₃ (TMP)], 36.0 [CH₃ (TMP)], 35.5 [CH₃ (TMP)], 35.0 [CH₃ (TMP)], 34.6 [C(CH₃)₃ (*t*Bu)], 20.5 [γ -CH₂ (TMP)], 20.1 [C(CH₃)₃ (*t*Bu)].

Crystal data for **5**: C₂₇H₅₂N₃NaOZn, *M* = 523.08, monoclinic, P2(1), *a* = 9.236(2) Å, *b* = 16.527(2) Å, *c* = 10.6095(19) Å, β = 114.39(3)°, *V* = 1475.0(5) Å³, *Z* = 2; 13428 reflections collected, 7511 were unique, *R*_{int} = 0.0261, *R* = 0.0309, *R*_w = 0.0658, GOF = 0.973, 311 refined parameters, max. and min. residual electron density = 0.599 and -0.295 e⁻Å⁻³.

Electrophilic Quenching Reactions

1-iodo-2-(methoxymethyl)benzene: An *in situ* hexane solution of the previously reported zincate **1** (2 mmol) was prepared as described above. Benzyl methyl ether (1 or 2 mmol) was then added to the base. The yellow solution was allowed to stir at ambient temperature for 48 hours. The resultant orange solution was treated with a freshly prepared solution of 1 M iodine in THF (4 mL, 4 mmol). Distilled water was then introduced. The organic phase was washed three times before being dried over MgSO₄. The NMR spectrum of the crude material was obtained to determine the yield of the

iodo-product relative to benzyl methyl ether. Yields of 1-iodo-2-(methoxymethyl)benzene were 88% and 59% when 1 mmol and 2 mmol of benzyl methyl ether, respectively were utilised. No other organic iodine-containing compounds were detected. ^1H NMR (400.13 MHz, 300 K, d_6 -benzene): δ 7.62 (d, 1H, H_{meta}), 7.38 [d { $^3\text{J}(\text{H,H})$ 7.64 Hz}, 1H, $H_{ortho'}$], 7.00 (t, 1H, $H_{meta'}$), 6.56 (t, 1H, H_{para}), 4.27 (s, 2H, PhCH_2), 3.10 (s, 3H, OCH_3).

Synthesis of [(TMEDA)Na $\{\mu$ -3,5-(2-C(O)NEt $_2$)-C $_4$ H $_1$ S}Zn(*t*Bu)] $_4$

Crystalline zincate **1** (0.45 g, 1 mmol) was dissolved in 2.5 mL benzene at room temperature producing a yellow solution. *N,N*-diethyl thiophene-2-carboxamide (0.18 g, 1 mmol) was introduced resulting in an instant colour change. The deep red solution was left standing for 72 hours depositing yellow crystalline material (0.21 g, 47%). ^1H NMR (400.13 MHz, 300 K, d_8 -toluene): δ 7.92 [s, 1H, $H_{(C4)}$], 3.86 [m, 1H, CH_2 (Ethyl)], 3.59 [m, 1H, CH_2 (Ethyl)], 3.43 [m, 2H, CH_2 (Ethyl)], 1.79 [br, 16H, NCH_3 & NCH_2 (TMEDA)], 1.57 [s, 9H, CH_3 (*t*Bu)], 1.23 [t { $^3\text{J}(\text{H,H})$ 7.44 Hz}, 6H, CH_3 (Ethyl)]. ^{13}C { ^1H } NMR (100.62 MHz, 300 K, d_8 -toluene): δ 176.4 (C=O), 173.0 [$\text{C}(2)$], 165.1 [$\text{C}(5)$], 145.9 [$\text{C}(4)$], 137.5 [$\text{C}(3)$], 56.8 [NCH_2 (TMEDA)], 44.9 [NCH_3 (TMEDA)], 44.0 [CH_2 (Ethyl)], 40.7 [CH_2 (Ethyl)], 35.1 [$\text{C}(\text{CH}_3)_3$ (*t*Bu)], 21.4 [$\text{C}(\text{CH}_3)_3$ (*t*Bu)], 14.9 [CH_3 (Ethyl)], 13.2 [CH_3 (Ethyl)].

Crystal data: $\text{C}_{76}\text{H}_{144}\text{N}_{12}\text{Na}_4\text{O}_4\text{S}_4\text{Zn}_4$, $M = 1771.71$, tetragonal, P4 $_2$ /n, $a = 21.2868(6)$ Å, $b = 21.2868(6)$ Å, $c = 12.2233(4)$ Å, $V = 5538.7(2)$ Å 3 , $Z = 2$; 5435 reflections collected, 5435 were unique, $R_{\text{int}} = 0.0000$, $R = 0.0607$, $R_w = 0.1709$, GOF = 1.017, 274 refined parameters, max. and min. residual electron density = 0.508 and -0.490 e \cdot Å $^{-3}$.

Recrystallisation of [(D)Na{ μ -3,5-(2-C(O)NEt₂)-C₄H₁S}Zn(*t*Bu)}]₄ **6****(where D is THF or TMEDA)**

The above prepared crystalline material (0.18 g, 0.1 mmol) was dissolved in 1.5 mL THF and stirred for 30 minutes before introducing hexane (~ 2.5 mL) until turbidity occurred. The Schlenk tube was transferred to the freezer where yellow crystalline material was produced (0.06 g, 31%). ¹H NMR (400.13 MHz, 300 K, *d*₈-toluene): δ 7.85 [s, 1H, *H*_(C4)], 3.92 [m, 1H, CH₂ (Ethyl)], 3.59-3.40 [m, 7H, CH₂ (Ethyl) and α -CH₂ (THF)], 1.78 [br, 9H, NCH₃ and NCH₂ (TMEDA)], 1.57 [s, 9H, CH₃ (*t*Bu)], 1.47 [br, 4H, β -CH₂ (THF)], 1.24 [t {³J(H,H) 7.28 Hz}, 6H, CH₃ (Ethyl)]. ¹³C {¹H} NMR (100.62 MHz, 300 K, *d*₈-toluene): δ 176.3 (C=O), 173.1 [C(2)], 164.8 [C(5)], 145.9 [C(4)], 137.5 [C(3)], 67.8 [α -CH₂ (THF)], 56.7 [NCH₂ (TMEDA)], 44.9 [NCH₃ (TMEDA)], 44.1 [CH₂ (Ethyl)], 40.7 [CH₂ (Ethyl)], 35.1 [C(CH₃)₃ (*t*Bu)], 21.4 [C(CH₃)₃ (*t*Bu)], 14.9 [CH₃ (Ethyl)], 13.2 [CH₃ (Ethyl)]. ¹H NMR donor solvent integrals vary due to the mixture previously discussed.

Crystal data for **6**: C_{87.36}H₁₆₀N_{8.64}Na₄O_{9.36}S₄Zn₄, *M* = 1962.81, monoclinic, C 2/c, *a* = 32.9619(8) Å, *b* = 12.4438(3) Å, *c* = 29.2420(7) Å, β = 118.645(3)°, *V* = 10526.2(4) Å³, *Z* = 4; 46910 reflections collected, 12035 were unique, *R*_{int} = 0.0345, *R* = 0.0586, *R*_w = 0.1770, GOF = 1.057, 622 refined parameters, max. and min. residual electron density = 0.851 and -0.677 e·Å⁻³.

Electrophilic quenching reactions

***N, N*-diethyl-5-iodothiophene-2-carboxamide**: Crystalline zincate **1** (0.92 g, 2 mmol) was dissolved in 5 mL THF and *N, N*-diethyl thiophene-2-carboxamide (0.37 g, 2 mmol) was added with the yellow solution allowed to stir at ambient temperature for 2 hours. The resultant solutions were treated with a freshly prepared solution of 1 M

iodine in THF (7 mL, 7 mmol) and allowed to stir for 2 hours. A 5 mL amount of NH_4Cl was added along with the addition of saturated $\text{Na}_2\text{S}_2\text{O}_3$ until bleaching occurred (5 mL). The organic layer was separated from the aqueous layer and dried over magnesium sulfate for 1 hour. After filtration, the solvent was removed under vacuum to give a light yellow oil. This was dissolved in a minimum amount of dichloromethane, which was purified by SiO_2 column chromatography with hexane/ethyl acetate (10:1) as the eluant to give *N, N*-diethyl-5-iodothiophene-2-carboxamide (0.49 g, 79%). ^1H NMR (400.13 MHz, 300 K, *d*-chloroform): δ 7.19 [d $\{^3\text{J}(\text{H,H})$ 3.83 Hz}, 1H, $H_{(C3)}$], 6.99 [d $\{^3\text{J}(\text{H,H})$ 3.83 Hz}, 1H, $H_{(C4)}$], 3.52 [q $\{^3\text{J}(\text{H,H})$ 7.12 Hz}, 4H, CH_2 (Ethyl)], 1.24 [t $\{^3\text{J}(\text{H,H})$ 7.10 Hz}, 6H, CH_3 (Ethyl)]. ^{13}C $\{^1\text{H}\}$ NMR (100.62 MHz, 300 K, *d*-chloroform): δ 162.3 (C=O), 144.3 [C(2)], 136.6 [C(3)], 129.6 [C(4)], 77.9 [C(5)], 42.1 [CH_2 (Ethyl)], 13.6 [CH_3 (Ethyl)].

***N, N*-diethyl-3,5-diiodothiophene-2-carboxamide:** Crystalline zincate **1** (0.92 g, 2 mmol) was dissolved in 5 mL benzene and *N, N*-diethyl thiophene-2-carboxamide (0.37 g, 2 mmol) was added with the red solution allowed to stir at ambient temperature for 72 hours. The resultant solutions were treated with a freshly prepared solution of 1 M iodine in THF (8 mL, 8 mmol) and allowed to stir for 2 hours. A 5 mL amount of NH_4Cl was added along with the addition of saturated $\text{Na}_2\text{S}_2\text{O}_3$ until bleaching occurred (5 mL). The organic layer was separated from the aqueous layer and dried over magnesium sulfate for 1 hour. After filtration, the solvent was removed under vacuum to give a yellow oil. This was dissolved in a minimum amount of dichloromethane, which was purified by SiO_2 column chromatography with hexane/ethyl acetate (10:1) as the eluant to give *N, N*-diethyl-3,5-diiodothiophene-2-carboxamide (0.47 g, 54%). ^1H NMR (400.13 MHz, 300 K, *d*-chloroform): δ 7.15 [s, 1H, $H_{(C4)}$], 3.43 [br, 4H, CH_2 (Ethyl)], 1.20 [br, 6H, CH_3 (Ethyl)]. ^{13}C $\{^1\text{H}\}$ NMR (100.62 MHz, 300 K, *d*-

chloroform): δ 162.5 (C=O), 143.1 [C(2)], 143.1 [C(4)], 78.7 [C(3)], 75.2 [C(5)], 43.1 [CH₂ (Ethyl)], 40.1 [CH₂ (Ethyl)], 13.4 [CH₃ (Ethyl)].

Chapter 2 - References

- [1] K. Godula, D. Sames, *Science* **2006**, *312*, 67 - 72.
- [2] (a) G. C. Hartung, V. Snieckus, in *Modern Arene Chemistry: Astruc, D., Ed.*, Wiley-VCH: New York, **2002**; (b) T. Macklin, V. Snieckus, in *Handbook of C-H Transformations; Dyker, G., Ed.*, Wiley-VCH: New York, **2005**; (c) J. Clayden, in *Organolithiums: Selectivity for Synthesis*, Pergamon, Elsevier Science: Oxford, **2002**.
- [3] (a) H. Gilman, R. L. Bebb, *J. Am. Chem. Soc.* **1939**, *61*, 109 - 112; (b) G. Wittig, G. Fuhrmann, *Ber. Dtsch. Chem. Ges.* **1940**, *73*, 1197 - 1218.
- [4] (a) P. Beak, R. A. Brown, *J. Org. Chem.* **1982**, *47*, 34 - 46; (b) T. G. Gant, A. I. Meyers, *Tetrahedron* **1994**, *50*, 2297 - 2360; (c) P. Beak, V. Snieckus, *Acc. Chem. Res.* **1982**, *15*, 306 - 312; (d) V. Snieckus, *Chem. Rev.* **1990**, *90*, 879 - 933.
- [5] F. N. Jones, M. F. Zinn, C. R. Hauser, *J. Org. Chem.* **1963**, *28*, 663 - 665.
- [6] D. W. Slocum, C. A. Jennings, *J. Org. Chem.* **1976**, *41*, 3653 - 3664.
- [7] M. C. Whisler, S. MacNeil, V. Snieckus, P. Beak, *Angew. Chem. Int. Ed.* **2004**, *43*, 2206 - 2225.
- [8] (a) N. S. Narasimhan, R. S. Mali, *Synthesis* **1983**, 957 - 986; (b) J. Clayden, C. S. Frampton, C. McCarthy, N. Westlund, *Tetrahedron* **1999**, *55*, 14161 - 14184 and references therein.
- [9] J. C. Riggs, K. J. Singh, M. Yun, D. B. Collum, *J. Am. Chem. Soc.* **2008**, *130*, 13709 - 13717.
- [10] W. H. Puterbaugh, C. R. Hauser, *J. Org. Chem.* **1964**, *29*, 853 - 856.
- [11] P. Beak, G. R. Brubaker, R. F. Farney, *J. Am. Chem. Soc.* **1976**, *98*, 3621 - 3627.
- [12] H. W. Gschwend, H. R. Rodriguez, *Org. React.* **1979**, *26*, 1 - 360.
- [13] P. Beak, R. A. Brown, *J. Org. Chem.* **1977**, *42*, 1823 - 1824.
- [14] W. Clegg, S. H. Dale, R. W. Harrington, E. Hevia, G. W. Honeyman, R. E. Mulvey, *Angew. Chem. Int. Ed.* **2006**, *45*, 2374 - 2377.
- [15] U. Schumann, U. Behrens, E. Weiss, *Angew. Chem. Int. Ed.* **1989**, *28*, 476 - 477.
- [16] K. Izod, J. C. Stewart, W. Clegg, R. W. Harrington, *Dalton Trans.*, **2007**, 257 - 264.

- [17] M. Steigelmann, Y. Nisar, F. Rominger, B. Goldfuss, *Chem. Eur. J.* **2002**, *8*, 5211 - 5218.
- [18] M. G. Gardiner, S. M. Lawrence, C. L. Raston, B. W. Skelton, A. H. White, *Chem. Commun.* **1996**, 2491 - 2492.
- [19] E. Bukhaltsev, I. Goldberg, A. Vigalok, *Organometallics* **2005**, *24*, 5732 - 5736.
- [20] M. P. Sibi, V. Snieckus, *J. Org. Chem.* **1983**, *48*, 1935 - 1937.
- [21] F. García, M. McPartlin, J. V. Morey, D. Nobuto, Y. Kondo, H. Naka, M. Uchiyama, A. E. H. Wheatley, *Eur. J. Org. Chem.* **2008**, 644 - 647.
- [22] P. C. Andrikopoulos, D. R. Armstrong, H. R. L. Barley, W. Clegg, S. H. Dale, E. Hevia, G. W. Honeyman, A. R. Kennedy, R. E. Mulvey, *J. Am. Chem. Soc.* **2005**, *127*, 6184 - 6185.
- [23] D. R. Armstrong, J. García-Álvarez, D. V. Graham, G. W. Honeyman, E. Hevia, A. R. Kennedy, R. E. Mulvey, *Chem. Eur. J.* **2009**, *15*, 3800 - 3807.
- [24] CSD version 5.31 see: F. H. Allen, *Acta Crystallogr., Sect. B* **2002**, *58*, 380 - 388.
- [25] *ortho*-Metallated ArPdI where Ar is [C₆H₄{OC(O)N(Me)-(CH₂CH=CH₂)}] has been prepared as the bis(PPh₃) solvate via oxidative addition; see: G. Bocelli, M. Catellani, G. P. Chiusoli, F. Cugini, B. Lasagni, M. N. Mari, *Inorg. Chim. Acta.* **1998**, *270*, 123 -129.
- [26] G. W. Klumpp, *Rec. Trav. Chim. Pays-Bas* **1986**, *105*, 1 - 21.
- [27] L. M. Hogg, PhD thesis, University of Strathclyde (Glasgow), **2009**.
- [28] U. Schöllkopf, *Angew. Chem. Int. Ed.* **1970**, *18*, 763 - 773.
- [29] (a) U. Azzena, L. Pilo, A. Sechi, *Tetrahedron* **1998**, *54*, 12389 - 12398; (b) U. Azzena, L. Pilo, E. Piras, *Tetrahedron* **2000**, *56*, 3775 - 3780; (c) U. Azzena, L. Pisano, S. Mocci, *J. Organomet. Chem.*, **2009**, *694*, 3619 - 3625.
- [30] A. Toshimitsu, T. Saeki, K. Tamao, *Chem. Lett.*, **2002**, 278 - 279.
- [31] H. Gilman, W. J. Meikle, J. W. Morton Jr, *J. Am. Chem. Soc.* **1952**, *74*, 6282 - 6284.
- [32] R. Jambor, L. Dostál, I. Císařová, A. Růžička, J. Holeček, *Inorg. Chim. Acta.* **2005**, *358*, 2422 - 2426.
- [33] Y. Kondo, M. Shilai, M. Uchiyama, T. Sakamoto, *J. Am. Chem. Soc.* **1999**, *121*, 3539 - 3540.
- [34] R. E. Mulvey, F. Mongin, M. Uchiyama, Y. Kondo, *Angew. Chem. Int. Ed.* **2007**, *46*, 3802 - 3824.

- [35] J. F. Biellman, J. B. Ducep, *Org. React.* **1982**, *27*, 1 - 344.
- [36] (a) R. D. McCullough, *Adv. Mater.* **1998**, *10*, 93 - 116; (b) I. Osaka, R. D. McCullough, *Acc. Chem. Res.* **2008**, *41*, 1202 - 1214.
- [37] S. Tanaka, S. Tamba, D. Tanaka, A. Sugie, A. Mori, *J. Am. Chem. Soc.* **2011**, *133*, 16734 - 16737.
- [38] (a) R. Romagnoli, P. G. Baraldi, M. D. Carrion, C. L. Cara, O. Cruz-Lopez, M. A. Iaconinoto, D. Preti, J. C. Shryock, A. R. Moorman, F. Vincenzi, K. Varani, P. A. Borea, *J. Med. Chem.* **2008**, *51*, 5875 - 5879; (b) L. Aurelio, H. Figler, B. L. Flynn, J. Linden, P. J. Scammells, *Bioorg. Med. Chem.* **2008**, *16*, 1319 - 1327.
- [39] E. Lamb, *Pharm. Times* **2008**, (May), 20.
- [40] M. Shilai, Y. Kondo, T. Sakamoto, *J. Chem. Soc., Perkin Trans. 1*, **2001**, 442 - 444.
- [41] (a) A. Krasovskiy, V. Krasovskaya, P. Knochel, *Angew. Chem. Int. Ed.* **2006**, *45*, 2958 - 2961; (b) F. M. Piller, P. Knochel, *Org. Lett.* **2009**, *11*, 445 - 448.
- [42] (a) D. W. H. MacDowell, T. B. Patrick, *J. Org. Chem.* **1966**, *31*, 3592 - 3595; (b) M. Watanabe, V. Snieckus, *J. Am. Chem. Soc.* **1980**, *102*, 1457 - 1460.
- [43] (a) L. DellaVecchia, I. Vlattas, *J. Org. Chem.* **1977**, *42*, 2649 - 2650; (b) D. J. Chadwick, M. V. McKnight, R. Ngochindo, *J. Chem. Soc., Perkin Trans. 1*, **1982**, 1343 - 1349.
- [44] E. G. Doadt, V. Snieckus, *Tetrahedron. Lett.* **1985**, *26*, 1149 - 1152.
- [45] D. J. Chadwick, A. J. Carpenter, *J. Org. Chem.* **1985**, *50*, 4362 - 4368.
- [46] T. Grimaldi, M. Romero, M. D. Pujol, *Synlett* **2000**, *12*, 1788 - 1792.
- [47] R. W. Saalfrank, S. Trummer, U. Reimann, M. M. Chowdhry, F. Hampel, O. Waldmann, *Angew. Chem. Int. Ed.* **2000**, *39*, 3492 - 3494.
- [48] V. L. Blair, A. R. Kennedy, J. Klett, R. E. Mulvey, *Chem. Commun.* **2008**, 5426 - 5428.
- [49] (a) W. Clegg, S. H. Dale, A. M. Drummond, E. Hevia, G. W. Honeyman, R. E. Mulvey, *J. Am. Chem. Soc.* **2006**, *128*, 7434 - 7435; (b) W. Clegg, J. García-Álvarez, P. García-Álvarez, D. V. Graham, R. W. Harrington, E. Hevia, A. R. Kennedy, R. E. Mulvey, L. Russo, *Organometallics* **2008**, *27*, 2654 - 2663.
- [50] A. L. Spek, N. Veldman, *Cambridge Crystallographic Database (Private Communication)* **1999**.

- [51] D. R. Powell, W. L. Whipple, H. J. Reich, *Acta Crystallogr., Sect. C: Cryst. Struct. Commun.* **1996**, *52*, 1346 - 1348.
- [52] A. L. Spek, *Cambridge Crystallographic Database (Private Communication)* **1999**.
- [53] C. Selinka, D. Stalke, *Z. Naturforsch., B: Chem. Sci.* **2003**, *58*, 291 - 298.
- [54] K. L. Jantzi, C. L. Pluckett, I. A. Guzei, H. J. Reich, *J. Org. Chem.* **2005**, *70*, 7520 - 7529.
- [55] A. L. Spek, W. J. J. Smeets, *Cambridge Crystallographic Database (Private Communication)* **1999**.
- [56] A. L. Spek, M. T. Lakin, R. Den Besten, *Cambridge Crystallographic Database (Private Communication)* **1999**.
- [57] V. L. Blair, A. R. Kennedy, R. E. Mulvey, C. T. O'Hara, *Chem. Eur. J.* **2010**, *16*, 8600 - 8604.
- [58] O. Bayh, H. Awad, F. Mongin, C. Hoarau, F. Trécourt, G. Quéguiner, F. Marsais, F. Blanco, B. Abarca, R. Ballesteros, *Tetrahedron* **2005**, *61*, 4779 - 4784.
- [59] D. R. Armstrong, W. Clegg, S. H. Dale, D. V. Graham, E. Hevia, L. M. Hogg, G. W. Honeyman, A. R. Kennedy, R. E. Mulvey, *Chem. Commun.* **2007**, 598 - 600.
- [60] (a) T. Imahori, M. Uchiyama, T. Sakamoto, Y. Kondo, *Chem. Commun.* **2001**, 2450 - 2451; (b) M. Uchiyama, Y. Kobayashi, T. Furuyama, S. Nakamura, Y. Kajihara, T. Miyoshi, T. Sakamoto, Y. Kondo, K. Morokuma, *J. Am. Chem. Soc.* **2008**, *130*, 472 - 480.
- [61] E. Baston, R. Maggi, K. Friedrich, M. Schlosser, *Eur. J. Org. Chem.* **2001**, 3985 - 3989.

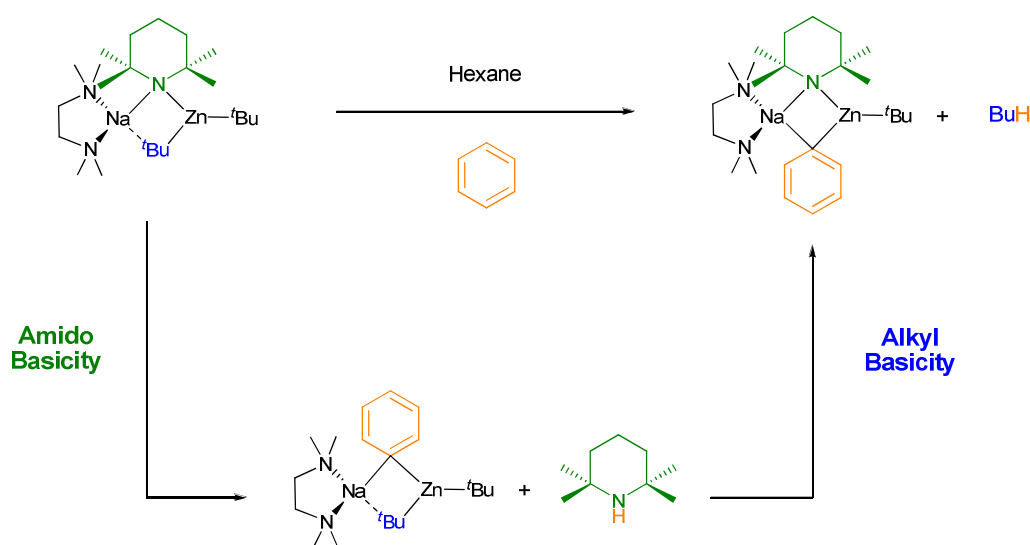
Chapter 3: Case Study – The Metallation Chemistry of *N, N*-dimethylaniline

3.1) Uncovering Synergic Surprises

As discussed in the previous chapter, Directed-*ortho*-Metallation (DoM) serves as a pioneering methodology in the production of substituted aromatic rings with versed heteroatom-containing functional groups ensuring excellent regio-control. However, by channelling the special synergic chemistry of sodium TMP-zincates, it is possible in certain cases to overcome DoM effects and direct metallation to more remote positions. Particularly germane to this work, we previously reported that *N, N*-dimethylaniline can be monozincated by the sodium zincate base [(TMEDA)Na(μ -TMP)(μ -*t*Bu)Zn(*t*Bu)] (**1**) at the normally inaccessible *meta*-position;^[1] while the group of Trahanovsky showed that complexation of *N, N*-dimethylaniline with Cr(CO)₃ leads to a mixture of *ortho*-, *meta*- and *para*-deprotonation upon lithiation.^[2] In general, other situations of *meta*-deprotonation require a special combination of substituents on the aromatic ring. Such situations, which because of the multiple substitution limit the number of sites available for deprotonation, are usually dictated by steric constraints and therefore should be clearly distinguished from mono-substituted aromatic rings in which *meta*-deprotonation is exceedingly more difficult to realise.^[3]

Another example of a synergic metallation can be found with the best known alkyl arene toluene. With conventional metallating reagents such as the activated alkyllithium *n*BuLi·TMEDA, toluene is normally deprotonated at the methyl (lateral) site to generate the resonance stabilised benzyl “carbanion” (PhCH₂⁻).^[4] In contrast, toluene has been directly zincated by reaction with the heteroleptic sodium zincate **1** to afford a statistical mixture of the *meta*- and *para*-regioisomers of [(TMEDA)Na(μ -TMP)(μ -C₆H₄-CH₃)Zn(*t*Bu)] with the methyl substituent retaining its three hydrogen atoms.^[5]

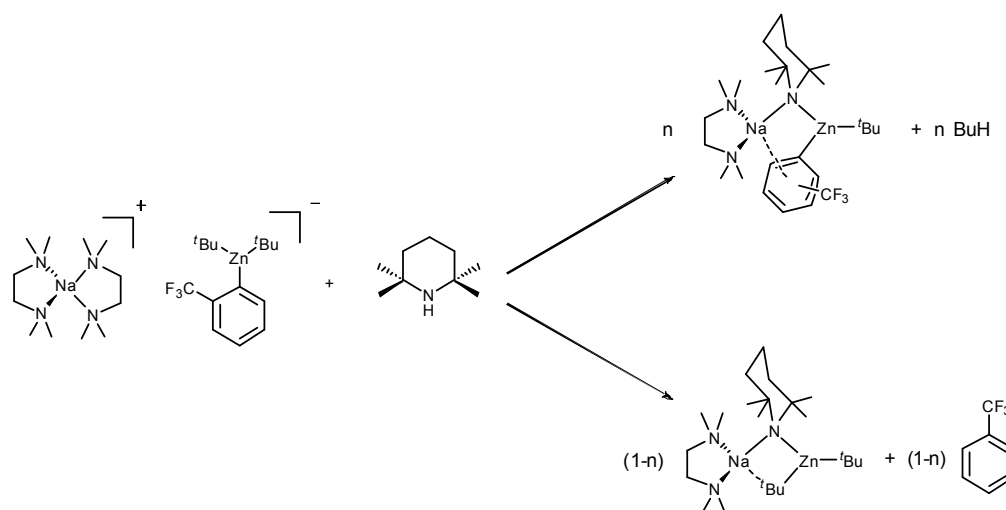
The structural insight offered by these synthetic findings has been augmented by a complementary theoretical study. Filling in the gaps between the crystallographically characterised starting materials and the thermodynamic final products, Uchiyama and Nobuto have deciphered the possible reaction pathways of the deprotonative metallation of benzene with sodium TMP-zincate **1** computationally.^[6] Their DFT calculations propose that these distinctive deprotonations proceed via a step-wise mechanism, whereby zincate **1** serves kinetically as an amide base (due to the greater kinetic lability of the Zn-N bonds) with concomitant release of TMP(H) with the formation of a bisalkyl(aryl) zincate intermediate (Scheme 3.1). In the second step, it follows that the co-existent, strongly acidic N-H bond of TMP(H) is deprotonated by this intermediate to afford the final thermodynamic product of the reaction identified by the aforementioned X-ray crystallographic studies, and isobutane.



Scheme 3.1: Proposed two-step mechanism for the zincation of benzene.

Recently, our group have sought to identify the structures of the reaction intermediates suggested by the theoretical studies. In addition to a closely related study for the AMMZn of anisole by the analogous lithium TMP-zincate [(THF)Li(μ -TMP)(μ -tBu)Zn(tBu)],^[7] these mechanistic and structural studies were then extended to the

metallation of trifluoromethylbenzene by the bimetallic base **1** (Scheme 3.2). Providing a greater understanding of the mechanisms involved, the reaction was structurally traced by the isolation of the kinetic solvent-separated *ortho*-deprotonated product $[\{(TMEDA)_2Na\}^+ \{Zn(o-C_6H_4-CF_3)(tBu)_2\}^-]$ before in turn exploring its reactivity towards TMP(H) mirroring the second, multipart step of the AMMZn process.^[8] Intriguingly, this second step was found to affect strongly the conclusion, swaying not only the product yield but also the final regioselectivity of the metallation with an intricate mixture of *ortho*-, *meta*- and *para*-regioisomeric products observed in solution. Supporting the earlier theoretical work, these findings provided the first experimental evidence for a two-step mechanism in deprotonative metallations with TMP-zincates but additionally pose the question; “is the unique *meta*-metallation of *N, N*-dimethylaniline a consequence of TMP-induced isomerisation?” This study attempts to answer this important question in gaining a more complete understanding of such special regioselective zincation reactions.



Scheme 3.2: TMP(H) induced structural reorganisation from solvent-separated ions to contact ions, facilitating rearrangement of some *ortho*-zincated molecules to *meta* and *para* isomers.

To this end, herein we investigate in detail the reaction of **1** with *N, N*-dimethylaniline, exploring the proposed two-step mechanism and shedding light on the special synergic

facet of the AMMZn by contrasting direct sodium-mediated zincation with indirect sodiation-dialkylzinc co-complexation by sequentially treating *N, N*-dimethylaniline with the homometallic components of bimetallic base **1**. Successful attempts to isolate and characterise the metallated intermediates and the regioselectivities afforded upon quenching the *in situ* mixtures will be discussed, offering increased understanding of the possible mechanisms involved in the reactions of TMP-zincates. Overall, this study provides an illustrative example of the subtle, yet prodigious reactivity of the bimetallic base **1**.

3.2) *The Original Direct meta-Zincation Reaction*

In comparison to the persuasive tertiary amides and *O*-carbamates, anilines are relatively modest metallation directing groups.^[9] Activation of *N, N*-dimethylaniline transpires primarily from the acidifying effect of the electronegative N atom; the coordination effect of the N atom is believed to be less important as result of the conjugation of its lone pair with the π -system of the ring, even so *N, N*-dimethylaniline undergoes DoM with PhLi in poor yield^[10] or *n*BuLi in good yield under forcing conditions.^[11] Varying the metallation agent from these mainstream homometallic species to heterometallic **1** remarkably switched the orientation of the deprotonation to the *meta*-site, with the metallated heterotri-anionic product of the reaction [(TMEDA)Na(TMP)(*m*-C₆H₄-NMe₂)Zn(*t*Bu)] (**7**) isolated at ambient temperature in a stable crystalline form which allowed its molecular structure to be ascertained by X-ray crystallography (Figure 3.1).^[1]

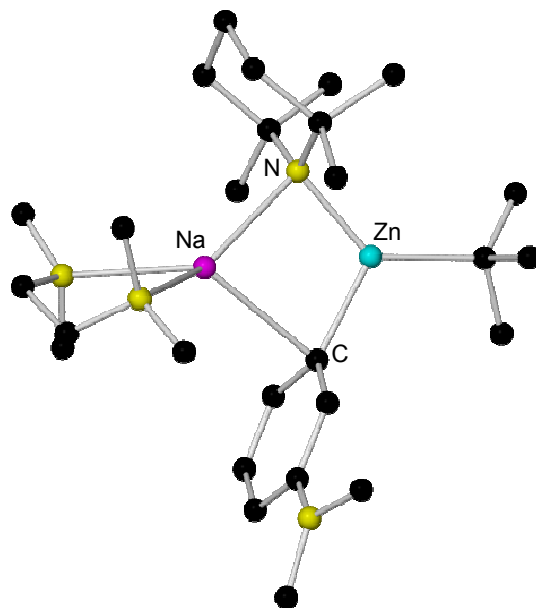


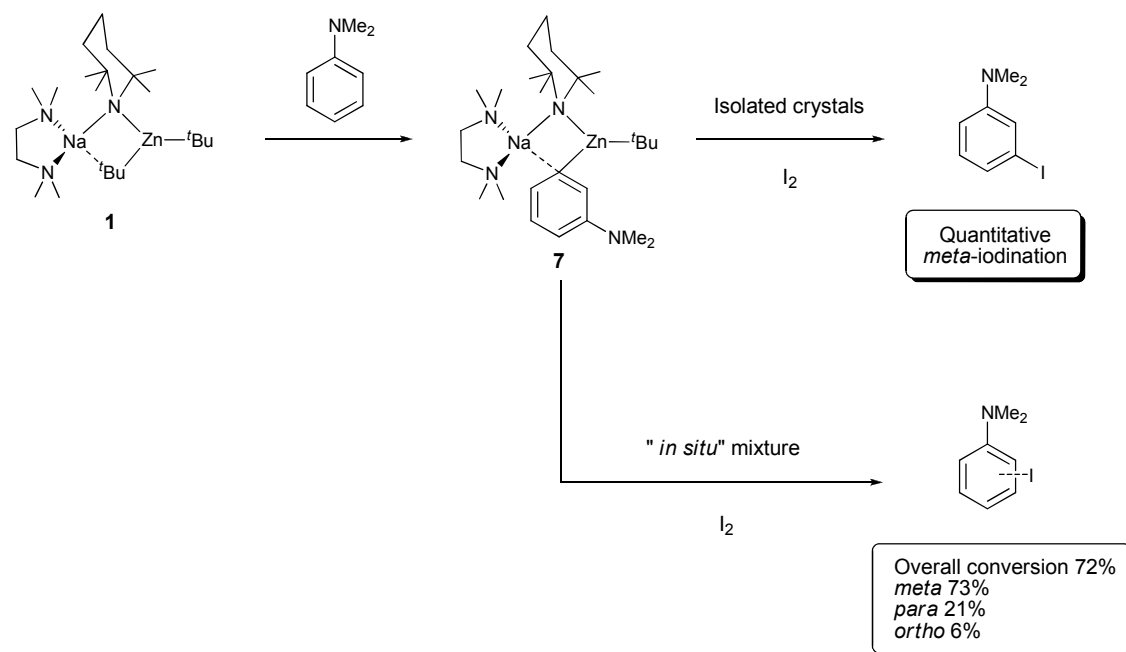
Figure 3.1: Molecular structure of 7 with selective atom labelling.

As reported, a preliminary reaction of isolated crystals of **7** in THF with iodine was carried out to establish whether these *meta*-zincated dimethylaniline complexes could be intercepted by electrophiles. ^1H NMR spectroscopic experiments revealed quantitative iodination and thus the selective formation of 3-iodo-*N, N*-dimethylaniline. Now we are looking to paint the complete picture of this surprising synergic *meta*-deprotonation of *N, N*-dimethylaniline.

3.3) The Direct *meta*-Zincation Reaction: A Closer Look

Revisiting the reaction, sodium TMP-zincate **1** was prepared *in situ* in hexane solution and reacted with one molar equivalent of *N, N*-dimethylaniline at room temperature to afford a yellow solution which was subsequently treated with iodine (Scheme 3.3). NMR spectroscopic analysis (^1H and ^1H - ^1H COSY NMR spectra in d_6 -benzene) of the crude reaction solution revealed a complicated mixture of iodinated products that contained all three possible ring regioisomers for the monometallation of *N, N*-dimethylaniline. In agreement with X-ray crystallographic analysis, the *meta*-isomer

was the principal product, but additionally in the aromatic region two doublets at 7.42 and 6.13 ppm were observed for the next most abundant product, that is, the *para*-product and finally four multiplets centred at 7.75, 6.99, 6.73 and 6.46 ppm for the minor *ortho*-product in an overall 11.6:3.0:1.0 ratio.



Scheme 3.3: Synergic metallation of *N, N*-dimethylaniline with sodium TMP-zincate **1 to generate **7**, which was subsequently quenched with I_2 to produce iodoanilines.**

3.4) The Indirect Sequential Sodiation-Dialkylzinc Co-complexation Approach

To begin, closely imitating the constituents of sodium zincate **1**, *N, N*-dimethylaniline was first *ortho*-sodiated with *n*BuNa in hexane at 0 °C to give the product as a light orange precipitate in 64% yield. Employment of the stronger base *n*BuNa was necessary because in our hands NaTMP, with or without TMEDA activation, was not sufficiently basic to abstract the *ortho*-hydrogen of *N, N*-dimethylaniline. Endeavouring to produce crystals of the resulting sodium anilide, the red filtrate (after isolation of the precipitate) was concentrated *in vacuo* to yield yellow/orange crystals following storage

in a refrigerator (at 5 °C). X-ray crystallographic analysis established the product as the dimeric, *ortho*-sodiated [(TMEDA)Na(*o*-C₆H₄-NMe₂)]₂ (**8**) (Figure 3.2).

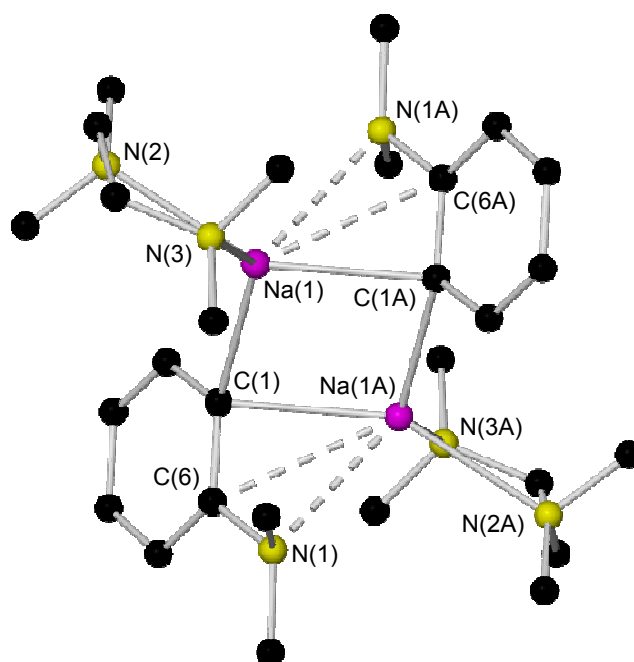


Figure 3.2: Molecular structure of **8** with selective atom labelling. Hydrogen atoms are omitted for clarity. The long Na \cdots C_{ipso} and Na \cdots N contacts are highlighted by dashed lines. Selected bond lengths (Å) and angles (deg): Na(1)-N(2) 2.5363(14), Na(1)-N(3) 2.5350(14), Na(1)-C(1) 2.5442(15), Na(1)-C(1A) 2.5903(16), Na(1) \cdots C(6A) 2.9231(15), Na(1) \cdots N(1A) 2.6749(14); N(3)-Na(1)-N(2) 73.37(5), N(3)-Na(1)-C(1) 129.64(5), N(2)-Na(1)-C(1) 104.31(5), N(3)-Na(1)-C(1A) 97.45(5), N(2)-Na(1)-C(1A) 150.27(5), C(1)-Na(1)-C(1A) 103.12(4), N(3)-Na(1)-N(1A) 106.68(4), N(2)-Na(1)-N(1A) 99.59(5), C(1)-Na(1)-N(1A) 122.86(5).

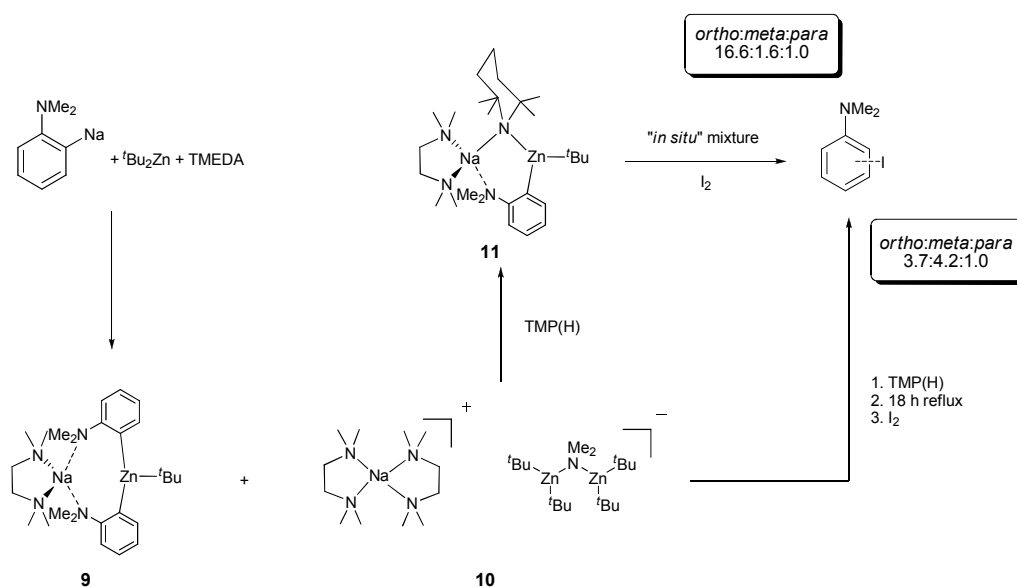
Sodiated aniline **8** adopts a simple dimeric centrosymmetric molecular structure based on a strictly planar four-membered [Na₂(μ -C)₂] ring. Occupying a tetrahedral geometry (mean angle around Na: 109.76°) the sodium atom in **8** is coordinated by a chelating TMEDA ligand and two deprotonated aniline units, the latter primarily through a close contact with the two symmetry-equivalent *ortho*-deprotonated carbon atoms of the aromatic ring [Na(1)-C(1) 2.5442(15); Na(1)-C(1A) 2.5903(16) Å]. In addition to these primary contacts, sodium also engages in longer, weaker secondary contacts with both

the *ipso*-carbon and nitrogen atom of the anilide unit [Na(1)···C(6A) 2.9231(15) and Na(1)···N(1A) 2.6749(14) Å]. The Na(1)-C(1A) distance is comparable to that of the corresponding bonds in the solvent-free sodium aryl derivative (NaC₆H₃-2,6-Mes₂)₂ prepared by Power (mean Na-C bond distance of 2.609 Å),^[12] whilst they are naturally longer than those in the lithium dimer [{1-(dimethylamino)-8-naphthyl}-lithium·THF]₂ [2.207(4) and 2.223(4) Å].^[13] In this latter compound the lithium atoms are located *ca.* 0.37 Å above and 1.05 Å below the naphthyl planes. By way of comparison, the sodium atoms in **8** are positioned 0.6565(5) Å above and 1.8248(5) Å below the aryl ring as a result of the increased size of sodium; a trend also reflected in the distance between the average main planes of the aromatic rings [1.176(1) Å in **8** and a surprisingly small 0.68 Å between the naphthyl rings of the lithium compound].

For the purposes of NMR spectroscopic analysis, the optimum solubility of **8** was achieved in *d*₁₂-cyclohexane solution. The salient observation from the NMR spectra of the solid material and indeed the reaction mixture is that there is no sign of any other metallated products/isomers. Therefore the *ortho*-sodiated *N, N*-dimethylaniline was the sole metallated product detected during the course of the reaction. ¹H NMR spectroscopic analysis of a *d*₁₂-cyclohexane solution of **8** revealed three multiplets at 7.78, 6.79 and 6.58 ppm representing the *ortho*-deprotonated aromatic ring (overlap at 6.58 ppm between the *ortho'*- and *para*-protons) with the NMe₂ singlet resonance of the anilide appearing at 2.83 ppm, a shift of 0.12 ppm to higher frequency from that in *N, N*-dimethylaniline. Completing the assignment, the TMEDA ligand signals are found at 2.22 and 2.04 ppm. Emphasising the synthetically limiting reactivity of **8**, it appears to attack THF, while undesired deprotonation of toluene furnished crystals of the known compound TMEDA solvated benzylna as confirmed by NMR analysis.^[14] Indeed, Slocum *et al.* have recently developed a selective *ortho*-metallation protocol which

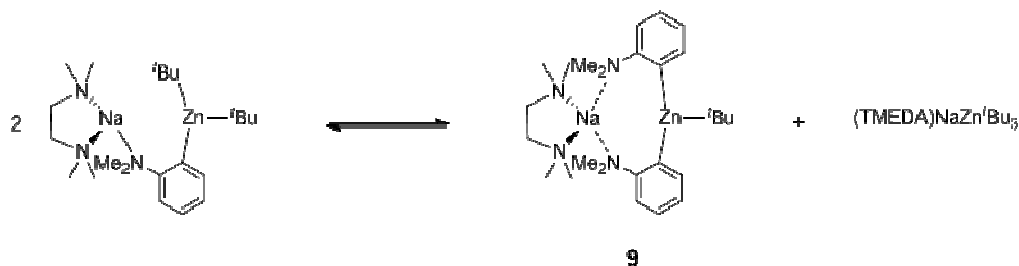
permits the retention of the bromine substituent in *para*-bromoanisole by the use of *ortho*-lithiodimethylaniline, which presumably must exhibit a reduced reactivity compared to its sodium analogue **8**, as the metallating agent.^[15] Indeed upon storage in a dry box, the shelf life of sodium anilide **8** is no better than a couple of days.

Continuing with the “imitating” experimental studies, to introduce the second metal component one molar equivalent of *t*Bu₂Zn (dissolved in hexane) was added to a suspension of **8** in hexane, which was prepared *in situ*, and the mixture was stirred at 0 °C for 1 hour and then a further 2 hours at room temperature (Scheme 3.4). Following gentle heating of the mixture, colourless crystals were deposited upon slow cooling of the Schlenk tube in a Dewar flask of hot water overnight. X-ray crystallography indicated that these crystals were not a single compound but a 2:1 co-crystalline mixture of two products, namely [(TMEDA)Na(*o*-C₆H₄-NMe₂)₂Zn(*t*Bu)] (**9**) and [{(TMEDA)₂Na⁺ } { (*t*Bu₂Zn)₂(μ-NMe₂) }⁻] (**10**).



Scheme 3.4: Indirect zincation of *N,N*-dimethylaniline producing **9, **10**, and **11**, which was then quenched with I₂ to produce iodo-anilines.**

Bis-aryl **9** can be considered a mixed-metal product of the co-complexation reaction between **8** and $t\text{Bu}_2\text{Zn}$, despite the incorporation of a second deprotonated organic substrate. Although, a *tert*-butyl group has been formally lost, the formation of **9** may not necessarily be a result of a second deprotonation, with a disproportionation pathway potentially at play (Scheme 3.5).



Scheme 3.5: The possible disproportionation reaction that leads to the formation of bis-aryl species **9**.

The molecular structure of **9** (Figure 3.3) can be described as a contacted ion pair with the anionic moiety containing a trigonal planar zinc centre bonded to three carbon atoms, two from the *ortho*-metallated fragments which bridge zinc to sodium and one from the terminally attached *tert*-butyl group. In addition to the nitrogen atoms of the chelating TMEDA, the sodium atoms primary coordination sphere is completed by bonding to the nitrogen of one anilide unit [Na(1)-N(1) 2.663(3) Å] and to the *ortho*-deprotonated carbon of the second aromatic ring [Na(1)-C(23) 2.663(3) Å], resulting in sodium adopting a distorted tetrahedral geometry (mean angle around Na: 107.87°). Furthermore, the multihapto-contacted sodium centre engages in weaker, secondary contacts to the *ipso*-carbons of both anilides [Na(1)⋯C(12) 2.848(3) and Na(1)⋯C(22) 2.884(3) Å] and additionally interacts with not only the second deprotonated carbon [Na(1)⋯C(13) 2.799(3) Å] but also the second aniline nitrogen atom [a long Na(1)⋯N(2) length of 2.851(2) Å compared to the Na-N_{TMEDA} bond lengths of Na(1)-

N(3) 2.473(2) and Na(1)-N(4) 2.473(3) Å]. Notably, the aryl carbanion which was initially bound to sodium is now directly attached to the more carbophilic zinc as illustrated by the short, strong zinc-carbon σ -bonds [Zn(1)-C(13) 2.025(3); Zn(1)-C(23) 2.042(3) Å]. Note there are no metal contacts, by zinc or sodium, to the *meta* positions on the anilide ring which still retain hydrogen atoms.

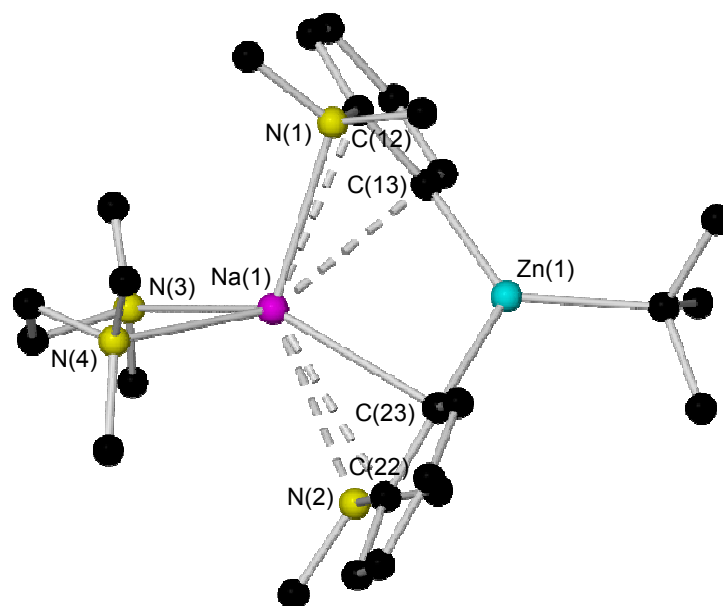


Figure 3.3: Molecular structure of bis-anilide **9** with selective atom labelling. Hydrogen atoms and a disordered component of TMEDA are omitted for clarity. Secondary contacts between sodium and the anilide rings are denoted by dashed lines. Only one crystallographically independent molecule is displayed, as the parameters for the other are the same within experimental error. Selected bond distances (Å) and angles (deg): Zn(1)-C(13) 2.025(3), Zn(1)-C(23) 2.042(3), Na(1)-N(1) 2.663(3), Na(1)⋯C(12) 2.848(3), Na(1)⋯C(13) 2.799(3), Na(1)⋯N(2) 2.851(2), Na(1)⋯C(22) 2.884(3), Na(1)-C(23) 2.663(3), Na(1)-N(3) 2.473(2), Na(1)-N(4) 2.473(3); C(13)-Zn(1)-C(23) 123.30(11), N(3)-Na(1)-N(4) 74.20(9), N(4)-Na(1)-C(23) 112.74(10), N(3)-Na(1)-C(23) 147.52(9), N(4)-Na(1)-N(1) 102.85(8), N(3)-Na(1)-N(1) 114.85(9), C(23)-Na(1)-N(1) 95.05(9).

A search of the Cambridge Crystallographic Database^[16] found that the bis-aryl model has precedent in alkali-metal zincate chemistry, for example, in the previously prepared

biscarboxamide [(TMEDA)Li{2-(1-C(O)N*i*Pr₂)C₆H₄}₂Zn(*t*Bu)}],^[17] however, the donor ability of the different directing groups limits comparison with **9**. A salient feature of this biscarboxamide structure is the bond between lithium and the Lewis basic carbonyl oxygen atoms which close a ten-membered ring, resulting in a contracted Ar-Zn-Ar bond angle of 111.76(10)°. In contrast, as a result of the dimethylamino groups modest directing ability, with coordination less important, the sodium atom in **9** engages the π -system of the arene ring, in turn widening the corresponding C(13)-Zn(1)-C(23) bond angle to 123.30(11)°.

The solvent-separated ion-pair co-product [$\{(TMEDA)_2Na^+\} \{(tBu_2Zn)_2(\mu-NMe_2)\}^-$] **10** (Figure 3.4) adopts a markedly different structural motif from that of **9**. Its cationic moiety comprises a nearly square planar sodium centre coordinated by two TMEDA molecules (note that near square planar alkali-metals are rare in comparison to the legion of tetrahedral coordinations documented^[18]), whereas the anionic moiety consists of two di-*tert*-butyl zinc units connected by a dimethylamino bridge. The unexpected manifestation of this bridging amide is almost certainly a consequence of utilising the overly aggressive homometallic reagent *n*BuNa at fairly ambient temperatures, with decomposition of either *N, N*-dimethylaniline or with precedent in the literature, TMEDA potentially leading to the presence of this cleaved amide fragment.^[19] The zinc-nitrogen distances in **10** [Zn(3)-N(13) 2.059(2) and Zn(4)-N(13) 2.062(2) Å] are the same within experimental error to each other and in good agreement with the distances of corresponding bonds in the zinc bisamide [$\{(PhCH_2)_2N\}Zn_2 \cdot C_6H_6$ [2.0083(13) and 2.0620(12) Å]^[20] and in dimeric MeZn(NPh₂) [average value of 2.072(8) Å for the four distinct Zn-N bond lengths].^[21] The best comparison for **10** is possibly provided by the dinuclear zinc guanidinate complex [$\{Zn(OAr)\}_2\{\mu-(Me_2NC(N*i*Pr)_2)\}(\mu-NMe_2)$] prepared by Coles.^[22] In both complexes, the zinc atoms

adopt a distorted trigonal planar geometry [sum of bond angles at Zn(3) and Zn(4) in **10** equal to 358.31° and 358.28°, respectively] but with each zinc atom additionally bound to a bulky aryloxyde and guanidinate ligand, the Zn-(μ -NMe₂)-Zn bond angle is compressed to 97.34°, in contrast to 103.67(9)° in the more open structure of **10**. A possible consequence of this increased steric hindrance in the guanidinate complex is the shorter Zn-N bond distances [1.990(3) and 1.982(3) Å] in comparison to those in **10**.

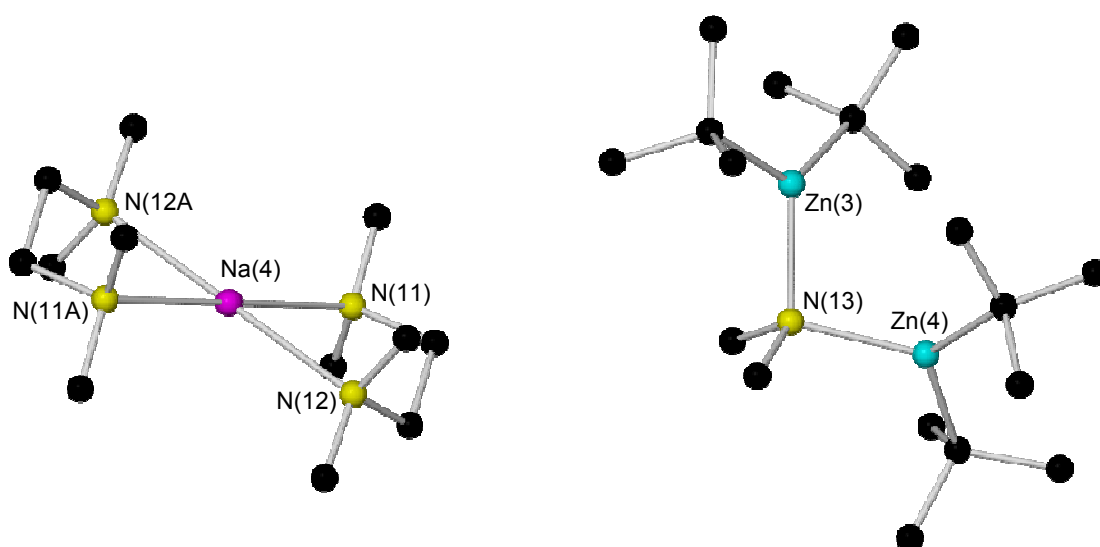


Figure 3.4: Solvent-separated ion-pair structure of **10** with selective atom labelling. Hydrogen atoms and disordered component of TMEDA are omitted for clarity. Only one crystallographically independent cation is displayed, the parameters for the other are the same within experimental error. Selected bond distances (Å) and angles (deg): Zn(3)-N(13) 2.059(2), Zn(4)-N(13) 2.062(2), Na(4)-N(11) 2.516(2), Na(4)-N(12) 2.494(3); Zn(3)-N(13)-Zn(4) 103.67(9), N(11)-Na(4)-N(12) 75.21(8), N(11)-Na(4)-N(11A) 180.0, N(11)-Na(3)-N(12A) 104.79(8), N(12)-Na(3)-N(12A) 180.0.

From ¹H NMR spectra in *d*₆-benzene solution of the reaction between **8** and *t*Bu₂Zn, which produced crystals of **9** and **10** the presence of a third distinct species was revealed. Four multiplets at 8.03, 7.17, 7.06 and 6.72 ppm are observed for the major *ortho*-metallated product but additionally, shadowing these signals, another distinct

ortho-metallated product is evident from a set of four different multiplets at 7.87, 7.01, 6.86 and 6.60 ppm. Potentially, this additional unidentified product could be the related dialkyl(aryl) sodium zincate [(TMEDA)Na(*o*-C₆H₄-NMe₂)*t*Bu-Zn-*t*Bu], reminiscent of the lithium congeners [(THF)₃Li(*o*-C₆H₄-OMe)*t*Bu-Zn-*t*Bu] and [(PMDETA)Li(*o*-C₆H₄-OMe)*t*Bu-Zn-*t*Bu] prepared by co-complexation reactions of lithiated anisole with *t*Bu₂Zn and the relevant Lewis base.^[7] The metallation regioselectivity exhibited in the crystalline material is confirmed by treatment of the *in situ* reaction mixture with iodine. Electrophilic quenching of the two different *ortho*-deprotonated organometallic compounds is depicted in the ¹H NMR spectrum of the crude residue, with a 20.2:1.0 mixture of the *ortho*- and *para*-isomers of iodo-*N, N*-dimethylaniline obtained and most significantly, a negligible quantity of the *meta*-iodinated product present.

According to theoretical studies, compound **9**'s related bisalkyl(aryl) derivative could be a putative intermediate in the first step of the metallation of *N, N*-dimethylaniline by TMP-zincates. Thus, the reactivity of this *in situ* mixture towards the amine TMP(H) was studied next, purposely for the formation of [(TMEDA)Na(TMP)(C₆H₄-NMe₂)Zn(*t*Bu)] products. First the reactivity towards one molar equivalent of TMP(H) at room temperature was investigated and within 30 minutes a white solid precipitated which could be recrystallised from hexane to afford a small amount of translucent crystals.

An X-ray crystallographic study showed the molecular structure of these crystals to be [(TMEDA)Na(TMP)(*o*-C₆H₄-NMe₂)Zn(*t*Bu)] (**11**) (Figure 3.5). Revealing a contact ion-pair structure, **11** comprises of the Na-TMP-Zn structural backbone of bimetallic base **1** where TMEDA chelates the sodium atom and zinc is bound to a terminal *tert*-butyl group. In keeping with previous illustrations of the AMM*Zn* reaction, zinc has filled the position vacated by the departing hydrogen atom and significantly in **11**, zinc

resides in the *ortho*-position of the aromatic ring, making **11** a regioisomer of **7**. Comparing these regioisomers, a strong zinc-carbon σ -bond exists between the metal and deprotonated carbon atom in both compounds [2.035(4) and 2.079(2) Å in **7** and **11**, respectively] as a result, the main distinction between the structures arises from the manner in which the metallated arene interacts with the alkali-metal. In **7**, with the NMe₂ unit detached from sodium, the alkali-metal interacts more with the π -system of the aromatic ring, principally with the deprotonated *meta*-carbon [2.691(4) Å] generating a four-membered (NaNZnC) ring. In contrast, for **11** the close proximity of the NMe₂ group enables it to bind with the sodium centre giving a slightly longer than average Na(1)-N(3) bond distance of 2.6991(19) Å [compared to a Na(1)-N(1) bond distance of 2.663(3) Å in **9** and Na-N bond distances in the range 2.448(8)-2.621(3) for a series of mononuclear zinc compounds deposited in the Cambridge Crystallographic Database^[16]], which closes a larger six-membered, highly puckered (NaNZnCCN) central ring. Nevertheless, sodium still engages with the aromatic ring [transannular distances of 2.917(2) and 2.768(2) Å] in a fashion characteristic of several AMMZn products.

The relatively simple ¹H NMR spectrum of the aforementioned white precipitate in *d*₈-THF solution revealed the solid to be exclusively product **11**, whereby *N, N*-dimethylaniline has been *ortho*-metallated with only four resonances, two doublets (7.48 and 6.81 ppm) and two triplets (6.92 and 6.75 ppm) observed in the aromatic region. Furthermore, analysis of the aliphatic region of both the ¹H and ¹³C NMR spectra showed resonances for both *tert*-butyl and TMEDA but notably, resonances which can be attributed to coordinated anionic TMP at 1.74, 1.37 and 1.20 ppm were observed (note that ¹H NMR resonances of TMP(H) in *d*₈-THF appear at 1.63, 1.29 and 1.06 ppm).

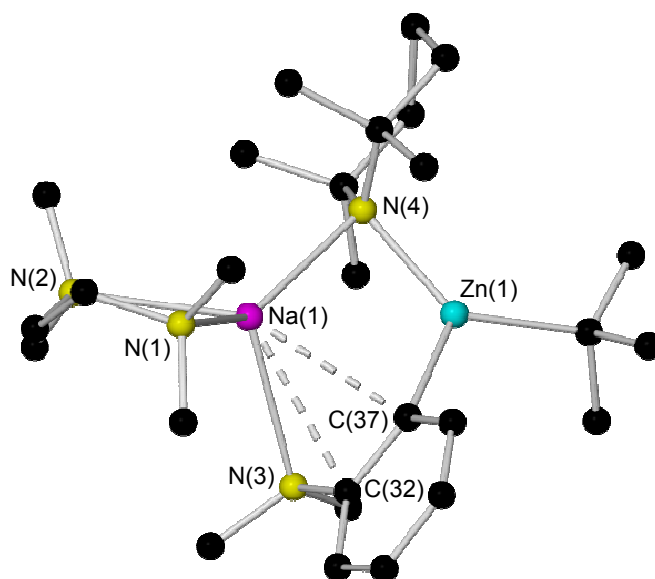


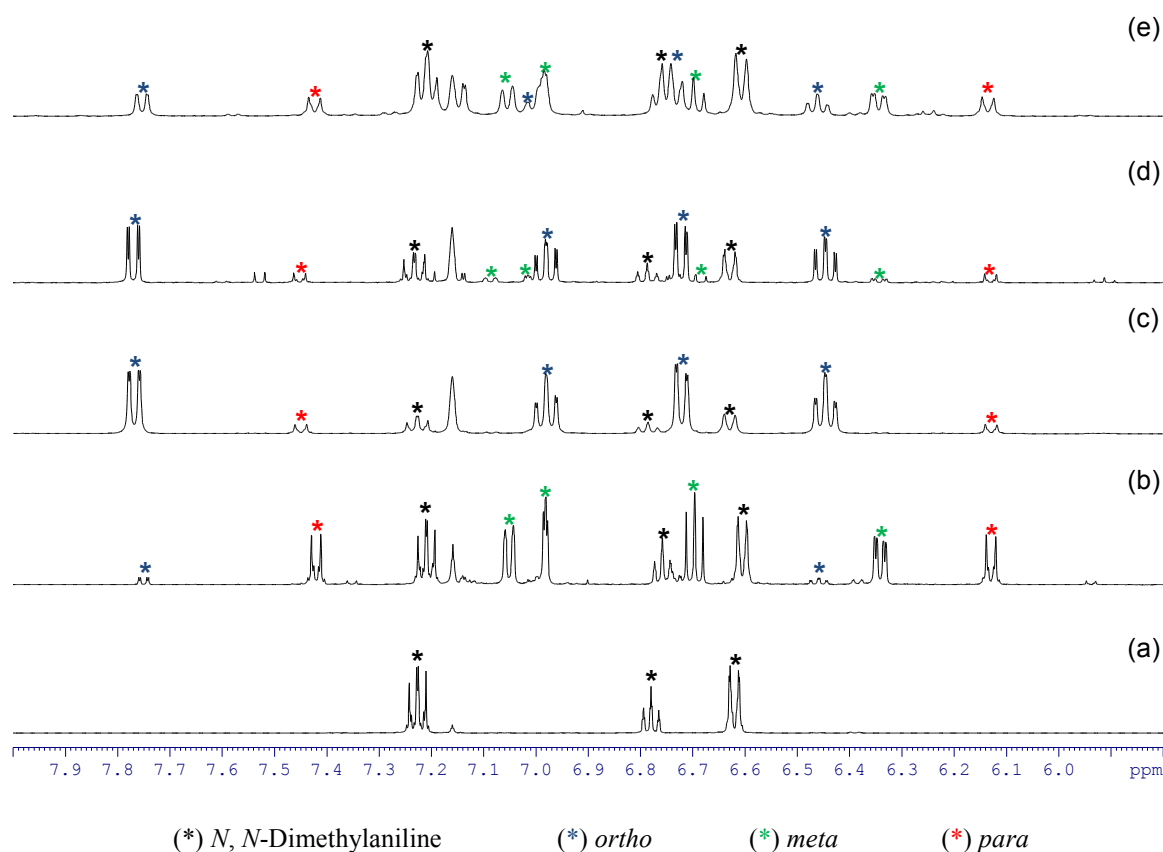
Figure 3.5: Molecular structure of **11** with selective atom labelling. Hydrogen atoms are omitted for clarity. Secondary contacts between sodium and the anilide rings are denoted by dashed lines. Selected bond distances (Å) and angles (deg): Na(1)-N(1) 2.586(2), Na(1)-N(2) 2.568(2), Na(1)-N(3) 2.6991(19), Na(1)-N(4) 2.469(2), Na(1)⋯C(32) 2.917(2), Na(1)⋯C(37) 2.768(2), Zn(1)-C(37) 2.079(2), Zn(1)-N(4) 2.0279(17); N(1)-Na(1)-N(4) 131.05(7), N(2)-Na(1)-N(4) 122.82(7), N(1)-Na(1)-N(2) 72.56(6), N(3)-Na(1)-N(4) 105.70(6), N(2)-Na(1)-N(3) 109.31(6), N(1)-Na(1)-N(3) 111.60(7), N(4)-Zn(1)-C(37) 114.27(8).

Regenerating the TMP bridge between sodium and zinc can be considered a copy of the second step of Uchiyama and Nobuto's theoretically proposed stepwise mechanism. However, should the AMMZn proceed by the two-step procedure, then the *meta*-isomer might emerge as the predominant product despite the isolation of **11**. To establish the complete constitution of an *in situ* reaction mixture, it was treated with iodine, the crude ^1H NMR spectrum revealing that while much of the *ortho*- and *para*-substitution pattern is retained, a small portion of these zincated aryl molecules have indeed isomerised to the *meta*-position [overall *ortho:meta:para* ratio of 16.6:1.6:1.0 from an *ortho:meta:para* ratio of 20.2:0:1.0 before TMP(H) addition]. For the addition of TMP(H) to the isolated, *ortho*-metallated kinetic intermediate [$\{(\text{TMEDA})_2\text{Na}\}^+\{\text{Zn}(o-$

$\text{C}_6\text{H}_4\text{-CF}_3(\text{tBu})_2\}^-]$, the Mulvey group previously reported that the secondary amine facilitates rearrangement of some *ortho*-zincated aryl molecules to *meta*- and *para*-isomers [in a 4.3:2.6:1.0 ratio, resulting from the amination reaction of TMP(H) with one *tert*-butyl group]^[8]. The smaller degree of isomerisation in the *N, N*-dimethylaniline system can be rationalised, at least in part, by considering the electronic nature of the different directing groups. With respect to NMe₂, CF₃ exerts an increased inductive effect thus weakening the Zn-C_{ortho} bond to a greater extent, potentially leading to its easier cleavage and thus isomerisation. However, stimulated by this result, the TMP-induced isomerisation was pursued with the aim of transforming more *ortho*-material (ideally in synthetically useful amounts) to *meta*. In order to meet this aspiration, the reaction mixture was refluxed overnight, aiding the solubility of **11** and thus presenting greater opportunity for the said regioisomerisation.

After the addition of TMP(H) and an 18 hour reflux, the yellow solution was treated with iodine. ¹H NMR spectroscopic analysis revealed that the make-up of the solution had dramatically changed, with each of the three regioisomers for the mono-iodination of *N, N*-dimethylaniline now present. Notably, the predominant isomer of iodo-*N, N*-dimethylaniline is now the *meta*-substituted product denoted by a set of three multiplets at 7.05, 6.70 and 6.34 and a singlet at 6.98 ppm (Spectrum 3.1). The *ortho*-product is still well represented denoted by four multiplets at 7.75, 7.02, 6.74 and 6.46 ppm, while two doublets at 7.42 and 6.13 ppm denote the minor *para*-product with the three regioisomers present in an overall *ortho:meta:para* 3.7:4.2:1.0 ratio. However, in what was initially surprising, the spectrum also revealed a substantial amount of free *N, N*-dimethylaniline (multiplets at 7.22, 6.77 and 6.60 ppm and a singlet at 2.55 ppm for the NMe₂ group). Simulating the multipart-step of the AMMZn reaction in the aforementioned trifluoromethylbenzene study – by reacting isolated crystals of

[{(TMEDA)₂Na}⁺{Zn(*o*-C₆H₄-CF₃)(*t*Bu)₂}⁻] with TMP(H) and monitoring by ¹H NMR spectroscopy – highlighted the significance of this second step in determining not only the final regioselectivity of the metallation but also the reaction yield with the amine found to partially target the metallated aryl anion regenerating sodium TMP-zincate **1** and trifluoromethylbenzene. The existence of such a parallel competitive reaction pathway here could promote the re-formation of *N, N*-dimethylaniline and when in the presence of concomitant zincate **1**, be responsible for the increase observed in the *meta*-deprotonated substrate concentration. Further evidence for the regeneration of bimetallic base **1** comes in the identity of two unknown products in the crude mixture, although evidently *N, N*-dimethylaniline derivatives, positive identification from NMR spectroscopic analysis was made difficult by the complexity of the aromatic region (two distinct singlets visible in the NMe₂ region at 2.35 and 2.29 ppm). GC-MS (CI mode) analysis verified the presence of the three regioisomers of iodo-*N, N*-dimethylaniline but also shed light on the identity of the two unknown species with the MH⁺ peaks at *m/z* 373.8 consistent with regioisomers of diiodo-*N, N*-dimethylaniline. Thus following the addition of TMP(H), the presence of sodium TMP-zincate **1** in conjunction with the harsher reflux conditions is likely to be the recipe for executing a degree of di-deprotonation of the aromatic molecule.



Spectrum 3.1: Aromatic region of ^1H NMR spectra for d_6 -benzene solutions of (a) a standard of *N, N*-dimethylaniline; (b) the crude mixture obtained from the reaction of [(TMEDA)Na(μ -TMP)(μ -*t*Bu)Zn(*t*Bu)] (**1**) with 1 equivalent of *N, N*-dimethylaniline at room temperature following iodine quenching; (c) the crude mixture obtained from the reaction of *n*BuNa·TMEDA, *N, N*-dimethylaniline and *t*Bu₂Zn at room temperature following iodine quenching; (d) the crude mixture obtained from the reaction of *n*BuNa·TMEDA, *N, N*-dimethylaniline, *t*Bu₂Zn and TMP(H) at room temperature following iodine quenching; (e) the crude mixture obtained from the reaction of *n*BuNa·TMEDA, *N, N*-dimethylaniline, *t*Bu₂Zn and TMP(H) following an overnight reflux and iodine quenching.

3.5) DFT Calculations

Endeavouring to rationalise the different metallation regioselectivities afforded by the homo and heterobimetallic bases, theoretical calculations at the DFT level using the B3LYP method and the 6-311G** basis set were employed in a collaboration with Dr

Armstrong of this department to compute the relative stabilities of the four possible regioisomers arising from the monometallation of *N, N*-dimethylaniline.

The relative stabilities of the four model regioisomers (*ortho*-, *meta*-, *para*- and methyl-positions), in which the aniline ring is sodium substituted were calculated and in support of the experimental studies, the *ortho*-isomer is the energetically preferred product (relative energy: 0.00 kcal mol⁻¹) with the presence of a Na–N donor-acceptor interaction helping its stability. Closely following is the methyl isomer (at 1.61 kcal mol⁻¹) but destabilised are the *meta*- and *para*-isomers (by 8.60 and 8.71 kcal mol⁻¹, respectively).

On modelling the introduction of TMEDA, the *ortho*-isomer remains the energy minimum structure at relative energy 0.00 kcal mol⁻¹, however, the energy gap to the other three regioisomers decreases slightly (methyl at 1.35 kcal mol⁻¹; *meta* at 6.93 kcal mol⁻¹; and *para* at 7.15 kcal mol⁻¹). Inspecting the dimensions of the *ortho*-product, TMEDA chelation of the Na atom results in a longer and thus weaker Na–NMe₂ secondary interaction (increase from 2.289 to 2.501 Å), while the *meta*- and *para*-isomers benefit from TMEDA's participation with the energies of TMEDA coordination equal to –20.86 and –20.74 kcal mol⁻¹, respectively. Tellingly, although the overall energy of reaction for these isomers is exothermic by –5.81 and –5.59 kcal mol⁻¹, by way of comparison the product of *ortho*-deprotonation is significantly more exothermic at –12.74 kcal mol⁻¹.

Taking account of aggregation the most disfavoured dimer is the methyl isomer (relative energy of 8.60 kcal mol⁻¹) but in contrast the *meta* (at 4.65 kcal mol⁻¹) and *para* (at 5.48 kcal mol⁻¹) regioisomers benefit in relation to the *ortho*-product (Figure 3.6). The –22.08 kcal mol⁻¹ energy of dimerisation gained by the *ortho*-isomer is

relatively low (compared to $-31.29 \text{ kcal mol}^{-1}$ for the *meta*-isomer) due to a combination of increased steric repulsions and loss of stabilising interactions. On dimerisation, the Na–N interaction in the *ortho*-product elongates in length from 2.501 to 2.662 Å with the Na atom now involved in bonding with two *ortho*-deprotonated C atoms, while there is also a noticeable increase in the Na–N(TMEDA) bond lengths from 2.521 and 2.533 Å to 2.604 and 2.674 Å. Through these modelling studies, *ortho*-deprotonation and dimerisation is found to be the energetically preferred metallation pathway by the homometallic reagent, with the overall reaction found to be exothermic by a substantial margin of $-47.55 \text{ kcal mol}^{-1}$. Incidentally, on addition of $t\text{Bu}_2\text{Zn}$ to each of the three monomeric sodiated regioisomers there is very little difference in the relative energies of the three products (*ortho* at $0.00 \text{ kcal mol}^{-1}$; *meta* at $0.32 \text{ kcal mol}^{-1}$; and *para* at $0.41 \text{ kcal mol}^{-1}$).

Turning to calculations on the sodium TMP-zincate **1**, concurring with the experimental findings and in marked contrast to the product obtained via monometallic $n\text{BuNa}\cdot\text{TMEDA}$, the *meta*-isomer (**A**) is found to be the minimum energy structure (relative energy: $0.00 \text{ kcal mol}^{-1}$) but is closely followed by the *para*-isomer (**B**) (at $0.66 \text{ kcal mol}^{-1}$). Notably, the *ortho*-isomer (**C**) is destabilised further (at $4.32 \text{ kcal mol}^{-1}$); and the least stable of all four isomers is the one where metallation takes place at the methyl group (at $9.01 \text{ kcal mol}^{-1}$). Hence in the synergic twofold metal system, the *meta*- and *para*-regioisomers are the thermodynamic products. Modelling studies reveal all four deprotonation reactions to be exothermic, with the energy minimum *meta*-isomer structure most exothermic by $-21.46 \text{ kcal mol}^{-1}$.

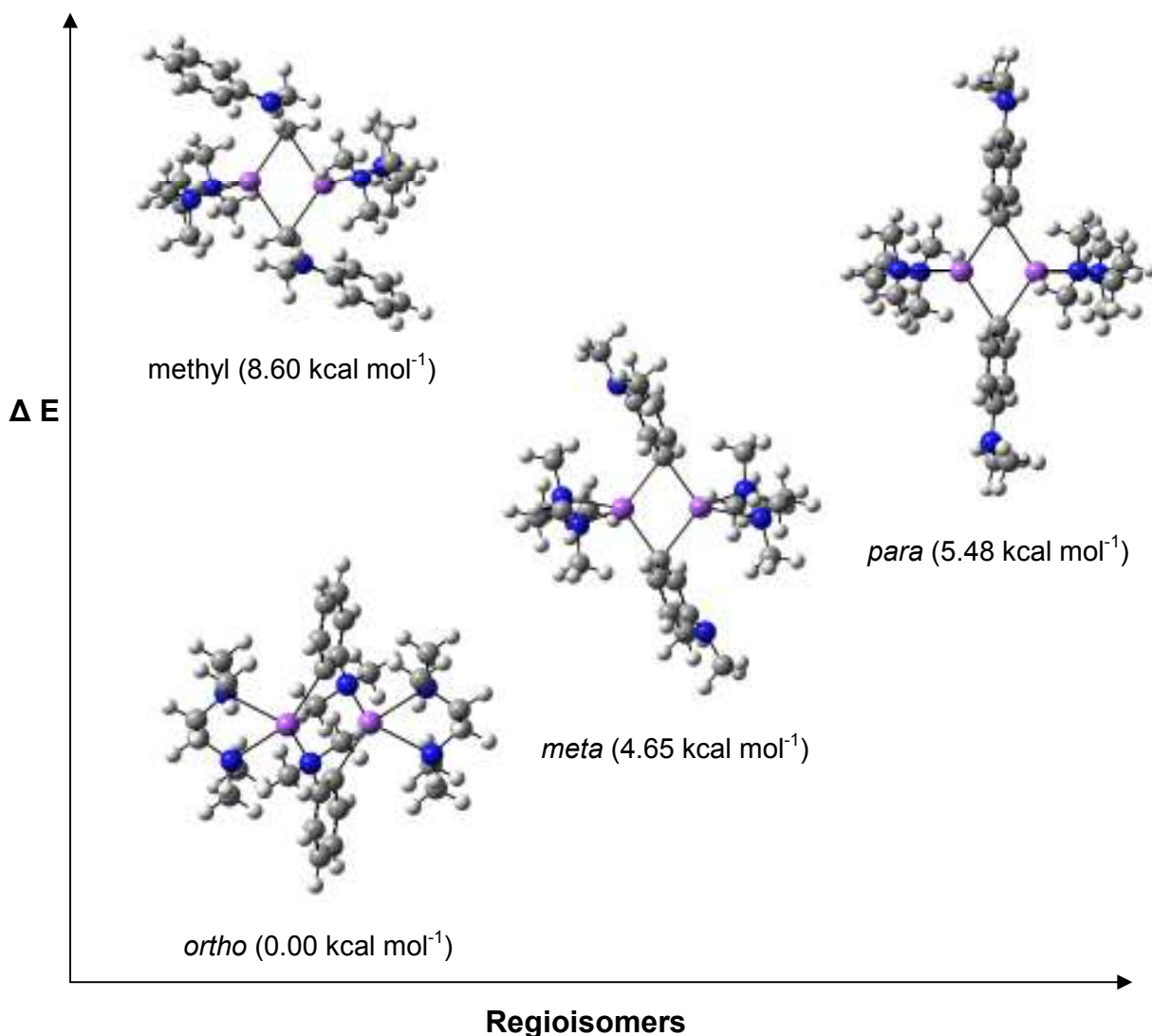
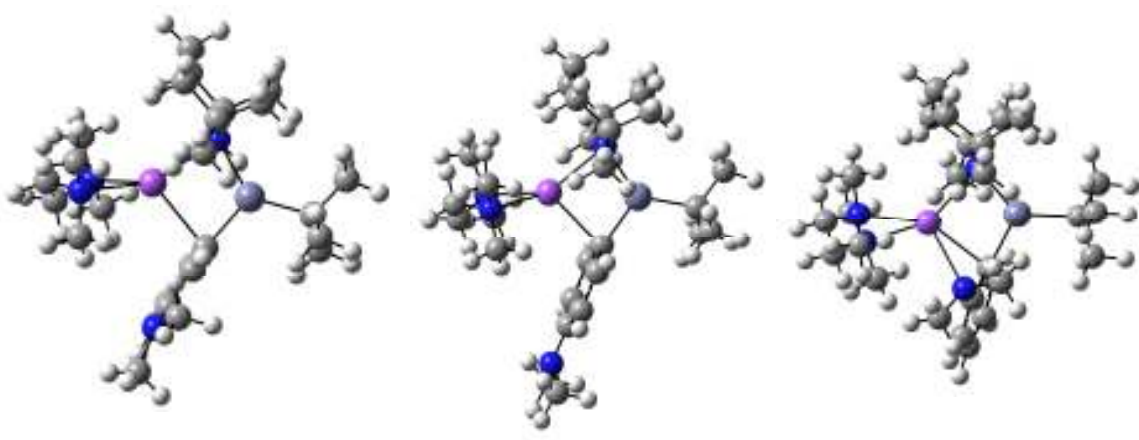


Figure 3.6: Relative energy sequence of the four theoretical regioisomers of the experimentally observed product 8.

The modest difference in the relative energies for **A** and **B** is consistent with the formation of the sizeable proportion of *para*-product observed experimentally. A comparison of the dimensions in these regioisomers, reveal that the Na contacts to the aryl C atoms are systematically shorter in the energetically preferred *meta*-isomer **A** (bond distances: 2.594, 3.070, 3.212, 3.959, 4.097, 4.403 Å) than in the analogous *para*-product **B** (bond distances: 2.596, 3.178, 3.239, 4.135, 4.185, 4.596 Å), whereas the Zn–C(aryl) bonds are within 0.001 Å of each other (2.084 and 2.083 Å, respectively)

(Table 3.1). In the *ortho*-isomer **C**, the product found previously to be expected from conventional (non-synergic, single metal) metallation, the Na–C(*ortho*) bond is decidedly longer (2.747 Å) and thus, weaker than the Na–C(*meta*) bond in the favoured *meta*-isomer **A** largely as a result of increased steric constraints. Additionally, with the sodium atom bonding to the NMe₂ group in **C**, lone pair–lone pair repulsion between the lone pair of the nitrogen and the nearby *ortho*-carbanion may be a factor in the relative instability of **C**. Consequently, the principal distinction lies in maximising the strength of the Na⋯C π contacts, and although they may be weak individually, collectively they must contribute appreciably to the overall stability of the unexpected *meta*-deprotonated product.

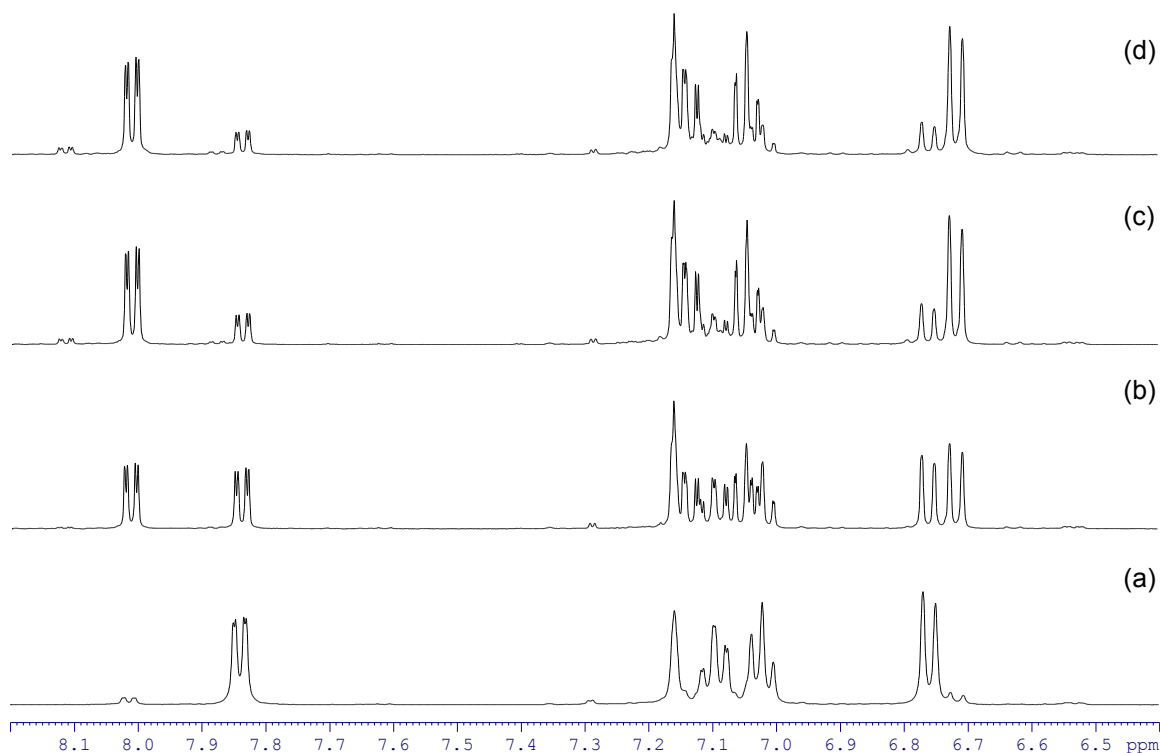
Table 3.1: Selected bond distances calculated for the three regioisomers A, B and C.



	A (0.00 kcal mol ⁻¹)	B (0.66 kcal mol ⁻¹)	C (4.32 kcal mol ⁻¹)
Bond distance (Å)	A	B	C
Zn–C _{metallated}	2.084	2.083	2.107
Na–C _{metallated}	2.594	2.596	2.747
Na⋯C _{aryl}	3.070, 3.212	3.178, 3.239	2.937

3.6) Attempted Thermal Isomerisation

Encouraged by the successful *in situ* regioisomerisation and the calculated energetics of the model structures, we revisited complex **11** exploring the possibility of thermal isomerisation. With the “{(TMEDA)Na(μ -TMP)Zn(*t*Bu)}” structural backbone of *meta*-zincated **7** already in place, no complications in the form of retro reactions re-forming *N, N*-dimethylaniline were anticipated. Isolated solid material of **11** was dissolved in hexane and the effects of time, and additionally heat were monitored by ^1H NMR spectroscopy in search of *meta*-zincated molecules forming from the rearrangement of pure *ortho*-metallated material. As illustrated in Spectrum 3.2, complex **11** undergoes a change in solution, however, as confirmed by the multiplicity pattern and ^1H - ^1H COSY NMR experiments, the aniline ring retains its *ortho*-deprotonated character, suggesting that through time or application of heat complex **11** unfortunately undergoes disproportionation rather than isomerisation, potentially forming a structure akin in nature to that of bis-anilide **9**.



Spectrum 3.2: Aromatic region of ^1H NMR spectra for d_6 -benzene solutions of **11 at various time intervals, probing possible regioisomerisation to the *meta*-isomer [(a) complex **11**; (b) 2 days; (c) 7 days; (d) 9 days].**

3.7) Concluding Remarks on Direct AMMZn versus Indirect Sodiation-Zinc Co-complexation Approaches

This study clearly brings to light the inherent complexity of these metallation reactions even at the active metal stage, with a diverse concoction of organometallic complexes isolated or identified in solution, prior to the recognised intricacies of subsequent electrophilic interception.

Collectively, these results emphasise the synthetic utility of the AMMZn reaction with the employment of a synergic bimetallic base providing entry to previously inaccessible metallation regioselectivities. The AMMZn of *N, N*-dimethylaniline by sodium zincate [(TMEDA)Na(μ -TMP)(μ -*t*Bu)Zn(*t*Bu)] **1** has been shown to afford a mixture of *ortho*-, *meta*- and *para*-regioisomers in solution, however, the predominant *meta*-substituted derivative [(TMEDA)Na(TMP)(*m*-C₆H₄-NMe₂)Zn(*t*Bu)] **7** – a regioselectivity normally

closed to synthetic aromatic chemistry – can be isolated in reasonable yields in a clean, pure crystalline form amenable to subsequent functionalisation.

In an attempt to try and advance our knowledge of the synergic facet of $AMMZn$, some informative control reactions with *N, N*-dimethylaniline were performed. With the toothless base tBu_2Zn , incapable of directly zincating aromatics, *N, N*-dimethylaniline was treated with $nBuNa \cdot TMEDA$ to afford dimeric $[(TMEDA)Na(o-C_6H_4-NMe_2)]_2$ **8**, which in keeping with conventional metallation (organolithium in particular) chemistry exhibits *ortho*-deprotonated anilines. The instability of **8** at ambient temperatures is reflected in its deprotonative attack of toluene under mild conditions and following co-complexation with the dialkyl zinc, a mixture of two products were isolated from the reaction, namely $[(TMEDA)Na(o-C_6H_4-NMe_2)_2Zn(tBu)]$ **9** and $[\{(TMEDA)_2Na^+\} \{(tBu_2Zn)_2(\mu-NMe_2)\}^-]$ **10**. The anomalous ion-pair product **10** contains a cleaved NMe_2 group, exemplifying nicely how the reactivity of an alkali-metal can be sedated when incorporated in a mixed-metal system but to a point where it is still able to play its part in conducting synthetically useful smooth metallations.

The final and arguably most important component of bimetallic base **1**, $TMP(H)$ was introduced at this stage, in what could be considered a copy of the second, multipart-step of the $AMMZn$ process and led to the isolation of $[(TMEDA)Na(TMP)(o-C_6H_4-NMe_2)Zn(tBu)]$ **11**, a regioisomer of **7** where the aromatic ring remains *ortho*-zincated. In search of the elusive *meta*-deprotonated derivative **7**, the reaction mixture was refluxed overnight and as a result of the harsher conditions, and almost certainly regeneration of sodium zincate **1**, the mono-deprotonated *meta*-derivative emerged as the predominant product.

Significantly, these results underscore the importance of the acid/base character of the TMP(H)/TMP^- couple and the synergic bridge the TMP anion provides between the two metals, for only when it is present, does the unique *meta*-regioselectivity materialise. Although this product has been engineered from the homometallic components, there are major disadvantages in this indirect approach versus the synergic direct approach. The low kinetic stability of the *ortho*-sodiated intermediate leads to undesired side reactions such as deprotonation of solvent and decomposition of reactants at temperatures tolerated by the synergic base, and the harsh reflux conditions required to bring about the presence of the *meta*-zincated derivative in a significant quantity offers less control, ultimately leading to competing di-metallation of the aromatic substrate.

DFT studies proved additionally informative. In probing the different metallation regioselectivities obtained from homometallic and heterobimetallic bases they highlight the importance of the interactions between the alkali-metal and the aromatic substrate. When executed by the conventional monometallic reagent $n\text{BuNa}\cdot\text{TMEDA}$, metallation is directed to the *ortho*-position in part by the secondary dative interaction between Na and the N atom of the NMe_2 group. In contrast, in the reaction of **1** with *N, N*-dimethylaniline, the *meta*-isomer is energetically the most preferred and analysis of the dimensions of the model structures suggest that the strength of the combined $\text{Na}\cdots\text{C}\pi$ contacts contribute at least in part to its stability. This favourable enthalpic effect, along with the communication between the metals provided by the TMP bridge, play a defining role in offering the unique regioselectivity observed in the AMMZn of *N, N*-dimethylaniline.

Finally, looking beyond the specifics of this reaction to its general implications, this study clearly demonstrates that bimetallic reagents can offer useful chemistry distinct to

that when two monometallic reagents of the corresponding metals are added sequentially to the same substrate. It follows that the secret to unlocking special synergic reactivity may be found in both metals communicating within the same bimetallic reagent. Future work is planned to capitalise on this advantage, investigating the generality of the concept across a broad spectrum of metal-mediated reactions.

3.8) Experimental section

Synthesis of [(TMEDA)Na(*o*-C₆H₄-NMe₂)]₂ **8**

Freshly prepared *n*BuNa (0.16 g, 2 mmol) was suspended in hexane (10 mL) and sonicated for 10 minutes to form a fine dispersion. The Schlenk tube was then cooled to 0 °C in an ice bath before the introduction of TMEDA (0.3 mL, 2 mmol) dropwise to give a clear yellow solution. *N, N*-dimethylaniline (0.25 mL, 2 mmol) was then introduced dropwise at this stage to give an orange solution which was stirred at 0 °C for 2 hours, producing a light orange precipitate which was isolated via filtration (0.33 g, 64% - based on monomeric unit). The deep red filtrate solution was concentrated *in vacuo* and stored in a refrigerator (at 5 °C), preceding the growth of a small amount of X-ray quality, orange crystalline material. ¹H NMR (400.13 MHz, 300 K, *d*₁₂-cyclohexane): δ 7.78 [d {³J(H,H) 6.22 Hz}, 1H, H_{meta}], 6.79 (t, 1H, H_{meta'}), 6.58 (m, 2H, H_{para} and H_{ortho'}), 2.83 [s, 6H, N(CH₃)₂], 2.22 [s, 4H, NCH₂ (TMEDA)], 2.04 [s, 12H, NCH₃ (TMEDA)]. ¹³C {¹H} NMR (100.62 MHz, 300 K, *d*₁₂-cyclohexane): δ 182.3 (C_{ortho}-Na), 164.1 (C_{ipso}), 142.7 (C_{meta}), 124.6 (C_{meta'}), 120.2 (C_{para}), 111.5 (C_{ortho'}), 58.6 [NCH₂ (TMEDA)], 46.0 [NCH₃ (TMEDA)], 45.0 [N(CH₃)₂].

Crystal data for **8**: C₂₈H₅₂N₆Na₂, *M* = 518.74, monoclinic, P2₁/c, *a* = 8.8060(9), *b* = 17.5089(12), *c* = 11.1635(11) Å, β = 111.693(12)°, *V* = 1599.3(3) Å³, *Z* = 2. 8277 reflections collected, 3797 were unique, *R*_{int} = 0.0454, *R* = 0.0471, *R*_w = 0.1133, GOF =

0.905, 169 refined parameters, max and min residual electron density = 0.233 and -0.161 e.Å⁻³.

Synthesis of a mixture of [(TMEDA)Na(TMP)(*o*-C₆H₄-NMe₂)₂Zn(*t*Bu)] **9 and [{(TMEDA)₂Na}⁺{(*t*Bu₂Zn)₂(μ-NMe₂)₂}⁻] **10****

To a suspension of **8**, prepared as described above, a hexane solution of *t*Bu₂Zn (0.36 g, 2 mmol) was added via cannula. The mixture was then allowed to stir for 1 hour at 0 °C, and was subsequently slowly warmed to room temperature where it was allowed to stir for a further two hours. The suspension was gently heated for a couple of minutes to obtain as close as possible to a yellow homogeneous solution, which was left to cool slowly in a Dewar flask filled with hot water overnight, resulting in the formation of 0.6 g of colourless crystals. ¹H NMR (400.13 MHz, 300 K, *d*₆-benzene): δ 8.03 [d {³J(H,H) 6.59 Hz}, 1H, H_{meta}], 7.87 [d {³J(H,H) 6.75 Hz}, 0.27H, H_{meta}], 7.17 [2.5H (overlap with solvent), H_{meta}], 7.06 (t, 1H, H_{para}), 7.01 (t, 0.29H, H_{para}), 6.86 (t, 0.29H, H_{meta}), 6.72 [d {³J(H,H) 7.96 Hz}, 1H, H_{ortho}], 6.60 [d {³J(H,H) 8.07 Hz}, 0.28H, H_{ortho}]. ¹³C {¹H} NMR (100.62 MHz, 300 K, *d*₆-benzene): δ 159.4 [C_{ortho}-Na (major)], 157.0 [C_{ipso} (major)], 140.2 [C_{meta} (major)], 139.5 [C_{meta} (minor)] 126.0 [C_{meta}' (major)], 125.4 [C_{para} (minor)], 120.9 [C_{para} (major)], 119.5 [C_{meta}' (minor)], 113.8 [C_{ortho}' (major)], 112.2 [C_{ortho}' (minor)]. The relevant resonances for the remaining quaternary carbons in the minor *ortho*-deprotonated product, C_{ipso} and Na-C_{aryl} could not be detected. Due to the presence of three species and resulting complexity, no correlation could be drawn between these signals and those in the aliphatic region.

Crystal data for **9/10**: C₈₂H₁₆₄N₁₃Na₃Zn₄, *M* = 1662.71, triclinic, P-1, *a* = 9.3229(2), *b* = 20.0052(4), *c* = 26.2813(6) Å, α = 86.732(2), β = 82.721(2)°, γ = 87.247(2), *V* = 4850.10(18) Å³, *Z* = 2. 57508 reflections collected, 19054 were unique, *R*_{int} = 0.0630, *R*

= 0.0413, $R_w = 0.0680$, GOF = 0.839, 956 refined parameters, max and min residual electron density = 0.969 and $-0.682 \text{ e.}\text{\AA}^{-3}$. Disorder in the TMEDA groups was treated as being over two sites, appropriate restraints on atom-atom distances and temperature factors in these groups were applied.

Synthesis of [(TMEDA)Na(TMP)(*o*-C₆H₄-NMe₂)Zn(*t*Bu)] **11**

The above-mentioned procedure for preparing the mixture of **9** and **10** was repeated but with TMP(H) (0.34 mL, 2 mmol) introduced to the mixture. The resulting yellow suspension was allowed to stir overnight, after which time the deposited white precipitate was collected by filtration (0.32 g, 31%). This precipitate was re-dissolved in warm hexane and allowed to cool to ambient temperature, affording a small amount of X-ray quality colourless crystals (recrystallised yield: 0.07 g, 7% - not optimised). ¹H NMR (400.13 MHz, 300 K, *d*₈-THF): δ 7.48 [d {³J(H,H) 6.59 Hz}, 1H, H_{meta}], 6.92 [t {³J(H,H) 7.93 Hz}, 1H, H_{meta'}], 6.81 [d {³J(H,H) 7.99 Hz}, 1H, H_{ortho'}], 6.75 [t {³J(H,H) 6.89 Hz}, 1H, H_{para}], 2.70 [s, 6H, N(CH₃)₂], 2.31 [s, 4H, NCH₂ (TMEDA)], 2.15 [s, 12H, NCH₃ (TMEDA)], 1.74 [m, 2H, γ -CH₂ (TMP)], 1.37 [br, 4H, β -CH₂ (TMP)], 1.20 [s, 12H, CH₃ (TMP)], 0.98 [s, 9H, CH₃ (*t*Bu)]. ¹³C {¹H} NMR (100.62 MHz, 300 K, *d*₈-THF): δ 165.0 (C_{ortho}-Zn), 160.1 (C_{ipso}), 141.2 (C_{meta}), 125.5 (C_{meta'}), 122.2 (C_{para}), 114.9 (C_{ortho'}), 58.9 [NCH₂ (TMEDA)], 53.1 [α -C (TMP)], 46.8 [N(CH₃)₂], 46.2 [NCH₃ (TMEDA)], 40.7 [β -CH₂ (TMP)], 36.1 [CH₃ (TMP)], 35.7 [C(CH₃)₃ (*t*Bu)], 20.6 [γ -CH₂ (TMP)], 19.8 [C(CH₃)₃ (*t*Bu)].

Crystal data for **11**: C₂₇H₅₃N₄NaZn, $M = 522.09$, orthorhombic, Pbc_a, $a = 16.1371(5)$, $b = 17.2078(5)$, $c = 21.6306(5) \text{ \AA}$, $V = 6006.5(3) \text{ \AA}^3$, $Z = 8$. 32010 reflections collected, 7240 were unique, $R_{\text{int}} = 0.0540$, $R = 0.0371$, $R_w = 0.0853$, GOF = 0.881, 311 refined parameters, max and min residual electron density = 0.804 and $-0.289 \text{ e.}\text{\AA}^{-3}$.

Electrophilic Quenching Reactions

The solutions prepared as described above, were treated with a freshly prepared solution of 1 M iodine in THF (7 mL, 7 mmol) and allowed to stir overnight. 5 mL of NH_4Cl were added along with the addition of saturated $\text{Na}_2\text{S}_2\text{O}_3$ solution until bleaching occurred (5 mL). The organic layer was separated from the aqueous layer and dried over MgSO_4 . After filtration, the solvent was removed under reduced pressure to give a yellow oil. The NMR spectrum of the crude material was obtained to determine the yield of the iodo-product relative to *N, N*-dimethylaniline.

2-Iodo-*N, N*-dimethylaniline ^1H NMR (400.13 MHz, 300 K, d_6 -benzene): δ 7.76 (d, 1H, H_{meta}), 6.98 (t, 1H, $\text{H}_{meta'}$), 6.72 (d, 1H, $\text{H}_{ortho'}$), 6.46 (t, 1H, H_{para}), 2.45 [s, 6H, $\text{N}(\text{CH}_3)_3$]. ^{13}C $\{^1\text{H}\}$ NMR (100.62 MHz, 300 K, d_6 -benzene): δ 155.4 (C_{ipso}), 140.5 (C_{meta}), 129.1 ($\text{C}_{meta'}$), 125.2 (C_{para}), 120.9 ($\text{C}_{ortho'}$), 97.9 (I-C_{ortho}), 44.7 [$\text{N}(\text{CH}_3)_3$].

3-Iodo-*N, N*-dimethylaniline ^1H NMR (400.13 MHz, 300 K, d_6 -benzene): δ 7.05 (d, 1H, H_{para}), 6.98 (s, 1H, H_{ortho}), 6.70 (t, 1H, $\text{H}_{meta'}$), 6.34 (d, 1H, $\text{H}_{ortho'}$), 2.32 [s, 6H, $\text{N}(\text{CH}_3)_3$]. ^{13}C $\{^1\text{H}\}$ NMR (100.62 MHz, 300 K, d_6 -benzene): δ 151.8 (C_{ipso}), 130.6 ($\text{C}_{meta'}$), 125.5 (C_{para}), 121.4 (C_{ortho}), 111.7 ($\text{C}_{ortho'}$), 96.0 (I-C_{meta}), 39.7 [$\text{N}(\text{CH}_3)_3$].

4-Iodo-*N, N*-dimethylaniline ^1H NMR (400.13 MHz, 300 K, d_6 -benzene): δ 7.42 [d $\{^3\text{J}(\text{H,H})$ 8.84 Hz}, 2H, H_{meta}], 6.13 [d $\{^3\text{J}(\text{H,H})$ 8.98 Hz}, 2H, H_{ortho}], 2.36 [s, 6H, $\text{N}(\text{CH}_3)_3$]. ^{13}C $\{^1\text{H}\}$ NMR (100.62 MHz, 300 K, d_6 -benzene): δ 150.9 (C_{ipso}), 137.8 (C_{meta}), 115.0 (C_{ortho}), 77.7 (I-C_{para}), 39.8 [$\text{N}(\text{CH}_3)_3$].

GC-MS (CI) Found $(\text{M} + \text{H})^+$ 247.9, $\text{C}_8\text{H}_{10}\text{IN}$ requires 246.9.

For unidentified species, GC-MS (CI) Found $(\text{M} + \text{H})^+$ 373.8, $\text{C}_8\text{H}_9\text{I}_2\text{N}$ requires 372.8.

Chapter 3 - References

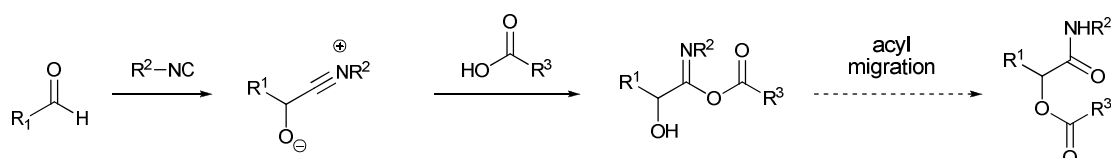
- [1] D. R. Armstrong, W. Clegg, S. H. Dale, E. Hevia, L. M. Hogg, G. W. Honeyman, R. E. Mulvey, *Angew. Chem. Int. Ed.* **2006**, *45*, 3775 - 3778.
- [2] R. J. Card, W. S. Trahanovsky, *J. Org. Chem.* **1980**, *45*, 2560 - 2566.
- [3] E. Baston, R. Maggi, K. Friedrich, M. Schlosser, *Eur. J. Org. Chem.* **2001**, 3985 - 3989.
- [4] (a) A. J. Chalk, T. J. Hoogeboom, *J. Organomet. Chem.* **1968**, *11*, 615 - 618; (b) C. D. Broaddus, *J. Am. Chem. Soc.* **1966**, *88*, 4174 - 4178.
- [5] D. R. Armstrong, J. García-Álvarez, D. V. Graham, G. W. Honeyman, E. Hevia, A. R. Kennedy, R. E. Mulvey, *Chem. Eur. J.* **2009**, *15*, 3800 - 3807.
- [6] D. Nobuto, M. Uchiyama, *J. Org. Chem.* **2008**, *79*, 1117 - 1120.
- [7] W. Clegg, B. Conway, E. Hevia, M. D. McCall, L. Russo, R. E. Mulvey, *J. Am. Chem. Soc.* **2009**, *131*, 2375 - 2384.
- [8] D. R. Armstrong, V. L. Blair, W. Clegg, S. H. Dale, J. García-Álvarez, G. W. Honeyman, E. Hevia, R. E. Mulvey, L. Russo, *J. Am. Chem. Soc.* **2010**, *132*, 9480 - 9487.
- [9] V. Snieckus, *Chem. Rev.* **1990**, *90*, 879 - 933.
- [10] G. Wittig, H. Merkle, *Ber. Dtsch. Chem. Ges. B* **1942**, *75*, 1491 - 1500.
- [11] A. R. Lepley, W. A. Khan, A. B. Giumanini, A. G. Giumanini, *J. Org. Chem.* **1966**, *31*, 2047 - 2051.
- [12] M. Niemeyer, P. P. Power, *Organometallics* **1997**, *16*, 3258 - 3260.
- [13] J. Betz, F. Hampel, W. Bauer, *J. Chem. Soc., Dalton Trans.* **2001**, 1876 - 1879.
- [14] C. Schade, P. v. R. Schleyer, H. Dietrich, W. Mahdi, *J. Am. Chem. Soc.* **1986**, *108*, 2484 - 2485.
- [15] D. W. Slocum, T. L. Reece, R. D. Sandlin, T. K. Reinscheld, P. E. Whitley, *Tetrahedron Lett.* **2009**, *50*, 1593 - 1595.
- [16] CSD version 5.31 see: F. H. Allen, *Acta. Crystallogr., Sect. B* **2002**, *58*, 380 - 388.
- [17] W. Clegg, S. H. Dale, R. W. Harrington, E. Hevia, G. W. Honeyman, R. E. Mulvey, *Angew. Chem. Int. Ed.* **2006**, *45*, 2374 - 2377.
- [18] L. M. Carella, C. Förster, A. R. Kennedy, J. Klett, R. E. Mulvey, E. Rentschler, *Organometallics* **2010**, *29*, 4756 - 4758.

- [19] N. P. Lorenzen, J. Kopf, F. Olbrich, U. Schümann, E. Weiss, *Angew. Chem. Int. Ed.* **1990**, *29*, 1441 - 1444.
- [20] D. R. Armstrong, G. C. Forbes, R. E. Mulvey, W. Clegg, D. M. Tooke, *J. Chem. Soc., Dalton Trans.* **2002**, 1656 - 1661.
- [21] N. A. Bell, H. M. M. Shearer, C. B. Spencer, *Acta. Crystallogr., Sect. C* **1983**, *39*, 1182 - 1185.
- [22] M. P. Coles, P. B. Hitchcock, *Eur. J. Inorg. Chem.* **2004**, 2662 - 2672.

Chapter 4: Synergic Synthesis of Benzannulated Metallacyclic Complexes

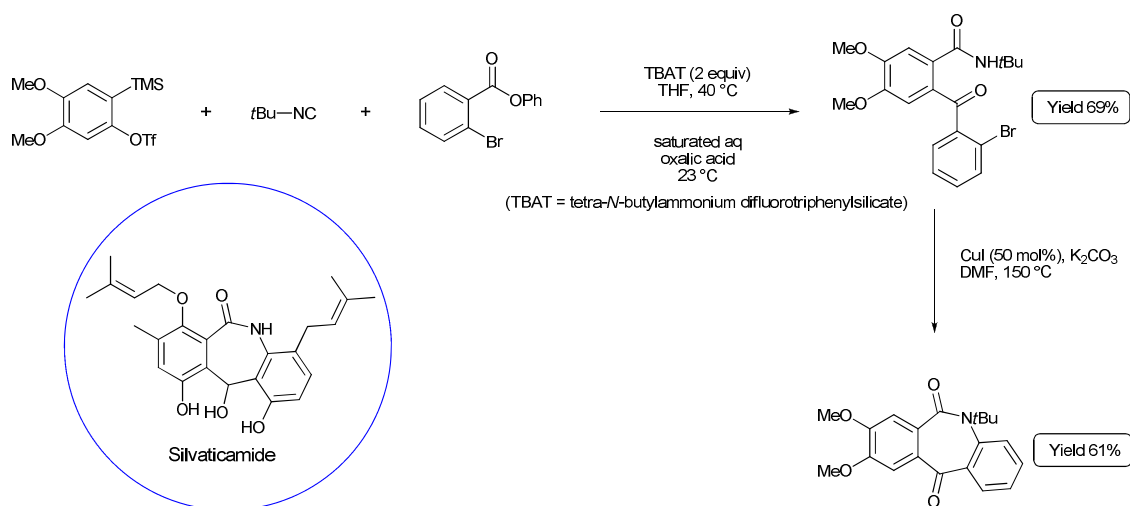
4.1) Multicomponent Reactions

Nowadays, the issue of chemical synthesis is under the spotlight more than ever. In the interest of meeting society's escalating demand for new chemical entities, creative solutions that fashion new molecules with specific properties are desired, but contemporary design must harmonise with increasing economical and ecological considerations. Evolving around rooted virtues such as simplicity, selectivity, succinct and high yielding; today's ideal synthesis should be simultaneously highly diverse, derived from readily available starting materials and environmentally benign. Comprising a chain reaction of organic processes, multicomponent reactions are the epitome of synthetic efficiency and reaction design.^[1] A multicomponent reaction is defined as a reaction in which three or more compounds react in a single operation to form a single product that contains essentially all of the atoms of the starting materials (with the exception of small condensation products such as H₂O, HCl or MeOH).^[2] However, with the simultaneous collision of three or more distinct molecules highly unlikely, multicomponent reactions frequently comprise of a number of subreactions. Largely flying under the radar in organic chemistry, an extension of the classic Passerini reaction (Scheme 4.1) unlocked the potential of this highly dynamic field.



Scheme 4.1: Generic example of the Passerini synthesis of α -acyloxyamides from isocyanides, carboxylic acids and carbonyl compounds.

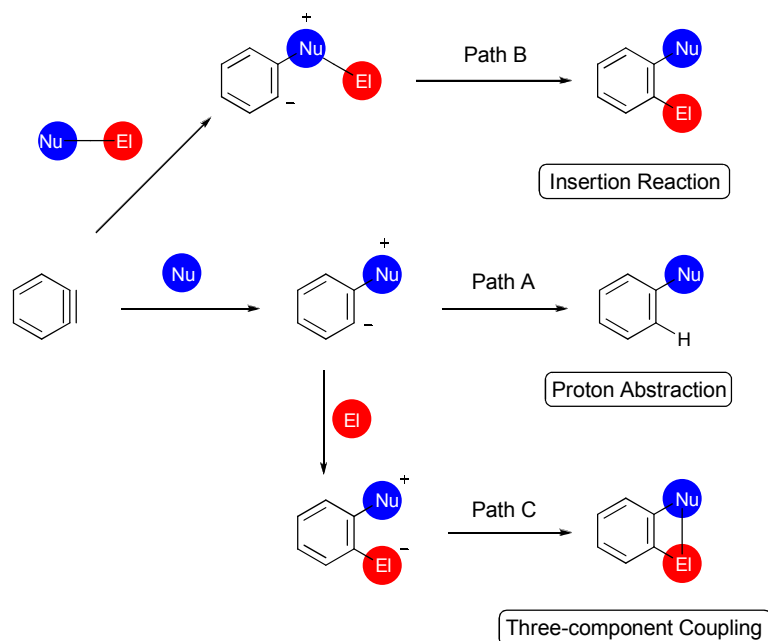
The Passerini reaction between carboxylic acids and carbonyl compounds with isonitriles is a widely applicable route for the synthesis of α -acyloxyamides where the aldehyde acts as both an electrophile and nucleophile during the course of the reaction.^[3] Over forty years would pass before Ugi, armed with prevailing reaction mechanisms performed the condensations of assorted amines and aldehydes or ketones with isonitriles revealing the generality of Passerini's methodology.^[4] Today adaptations of the Passerini reaction are still forthcoming, assembling new innovative types of multicomponent reactions. Replacing the aldehyde component with an aryne, Stoltz *et al.* have successfully prepared *o*-ketobenzamides using a multicomponent approach (Scheme 4.2).^[5] Illustrating their synthetic utility, intramolecular cyclisation of bromobenzamides generates caprolactams that share structural similarity with the bioactive natural product, silvaticamide intimating a potential future role in total synthesis for this multicomponent methodology.



Scheme 4.2: Three-component one-pot synthesis of *o*-ketobenzamides and their intramolecular cyclisation to produce caprolactams.

Benzyne has played an intrinsic role in the discovery of novel multicomponent reactions for over seventy years,^[6] by virtue of their low-lying LUMO, the salient

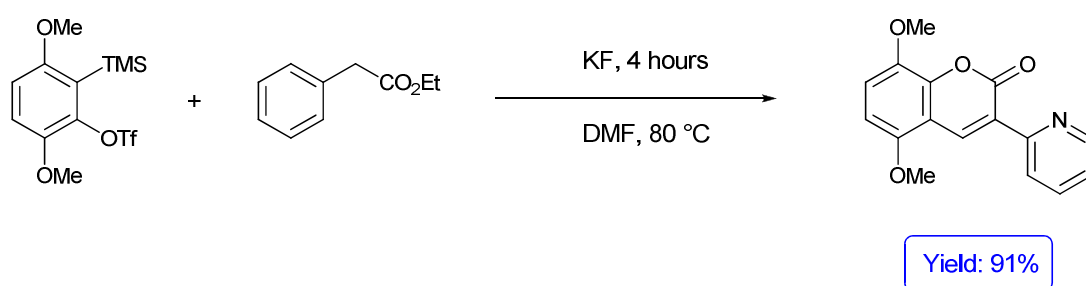
electrophilic character of arynes initiates facile addition of neutral nucleophiles of moderate nucleophilicity, producing zwitterionic intermediates which can then follow one of three reaction pathways (Scheme 4.3). Generally, the emanating aryl anion is primed for proton abstraction from the cationic site producing monosubstituted arenes (Path A)^[7] but on occasion double functionalisation of the aryne is attainable. Insertion reactions into a nucleophilic-electrophilic σ -bond provides a conducive method for installing functionality to both ends of the triple bond (Path B)^[8] while for greater structural complexity and diversity, cyclisation by capturing the zwitterion intermediates with an electrophile represents an attractive synthetic prototype (Path C).



Scheme 4.3: Generation of zwitterionic intermediates from the addition of nucleophiles to arynes, and three potential subsequent reaction pathways.

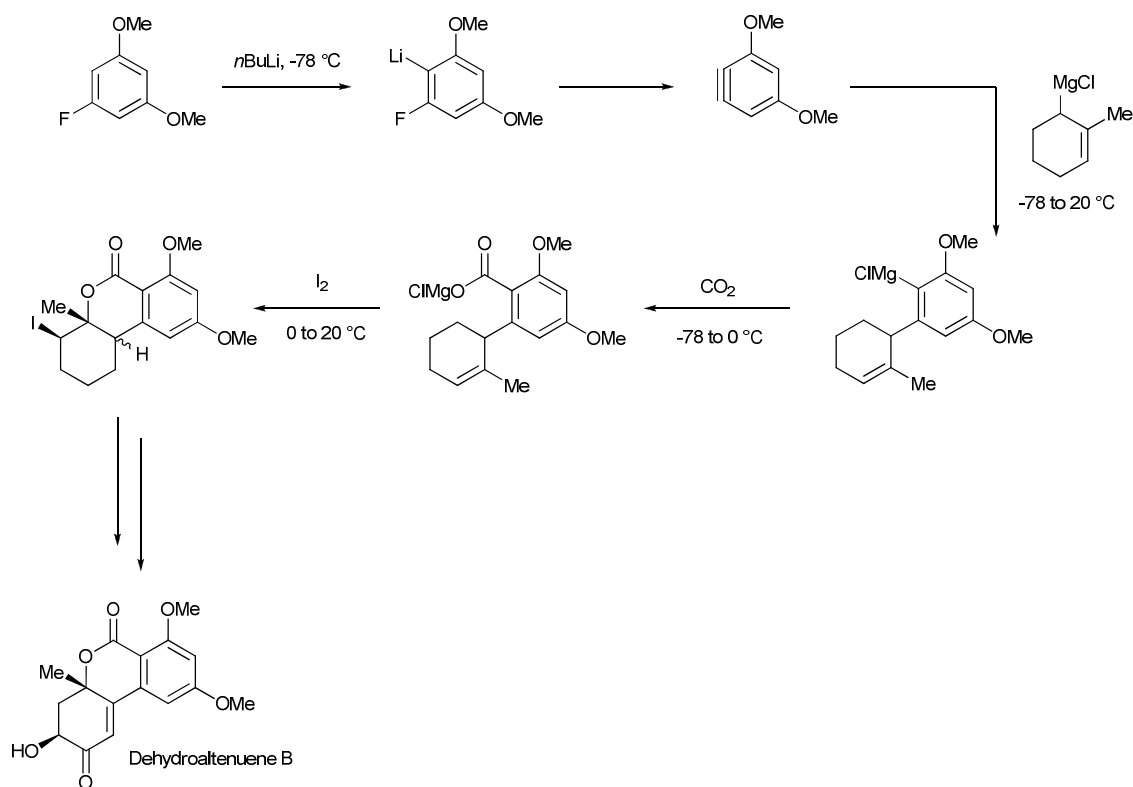
Elegantly described as three-component couplings of benzyne, unsaturated nucleophiles and electrophiles, Kunai and Yoshida have implemented this protocol for the *ortho*-selective double functionalisation of aromatic skeletons^[9] and as a convenient avenue to benzo-annulated nitrogen or oxygen heterocycles.^[10] Despite their transient

nature, a selection of substituted arynes can be utilised in a selective three-component one-pot reaction to provide a myriad of benzo-annulated iminofuran and iminoindole derivatives which are difficult to prepare by orthodox methods. Supplementing these offerings, *ortho*-quinone methides, prepared from arynes and DMF (dimethylformamide), are smoothly coupled with active methylene compounds or arylacetic acid esters tendering a previously concealed route to diverse coumarins which constitute a significant class of biologically active compounds (Scheme 4.4).^[11]



Scheme 4.4: Synthesis of coumarins via substituted arynes using a three-component coupling methodology.

From an inorganic perspective, the generation and capture of benzyne by organometallic reagents (including lithium amides) has been well documented in a review article^[12] but in relation to multicomponent reactions in organic synthesis a worthy example has been provided by Barrett.^[13] In the first total synthesis of the antibacterial marine natural product dehydroaltenune B (Scheme 4.5), a key step is the preparation of the iodide **A**, by a four-component coupling strategy involving nucleophilic addition of the benzyne with the Grignard reagent to regioselectively afford the arylmagnesium chloride primed for carboxylation and iodolactonisation.



Scheme 4.5: Four-component benzyne coupling reaction for the total synthesis of dehydroaltenuene B.

In these austere times, multicomponent reactions are most definitely in vogue when it comes to the generation of small organic molecules. However, with regard to properties such as biological activity, there is a perpetual requisite for fresh reactions to ensure sufficient molecular diversity. The diversity sought can be broken down into different levels, prominent are appendage and scaffold diversity.^[2] Appendage diversity revolves around a common molecular skeleton (scaffold) and the introduction of different appendages producing compounds with a general molecular shape but particularly important is scaffold diversity, the synthesis of compounds with different molecular scaffolds. As with many aspects of science, serendipity has and will always be a factor in the discovery of new multicomponent reactions but with the knowledge accrued in times gone by, rational design strategies have become more prominent over the past decade. Nevertheless, with possible combinations of the traditional building blocks [e.g.

isocyanides^[14] (Passerini, Ugi) and the combination of β -dicarbonyl compounds, amines, and aldehydes (Hantzsch, Biginelli)^[15] limited, future multicomponent protocols are likely to focus on the one-pot combination of sequential, orthogonal reactions ensuring highly atom- and step-economical procedures.

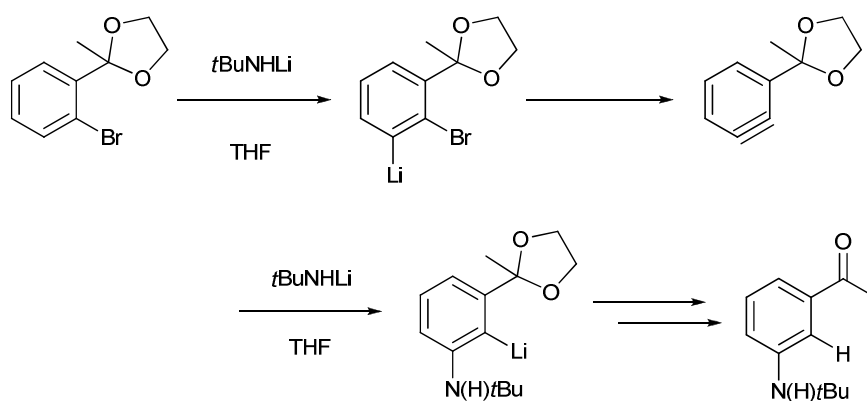
4.2) Background To Arynes

Benzynes (arynes) are highly reactive chemical intermediates, which due to their flexibility to act as electrophiles, nucleophiles, dienophiles, alkynes and two or four electron donors have found widespread application in organic synthesis.^[16] A transient species, there are various representations of the structure of benzyne (Figure 4.1); the most common in terms of reaction mechanism being the cycloalkynyl structure which is advocated by low temperature (8 K) IR spectra in an argon matrix^[17] and microwave spectra in the gas phase.^[18]



Figure 4.1: The classic representations of benzyne.

However, the exact nature of the structure of benzyne is far from definite. The zwitterionic representation reflects a habitual journey to benzynes and parallel aryne; *ortho*-metallation of a mono-substituted aryl ring, furnishing an electron-rich, metal-bound carbon adjacent to one harbouring a leaving group represents a time-honoured route to aryne. From a synthetic viewpoint, the obligation for a solitary mono-functionalised aromatic substrate offers an advantage over alternative routes but on occasion, strategic placement of a second aryl substituent can be beneficial in effecting a 1,2-transposition of functionality (Scheme 4.6).^[19]



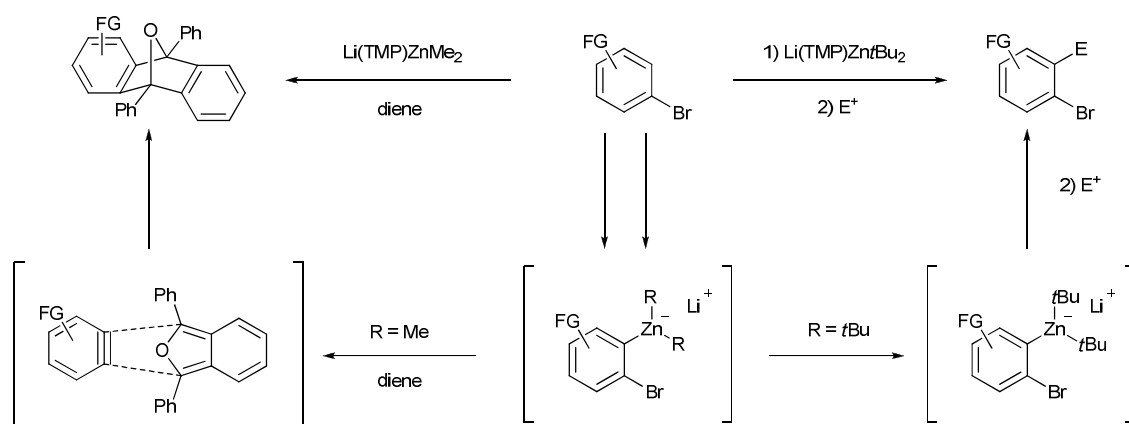
Scheme 4.6: An efficient synthesis of *meta* *N*-*tert*-butylamino acetophenone that exploits *in situ* aryne formation.

This propensity to benzyne formation is a limiting feature for the use of haloaromatics in Directed-*ortho*-Metallation with reaction conditions consequently, carefully controlled. Deprotonation of chlorobenzene is feasible with *s*BuLi in THF, but only at -105 °C to prevent collapse to a benzyne^[20] and similarly chlorobenzene and bromobenzene can be lithiated with moderate yield and selectivity by LDA or LiTMP at -75 or -100 °C.^[21] However, often at these extreme temperatures there is a trade-off as metallation is slow and cannot be completely accomplished. Therefore in this section, AMMZn is introduced to haloaromatics and attempts to isolate and characterise the metallated intermediates generated at ambient temperature will be discussed. However, echoing the abovementioned difficulties experienced in organolithium-mediated *ortho*-deprotonation, an unexpected series of compounds were subsequently prepared.

4.3) The Unexpected Synthesis of Zincabicyclic Complexes

In the few previous studies of reactions of aryl halides and TMP-zincates,^[22] no experimental evidence has been collected on the chemistry taking place between the limits of the starting materials and the zinc-free quenched products (Scheme 4.7).

Therefore, to shed light on the critical metal (and bimetal) activity stage of these reactions, our primary objective was to get inside these limits by isolating and characterising representative zinc-containing intermediates. With conditions stringently controlled for its lithiation, the zincation of chlorobenzene was investigated by treatment with an equimolar quantity of sodium TMP-zincate [(TMEDA)Na(μ -TMP)(μ -*t*Bu)Zn(*t*Bu)] (**1**). However, fully characterised by X-ray crystallography and NMR spectroscopy, the unexpected final product isolated from this reaction is the remarkable zwitterionic benzannulated bicyclic zinc complex [$\{1\text{-Zn}(t\text{Bu})\}^- \cdot \{2\text{-N}(\text{Me})(\text{CH}_2\text{CH}_2\text{CH}_2\text{NMe}_2\}^+ \cdot \text{C}_6\text{H}_4\}$] (**12**) (Scheme 4.8). This product was obtained as small colourless block crystals in a 20.7% yield. To obtain a higher yield, a mixture of **1** (2 mmol) and chlorobenzene (1 mmol), following 48 hours stirring at room temperature, produces a powder of **12** in a refined yield of 51%.



Scheme 4.7: Summary of the previous reactions of TMP-zincates and aryl halides.

Since it was reported earlier that reaction of “ $\text{LiZn}(\text{TMP})t\text{Bu}_2$ ” with haloarenes followed by electrophilic trapping produced polyfunctional haloarenes (*i.e.*, with retention of the original halogen substituent),^[22] we expected **12** to be an *ortho*-zincated chlorobenzene derivative. Surprisingly, however, chloride is absent and while its aromatic ring appears to have been *ortho*-zincated, **12** has several other unexpected new

bonding features. Thus, a nitrogen from TMEDA that links to the zinc atom through a CH₂ bridge and a CH₂CH₂N(Me)₂ bridge, is now attached to the ring. Terminal methyl and *tert*-butyl groups on the aryl-attached nitrogen and zinc atoms respectively, complete the formulation, which can be interpreted as a mesoionic zwitterion^[23] with a ⁺NR₃-CH₂-Zn⁻ β-dipole. Alternatively, **12** can be classified as an α-zincated N ylide.

Determined by X-ray crystallography the molecular structure of **12** (Figure 4.2) is mononuclear, with both the Zn and N(1) atoms chiral as attached to four different substituents, though overall the crystal structure is centrosymmetric and hence the material is racemic. Three anionic carbon atoms (two aliphatic sp³ atoms from the *t*Bu and deprotonated CH₂N groups and one aryl sp² atom) bind to zinc [bond distances of 2.0245(15)/2.0611(16) and 2.0615(15) Å, respectively] with a dative interaction from the N(Me)₂ atom [2.3313(13) Å] completing the distorted tetrahedral coordination of the metal. Ring constraints severely distort this geometry with bond angles ranging from 84.54(6)° [C(2)-Zn(1)-C(10)] to 134.05(6)° [C(10)-Zn(1)-C(13)] and a mean value of 107.39°. The Zn and N(1) atoms lie slightly to one side of the benzene ring plane (by 0.138 and 0.090 Å, respectively). A search of the Cambridge Crystallographic Database revealed only six structures which contain zinc and a non-hydrogen atom at adjacent positions on an aromatic ring and significantly, no precedent for this structure.^[24] There is one example of an α-zincated phosphorus ylide [$\{1\text{-Zn(HMDS)(py)}\}^- \{2\text{-P(Ph)}_2\text{(CH}_2\text{)}\}^+ \text{-C}_6\text{H}_4$] formed by reaction of the phosphorus ylide Ph₃P=CH₂, Zn(HMDS)₂ and pyridine at 60 °C.^[25] While the zinc-C_{aryl} bond in this complex [2.050(3) Å] is only slightly shorter than that in **12**, the bridging zinc-carbon bond is long at 2.138(4) Å possibly affected by the electron-withdrawing phenyl groups on phosphorus. This results in a larger C-Zn-C angle in this complex 92.9(1)° in comparison to that in **12** [C(2)-Zn(1)-C(10) 84.54(6)°].

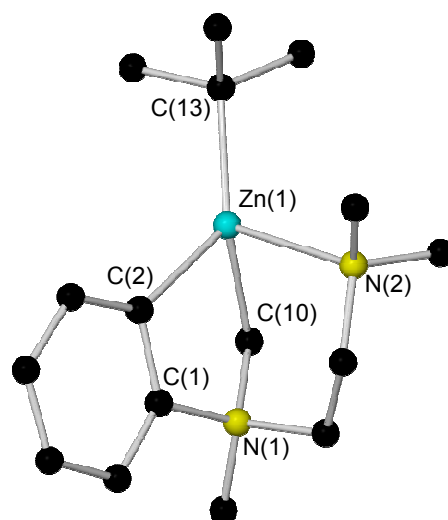
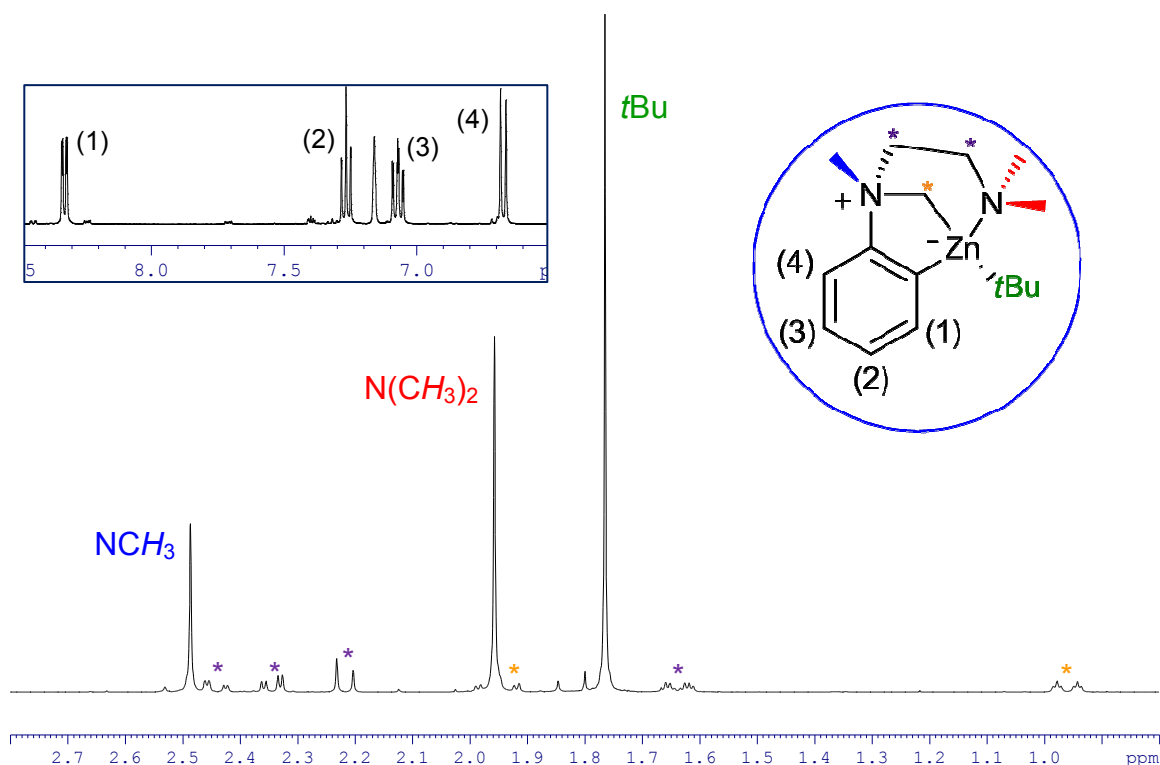


Figure 4.2: Molecular structure of zincabicyclic **12** with selective atom labelling. Hydrogen atoms are omitted for clarity. Selected bond lengths (Å) and angles (deg): Zn(1)-C(2) 2.0615(15), Zn(1)-C(10) 2.0611(16), Zn(1)-C(13) 2.0245(15), Zn(1)-N(2) 2.3313(13), N(1)-C(1) 1.5173(18), N(1)-C(10) 1.5374(19); C(2)-Zn(1)-N(2) 92.53(5), C(2)-Zn(1)-C(10) 84.54(6), C(2)-Zn(1)-C(13) 130.80(6), N(2)-Zn(1)-C(10) 89.63(5), N(2)-Zn(1)-C(13) 112.84(6), C(10)-Zn(1)-C(13) 134.05(6).

All the anticipated different types of hydrogen atom in **12** are accounted for and well resolved in its ^1H NMR spectrum recorded from d_6 -benzene solution (Spectrum 4.1). Belonging to metallated TMEDA, the Me_2N and $\text{Me}'\text{N}$ resonances appear at 1.96 and 2.49 ppm, respectively, while all six H atoms of the three unique CH_2 groups are inequivalent having separate resonances at 0.96/1.94, 1.63/2.44 and 2.22/2.34 ppm, consistent with the rigid, bicyclic conformation of the structure. The pairing most upfield can be attributed to the deprotonated NCH_2 unit of TMEDA. Four aromatic resonances at 6.67, 7.07, 7.26 and 8.32 ppm denote the H atoms at the 3 (*ortho* to N), 4, 5 and 6 (*ortho* to Zn) positions and the *t*Bu resonance at 1.76 ppm completes the assignment. Similarly, the ^{13}C NMR spectrum of **12** is easily fully assignable.

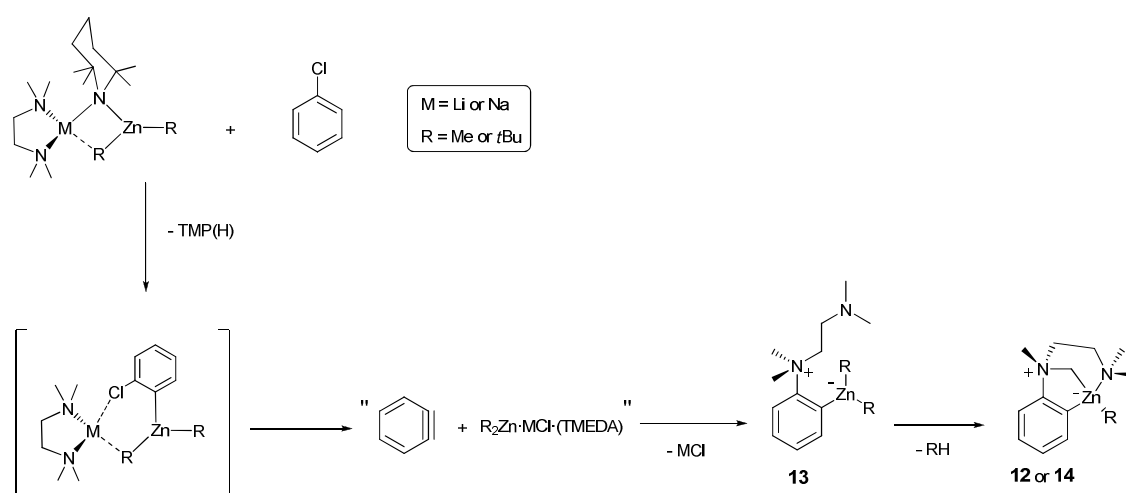


Spectrum 4.1: Aliphatic region of the ^1H NMR (400.13 MHz, 300 K) spectrum of **12 in d_6 -benzene solution, and inset the aromatic region.**

Formation of **12** can be rationalised by a novel four-step *ortho*-zincation, zincate (or sodium chloride) elimination, azazincation-addition, amine α -zincation domino^[26] sequence. An intermediate along this path formed prior to the final step (amine α -zincation), $[\{1\text{-Zn}(t\text{Bu})_2\}^- \{-2\text{-N}(\text{Me})_2\text{CH}_2\text{CH}_2\text{NMe}_2\}^+ \text{-C}_6\text{H}_4]$ (**13**) has also been isolated from the reaction and characterised crystallographically and by NMR spectroscopy.

Scheme 4.8 proposes a pathway for the formation of zincacyclic **12**. *Ortho*-zincation of chlorobenzene would be the first step, almost certainly through heteroleptic **1** functioning kinetically as a TMP base with concomitant release of TMP(H).^[27] As mentioned previously, **1** appears to generally react firstly as a TMP base in reactions with aromatic substrates. This would generate a sodium monoaryl-bisalkylzincate intermediate for which there are close analogies in lithium^[28] and sodium-TMP

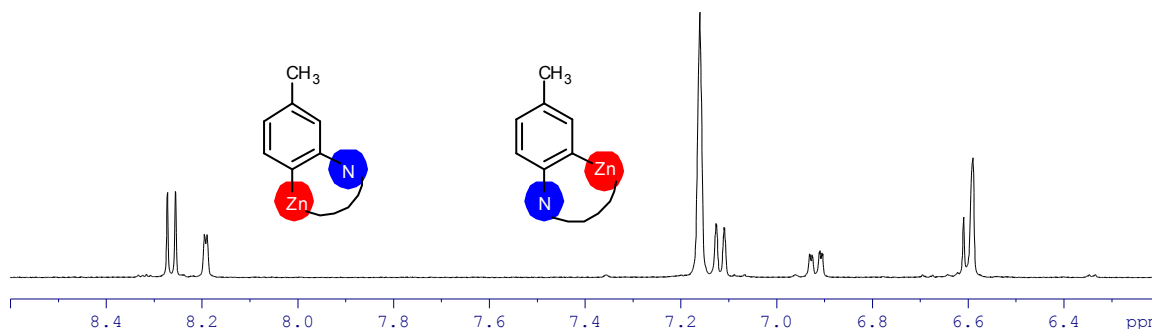
chemistry,^[29] but the lack of TMP in the later intermediate **13** is perhaps the strongest evidence. Next, the Zn and Cl σ -attachments to the benzene ring could both cleave to generate an *o*-benzyne intermediate and “(*t*Bu₂Zn)·NaCl·TMEDA” or fragments thereof. Militating against this mechanism are Uchiyama’s aforementioned studies of “LiZn(TMP)*t*Bu₂”,^[22] which reveal no evidence for benzyne formation towards haloarenes, but that reaction must follow a different pathway to ours as the halogen substituent is retained on the aryl ring, whereas it is cleaved in our case.



Scheme 4.8: Proposed formation of 12, 13 and 14 through sodium-TMEDA-mediated zincation of chlorobenzene.

Note that at this stage in our reaction the benzyne molecule may not be “naked” but could be involved in a benzyne-zincate intermediate in which one of the metals interacts with the π -system of the benzyne triple bond. Evidence for this type of cation- π intermediate comes from DFT calculations on model zincates in the aforesaid Uchiyama paper.^[22] Subsequent addition of TMEDA and *t*Bu₂Zn across the benzyne triple bond leads to **13** and elimination of NaCl. The unexpected attachment of TMEDA might be interpreted as a type of complex-induced proximity effect (CIPE)^[30] due to the Na(TMEDA) unit lying close to the C atom originally carrying the Cl substituent. By repeating the reaction with 4-chlorotoluene in place of chlorobenzene to get a fix on the

position of zincation, we observed zinc adding to both the 3 and 4 positions, which supports the existence, at least in part, of such a benzyne mechanism. From Spectrum 4.2, it can be seen that the isomers form in an approximate ratio of 60:40, rather than the expected 50:50 proportion associated with a benzyne intermediate (the 10% deviation could be due to the added steric/electronic influence of the methyl group).



Spectrum 4.2: Aromatic region of the ¹H NMR spectrum (400.13 MHz, 300 K) of the crystalline product isolated from reaction of sodium TMP-zincate **1 and 4-chlorotoluene in *d*₆-benzene solution, showing the two possible aryl zincacycles.**

Intermediate **13** provides convincing proof of this stage of the reaction sequence. Made by easing the experimental conditions (no refluxing of the solution), **13** has a molecular structure (Figure 4.3) akin to that of **12** but with two *t*Bu ligands attached to zinc and with an intact TMEDA molecule occupying an *ortho*-position next to, but not attached to the Zn(*t*Bu)₂ unit. In the final step, one *t*Bu ligand deprotonates one NMe₂ arm of TMEDA to build an N-CH₂-Zn bridge, while concomitantly reduced steric constraints around the zinc centre allow the free Me₂N terminal of the benzene-tethered TMEDA to datively bind to Zn to close a seven-atom (ZnCCNCCN) ring. Usually α -metallations of amines have high kinetic barriers due to the destabilisation incited by the repulsive interaction of the carbanion with the adjacent nitrogen lone pair^[31] and would conventionally be considered impossible for only mildly electropositive zinc, but here the barrier must be reduced substantially by the close proximity of the tethered *t*Bu₂Zn

and TMEDA units which sets up a favourable intramolecular Zn-H exchange reaction with loss of BuH; while it is also noted that the positive charge of the N atom is also a factor in making the α -CH₃ more acidic, akin to Lewis acid (e.g. borane)-activated amines.^[32]

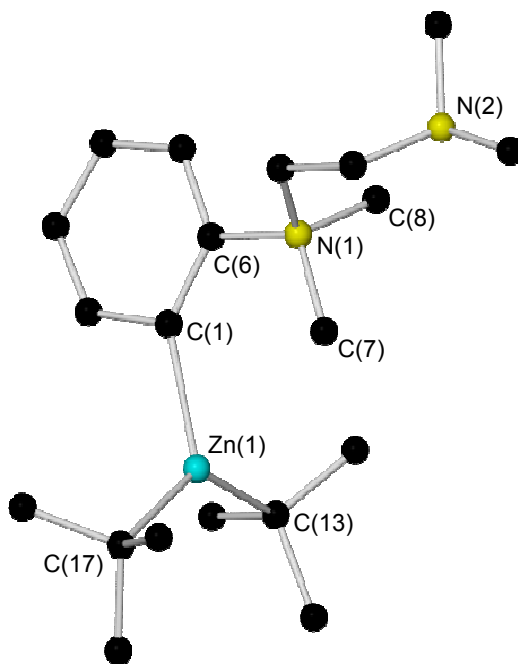


Figure 4.3: Molecular structure of **13** with selective atom labelling. Hydrogen atoms are omitted for clarity. Selected bond lengths and distances (Å): Zn(1)-C(1) 2.079(4), Zn(1)-C(13) 2.041(5), Zn(1)-C(17) 2.036(5), N(1)-C(6) 1.542(5), N(1)-C(7) 1.494(5), N(1)-C(8) 1.508(5), C(7)⋯C(13) 4.007(7), C(7)⋯C(17) 4.220(6), C(8)⋯C(13) 4.939(7), C(8)⋯C(17) 6.235(7).

As aforementioned, loss of the halogen substituent distinguishes this new AMMZn reaction from those of “LiZn(TMP)*t*Bu₂” which, when intercepted by electrophiles, give polysubstituted haloarenes. Emphasising the strong solvent dependency of AMMZn reactions, significantly the former was performed in hexane solution containing TMEDA, whereas the latter were performed in THF with no TMEDA. Zincate reactions are also sensitive to the alkyl group on zinc. Interestingly, Uchiyama reports that “LiZn(TMP)Me₂” behaves differently from “LiZn(TMP)*t*Bu₂” towards

haloarenes, generating benzyne intermediates which can be trapped by dienes to produce polysubstituted halogen-free aromatic compounds (see Scheme 4.7),^[22] the reaction leading to **12** thus represents a new, third variation on this theme.

Probing alkyl effects in our system, significantly, we isolated the methyl analogue of **12**, [$\{1\text{-Zn(Me)}\}^- \{2\text{-N(Me)(CH}_2\text{)CH}_2\text{CH}_2\text{NMe}_2\}^+ \text{-C}_6\text{H}_4$] (**14**), from the reaction of chlorobenzene and the lithium methylzincate “(TMEDA)·LiZn(TMP)Me₂”. Reflecting its high solubility **14** was isolated in a poor crystalline yield of only 13%. Here the construction of the N-CH₂-Zn bridge must involve a methyl deprotonation (through a “Me-Zn” unit) of an N-Me group, a reaction normally even more difficult than a *tert*-butyl deprotonation (through a “*t*Bu-Zn” unit). Determined by X-ray crystallography, the molecular structure of **14** (Figure 4.4) is essentially identical to that of **12** with a Me instead of a *t*Bu ligand terminally attached to zinc.

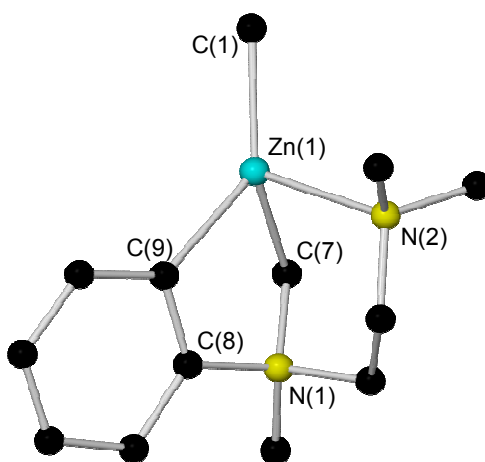


Figure 4.4: Molecular structure of **14** with selective atom labelling. Hydrogen atoms are omitted for clarity. Selected bond lengths (Å) and angles (deg): Zn(1)-C(1) 2.000(3), Zn(1)-C(7) 2.061(3), Zn(1)-C(9) 2.069(3), Zn(1)-N(2) 2.256(2), N(1)-C(7) 1.537(4), N(1)-C(8) 1.521(4); C(9)-Zn(1)-N(2) 93.82(10), C(9)-Zn(1)-C(7) 84.43(12), C(9)-Zn(1)-C(1) 134.60(12), N(2)-Zn(1)-C(7) 91.57(12), N(2)-Zn(1)-C(1) 108.12(12), C(7)-Zn(1)-C(1) 132.27(13).

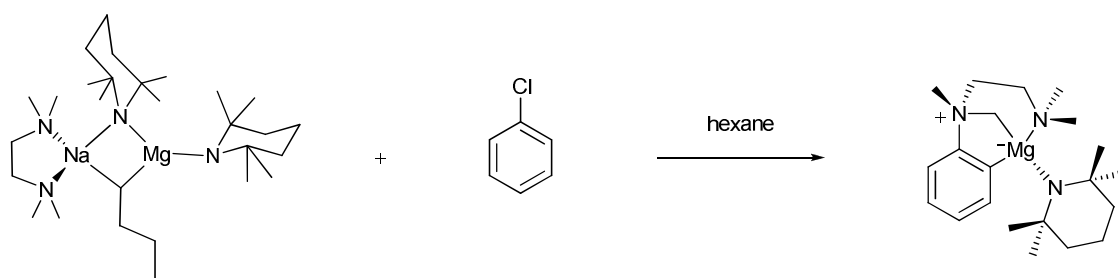
It is worth commenting that the primary role of TMEDA in organometallic and coordination chemistry is as a didentate N donor ligand, but here in the formation of **12** and **14** it has an unusual three-fold function. It acts first as a neutral N nucleophile towards an electron-deficient aromatic C atom; second as an anionic C nucleophile towards Zn (through an unprecedented direct zincation of TMEDA); and third as a neutral N ligand towards Zn.

Formally, **12**, **13** and **14** could be considered the products of three component couplings of PhCl, R₂Zn (R = *t*Bu or Me) and TMEDA. It was therefore decided to try such reactions by mixing these three components in hexane solution. However, such reaction mixtures do not lead to zincacyclic products (on the evidence of NMR spectroscopic studies there was no trace of a zinc-aryl product even when harsh reflux conditions were applied). In practice, NaTMP or LiTMP must be present, so it appears to be cooperativity between the different components within **1** and related zincates that are behind the construction of **12** and **14**, hence these reactions can be interpreted as new and novel examples of “synergic synthesis”.

4.4) The Quest for Molecular Diversity

An intriguing question raised by these results centred on whether this zincacycle-producing reaction could be extended to a wide range of metals and neutral nucleophiles to provide access to new families of metallacyclic compounds. Exploration of a different metal proved promising. The monoalkyl-bisamido magnesiate complex [(TMEDA)Na(μ-TMP)(μ-*n*Bu)Mg(TMP)] has previously showcased its deprotonative ability towards benzene^[33] and in the regioselective *meta*-magnesiumation of toluene,^[34] thus preliminary reactions of it with chlorobenzene were performed at ambient temperature. Accordingly, the reaction reproducibly affords the cognate

zwitterionic benzannulated magnesacycle complex $[\{1\text{-Mg(TMP)}\}^- \{-2\text{-N(Me)(CH}_2\text{)CH}_2\text{CH}_2\text{NMe}_2\}^+ \text{-C}_6\text{H}_4\text{}]$ (**15**) in a crystalline yield of 44% (Scheme 4.9). In addition to increasing the base:substrate ratio to attempt to boost product yields, complex **15** can be isolated in powder form in an increased 71% yield when generating *in situ* $n\text{Bu}_2\text{Mg}$ (from a mixture of $n\text{BuMgCl}$ and $n\text{BuLi}$) sidestepping issues presented by aluminium additives in commercial $n\text{Bu}_2\text{Mg}$ solutions.^[35]



Scheme 4.9: Synthesis of magnesacycle complex 15 through sodium-TMEDA-mediated magnesiation of chlorobenzene.

The molecular structure of magnesacycle **15** (Figure 4.5) is constructed upon the same scaffold as **12** and **14**, but where zinc carries a terminal alkyl group in the latter complexes (*t*Bu in **12** and Me in **14**) the metal in **15** retains a TMP ligand reflecting magnesium's greater affinity for nitrogen and the fact the precursor was a bis(amide) as opposed to a bis(alkyl). The products of Alkali-Metal-Mediated Magnesiation typically preserve their TMP ligands, displaying overall thermodynamic alkyl basicity but as with TMP-zincate **1**, evidence exists for the potassium TMP-magnesiate $[(\text{PMDETA})\text{K}(\mu\text{-TMP})(\mu\text{-CH}_2\text{SiMe}_3)\text{Mg}(\text{TMP})]$ exhibiting kinetic amido basicity in the metallation of anisole.^[36] The tetrahedrally distorted (mean angle 107.42°) chiral magnesium essentially lies in the plane of the benzene ring as does the aryl bound N3, and bonds comparably to the aryl and bridging carbon atoms [Mg(1)-C(1) 2.184(2) and Mg(1)-C(25) 2.172(3) Å, respectively]; while the same can be said for the parallel nitrogen-carbon bond distances [N(3)-C(2) 1.519(3) and N(3)-C(25) 1.542(3) Å,

respectively]. As anticipated, the Mg-N(TMP) bond is significantly shorter than the dative Mg-N(TMEDA) bond [Mg(1)-N(1) 1.9924(19) and Mg(1)-N(2) 2.227(2) Å, respectively]; a trend consistent with the bond distances found for Mountford and Breher's zwitterionic magnesium amide complex [Mg{C-Me₂pz}₃{N(SiMe₃)₂}] that is prepared by deprotonation of the poly(pyrazolyl)methane ligand with Mg(HMDS)₂ (in which pz is pyrazolyl) where the Mg-N(SiMe₃)₂ and Mg-Npz distances are within the expected range [1.987(2) and 2.094(2), 2.152(2), 2.098(2) Å, respectively].^[37]

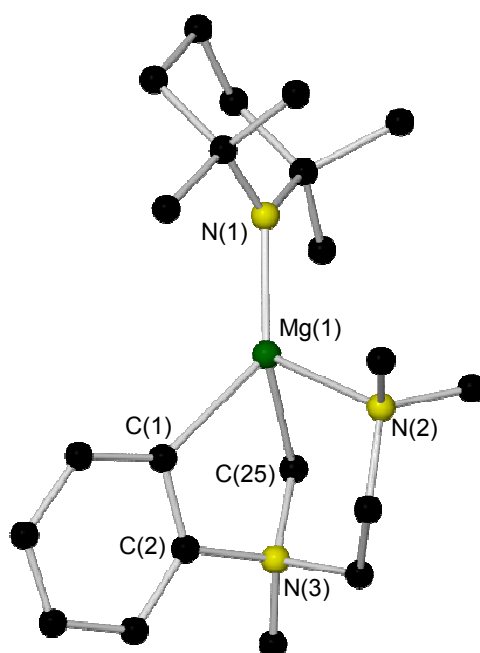


Figure 4.5: Molecular structure of magnesiumacycle **15** with selective atom labelling. Hydrogen atoms are omitted for clarity. Selected bond lengths (Å) and angles (deg): Mg(1)-C(1) 2.184(2), Mg(1)-C(25) 2.172(3), Mg(1)-N(1) 1.9924(19), Mg(1)-N(2) 2.227(2), N(1)-C(2) 1.519(3), N(1)-C(25) 1.542(3); C(1)-Mg(1)-N(1) 134.79(9), C(1)-Mg(1)-N(2) 94.66(8), C(1)-Mg(1)-C(25) 79.48(10), N(1)-Mg(1)-N(2) 115.30(8), N(1)-Mg(1)-C(25) 129.81(9), N(2)-Mg(1)-C(25) 90.45(9).

As expected, the ¹H NMR spectrum of **15** in *d*₆-benzene bears more than a passing resemblance to those of **12** and **14** with the key, diagnostic chemical shifts of all three complexes detailed in Table 4.1. The only distinguishing feature is the upfield shift of the bridging NCH₂ resonance upon bonding to the more electropositive magnesium

(0.96/1.14 and 0.84 ppm in **12**, **14** and **15**, respectively). Additionally, where it is a sharp signal in ^1H NMR spectra of **12** and **14**, the TMEDA NMe_2 resonance is broader in that of **15** and indicating hindered rotation only a slight hump (spreading over 44-48 ppm) in the baseline is discernible for the methyl peaks in the ^{13}C NMR spectrum. Undertaking a variable temperature NMR experiment in d_8 -toluene, two sharp signals emerge at 42.9 and 47.7 ppm from the baseline upon cooling, consistent with impediment of fluxional processes at 210 K (Spectrum 4.3).

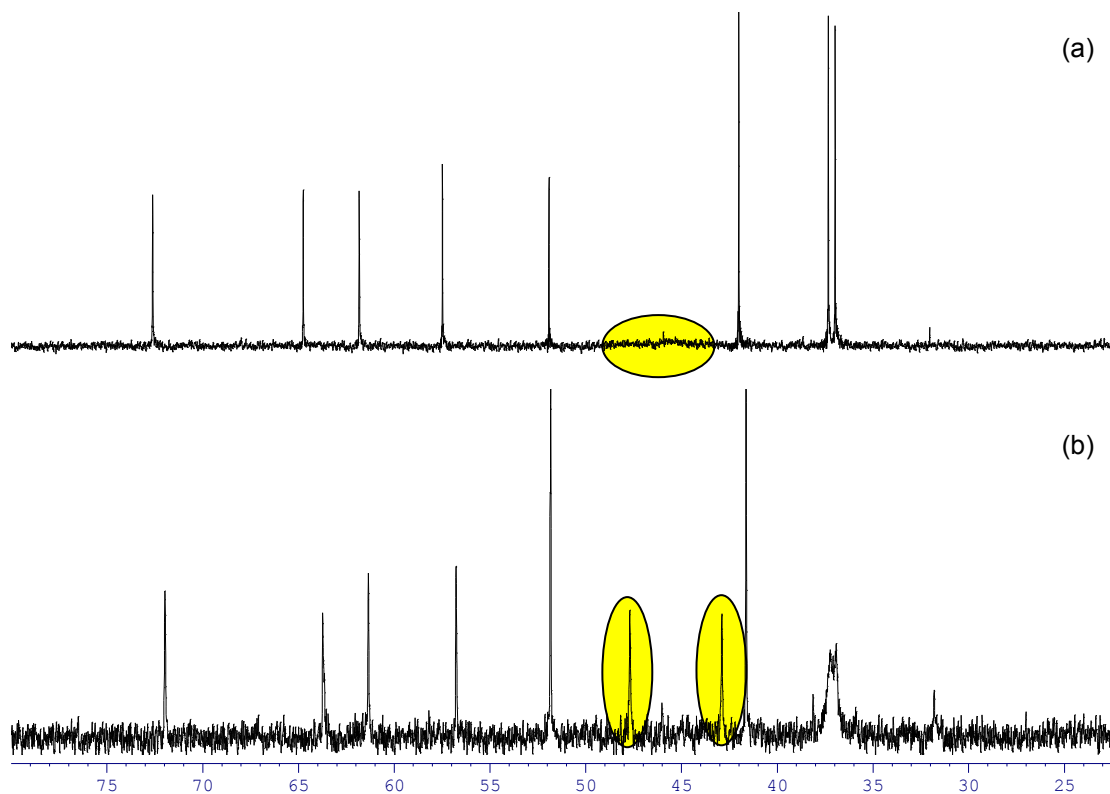
Table 4.1: Comparison of common ^1H NMR (400.13 MHz, 300 K) chemical shifts (δ in ppm) for complexes **12, **14** and **15** in d_6 -benzene solution.**

Compound	$\delta(\text{NCH}_2\text{-br}^*)$	$\delta(\text{NCH}_2)$	$\delta(\text{NCH}_3)$	$\delta(\text{N}(\text{CH}_3)_2)$	$\delta(\text{Aromatic})$
12	1.94, 0.96	2.44, 2.34, 2.22, 1.63	2.49	1.96	8.32, 7.26, 7.06, 6.67
14	1.93, 1.14	2.56, 2.41, 2.33, 1.77	2.59	1.94	8.31, 7.26, 7.07, 6.73
15	2.20, 0.84	2.44, 2.29, 1.70, 1.63	2.56	1.94	8.31, 7.30, 7.09, 6.70

* where br stands for bridging

Switching the metal from zinc to the more electropositive magnesium involved the introduction of a different appendage to a common molecular skeleton, creating appendage diversity. As touched on at the outset of this chapter, scaffold diversity remains the most pronounced element of diversity. Preliminary investigations into different donor solvents to try and mimic the neutral nucleophile role of TMEDA, namely PMDETA and chiral (*R,R*)-TMCDA (*N,N,N',N'*-tetramethylcyclohexane-1,2-diamine) have thus far proved unsuccessful in the isolation of related zwitterions, however, the scope of this area in terms of accessing new metallacyclic, zwitterionic and ylidic compounds remains vast. For example, in addition to mono-halogenated arenes, di-chlorinated benzenes are routinely commercially available; while of even

more interest in creating new building blocks, are the variety of accessible mono- and di-substituted naphthalenes and anthracenes that are ripe for exploring (Figure 4.6), meaning the surface and potential of this particularly exciting reaction has only been scratched and therefore the reaction of sodium TMP-zincate **1** with additional haloaromatics should be pursued further.



Spectrum 4.3: Selected aliphatic region of the ^{13}C NMR spectrum of **15** in d_8 -toluene solution, showing the NMe_2 resonances of the deprotonated TMEDA ligand at various temperatures [(a) 300 K; (b) 210 K].

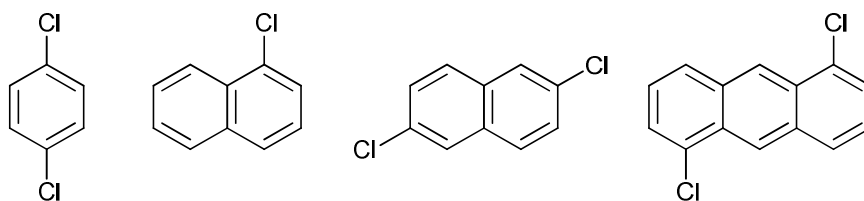


Figure 4.6: Some possible future candidates for transformation in metallacycles.

4.5) Experimental Section

Synthesis of $\{1\text{-Zn}(t\text{Bu})\}^- \{2\text{-N}(\text{Me})(\text{CH}_2)\text{CH}_2\text{CH}_2\text{NMe}_2\}^+ \text{-C}_6\text{H}_4\}$ **12**

A hexane solution of **1** (2 mmol) was prepared as described previously, chlorobenzene (0.2 mL, 2 mmol) was added, and the mixture was heated to reflux for 1 hour to produce a slightly cloudy yellow solution. The Schlenk tube was surrounded with a Dewar flask of hot water to allow the solution to cool slowly. This yielded small, colourless, X-ray quality crystals (0.13 g, 21%). To obtain a higher yield, a mixture of **1** (2 mmol) and chlorobenzene (1 mmol) was stirred for 48 hours, which produced a powder of **12** (0.16 g, 51% based on consumption of chlorobenzene). ^1H NMR (400.13 MHz, 300 K, d_6 -benzene): δ 8.32 (d, 1H, $H_{ortho\ to\ metal}$), 7.26 (t, 1H, H_{meta}), 7.06 (t, 1H, H_{para}), 6.67 [d $\{^3J(\text{H,H})\}$ 8.19 Hz], 1H, $H_{meta'}$], 2.49 (s, 3H, NCH_3), 2.44 (m, 1H, NCH_2), 2.34 (m, 1H, NCH_2), 2.22 (m, 1H, NCH_2), 1.96 [s, 6H, $\text{N}(\text{CH}_3)_2$], 1.94 (m, 1H, CH_2), 1.76 [s, 9H, CH_3 ($t\text{Bu}$)], 1.63 (m, 1H, NCH_2), 0.96 (m, 1H, CH_2). ^{13}C $\{^1\text{H}\}$ NMR (100.62 MHz, 300 K, d_6 -benzene): δ 168.8 ($\text{C}_{metallated}$), 154.7 ($\text{C}_{nitrogen}$), 140.1 (C_{ortho}), 126.7 (C_{meta}), 125.3 (C_{para}), 114.9 ($\text{C}_{meta'}$), 70.5 (NCH_2), 64.8 (NCH_2), 60.2 [$\text{N}(\text{CH}_3)$], 57.1 (CH_2), 45.6 [$\text{N}(\text{CH}_3)_2$], 36.3 [$\text{C}(\text{CH}_3)_3$ ($t\text{Bu}$)], 19.8 [$\text{C}(\text{CH}_3)_3$ ($t\text{Bu}$)].

Crystal data for **12**: $\text{C}_{16}\text{H}_{28}\text{N}_2\text{Zn}$, $M = 313.77$, monoclinic, $\text{P}2_1/c$, $a = 9.7870(11)$ Å, $b = 9.4959(10)$ Å, $c = 18.276(2)$ Å, $\beta = 97.588(2)^\circ$, $V = 1683.6(3)$ Å³, $Z = 4$; 14315 reflections collected, 3862 were unique, $R_{\text{int}} = 0.0222$, $R = 0.0255$, $R_w = 0.0663$, GOF = 1.088, 178 refined parameters, max. and min. residual electron density = 0.40 and -0.27 $\text{e} \cdot \text{Å}^{-3}$.

Synthesis of $\{1\text{-Zn}(t\text{Bu})_2\}^- \{2\text{-N}(\text{Me})_2\text{CH}_2\text{CH}_2\text{NMe}_2\}^+ \text{-C}_6\text{H}_4\}$ **13**

A hexane solution of **1** (2 mmol) was prepared as described previously, chlorobenzene (0.2 mL, 2 mmol) was added, and the slightly cloudy yellow solution was transferred to

a freezer operating at $-28\text{ }^{\circ}\text{C}$. Overnight, this yielded a mixture of small, yellow, X-ray quality crystals of **13** and colourless crystals of **12** (crude yield, 0.15 g, which equates to 12% of each as determined from an NMR analysis). ^1H NMR (400.13 MHz, 300 K, d_6 -benzene): δ 7.96 (d, 1H, $H_{ortho\ to\ metal}$), 7.13 (t, 1H, H_{meta}), 6.90 (t, 1H, H_{para}), 6.51 [d { $^3\text{J}(\text{H,H})$ 8.43 Hz}, 1H, $H_{meta'}$], 2.83 [t { $^3\text{J}(\text{H,H})$ 5.72 Hz}, 2H, NCH_2], 2.52 [s, 6H, $\text{N}(\text{CH}_3)_2$], 1.90 [t { $^3\text{J}(\text{H,H})$ 5.61 Hz}, 2H, NCH_2], 1.63 [s, 6H, $\text{N}(\text{CH}_3)_2$], 1.60 [s, 18H, CH_3 ($t\text{Bu}$)]. ^{13}C { ^1H } NMR (100.62 MHz, 300 K, d_6 -benzene): δ 168.0 ($C_{metallated}$), 151.7 ($C_{nitrogen}$), 139.8 (C_{ortho}), 126.9 (C_{meta}), 124.3 (C_{para}), 115.8 ($C_{meta'}$), 64.5 (NCH_2), 54.5 (NCH_2), 53.0 [$\text{N}(\text{CH}_3)_2$], 44.8 [$\text{N}(\text{CH}_3)_2$], 35.7 [$\text{C}(\text{CH}_3)_3$ ($t\text{Bu}$)], 22.8 [$\text{C}(\text{CH}_3)_3$ ($t\text{Bu}$)].

Crystal data for **13**: $\text{C}_{20}\text{H}_{38}\text{N}_2\text{Zn}$, $M = 371.93$, orthorhombic, $Pbca$, $a = 9.6006(8)\text{ \AA}$, $b = 19.4973(13)\text{ \AA}$, $c = 22.8263(16)\text{ \AA}$, $V = 4272.8(5)\text{ \AA}^3$, $Z = 8$; 11581 reflections collected, 4168 were unique, $R_{\text{int}} = 0.1237$, $R = 0.0673$, $R_w = 0.1234$, $\text{GOF} = 0.959$, 218 refined parameters, max. and min. residual electron density = 0.720 and $-0.411\text{ e}\cdot\text{\AA}^{-3}$.

Synthesis of [$\{1\text{-Zn}(\text{Me})\}^-$ - $\{2\text{-N}(\text{Me})(\text{CH}_2)\text{CH}_2\text{CH}_2\text{NMe}_2\}^+$ - C_6H_4] **14**

A solution of TMPH (0.34 mL, 2 mmol) in 10 mL of dry hexane was treated with 1.25 mL of $n\text{BuLi}$ (1.6 M solution in hexane, 2 mmol). The solution was stirred at room temperature for 30 minutes. Me_2Zn (2 mL of 1.0 M solution in heptane, 2 mmol) was then added, before the addition of TMEDA (0.3 mL, 2 mmol). The mixture was stirred for 1 hour to give a pale yellow solution. Chlorobenzene (0.2 mL, 2 mmol) was added, and the solution was heated at reflux for 1 hour resulting in a slightly cloudy yellow solution. The solution was filtered through Celite to remove a small amount of precipitate in an effort to aid crystallization. The yellow solution was concentrated with the removal of solvent *in vacuo* and was transferred to a refrigerator operating at $5\text{ }^{\circ}\text{C}$.

A small amount of highly hydrocarbon-soluble colourless, cubic crystals were deposited (0.07 g, 13%). ^1H NMR (400.13 MHz, 300K, d_6 -benzene): δ 8.31 (d, 1H, H_{ortho} to metal), 7.26 (t, 1H, H_{meta}), 7.07 (t, 1H, H_{para}), 6.73 [d $\{^3J(\text{H,H})$ 8.28 Hz}, 1H, H_{meta}], 2.59 (s, 3H, NCH_3), 2.56 (m, 1H, NCH_2), 2.41 (m, 1H, NCH_2), 2.33 (m, 1H, NCH_2), 1.94 [s, 6H, $\text{N}(\text{CH}_3)_2$], 1.93 (m, 1H, CH_2), 1.77 (m, 1H, NCH_2), 1.14 (m, 1H, CH_2), -0.14 (s, 3H, CH_3). ^{13}C $\{^1\text{H}\}$ NMR (100.62 MHz, 300 K, d_6 -benzene): δ 168.9 ($C_{metallated}$), 154.7 ($C_{nitrogen}$), 139.9 (C_{ortho}), 126.73 (C_{meta}), 125.4 (C_{para}), 115.1 ($C_{meta'}$), 71.7 (NCH_2), 64.8 (NCH_2), 60.5 [$\text{N}(\text{CH}_3)$], 56.4 (CH_2), 45.2 [$\text{N}(\text{CH}_3)_2$], -16.8 (CH_3).

Crystal data for **14**: $\text{C}_{16}\text{H}_{28}\text{N}_4\text{Zn}_2$, $M = 543.39$, monoclinic, $C2/c$, $a = 21.489(3)$ Å, $b = 10.4262(13)$ Å, $c = 15.130(2)$ Å, $\beta = 125.198(16)^\circ$, $V = 2770.1(6)$ Å³, $Z = 4$; 9212 reflections collected, 2355 were unique, $R_{\text{int}} = 0.0310$, $R = 0.0440$, $R_w = 0.1107$, GOF = 1.067, 157 refined parameters, max. and min. residual electron density = 0.548 and -0.365 $e \cdot \text{Å}^{-3}$.

Synthesis of $[\{1\text{-Mg}(\text{TMP})\}^- \{2\text{-N}(\text{Me})(\text{CH}_2)\text{CH}_2\text{CH}_2\text{NMe}_2\}^+ \text{-C}_6\text{H}_4]$ **15**

Freshly prepared $n\text{BuNa}$ (0.16 g, 2 mmol) was suspended in hexane and sonicated for 10 minutes to form a fine dispersion. $\text{TMP}(\text{H})$ (0.68 mL, 4 mmol) was added and the yellow suspension was stirred for 1 hour before the addition of 2 mL $n\text{Bu}_2\text{Mg}$ (1.0 M solution in heptane, 2 mmol) and TMEDA (0.3 mL, 2 mmol) to give a clear yellow solution. After 20 minutes, chlorobenzene (2 mmol, 0.2 mL) was added and the resulting cloudy yellow mixture was stirred for 10 minutes before being transferred to the freezer (at -28 °C). Colourless crystals were deposited after 4 days (0.31 g, 44%). To obtain a higher yield, $n\text{BuMgCl}$ (1 mL of 2 M solution in THF, 2 mmol) was suspended in hexane (10 mL). The Schlenk tube was then cooled to 0 °C in an ice bath before the introduction of 1.25 mL $n\text{BuLi}$ (1.6 M solution in hexane, 2 mmol) and the

white suspension was left to stir for 3 hours. The mixture was then filtered through Celite and glass wool to remove the precipitated LiCl, and the solvent was removed *in vacuo* producing $n\text{Bu}_2\text{Mg}$ as a colourless oil which was redissolved in hexane (5 mL). This solution was then transferred by cannula to a pre-prepared NaTMP suspension and TMEDA (0.3 mL, 2 mmol) was added to give a clear yellow solution. Finally, chlorobenzene (1 mmol) was introduced and the mixture was stirred for 48 hours, which produced a powder of **15** (0.25 g, 71% based on consumption of chlorobenzene). ^1H NMR (400.13 MHz, 300 K, d_6 -benzene): δ 8.31 (d, 1H, $H_{ortho\ to\ metal}$), 7.30 [t { $^3J(\text{H,H})$ 6.75 Hz}, 1H, H_{meta}], 7.09 (t, 1H, H_{para}), 6.70 [d { $^3J(\text{H,H})$ 8.18 Hz}, 1H, $H_{meta'}$], 2.56 (s, 3H, NCH_3), 2.44 (m, 1H, NCH_2), 2.29 (m, 1H, NCH_2), 2.20 (m, 1H, CH_2), 2.11 [m, 2H, $\gamma\text{-CH}_2$ (TMP)], 1.94 [s, 6H, $\text{N}(\text{CH}_3)_2$], 1.75 [m, 4H, $\beta\text{-CH}_2$ (TMP)], 1.70 (m, 1H, NCH_2), 1.69 [s, 6H, CH_3 (TMP)], 1.63 (m, 1H, NCH_2), 1.61 [s, 6H, CH_3 (TMP)], 0.84 (m, 1H, CH_2). ^{13}C { ^1H } NMR (100.62 MHz, 300 K, d_6 -benzene): δ 173.3 ($\text{C}_{metallated}$), 156.6 ($\text{C}_{nitrogen}$), 140.8 (C_{ortho}), 126.4 (C_{meta}), 125.2 (C_{para}), 114.8 ($\text{C}_{meta'}$), 72.7 (NCH_2), 64.6 (NCH_2), 61.9 [$\text{N}(\text{CH}_3)$], 57.3 (CH_2), 51.9 [$\alpha\text{-C}$ (TMP)], 48-44 [$\text{N}(\text{CH}_3)_2$, br], 42.0 [$\beta\text{-CH}_2$ (TMP)], 37.3 [CH_3 (TMP)], 37.0 [CH_3 (TMP)], 20.9 [$\gamma\text{-CH}_2$ (TMP)].

Crystal data for **15**: $\text{C}_{21}\text{H}_{37}\text{N}_3\text{Mg}$, $M = 355.85$, monoclinic, $\text{P}2_1/\text{c}$, $a = 14.1235(6)$ Å, $b = 14.5517(6)$ Å, $c = 10.5427(5)$ Å, $\beta = 101.577(4)^\circ$, $V = 2122.67(16)$ Å³, $Z = 4$; 15271 reflections collected, 3719 were unique, $R_{\text{int}} = 0.0682$, $R = 0.0463$, $R_w = 0.0911$, GOF = 0.853, 241 refined parameters, max. and min. residual electron density = 0.188 and -0.172 e \cdot Å⁻³.

Chapter 4 - References

- [1] J. Zhu, H. Bienaymé, in *Multicomponent Reactions*, Wiley-VCH: Weinheim, Germany, **2005**.
- [2] E. Ruijter, R. Scheffelaar, R. V. A. Orru, *Angew. Chem. Int. Ed.* **2011**, *50*, 6234 - 6246.
- [3] M. Passerini, *Gazz. Chim. Ital.* **1921**, *51*, 181 - 189.
- [4] I. Ugi, *Angew. Chem. Int. Ed.* **1962**, *1*, 8 - 21.
- [5] K. M. Allan, C. D. Gilmore, B. M. Stoltz, *Angew. Chem. Int. Ed.* **2011**, *50*, 4488 - 4491.
- [6] (a) G. Wittig, G. Pieper, G. Fuhrmann, *Ber. Dtsch. Chem. Ges.* **1940**, *73*, 1193 - 1197; (b) G. Wittig, G. Fuhrmann, *Ber. Dtsch. Chem. Ges.* **1940**, *73*, 1197 - 1218.
- [7] (a) Y. Sato, T. Toyooka, T. Aoyama, H. Shirai, *J. Org. Chem.* **1976**, *41*, 3559 - 3564; (b) J. Nakayama, S. Takeue, M. Hoshino, *Tetrahedron. Lett.* **1984**, *25*, 2679 - 2682.
- [8] (a) H. Yoshida, E. Shirakawa, Y. Honda, T. Hiyama, *Angew. Chem. Int. Ed.* **2002**, *41*, 3247 - 3249; (b) H. Yoshida, T. Terayama, J. Ohshita, A. Kunai, *Chem. Commun.* **2004**, 1980 - 1981; (c) H. Yoshida, M. Watanabe, J. Ohshita, A. Kunai, *Chem. Commun.* **2005**, 3292 - 3294; (d) U. K. Tambar, B. M. Stoltz, *J. Am. Chem. Soc.* **2005**, *127*, 5340 - 5341.
- [9] T. Morishita, H. Fukushima, H. Yoshida, J. Ohshita, A. Kunai, *J. Org. Chem.* **2008**, *73*, 5452 - 5457.
- [10] (a) H. Yoshida, H. Fukushima, J. Ohshita, A. Kunai, *Angew. Chem. Int. Ed.* **2004**, *43*, 3935 - 3938; (b) H. Yoshida, H. Fukushima, J. Ohshita, A. Kunai, *Tetrahedron. Lett.* **2004**, *45*, 8659 - 8662; (c) H. Yoshida, H. Fukushima, T. Morishita, J. Ohshita, A. Kunai, *Tetrahedron* **2007**, *63*, 4793 - 4805.
- [11] H. Yoshida, Y. Ito, J. Ohshita, *Chem. Commun.* **2011**, *47*, 8512 - 8514.
- [12] A. M. Dyke, A. J. Hester, G. C. Lloyd-Jones, *Synthesis* **2006**, 4093 - 4112.
- [13] D. Soorukram, T. Qu, A. G. M. Barrett, *Org. Lett.* **2008**, *10*, 3833 - 3835.
- [14] A. Dömling, *Chem. Rev.* **2006**, *106*, 17 - 89.
- [15] C. Simon, T. Constantieux, J. Rodriguez, *Eur. J. Org. Chem.* **2004**, 4957 - 4980.
- [16] (a) H. Pellisier, M. Santelli, *Tetrahedron* **2003**, *59*, 701 - 730; (b) H. H. Wenk, M. Winkler, W. Sander, *Angew. Chem. Int. Ed.* **2003**, *42*, 502 - 528.

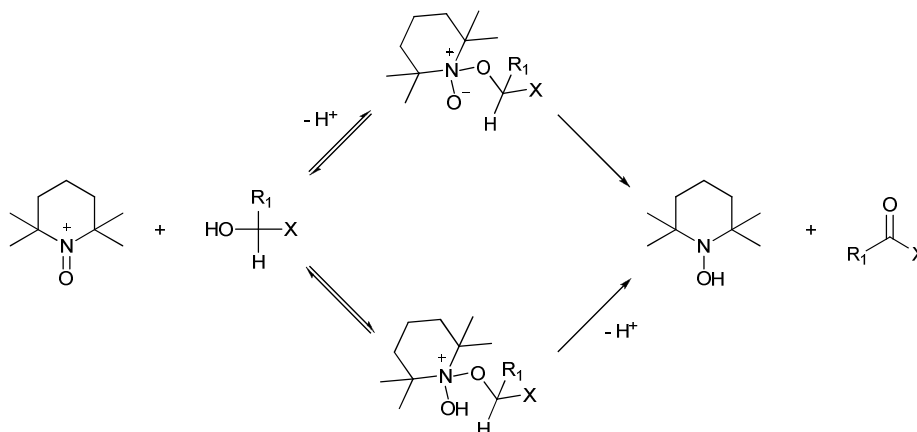
- [17] O. L. Chapman, K. Mattes, C. L. McIntosh, J. Pacansky, G. V. Calder, G. Orr, *J. Am. Chem. Soc.* **1973**, *95*, 6134 - 6135.
- [18] R. D. Brown, P. D. Godfrey, M. Rodler, *J. Am. Chem. Soc.* **1986**, *108*, 1296 - 1297.
- [19] J. D. Albright, D. F. Lieberman, *J. Heterocycl. Chem.* **1994**, *31*, 537 - 539.
- [20] M. Iwao, *J. Org. Chem.* **1990**, *55*, 3622 - 3627.
- [21] F. Mongin, M. Schlosser, *Tetrahedron. Lett.* **1997**, *38*, 1559 - 1562.
- [22] (a) M. Uchiyama, T. Miyoshi, Y. Kajihara, T. Sakamoto, Y. Otani, T. Ohwada, Y. Kondo, *J. Am. Chem. Soc.* **2002**, *124*, 8514 - 8515; (b) M. Uchiyama, Y. Kobayashi, T. Furuyama, S. Nakamura, Y. Kajihara, T. Miyoshi, T. Sakamoto, Y. Kondo, K. Morokuma, *J. Am. Chem. Soc.* **2008**, *130*, 472 - 480.
- [23] R. Chauvin, *Eur. J. Org. Chem.* **2000**, 577 - 591.
- [24] CSD version 5.31 see: F. H. Allen, *Acta Crystallogr., Sect. B* **2002**, *58*, 380 - 388.
- [25] M. Steiner, H. Grützmacher, H. Prtitzkow, L. Zsolani, *Chem. Commun.* **1998**, 285 - 286.
- [26] (a) M. J. Monreal, S. Khan, P. L. Diaconescu, *Angew. Chem. Int. Ed.* **2009**, *48*, 8352 - 8355; (b) D. Ma, X. Lu, L. Shi, H. Zhang, Y. Jiang, X. Liu, *Angew. Chem. Int. Ed.* **2011**, *50*, 1118 - 1121; (c) V. L. Blair, W. Clegg, A. R. Kennedy, Z. Livingstone, L. Russo, E. Hevia, *Angew. Chem. Int. Ed.* **2011**, *50*, 9857 - 9860.
- [27] D. Nobuto, M. Uchiyama, *J. Org. Chem.* **2008**, *73*, 1117 - 1120.
- [28] W. Clegg, B. Conway, E. Hevia, M. D. McCall, L. Russo, R. E. Mulvey, *J. Am. Chem. Soc.* **2009**, *131*, 2375 - 2384.
- [29] D. R. Armstrong, V. L. Blair, W. Clegg, S. H. Dale, J. García-Álvarez, G. W. Honeyman, E. Hevia, R. E. Mulvey, L. Russo, *J. Am. Chem. Soc.* **2010**, *132*, 9480 - 9487.
- [30] M. C. Whisler, S. MacNeil, V. Snieckus, P. Beak, *Angew. Chem. Int. Ed.* **2004**, *43*, 2206 - 2225.
- [31] (a) D. Bojer, I. Kamps, X. Tian, A. Hepp, T. Pape, R. Fröhlich, N. W. Mitzel, *Angew. Chem. Int. Ed.* **2007**, *46*, 4176 - 4179; (b) V. H. Gessner, C. Strohmann, *J. Am. Chem. Soc.* **2008**, *130*, 14412 - 14413.
- [32] S. V. Kessar, P. Singh, *Chem. Rev.* **1997**, *97*, 721 - 737.

- [33] E. Hevia, D. J. Gallagher, A. R. Kennedy, R. E. Mulvey, C. T. O'Hara, C. Talmard, *Chem. Commun.* **2004**, 2422 - 2423.
- [34] P. C. Andrikopoulos, D. R. Armstrong, D. V. Graham, E. Hevia, A. R. Kennedy, R. E. Mulvey, C. T. O'Hara, C. Talmard, *Angew. Chem. Int. Ed.* **2005**, *44*, 3459 - 3462.
- [35] A. R. Kennedy, R. E. Mulvey, S. D. Robertson, *Dalton Trans.*, **2010**, *39*, 9091 - 9099.
- [36] W. Clegg, B. Conway, P. García-Álvarez, A. R. Kennedy, R. E. Mulvey, L. Russo, J. Sassmannhausen, T. Tuttle, *Chem. Eur. J.* **2009**, *15*, 10702 - 10706.
- [37] M. G. Cushion, J. Meyer, A. Heath, A. D. Schwarz, I. Fernández, F. Breher, P. Mountford, *Organometallics* **2010**, *29*, 1174 - 1190.

Chapter 5: Redox Reactions in Sodium-Zinc Chemistry

5.1) Nitroxides: Applications in Synthesis

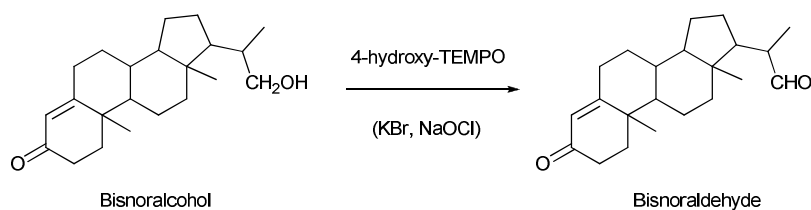
A stable nitroxyl free radical, TEMPO (2, 2, 6, 6-tetramethyl-1-piperidinyloxy) attracts an exceptional level of interest.^[1] First synthesised by Lebelev and Kazarnowskii in 1960,^[2] it is utilised within a number of surprisingly distinct areas. TEMPO is employed as a probe in biological systems using electron spin resonance spectroscopy and also finds utility as a radical trapping agent.^[3] A significant constituent in the development of “living” free radical polymerisation, it is often the reagent of choice for effecting mild and selective oxidation.^[4] Of particular interest in organic synthesis for the production of pharmaceuticals, agrochemicals and other speciality chemicals; TEMPO-mediated oxidation is widely practiced in industry for the conversion of primary and secondary alcohols into aldehydes, ketones and other carbonyl compounds via the oxoammonium cation (Scheme 5.1).^[5]



Scheme 5.1: TEMPO-mediated oxidation of alcohols via the oxoammonium cation.

With TEMPO considered a fairly expensive chemical (£94.70 for 5g from Sigma-Aldrich),^[6] industry typically exploits 4-substituted nitroxyl derivatives such as 4-hydroxy-TEMPO prepared from the readily available, cost-effective precursor

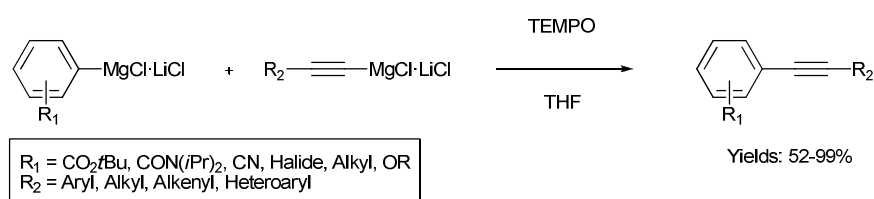
triacetoneamine. The potential of the TEMPO-mediated oxidation to industry was first unearthed in the mid 1990s by Pharmacia and Upjohn in the synthesis of the important steroidal precursor bisnoraldehyde from waste soya bean residues (Scheme 5.2).^[7] Formulated around the oxidation of bisnoralcohol with 4-hydroxy-TEMPO and bleach, this catalytic methodology possesses many economic and environmental benefits, for instance avoiding the use of heavy metal based oxidants and increasing the utilisation of soya sterol feedstock from 15% to 100%. Additionally, the multi-kilogram synthesis of a key intermediate of a HIV protease inhibitor at Pfizer encompasses a ketone fluorination, with the inherent ketone generated through homogeneous TEMPO-mediated oxidation.^[8]



Scheme 5.2: Synthesis of Bisnoraldehyde based on oxidation of Bisnoralcohol with bleach and 4-hydroxy-TEMPO providing the requisite oxoammonium cation.

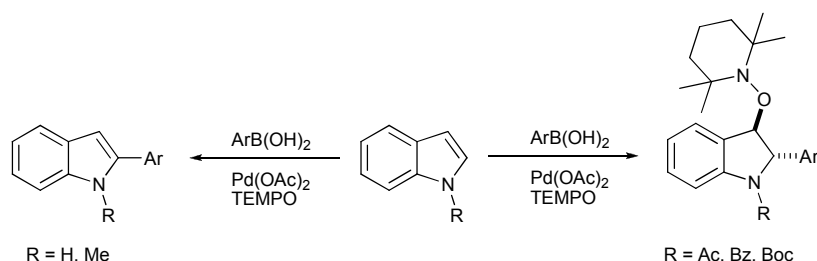
In recent years, reports of TEMPO aiding organic synthesis have grown with the group of Studer being particularly active in it. The Sonogashira cross coupling reaction is commonly utilised for the construction of compounds bearing an internal alkyne motif.^[9] Transition-metal catalysed, the original Sonogashira methodology uses a Pd(II)-salt and CuI as the co-catalyst.^[10] Although, contemporary adaptations have been reported by Knochel^[11] and Cahiez^[12] that utilise chloranil and molecular oxygen as oxidants, both protocols require the presence of transition metals (stoichiometric Cu and catalytic Mn, respectively). Studer and co-workers have elegantly shown that oxidative homocoupling of Grignard reagents in the presence of TEMPO and dioxygen is

possible in high yields^[13] and additionally, described a highly efficient transition-metal-free cross coupling of *ortho*-substituted aryls with alkynyl “turbo-Grignard” reagents by using TEMPO as a mild, environmentally benign organic oxidant (Scheme 5.3).^[14] Notably, the reaction scope was investigated and it was found that the couplings could be performed with various aryl and alkynyl Grignard reagents with sensitive functional groups such as esters, amides and cyanides tolerated, delivering the products in high yields.



Scheme 5.3: Oxidative coupling of various substituted aryl and alkynyl Grignard reagents using TEMPO as an oxidant.

Augmenting an already impressive portfolio, Studer revealed that atypical palladium-catalysed chemical transformations of several indoles could be effected with commercially available arylboronic acids and TEMPO as a mild oxidant.^[15] Depending on the substituent on the indole N atom, either direct C(2) arylation or an unprecedented highly stereoselective oxidative arylcarboaminoxylation reaction occurs under mild conditions rendering biologically interesting structures (Scheme 5.4).



Scheme 5.4: Protecting group dependent C(2) arylation or diastereoselective arylcarboaminoxylation.

Perhaps most pertinent to this study, the radical has also been utilised in coordination chemistry yielding an interesting and varied selection of ligation modes, as well as flexibility in the ligands electronic structure. Most TEMPO coordination chemistry lies with the *d*-block metals, with complexes known where it binds to Ti,^[16] Mn,^[17] Co,^[18] Ni,^[19] Cu,^[20] Zn,^[21] Mo,^[22] Ru,^[23] Rh,^[24] Pd^[25] and Hg.^[26]

In 2001, Mulvey and co-workers revealed that TEMPO could behave as a “chameleonic ligand” towards *s*-block metal amides,^[27] that is, it can retain its radical (paramagnetic) nature or be reduced to an anionic (diamagnetic) entity in different ligation modes depending on the composition of the *s*-block metal amide (Figure 5.1).

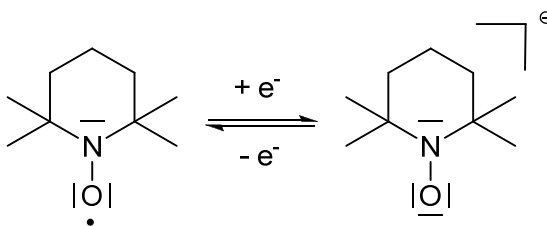


Figure 5.1: Radical and anionic forms of the TEMPO ligand.

As well as coordinating to a metal centre as an anion or radical, the TEMPO unit can act solely as an O donor (η^1) or as a bidentate N/O donor (η^2). This series established that TEMPO was a flexible ligand for these electropositive metals, presenting greater scope in its ligation and electronic structure than the standard O-based donors frequently encountered in *s*-block chemistry (Figure 5.2).

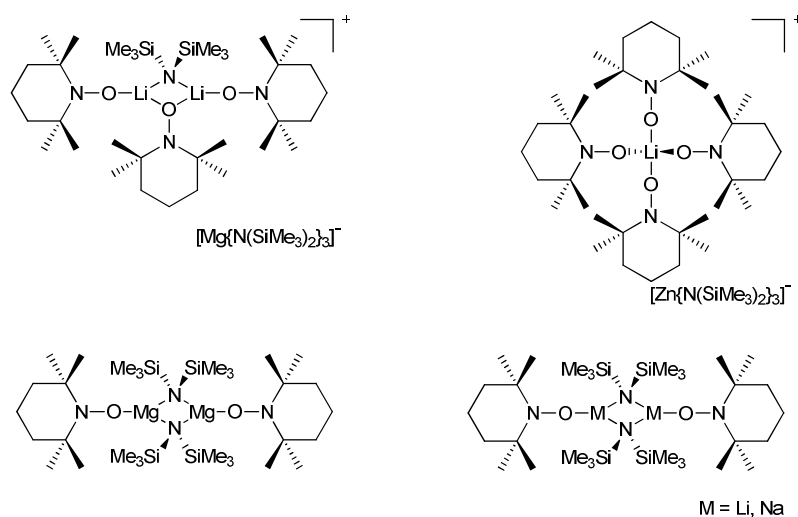
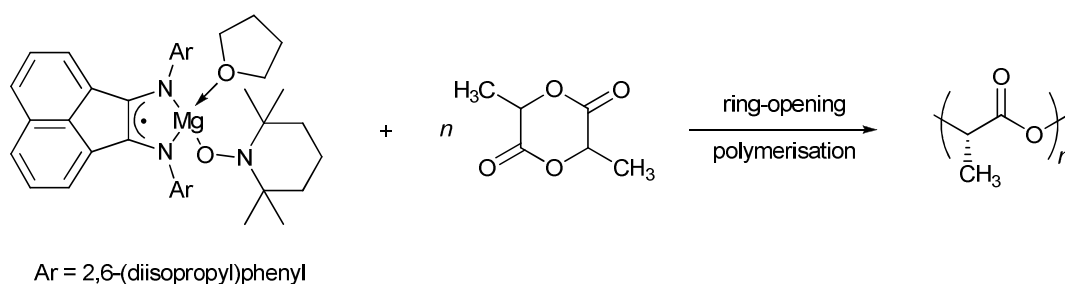


Figure 5.2: ChemDraw representations of known *s*-block/TEMPO complexes.

Coordination complexes of main group metals are regularly touted as catalysts for the ring-opening polymerisation (ROP) of cyclic esters, particularly lactides.^[28] Polylactides are very attractive materials as they are biologically degradable and are manufactured from renewable plant resources.^[29] The eminent active catalytic systems for ROP of cyclic esters consist of aluminium, zinc, yttrium and magnesium alkoxides and amides supported by N- and O-bi(poly)dentate ligands. Recently, a monomeric magnesium complex carrying a terminal TEMPO ligand has been prepared from an ancillary acenaphthene-1,2-diimine ligand.^[30] Consisting of an oxophilic metal and a rigid, bulky diimine ligand, this complex proved to be a very active catalyst for the ROP of lactides in solution as well as in the melt of the monomer affording isotactic poly-L-lactide (Scheme 5.5). With the wealth of uses outlined, it is clear this ligand warranted additional study, thus we have investigated TEMPO in the context of sodium-zinc chemistry.



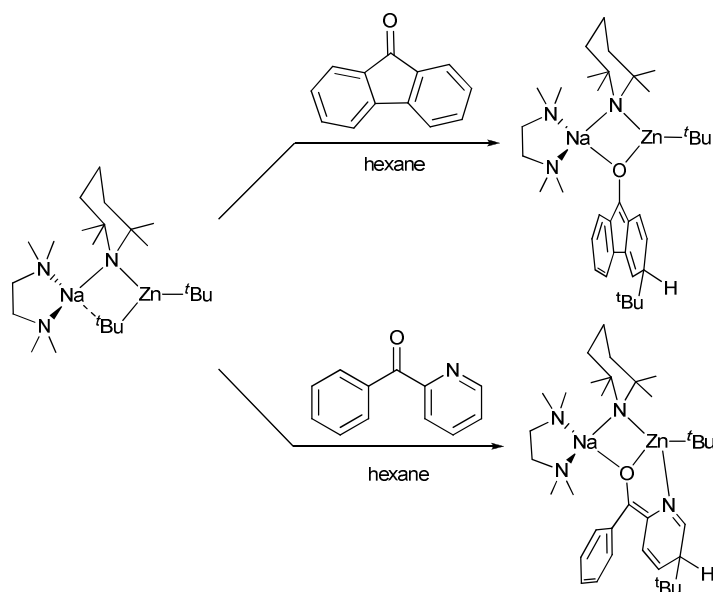
Scheme 5.5: Ring-opening polymerisation of lactides catalysed by a magnesium complex bearing a terminal TEMPO ligand.

5.2) Single Electron Transfer Activity of the Sodium TMP-Zincate

Contrasting with its extensive application as a Brønsted base, sodium TMP-zincate [(TMEDA)Na(μ -TMP)(μ -*t*Bu)Zn(*t*Bu)] (**1**) can alternatively be used as a *tert*-butyl source to formally introduce a *tert*-butyl ligand in a 1,6-fashion towards the ketones benzophenone,^[31] fluorenone^[32] and 2-benzoylpyridine^[32] as shown by the Mulvey and O'Hara groups (Scheme 5.6). In all three cases, the intermediate enolate adduct has been trapped and characterised in both the solid-state and solution. Earlier in 1991, Olah and co-workers, reported that benzophenone can undergo 1,6-*tert*-butylation in ethereal solvents at -100 °C in 46% yield using *t*BuLi.^[33] It was suggested that the reaction mechanism proceeds via single electron transfer (SET) from *t*BuLi to benzophenone.^[34]

Returning to the work of this PhD project, we aimed to study the reaction chemistry of TEMPO with sodium TMP-zincate **1** before investigating the redox chemistry of dialkyl zinc reagents and alkali-metals towards the free radical, attempting to grow crystalline samples of metal-TEMPO products for X-ray crystallographic study. The SET activity of the TMP-zincate system was ascertained by reaction of **1** with the nitroxyl radical TEMPO. Following a 1:1 stoichiometric reaction between **1** and

TEMPO in bulk hexane solution, the new anionic TEMPO complex [(TMEDA)Na(μ -TMP)(μ -TEMPO⁻)Zn(*t*Bu)] (**16**) was isolated in 34% yield.



Scheme 5.6: Sodium TMP-zincate **1 effecting the selective 1,6-addition across fluorenone and 2-benzoylpyridine.**

The molecular structure of heterotrimeric **16** (Figure 5.3) revealed a contacted ion-pair, bimetallic motif with a tetracoordinate Na centre [range of angles subtended at Na(1) 73.19(4)-136.10(5)^o; mean angle: 111.06^o] and a distorted trigonal planar zinc centre. The connectivity framework and composition of **1** is retained except that a *t*Bu bridge is replaced by a TEMPO ligand, furnishing a smaller four-membered, four-element (NaNZnO) ring at the core that results in a more acute Na-N_{TMPO}-Zn angle of 88.55(5)^o in comparison to that of its precursor [98.6(2)^o]. By comparing the N(2)-O(1) bond length [1.4479(15) Å] in **16** with that in related TEMPO-containing complexes [in TEMPO radical complexes the N-O bond ranges from 1.26-1.30 Å in length and between 1.40-1.48 Å in its anionic form] it is clear that the nitroxide ligand here is anionic as it must be from valency considerations.

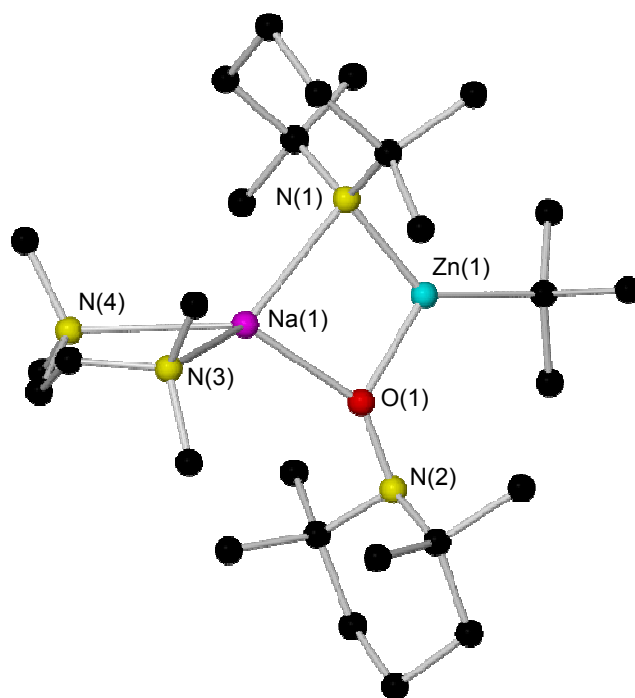
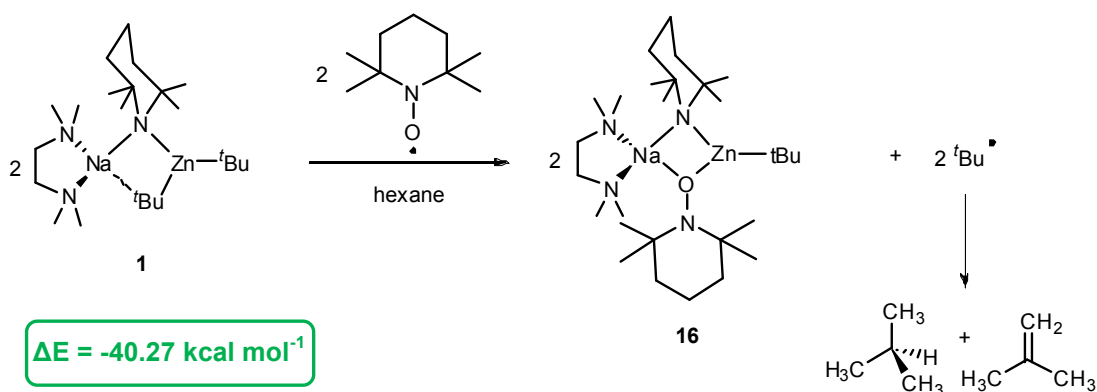


Figure 5.3: Molecular structure of **16** with selective atom labelling. Hydrogen atoms and disordered component of *tert*-butyl group are omitted for clarity. Selected bond distances (Å) and angles (deg): Na(1)–O(1) 2.2492(12), Na(1)–N(1) 2.4902(13), Na(1)–N(3) 2.6167(15), Na(1)–N(4) 2.6190(14), Zn(1)–O(1) 1.9678(10), Zn(1)–N(1) 2.0062(12), Zn(1)–C(1) 2.063(6), N(2)–O(1) 1.4479(15); O(1)–Na(1)–N(1) 77.33(4), O(1)–Na(1)–N(3) 124.57(5), O(1)–Na(1)–N(4) 131.46(5), N(1)–Na(1)–N(3) 136.10(5), N(1)–Na(1)–N(4) 123.69(5), N(3)–Na(1)–N(4) 73.19(4), O(1)–Zn(1)–N(1) 96.58(5), O(1)–Zn(1)–C(1) 127.42(19), N(1)–Zn(1)–C(1) 135.37(18), Na(1)–O(1)–Zn(1) 96.76(4), Na(1)–N(1)–Zn(1) 88.55(8).

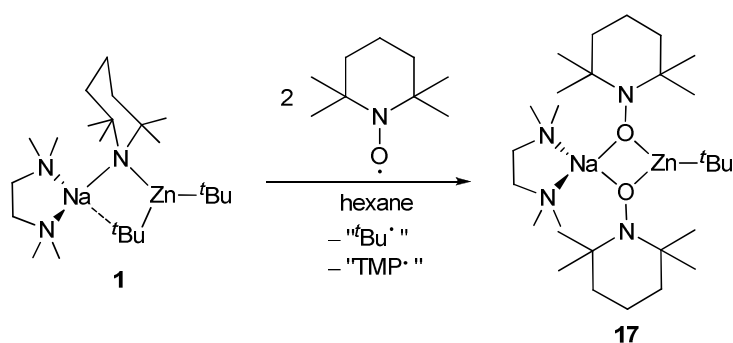
A key feature in the synthesis of **16** is the reduction of a TEMPO[•] radical to a TEMPO[−] anion (with presumably concomitant oxidation of a *t*Bu[−] anion to a *t*Bu[•] radical). It is envisaged that the putative tertiary alkyl radicals combine to give isobutene and isobutane. Indeed from DFT calculations carried out in collaboration with Dr Armstrong of this department, it is estimated that the conversion of **1** and TEMPO to **16** and hydrocarbon co-products is exothermic by 40.27 kcal mol^{−1} (Scheme 5.7). Reaffirming the experimentally observed product, the thermodynamically most

favoured reaction pathway as suggested by these calculations involves displacement of the bridging *t*Bu by TEMPO (exothermic by 13.86 kcal mol⁻¹). The respective cleavage of the terminal *t*Bu and bridging TMP ligands, and replacement by TEMPO are both estimated to be endothermic (by 3.31 and 1.51 kcal mol⁻¹, respectively) and as such are clearly less likely to be the path taken experimentally.



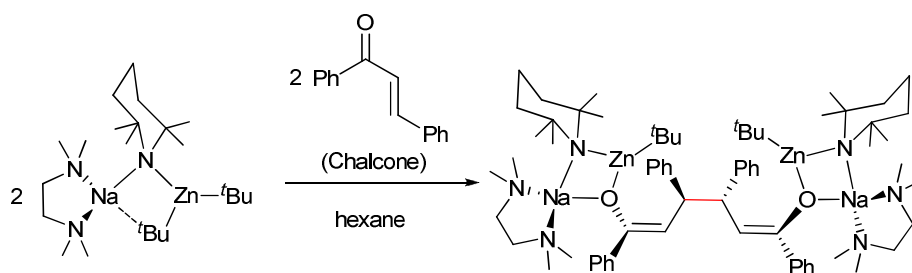
Scheme 5.7: Exothermic conversion of 1 and TEMPO to the heterotri-anion zincate 16 and hydrocarbon co-products. The stoichiometry chosen for the calculation takes into account the structure of the *t*Bu[•] radical.

In an effort to trap the *t*Bu radical thought to be released in the reaction (to give TEMPO-*t*Bu), we added two molar equivalents of TEMPO to the zincate **1** (Scheme 5.8). To our surprise, this reaction did not yield **16**, instead the bis-nitroxide [(TMEDA)Na(μ-TEMPO⁻)₂Zn(*t*Bu)] (**17**) was isolated as colourless crystals (31% yield). The structure of **17** was elucidated using X-ray crystallography which due to its poor quality will not be discussed herein. It is unlikely that **17** forms due to a disproportionation reaction as it was never detected by NMR spectroscopic analysis when only one equivalent of TEMPO is used; therefore to produce **17**, it seems that **1** has acted as a dual SET reagent whereby both a *t*Bu radical and a TMP radical^[35] have been generated *in situ*.



Scheme 5.8: The synthesis of bis(TEMPO) zincate 17.

These experimental and theoretical investigations support the hypothesis that SET could be at play in the aforementioned previously reported 1,6-addition reactions. After realising that **1** could function as an SET reagent, O'Hara and co-workers decided to further probe its chemistry with the pharmaceutically important aromatic α , β -unsaturated ketone, chalcone (1,3-diphenyl-2-propen-1-one).^[36] On treating **1** with an equimolar quantity of chalcone, the crystalline product revealed that no *t*Bu addition had occurred and that $[\{(\text{TMEDA})\text{Na}(\mu\text{-TMP})\text{Zn}(\text{tBu})\}_2(\mu\text{-OCPPhCH=CHPhCHPhCH=CPh-}\mu\text{-O})]$ was isolated as the sole product (Scheme 5.9). The formation of this unexpected product can be rationalised in terms of a SET reaction. One canonical form of chalcone can be compared to that of TEMPO – it has an oxy radical centre (as well as a benzyl radical centre) and when treated with **1** it was proposed that a dinuclear sodium zincate containing the familiar Na-N_{TMP}-Zn-O ring forms, and spontaneously dimerises due to the presence of the reactive benzyl radical to afford the bimetallic tetranuclear species.



Scheme 5.9: Synthesis of the tetranuclear chalcone species with site of dimerisation and new C-C bond highlighted in red.

The next undertaking in our own research was to extend this TEMPO methodology to other alkyl zincates. Surveying alkyl effects, the methyl analogue of **16**, [(TMEDA)Na(μ-TMP)(μ-TEMPO⁻)Zn(Me)] (**18**) was isolated from the analogous 1:1 reaction of TEMPO and the sodium methylzincate “(TMEDA)·NaZn(TMP)Me₂” in a crystalline yield of 25%. Compound **18** presents an analogous structure to that of **16**, with the same inorganic backbone and central four-membered (NaNZnO) ring where the metals are bridged by TMP and anionic TEMPO ligands (Figure 5.4). Unfortunately, disorder in both the TMEDA and TEMPO ligands affects the accuracy of the bond lengths and angles, and therefore prevents their discussion.

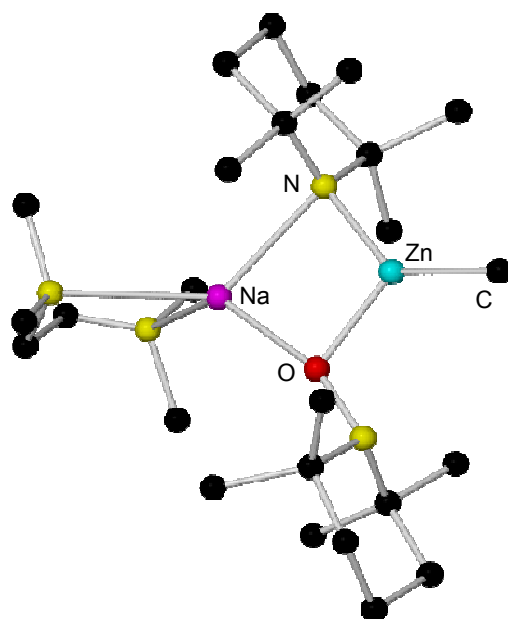


Figure 5.4: Molecular structure of 18 with selective atom labelling. Hydrogen atoms omitted for clarity.

NMR spectroscopic studies of d_8 -THF solutions of **16-18** revealed that TMEDA is displaced by the ethereal solvent, but otherwise the solid-state structures appear to be retained in solution with the ^1H NMR chemical shifts detailed in Table 5.1. As a radical, TEMPO produces broad resonances outwith the standard ^1H NMR spectroscopy window, therefore, the fact that NMR spectra could be obtained for all three complexes is further evidence that the paramagnetic TEMPO radical converts to the diamagnetic TEMPO anion in these structures. Making use of 2D spectroscopy techniques (^1H - ^1H COSY and ^1H - ^{13}C HSQC experiments) the ^1H NMR spectra have been fully assigned, identifying overlap of the β - and γ -TEMPO resonances. The structural similarity between TEMPO and TMP makes any advancement on the crystalline yield difficult on the basis of NMR spectroscopic analysis of the filtrates with significant overlap between the starting zincate reagents and anionic TEMPO products.

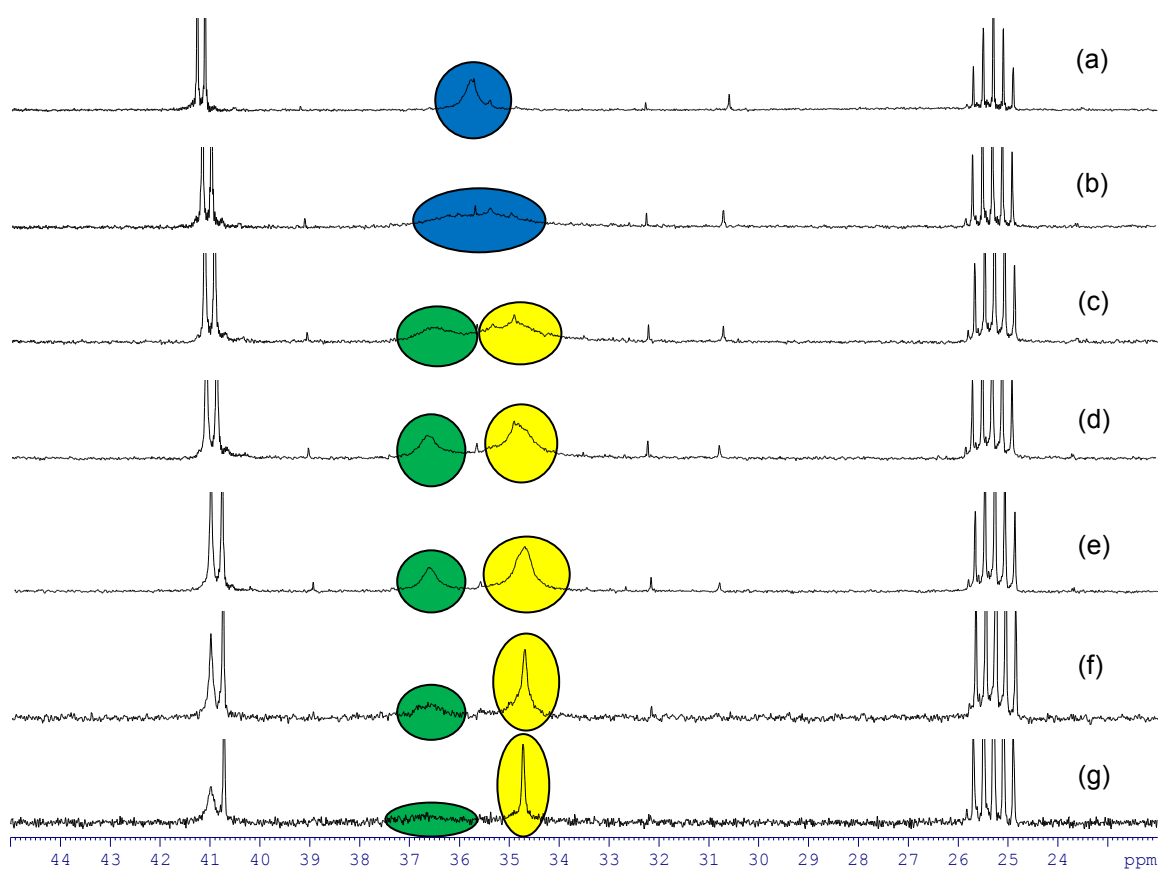
Table 5.1: Comparison of selected ^1H NMR (400.13 MHz, 300 K) chemical shifts (δ in ppm) for zincates **16, **17** and **18** in d_8 -THF.**

Compound	$\delta(\text{TMP-CH}_3)$	$\delta(\beta\text{-TMP})$	$\delta(\gamma\text{-TMP})$	$\delta(\beta/\gamma\text{-TEMPO})$	$\delta(\text{TEMPO-CH}_3)$	$\delta(\text{Zn-C})^a$
16	1.16, 0.96	1.44, 1.22	1.71	1.44	1.16, 1.09	1.08
17	-	-	-	1.44, 1.39	1.08	1.10
18	1.13	1.28	1.69	1.42	1.02	-0.86

^awhere C is *t*Bu for **16** and **17**, and Me for **18**.

While assigning the ^1H NMR spectra proved more straightforward, the ^{13}C NMR spectrum of **18** provided a new difficulty. Utilising the ^1H - ^{13}C HSQC spectra, the ^{13}C NMR could be deciphered with the exception of the methyl groups of the TMP and TEMPO, as a very broad signal appeared in the anticipated region (centred at 35.7 ppm). In previous TEMPO work within the group, broad ^{13}C resonances have often been observed, thus we decided to carry out a low temperature NMR study on

compound **18**. As shown in Spectrum 5.1, reducing the temperature to $-50\text{ }^{\circ}\text{C}$ sees the splitting of the broad hump into a much sharper, defined peak, while a broad peak is also retained. With the broadness of TEMPO peaks already established we tentatively propose the sharper peak corresponds to the TMP ligand. Interestingly, the resonances of the β -TMP and TEMPO carbon atoms are also very close to one another, and as can be observed we also see one of these peaks starting to broaden in the low temperature study.



Spectrum 5.1: Selected aliphatic region of the ^{13}C NMR spectrum of **18** in d_8 -THF solution, showing Me resonances of TMP (yellow) and TEMPO (green) ligands at various temperatures [(a) 300 K; (b) 273 K; (c) 263 K; (d) 253 K; (e) 243 K; (f) 233 K; (g) 223 K].

Putting our results into a broader context it should be mentioned that structural characterisation of zinc-TEMPO species is rare, irrespective of the nature of the

TEMPO (anionic or neutral). While there are no neutral TEMPO examples deposited in the Cambridge Crystallographic Database,^[37] Power reported the synthesis of 4-Me₃Si-Ar*Zn(TEMPO⁻), prepared by reaction of an arylzinc hydride [(4-Me₃Si-Ar*)Zn(μ-H)₂Zn(Ar*-SiMe₃-4)] and TEMPO [where 4-Me₃Si-Ar* = C₆H₂-2,6-(C₆H₂-2,4,6-*i*Pr₃)₂-SiMe₃-4].^[21b] In this neutral zinc complex, TEMPO is bound to the zinc in a novel quasi “side-on” fashion with a significant secondary interaction between zinc and the nitrogen atom to afford a three-membered Zn-N-O metallacycle. The second structure featuring TEMPO bonded to zinc was reported in 2007.^[21a] Carmona’s solvent-free dimeric compound [EtZn(TEMPO⁻)]₂ (Figure 5.5) was formed as a by-product in small, albeit isolable amounts in the synthesis of the (η⁵-C₅Me₅)ZnEt half sandwich complex. Significantly, it was observed that the radical TEMPO does not react separately with Et₂Zn, and this compound was only produced when TEMPO was added to a mixture of two organozinc reagents, Et₂Zn and Zn(C₅Me₅)₂. Intrigued by this result, we set out to investigate whether the apparently direct redox reaction was possible for other dialkyl zinc reagents.

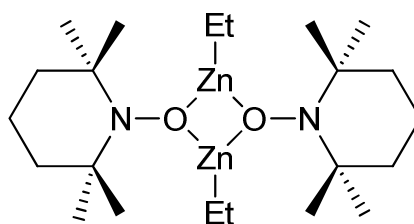


Figure 5.5: ChemDraw representation of Carmona’s [EtZn(TEMPO⁻)]₂ dimer.

To examine the possibility of SET reactions with dialkyl zinc compounds, TEMPO was treated with one molar equivalent of Me₂Zn in hexane solution and [MeZn(TEMPO⁻)]₂ (**19**) was isolated as colourless crystals in a low yield of 15%. Compound **19** (Figure 5.6) adopts a simple dimeric centrosymmetric structure based on a four-membered [Zn₂(μ-O)₂] ring with terminal methyl groups, completing the distorted trigonal planar

geometry of the zinc centres. The interior ring adopts a planar disposition (sum of its internal angles is exactly 360°); while the Zn-O bond lengths in **19** [Zn(1)-O(1) 1.978(10) and Zn(1)-O(2) 1.930(10) Å] are in good agreement with those found in Carmona's aforementioned structure [1.975 and 1.922 Å]. Furthermore, the N(1)-O(1) bond length in **19** [1.443(14) Å] is comparable to those in the ethyl congener and **16** [1.439 and 1.4479(15) Å, respectively], underlining the anionic character of the bridging TEMPO ligands.

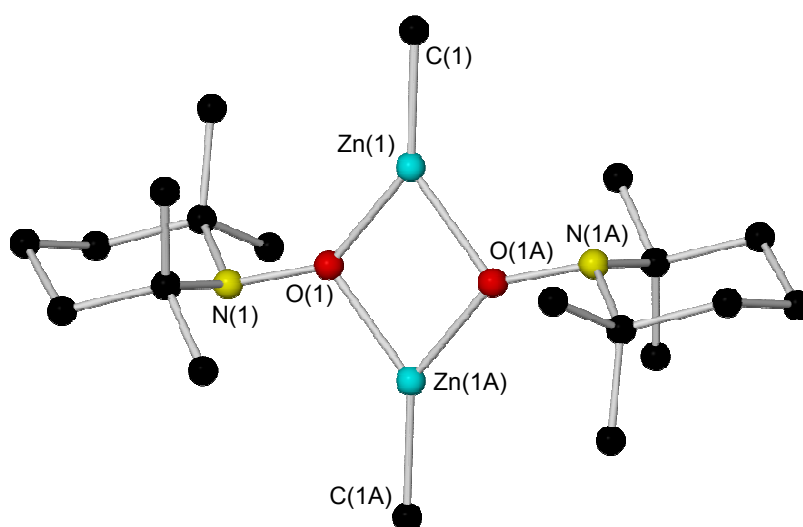
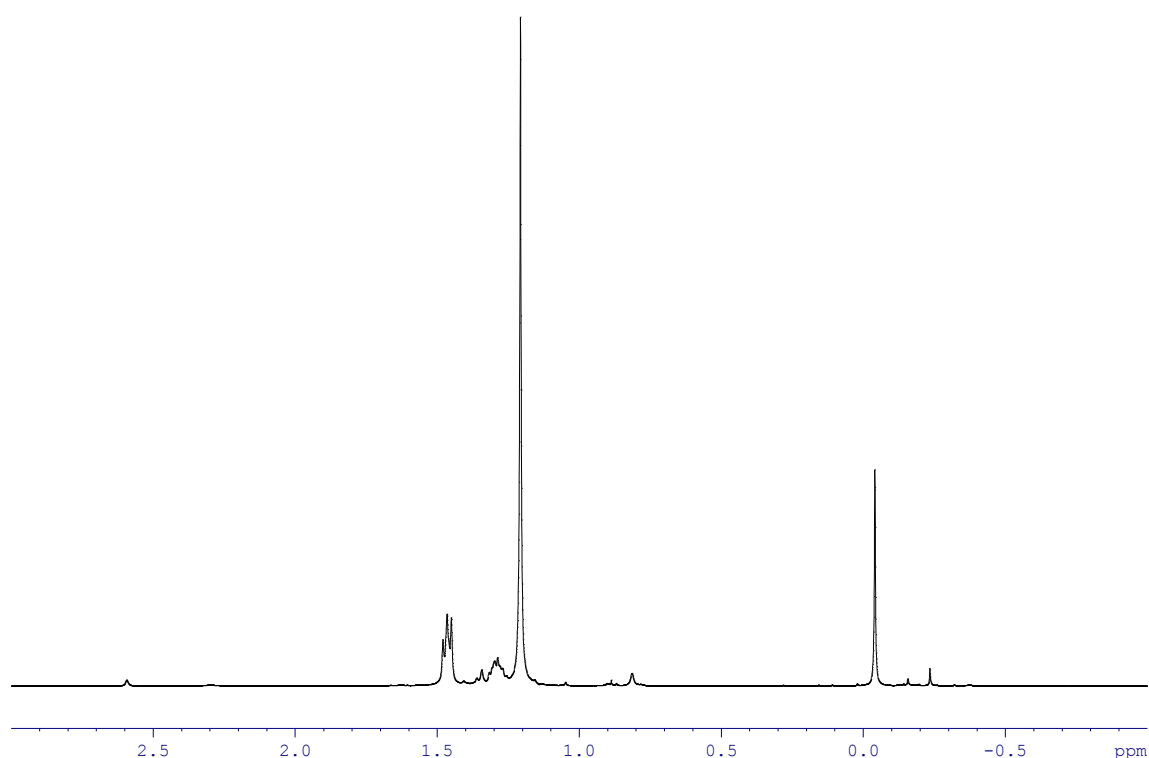


Figure 5.6: Molecular structure of **19** with selective atom labelling. Hydrogen atoms are omitted for clarity. Selected bond distances (Å) and angles (deg): Zn(1)-O(1) 1.9775(10), Zn(1)-O(1A) 1.9299(10), Zn(1)-C(1) 1.9361(18), N(1)-O(1) 1.4433(14); O(1)-Zn(1)-C(1) 142.58(6), O(1)-Zn(1)-O(1A) 77.77(4), C(1)-Zn(1)-O(1A) 139.59(6).

The solubility of **19** in d_6 -benzene solution, along with its diamagnetic nature allowed the complex to be studied by NMR spectroscopy. The ^1H NMR spectra (Spectrum 5.2) is comparatively straightforward containing three resonances for the TEMPO anion at 1.21 (CH_3), 1.29 ($\gamma\text{-CH}_2$) and 1.47 ppm ($\beta\text{-CH}_2$). The most upfield signal was found to be the terminal zinc-bonded methyl group at -0.04 ppm. However, in comparison to other Zn-Me complexes this shift is relatively downfield. For instance, in

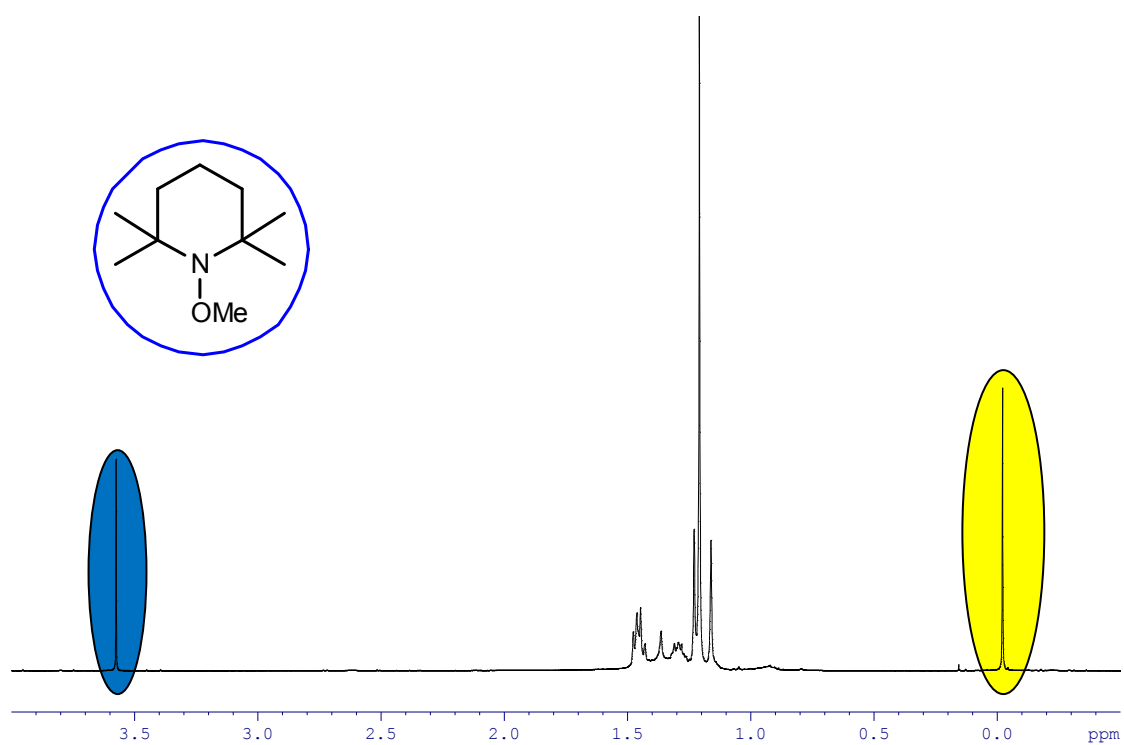
$\text{Me}_2\text{Zn}\cdot\text{TMEDA}$ the resonance for the methyl group appears at -1.16 ppm, admittedly in a different solvent (d_8 -THF). The less negative value of δ for **19** can be attributed to the greater electronegativity of oxygen (in comparison to the chelating nitrogen's of TMEDA) which results in the methyl protons being situated in a region of lower electron density and allied to TEMPO being a poorer electron donor, the Me group consequently has to donate more of its electron density to the zinc causing resonance to occur at a relatively low field.



Spectrum 5.2: ^1H NMR (400.13 MHz, 300 K) spectrum of **19** obtained in d_8 -THF solution.

As detailed previously, complex **19** was isolated in a low crystalline yield of just 15%; to establish the complete constitution of an *in situ* reaction mixture, an aliquot of solution was taken for ^1H NMR spectroscopic analysis (Spectrum 5.3). In addition, to complex **19**, the second species present with evident singlets located at 1.16, 1.23 and 3.58 ppm was identified as TEMPO-Me (formed by TEMPO act as a radical scavenger,

mopping up the liberated Me^\bullet radical) by comparison to NMR chemical shifts documented in the literature.^[38] These two species were found to be present in an 66:34 (**19**:TEMPO-Me) ratio. However, if it is to be envisaged that the Me^\bullet radicals exclusively combine with free TEMPO this ratio should correspond exactly to a 50:50 mixture. The deviation noted from this perfect value can be attributed to some extent to two alkyl radicals combining to evolve ethane or upon removing the hexane prior to NMR spectroscopic analysis, the volatile, unreacted Me_2Zn is also removed from the reaction mixture *in vacuo*.



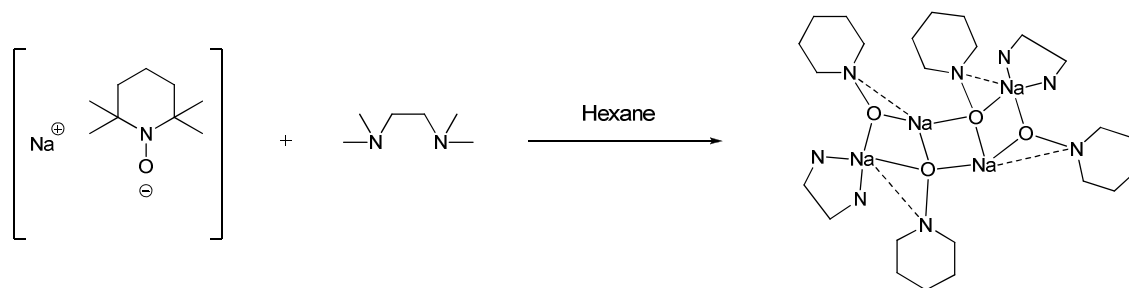
Spectrum 5.3: ^1H NMR (400.13 MHz, 300 K) spectra of a solution aliquot from the 1:1 reaction of Me_2Zn and TEMPO giving **19** (yellow circle) and TEMPO-Me (blue circle) (inset) in a 66:34 ratio.

5.3) Elemental Metal Reduction

Throughout this chapter, work has been presented that has involved the reduction of TEMPO to its monoanionic form. Recently, Mulvey reported the first examples of elemental-metal single electron reduction of this important radical to the TEMPO^-

anion.^[39] Treatment of TEMPO with a group 1 metal (Li, Na, K, Rb or Cs), resulted in direct reduction of the radical to the TEMPO⁻ anion with a variety of structural motifs being encountered depending on the specific choice of metal and/or solvent.

In general, the complexes were formed by direct reaction of the alkali-metal with an equimolar quantity of TEMPO in the respective solvent medium. For example, during the course of this PhD project, TMEDA was added to a suspension of freshly prepared Na⁺TEMPO⁻ (a powder which was prepared by reacting elemental sodium with TEMPO in hexane) in hexane solution (Scheme 5.10). After stirring the solution overnight and cooling to -24 °C, crystals precipitated from it in a 59% yield. X-ray crystallographic analysis revealed these crystals to be [Na⁺₄(μ₃-TEMPO⁻)₂(μ₂-TEMPO⁻)₂(TMEDA)₂] (**20**).



Scheme 5.10: Preparation of the Na⁺TEMPO⁻ complex 20. For clarity, the Na-N_{TEMPO} bonds have been drawn as dashed lines and TEMPO and TMEDA Me groups have been omitted.

The molecular structure of **20** is shown in Figure 5.7. Complex **20** exists as a tetranuclear pseudodimer which adopts a ladder-like conformation. The Na atoms which occupy positions in the outer rungs [Na(1) and Na(4)] are five-coordinate, coordinated to one μ₂-O, one μ₃-O, one N_{TEMPO} and two N_{TMEDA} atoms. Those occupying the central rungs [Na(2) and Na(3)] adopt a highly distorted tetrahedral geometry [mean angles: 108.72 and 104.91°, respectively]. The mean acute O-Na-

N_{TEMPO} and TMEDA bite angles are 35.08 and 70.64°, respectively. Turning to the bond distances in **20**, the shortest Na-O bonds are those belonging to the end rungs of the ladder [2.1992(12) and 2.1941(12) Å for Na(1)-O(1) and Na(4)-O(4), respectively]. The remaining Na-O bonds range in length from 2.2446(11) to 2.4399(12) Å. The average of these distances fits nicely with the Na-O distance [2.342 Å] in the sodium salt of 4-carboxy-TEMPO,^[40] the only relatively comparative structure in the Cambridge Crystallographic Database.^[37]

Ladder motifs are commonly observed in the organometallic chemistry of the alkali-metals.^[41] As illustrated in Section 1.1, lithium alkyls are normally associated species such as tetramers and hexamers with such structures reflecting lithium's desire to fully maximise its coordination number due to its ionic nature. Often the lithium cation is surrounded by four negatively charged or donor atoms/groups and though the bonding is predominantly ionic, this coincides with the four valence-shell orbitals on lithium. The idea of ring-stacking was put forward to account for recurring patterns within the structural chemistry of lithium and is demonstrated in crystalline iminolithium, alkynyllithium and alkoxy- or aryloxy-lithium species where the basic unit is a four-membered or six-membered ring of Li and X atoms (X = N, C and O, respectively).^[42] Significantly, such ring species are flat up to and including the primary atom of the group facilitating vertical aggregation and raising the metal coordination number from two to three. Accordingly, the oligomeric (tetrameric and hexameric) clusters can be thought of as double stacks of dimeric or trimeric rings. In contrast, generally lithium amides cannot adopt such stacked structures because in cyclic dimers or trimers the substituents generally project above and below the (NLi)_n core ring plane precluding vertical association of the rings. Provided the substituents are not too bulky, the tendency to aggregate can be realised by lateral association to form ladder structures.

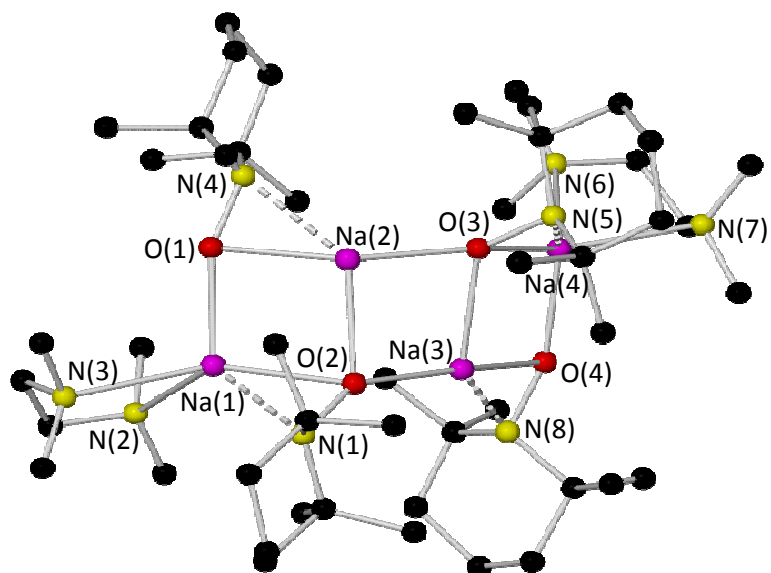


Figure 5.7: Molecular structure of **20** with selective atom labelling. Hydrogen atoms and disordered component of TMEDA are omitted for clarity. Selected bond distances (Å) and angles (deg): Na(1)-O(1) 2.1992(12), Na(1)-O(2) 2.3107(11), Na(1)-N(1) 2.4705(13), Na(1)-N(2) 2.6986(15), Na(1)-N(3) 2.4726(14), Na(2)-O(1) 2.3059(11), Na(2)-O(2) 2.3443(11), Na(2)-O(3) 2.2673(11), Na(2)-N(4) 2.4287(14), Na(3)-O(2) 2.2446(11), Na(3)-O(3) 2.3059(11), Na(3)-O(4) 2.2919(12), Na(3)-N(8) 2.3815(13), Na(4)-O(3) 2.4399(12), Na(4)-O(4) 2.1941(12), Na(4)-N(5) 2.4347(13), Na(4)-N(6) 2.8080(15), Na(4)-N(7) 2.5299(14), O(1)-N(4) 1.4345(15), O(2)-N(1) 1.4447(14), O(3)-N(5) 1.4436(14), O(4)-N(8) 1.4376(15); O(1)-Na(1)-O(2) 99.92(4), O(1)-Na(1)-N(1) 120.14(5), O(1)-Na(1)-N(2) 109.43(5), O(1)-Na(1)-N(3) 101.24(5), O(2)-Na(1)-N(1) 34.97(3), O(2)-Na(1)-N(2) 130.19(5), O(2)-Na(1)-N(3) 140.71(5), N(1)-Na(1)-N(2) 129.47(5), N(1)-Na(1)-N(3) 105.95(5), N(2)-Na(1)-N(3) 71.49(5), O(1)-Na(2)-O(2) 95.91(4), O(1)-Na(2)-O(3) 164.94(5), O(1)-Na(2)-N(4) 35.15(4), O(2)-Na(2)-O(3) 91.51(4), O(2)-Na(2)-N(4) 130.55(4), O(3)-Na(2)-N(4) 134.23(5), O(2)-Na(3)-O(3) 93.10(4), O(2)-Na(3)-O(4) 146.76(5), O(2)-Na(3)-N(8) 122.15(4), O(3)-Na(3)-O(4) 98.20(4), O(3)-Na(3)-N(8) 133.46(4), O(4)-Na(3)-N(8) 35.76(4), O(3)-Na(4)-O(4) 97.04(4), O(3)-Na(4)-N(6) 129.86(4), O(3)-Na(4)-N(7) 143.77(5), O(4)-Na(4)-N(5) 118.43(5), O(4)-Na(4)-N(6) 112.72(5), O(4)-Na(4)-N(7) 101.31(5), N(5)-Na(4)-N(6) 127.41(5), N(5)-Na(4)-N(7) 109.74(5), N(6)-Na(4)-N(7) 69.79(4), Na(1)-O(1)-Na(2) 83.70(4), Na(1)-O(2)-Na(2) 80.47(4), Na(2)-O(2)-Na(3) 84.03(4), Na(2)-O(3)-Na(3) 84.40(4), Na(3)-O(3)-Na(4) 79.27(4), Na(3)-O(4)-Na(4) 84.91(4).

For instance, Snaith has previously prepared the complexes $[\{\text{H}_2\text{C}(\text{CH}_2)_3\text{NLi}\}_2\text{TMEDA}]_2$ and $[\{\text{H}_2\text{C}(\text{CH}_2)_3\text{NLi}\}_3\text{PMDETA}]_2$, derived by alkyl lithiation of the small cyclic amine pyrrolidine (Figure 5.8).^[43] Both adopt ladder structures of four (N-Li) rungs in length, though the latter carries two additional lithium atoms broken away from the ladder framework. The central rings of the ladders and the N atoms of the outer rings are approximately co-planar but the lithium atoms of the outer rings straddle this plane.

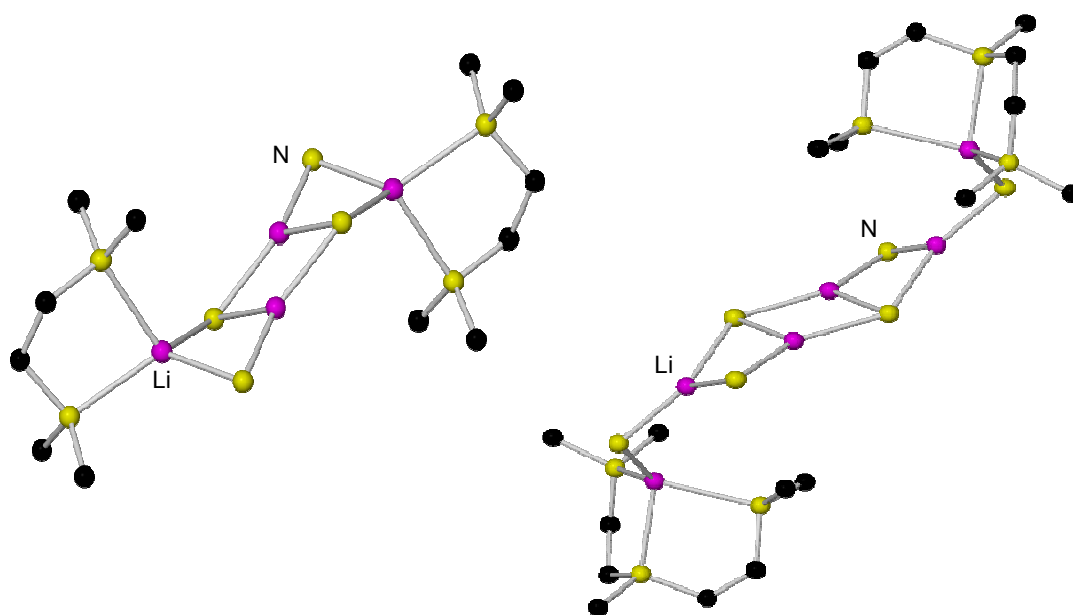


Figure 5.8: The ladder structures of $[\{\text{H}_2\text{C}(\text{CH}_2)_3\text{NLi}\}_2\text{TMEDA}]_2$ (L.H.S) and $[\{\text{H}_2\text{C}(\text{CH}_2)_3\text{NLi}\}_3\text{PMDETA}]_2$ (R.H.S). For clarity the hydrogen atoms and pyrrolidine ligands carbon skeleton have been removed.

The ladder core of **20** comprises three Na_2O_2 rhombi (Figure 5.9); the outermost rings are essentially planar, while the central ring deviates significantly from planarity [sum of endocyclic angles for $\text{Na}(1)\text{-O}(1)\text{-Na}(2)\text{-O}(2)$, $\text{O}(2)\text{-Na}(2)\text{-O}(3)\text{-Na}(3)$ and $\text{Na}(3)\text{-O}(3)\text{-Na}(4)\text{-O}(4)$ are 360 , 353.04 and 359.42° , respectively]. The dihedral angles between planes $\text{Na}(1)\text{-O}(1)\text{-Na}(2)\text{-O}(2)$ and $\text{O}(2)\text{-Na}(2)\text{-O}(3)\text{-Na}(3)$, and $\text{O}(2)\text{-Na}(2)\text{-O}(3)\text{-Na}(3)$ and $\text{Na}(3)\text{-O}(3)\text{-Na}(4)\text{-O}(4)$ are $154.44(3)^\circ$ and $133.92(3)^\circ$, respectively, resulting in the ladder adopting a cisoidal conformation.

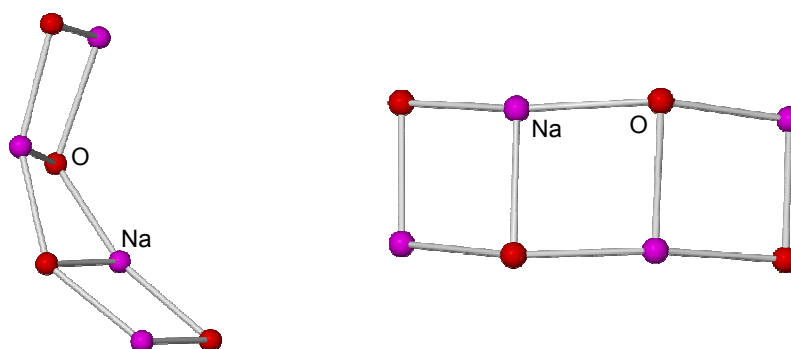


Figure 5.9: Two different representations of the ladder core of complex **20** illustrating its cisoidal conformation.

Searching for comparisons with **20**, the novel sodium amide-amine complex $[\{t\text{BuN}(\text{H})\text{Na}\}_3 \cdot \text{H}_2\text{N}t\text{Bu}]_\infty$, previously reported by the Mulvey group, forms an infinite wave like ladder structure (Figure 5.10).^[44] Covering three nitrogen-sodium rings, its curved sections also display a cisoid conformation of amide substituents; but where the curved sections fuse, a transoid conformation is found. This contrasts with the situation found in the lithium analogue, where the lack of solvent ligands leads to an exclusively cisoid conformation; this results in a closed cyclic structure comprising eight N-Li rings.

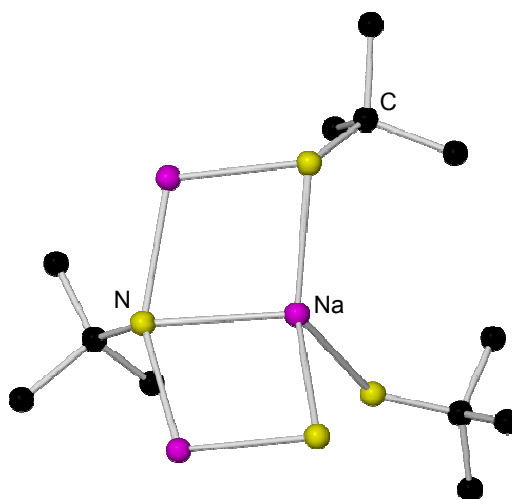


Figure 5.10: Section of the polymeric structure of $[\{t\text{BuN}(\text{H})\text{Na}\}_3 \cdot \text{H}_2\text{N}t\text{Bu}]_\infty$ with hydrogen atoms omitted for clarity.

The solubility of **20** in both d_8 -THF and d_6 -benzene allowed a detailed solution study of the complex by NMR spectroscopy. The ^1H NMR spectrum in the former polar solvent is relatively simple containing two broad resonances for the TEMPO anion at 1.06 (Me protons) and 1.44 ppm (overlap of β and γ protons) and as expected, upon dissolution in d_8 -THF, the TMEDA ligand is no longer coordinated to the sodium centre but is replaced by d_8 -THF ligands. These NMR spectroscopic data (Table 5.2) can be compared those found for the $[(\text{THF})\cdot\text{Na}^+(\text{TEMPO}^-)]_4$ and $[(\text{THF})\cdot\text{K}^+(\text{TEMPO}^-)]_4$ complexes that adopt cubane structures in the solid-state.^[39] This would seem to indicate that in polar solvent a solvent-separated ion-pair or a solvated, lower oligomeric form of the complexes exist; in essence, the data show that the local coordination environment of the TEMPO⁻ ligand is sensitive to the charge-balancing cation.

Table 5.2: Comparison of selected ^1H NMR (400.13 MHz, 300 K) chemical shifts (δ in ppm) for a selection of alkali metal - TEMPO complexes in d_8 -THF solution.

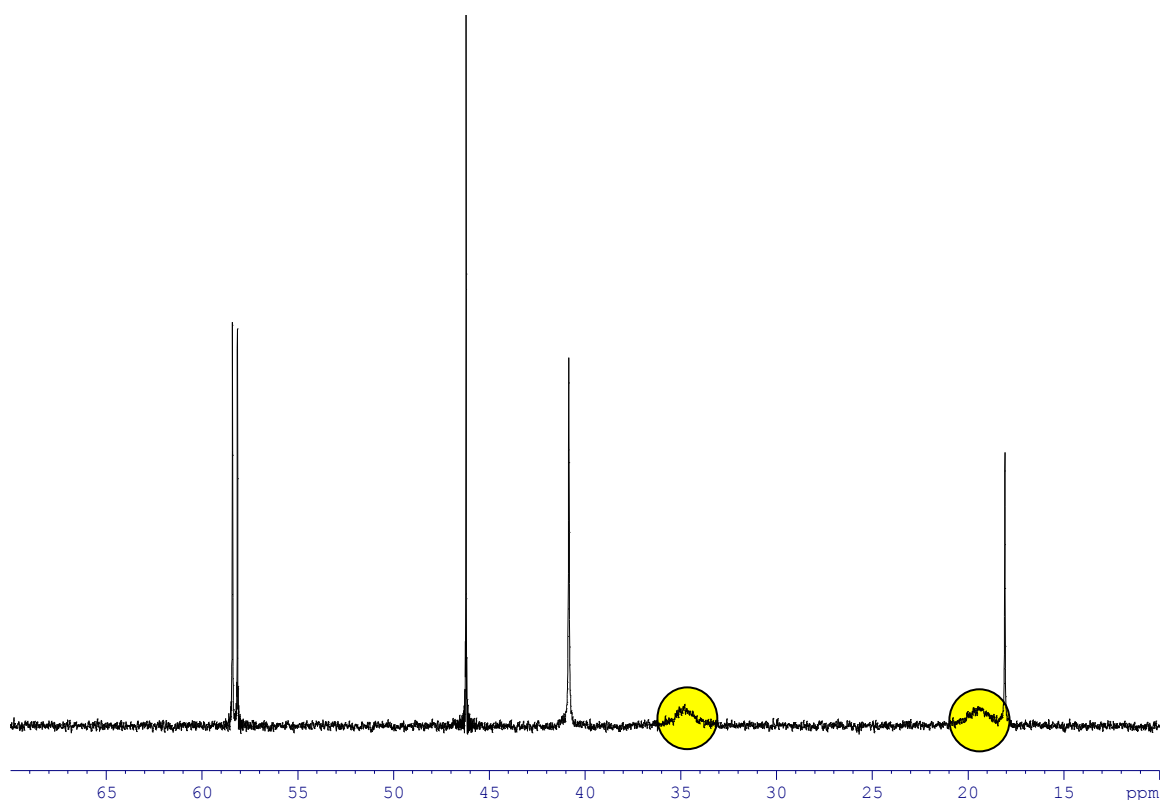
Compound	$\delta(\beta\text{-CH}_2 \text{ and } \gamma\text{-CH}_2 \text{ TEMPO})$	$\delta(\text{TEMPO-CH}_3)$
20	1.44	1.06
$[(\text{THF})\cdot\text{Na}^+(\text{TEMPO}^-)]_4$	1.45	1.10
$[(\text{THF})\cdot\text{K}^+(\text{TEMPO}^-)]_4$	1.42	1.00

The TEMPO anion in d_6 -benzene is also depicted by two broad resonances in the ^1H NMR spectrum (Table 5.3). Turning to the ^{13}C NMR data, the spectrum provides an insight into the solution dynamics of complex **20**. In general, three sharp resonances [at 18.1 (γ -C), 40.8 (β -C) and 58.4 (α -C) ppm] are observed in d_6 -benzene, along with two extremely broad signals (Spectrum 5.4) at 19.5 and 34.8 ppm (note these resonances were not observed in d_8 -THF). Using ^1H - ^{13}C HSQC NMR spectroscopy, the broader

signals can be attributed to two chemically distinct Me-TEMPO groups (Me groups are diastereotopic). This observation suggests that rotation around the O-N axis of the TEMPO⁻ anion appears to be highly restricted (hence two independent resonances) and that rotation is slow on the NMR time scale under the conditions studied.

Table 5.3: ¹H NMR (400.13 MHz, 300 K) and ¹³C NMR (100.62 MHz, 300 K) chemical shifts (δ in ppm) for the TEMPO ligand in **20 in *d*₆-benzene solution.**

Nucleus	δ(CH ₃)	δ(β-CH ₂)	δ(γ-CH ₂)	δ(α-C)
¹ H	1.33	1.60	1.60	-
¹³ C { ¹ H}	19.5, 34.8	40.8	18.1	58.4



Spectrum 5.4: ¹³C NMR (100.62 MHz, 300 K) spectrum of **20 in *d*₆-benzene solution illustrating the two diastereotopic methyl groups** ● .

In summary, we have shown that sodium zincate **1** can function as an SET agent towards TEMPO, providing experimental evidence that supports the hypothesis that

SET could be at play in the Mulvey and O'Hara groups previously reported 1,6-additions. Future studies could investigate the scope of this work by utilising **16** in other synthetic procedures, determining whether it can be a useful synthetic reagent in deprotonative metallation and/or addition reactions. In an extension of this work, new metal-TEMPO complexes were prepared by treating TEMPO with a dialkyl zinc reagent or an alkali-metal, with the latter synthesis of **20** representing one of the first examples of elemental-metal reduction of the TEMPO radical.

5.4) Experimental section

Synthesis of [(TMEDA)Na(μ -TMP)(μ -TEMPO⁻)Zn(*t*Bu)] **16**

A hexane solution of **1** was prepared as described previously (2 mmol in 20 mL). TEMPO (0.31 g, 2 mmol) was added via a solid addition tube and the reaction mixture was allowed to stir at ambient temperature for 2 hours. The resulting orange solution was concentrated *in-vacuo* and transferred to a freezer operating at -28 °C, which deposited a crop of colourless crystals overnight (0.38 g, 34%). ¹H NMR (400.13 MHz, 300 K, *d*₈-THF): δ 2.30 [s, 4H, NCH₂ (TMEDA)], 2.15 [s, 12H, NCH₃ (TMEDA)], 1.71 [m, 2H, γ -CH₂ (TMP)], 1.44 [m, 8H, γ -CH₂ and β -CH₂ (TEMPO) and β -CH₂ (TMP)], 1.22 [m, 2H, β -CH₂ (TMP)], 1.16 [s, 12H, CH₃ (TMP) and CH₃ (TEMPO)], 1.09 [s, 6H, CH₃ (TEMPO)], 1.08 [s, 9H, CH₃ (*t*Bu)], 0.96 [br, 6H, CH₃ (TMP)]. ¹³C {¹H} NMR (100.62 MHz, 300 K, *d*₈-THF): δ 58.9 [NCH₂ (TMEDA)], 58.3 [α -C (TEMPO)], 52.5 [α -C (TMP)], 46.2 [NCH₃ (TMEDA)], 41.3 [β -CH₂ (TEMPO)], 40.9 [β -CH₂ (TMP)], 36.5 [CH₃ (TMP/TEMPO)], 35.9 [C(CH₃)₃ (*t*Bu)], 35.8 [CH₃ (TEMPO)], 34.1 [CH₃ (TMP/TEMPO)], 20.6 [γ -CH₂ (TMP)], 20.3 [C(CH₃)₃ (*t*Bu)], 19.3 [CH₃ (TMP)], 18.9 [γ -CH₂ (TEMPO)].

Crystal data for **16**: C₂₈H₆₁N₄NaOZn, M = 558.17, monoclinic, C2/c, $a = 17.3607(4)$ Å, $b = 13.0692(4)$ Å, $c = 28.9589(8)$ Å, $\beta = 98.010(1)^\circ$, $V = 6506.4(3)$ Å³, $Z = 8$; 121087 reflections collected, 9475 were unique, $R_{\text{int}} = 0.112$, $R = 0.0382$, $R_w = 0.0809$, GOF = 1.008, 371 refined parameters, max. and min. residual electron density = 0.562 and -0.583 e⁻Å⁻³.

Synthesis of [(TMEDA)Na(μ-TEMPO⁻)₂Zn(*t*Bu)] **17**

A hexane solution of **1** was prepared (2 mmol in 20 mL). TEMPO (0.62 g, 4 mmol) was added via a solid addition tube and the reaction mixture was allowed to stir at ambient temperature for 2 hours. The resulting orange solution was concentrated *in-vacuo* and transferred to a freezer operating at -28 °C, which deposited a crop of colourless crystals overnight (0.37 g, 32%). ¹H NMR (400.13 MHz, 300 K, *d*₈-THF): δ 2.30 [s, 4H, NCH₂ (TMEDA)], 2.14 [s, 12H, NCH₃ (TMEDA)], 1.44 [br, 8H, β-CH₂ (TEMPO)], 1.39 [m, 4H, γ-CH₂ (TEMPO)], 1.10 [s, 9H, CH₃ (*t*Bu)], 1.08 [br, 24H, CH₃ (TEMPO)]. ¹³C {¹H} NMR (100.62 MHz, 300 K, *d*₈-THF): δ 58.9 [NCH₂ (TMEDA)], 58.5 [α-C (TEMPO)], 46.2 [NCH₃ (TMEDA)], 41.2 [β-CH₂ (TEMPO)], 35.3 [C(CH₃)₃ (*t*Bu)], 21.7 [C(CH₃)₃ (*t*Bu)], 18.7 [γ-CH₂ (TEMPO)]. *No resonances could be observed for the TEMPO methyl groups. Extremely broad ¹³C signals have previously been noted for the methyl groups of alkali-metal TEMPO complexes.^[39] Unfortunately, because of the relatively low boiling point of *d*₈-THF, a high temperature NMR study could not be conducted.

Synthesis of [(TMEDA)Na(μ-TMP)(μ-TEMPO⁻)Zn(Me)] **18**

The sodium amide NaTMP was prepared *in situ* by reaction of *n*BuNa (0.16 g, 2 mmol) with TMPH (0.34 g, 2 mmol) in 10 mL of dry hexane. The yellow suspension formed was allowed to stir for 2 hours. Me₂Zn (2 mL of 1M solution in heptane, 2 mmol) was

then added to the already prepared NaTMP. TMEDA (0.3 mL, 2 mmol) was then added to the contents of the Schlenk tube. After stirring for 10 minutes, TEMPO (0.31 g, 2 mmol) was introduced and the mixture was left stirring overnight. The solution was filtered, resulting in a clear transparent orange solution. The solution was concentrated with the removal of solvent *in vacuo* and placed in the freezer (at -28 °C) which deposited a crop of colourless crystals (0.26 g, 25%). ^1H NMR (400.13 MHz, 300 K, d_8 -THF): δ 2.37 [s, 4H, NCH_2 (TMEDA)], 2.19 [s, 12H, NCH_3 (TMEDA)], 1.69 [m, 2H, γ - CH_2 (TMP)], 1.42 [br, 6H, γ - CH_2 and β - CH_2 (TEMPO)], 1.28 [br, 4H, β - CH_2 (TMP)], 1.13 [s, 12H, CH_3 (TMP)], 1.02 [s, 12H, CH_3 (TEMPO)], -0.86 (s, 3H, CH_3). ^{13}C $\{^1\text{H}\}$ NMR (100.62 MHz, 300 K, d_8 -THF): δ 58.32 [NCH_2 (TMEDA)], 57.86 [α -C (TEMPO)], 52.86 [α -C (TMP)], 46.57 [NCH_3 (TMEDA)], 41.28/41.12 [β - CH_2 (TMP) and β - CH_2 (TEMPO)], 35.79 [br, CH_3 (TMP) and CH_3 (TEMPO)], 20.62 [γ - CH_2 (TMP)], 18.83 [γ - CH_2 (TEMPO)], -10.43 (CH_3).

Crystal data for **18**: $\text{C}_{25}\text{H}_{55}\text{N}_4\text{NaOZn}$, $M = 516.09$, monoclinic, $\text{P}2_1/n$, $a = 11.9364(3)$ Å, $b = 19.0869(4)$ Å, $c = 13.4897(3)$ Å, $\beta = 102.538(2)^\circ$, $V = 3000.05(12)$ Å³, $Z = 4$; 40371 reflections collected, 8561 were unique, $R_{\text{int}} = 0.0384$, $R = 0.0556$, $R_w = 0.1252$, GOF = 1.064, 326 refined parameters, max. and min. residual electron density = 0.769 and -0.607 e \cdot Å⁻³.

Synthesis of $[\text{MeZn}(\text{TEMPO}^-)]_2$ **19**

Me_2Zn (2 mL of 1M solution in heptane, 2 mmol) was added to 10 mL of dry hexane. TEMPO (0.31 g, 2 mmol) was added and the clear transparent red solution was stirred overnight. The subsequent colourless solution was filtered and concentrated with the removal of solvent *in vacuo*. The Schlenk tube was placed in the freezer (at -28 °C) and the solution subsequently deposited a small amount of colourless crystals (0.07 g, 15%).

^1H NMR (400.13 MHz, 300 K, d_6 -benzene): δ 1.47 [m, 4H, β -CH₂ (TEMPO)], 1.29 [m, 2H, γ -CH₂ (TEMPO)], 1.21 [s, 12H, CH₃ (TEMPO)], -0.04 (s, 3H, CH₃). ^{13}C { ^1H } NMR (100.62 MHz, 300 K, d_6 -benzene): δ 60.42 [α -C (TEMPO)], 39.83 [β -CH₂ (TEMPO)], 26.77 [CH₃ (TEMPO)], 17.46 [γ -CH₂ (TEMPO)], -11.41 (CH₃).

Crystal data for **19**: C₂₀H₄₂N₂O₂Zn₂, M = 473.30, triclinic, P-1, $a = 7.8065(3)$ Å, $b = 7.8516(3)$ Å, $c = 10.1371(3)$ Å, $\alpha = 78.092(3)^\circ$, $\beta = 88.211(3)^\circ$, $\gamma = 74.104(4)^\circ$, $V = 584.51(4)$ Å³, $Z = 1$; 12552 reflections collected, 3396 were unique, $R_{\text{int}} = 0.0236$, $R = 0.0251$, $R_w = 0.0595$, GOF = 1.098, 122 refined parameters, max. and min. residual electron density = 0.410 and -0.294 e \cdot Å⁻³.

Synthesis of Na⁺ TEMPO⁻ Powder

A Schlenk tube was charged with freshly cleaned elemental sodium (0.46 g, 20 mmol). To enhance the reactivity of the metal, the sodium was melted to a mirror using a heat gun. Hexane (40 mL) and TEMPO (3.12 g, 20 mmol) were added to the Schlenk tube, and this orange coloured mixture was heated to reflux for 12 hours, resulting in the precipitation of a white solid. On reducing the solvent *in vacuo* by approximately 50%, further precipitation occurred. The solid was collected by filtration (typical yield: 2.3 g, 65%).

Synthesis of [Na⁺₄(μ_3 -TEMPO⁻)₂(μ -TEMPO⁻)₂(TMEDA)₂] **20**

Freshly prepared Na⁺TEMPO⁻ (0.36 g, 2 mmol) was suspended in hexane in a Schlenk tube. TMEDA (0.15 mL, 1 mmol) was added, and the mixture was stirred overnight. The subsequent mixture was filtered, and the red filtrate was concentrated by removal of some solvent *in vacuo* and placed in the freezer at -28 °C. A crop of colourless crystals was deposited after 24 hours. Yield: 0.28 g, 59%. ^1H NMR (400.13 MHz, 300

K, d_6 -benzene): δ 2.27 [s, 4H, NCH_2 (TMEDA)], 2.14 [s, 12H, NCH_3 (TMEDA)], 1.60 [br s, 12H, β - CH_2 and γ - CH_2 (TEMPO)], 1.33 [br s, 24H, CH_3 (TEMPO)]. ^{13}C { 1H } NMR (100.62 MHz, 300 K, d_6 -benzene): δ 58.41 [α -C (TEMPO)], 58.14 [NCH_2 (TMEDA)], 46.20 [NCH_3 (TMEDA)], 40.84 [β - CH_2 (TEMPO)], 34.81 [CH_3 (TEMPO)], 19.50 [CH_3 (TEMPO)], 18.7 [γ - CH_2 (TEMPO)].

Crystal data for **20**: $C_{48}H_{104}N_8Na_4O_4$, $M = 949.35$, triclinic, P-1, $a = 11.5872(4)$ Å, $b = 12.6446(4)$ Å, $c = 20.7262(4)$ Å, $\alpha = 90.066(2)^\circ$, $\beta = 90.989(3)^\circ$, $\gamma = 112.001(3)^\circ$, $V = 2815.28(14)$ Å³, $Z = 2$; 52741 reflections collected, 13559 were unique, $R_{int} = 0.0381$, $R = 0.0479$, $R_w = 0.1171$, GOF = 1.028, 662 refined parameters, max. and min. residual electron density = 0.278 and -0.252 e \cdot Å⁻³.

Chapter 5 - References

- [1] (a) S. Barriga, *Synlett* **2001**, 4, 563; (b) M. V. N. De Souza, *Mini-Rev. Org. Chem.* **2006**, 3, 155 - 165.
- [2] O. Lebelev, S. N. Kazarnovskii, *Zhur. Obshch. Khim.* **1960**, 30, 1631 - 1635.
- [3] F. Montanari, S. Quici, H. Henry-Riyad, T. T. Tidwell, in "2,2,6,6-Tetramethylpiperidin-1-oxyl" *Encyclopedia of Reagents for Organic Synthesis*, John Wiley & Sons: New York, **2005**.
- [4] T. Vogler, A. Studer, *Synthesis* **2008**, 13, 1979 - 1993.
- [5] (a) A. E. J. de Nooy, H. van Bekkum, A. Besemer, *Synthesis* **1996**, 1153 - 1174; (b) R. A. Sheldon, I. W. C. E. Arends, *Adv. Synth. Catal.* **2004**, 346, 1051 - 1071; (c) J. A. Bäckvall, in *Modern Oxidation Methods*, Wiley-VCH: Weinheim, **2004**; (d) R. Ciriminna, M. Pagliaro, *Org. Process. Res. Dev.* **2010**, 14, 245 - 251.
- [6] www.sigmaaldrich.com, **November 2011**.
- [7] B. D. Hewitt, Conversion of bisnoralcohol to bisnoraldehyde (Upjohn Co., USA) WO 016698, **1995**.
- [8] F. Rossi, F. Corcella, F. S. Caldarelli, F. Heidempergher, C. Marchionni, M. Auguadro, M. Cattaneo, L. Ceriani, G. Visentin, G. Ventrella, V. Pincioli, G. Ramella, I. Candiani, A. Bedeschi, A. Tomasi, B. J. Kline, C. A. Martinez, D. Yazbeck, D. J. Kucera, *Org. Process. Res. Dev.* **2008**, 12, 322 - 338.
- [9] (a) R. Chinchilla, C. Nájera, *Chem. Rev.* **2007**, 107, 874 - 922; (b) H. Doucet, J. C. Hierso, *Angew. Chem. Int. Ed.* **2007**, 46, 834 - 871.
- [10] K. Sonogashira, Y. Tohda, N. Hagihara, *Tetrahedron Lett.* **1975**, 16, 4467 - 4470.
- [11] S. R. Dubbaka, M. Kienle, H. Mayr, P. Knochel, *Angew. Chem. Int. Ed.* **2007**, 46, 9093 - 9096.
- [12] G. Cahiez, C. Duplais, J. Buendia, *Angew. Chem. Int. Ed.* **2009**, 48, 6731 - 6734.
- [13] M. S. Maji, T. Pfeifer, A. Studer, *Angew. Chem. Int. Ed.* **2008**, 47, 9547 - 9550.
- [14] M. S. Maji, M. Murarka, A. Studer, *Org. Lett.* **2010**, 12, 3878 - 3881.
- [15] S. Kirchberg, R. Fröhlich, A. Studer, *Angew. Chem. Int. Ed.* **2009**, 48, 4235 - 4238.

- [16] (a) M. K. Mahanthappa, A. P. Cole, R. M. Waymouth, *Organometallics* **2004**, *23*, 836 - 845; (b) M. K. Mahanthappa, K. W. Huang, A. P. Cole, R. M. Waymouth, *Chem. Commun.* **2002**, 502 - 503; (c) K. Schröder, D. Haase, W. Saak, R. Beckhaus, W. P. Kretschmer, A. Lutzen, *Organometallics* **2008**, *27*, 1859 - 1868.
- [17] (a) M. H. Dickman, L. C. Porter, R. J. Doedens, *Inorg. Chem.* **1986**, *25*, 2595 - 2599; (b) P. Jaitner, W. Huber, G. Huttner, O. Scheidsteger, *J. Organomet. Chem.* **1983**, *259*, C1 - C5.
- [18] (a) M. H. Dickman, *Acta Crystallogr. Sect. C: Cryst. Struct. Commun.* **1997**, *53*, 1192 - 1195; (b) P. Jaitner, W. Huber, A. Gieren, H. Betz, *J. Organomet. Chem.* **1986**, *311*, 379 - 385.
- [19] (a) D. J. Mindiola, R. Waterman, D. M. Jenkins, G. L. Hillhouse, *Inorg. Chim. Acta.* **2003**, *345*, 299 - 308; (b) D. Isrow, B. Captain, *Inorg. Chem.* **2011**, *50*, 5864 - 5866; (c) M. Ito, T. Matsumoto, K. Tatsumi, *Inorg. Chem.* **2009**, *48*, 2215 - 2223.
- [20] (a) A. Caneschi, A. Grand, J. Laugier, P. Rey, R. Subra, *J. Am. Chem. Soc.* **1988**, *110*, 2307 - 2309; (b) M. H. Dickman, R. J. Doedens, *Inorg. Chem.* **1981**, *20*, 2677 - 2681; (c) J. Laugier, J. M. Latour, A. Caneschi, P. Rey, *Inorg. Chem.* **1991**, *30*, 4474 - 4477; (d) L. C. Porter, M. H. Dickman, R. J. Doedens, *Inorg. Chem.* **1983**, *22*, 1962 - 1964.
- [21] (a) A. Gorrane, I. Resa, A. Rodriguez, E. Carmona, E. Alvarez, E. Gutierrez-Puebla, A. Monge, A. Galindo, D. del Rio, R. A. Andersen, *J. Am. Chem. Soc.* **2007**, *129*, 693 - 703; (b) Z. Zhu, J. C. Fettinger, M. M. Olmstead, P. P. Power, *Organometallics* **2009**, *28*, 2091 - 2095.
- [22] P. Jaitner, W. Huber, A. Gieren, H. Betz, *Z. Anorg. Allg. Chem.* **1986**, *538*, 53 - 60.
- [23] (a) A. Cogne, E. Belorizky, J. Laugier, P. Rey, *Inorg. Chem.* **1994**, *33*, 3364 - 3369; (b) M. Handa, Y. Sayama, M. Mikuriya, R. Nukada, I. Hiromitsu, K. Kasuga, *Bull. Chem. Soc. Jpn.* **1995**, *68*, 1647 - 1653; (c) J. W. Seyler, P. E. Fanwick, C. R. Leidner, *Inorg. Chem.* **1992**, *31*, 3699 - 3700.
- [24] (a) T. Y. Dong, D. N. Hendrickson, T. R. Felthouse, H. S. Shieh, *J. Am. Chem. Soc.* **1984**, *106*, 5373 - 5375; (b) T. R. Felthouse, T. Y. Dong, D. N. Hendrickson, H. S. Shieh, M. R. Thompson, *J. Am. Chem. Soc.* **1986**, *108*, 8201 - 8214.

- [25] (a) M. H. Dickman, R. J. Doedens, *Inorg. Chem.* **1982**, *21*, 682 - 684; (b) L. C. Porter, R. J. Doedens, *Acta Crystallogr. Sect. C: Cryst. Struct. Commun.* **1985**, *41*, 838 - 840.
- [26] M. R. Haneline, F. P. Gabbai, *Inorg. Chem.* **2005**, *44*, 6248 - 6255.
- [27] G. C. Forbes, A. R. Kennedy, R. E. Mulvey, P. J. A. Rodger, *Chem. Commun.* **2001**, 1400 - 1401.
- [28] (a) O. Dechy-Cabaret, B. Martin-Vaca, D. Borissou, *Chem. Rev.* **2004**, *104*, 6147 - 6176; (b) A. P. Dove, *Chem. Commun.* **2008**, 6446 - 6470.
- [29] S. Mecking, *Angew. Chem. Int. Ed.* **2004**, *43*, 1078 - 1085.
- [30] I. L. Fedushkin, A. G. Morozov, V. A. Chudakova, G. K. Fukin, V. K. Cherkasov, *Eur. J. Inorg. Chem.* **2009**, 4995 - 5003.
- [31] E. Hevia, G. W. Honeyman, A. R. Kennedy, R. E. Mulvey, *J. Am. Chem. Soc.* **2005**, *127*, 13106 - 13107.
- [32] J. J. Crawford, B. J. Fleming, A. R. Kennedy, J. Klett, C. T. O'Hara, S. A. Orr, *Chem. Commun.* **2011**, *47*, 3772 - 3774.
- [33] G. A. Olah, A. H. Wu, O. Farooq, *Synthesis* **1991**, 1179 - 1182.
- [34] E. C. Ashby, A. B. Goel, *J. Am. Chem. Soc.* **1981**, *103*, 4983 - 4985.
- [35] (a) H. A. Göttinger, V. E. Zubarev, O. Brede, *J. Chem. Soc. Perkin Trans. 2* **1997**, 2167 - 2172; (b) M. M. Vyushkova, V. I. Borovkov, L. N. Shchegoleva, I. V. Beregovaya, V. A. Bagryanskii, Y. N. Molin, *Doklady Physical Chemistry* **2008**, *420*, 125 - 127.
- [36] D. R. Armstrong, L. Balloch, J. J. Crawford, B. J. Fleming, L. M. Hogg, A. R. Kennedy, J. Klett, R. E. Mulvey, C. T. O'Hara, S. A. Orr, S. D. Robertson, *Chem. Commun.* **2012**, *48*, 1541 - 1543.
- [37] CSD version 5.31 see: F. H. Allen, *Acta Crystallogr., Sect. B* **2002**, *58*, 380 - 388.
- [38] J. Edgar Anderson, D. Casarini, J. E. T. Corrie, L. Lunazzi, *J. Chem. Soc. Perkin Trans. 2* **1993**, 1299 - 1304.
- [39] L. Balloch, A. M. Drummond, P. García-Álvarez, D. V. Graham, A. R. Kennedy, J. Klett, R. E. Mulvey, C. T. O'Hara, P. J. A. Rodger, I. D. Rushworth, *Inorg. Chem.* **2009**, *48*, 6934 - 6944.
- [40] A. Misiolek, R. Huang, B. Kahr, J. E. Jackson, *Chem. Commun.* **1996**, 2119 - 2120.

- [41] (a) R. E. Mulvey, *Chem. Soc. Rev.* **1991**, 20, 167 - 209; (b) K. Gregory, P. V. Schleyer, R. Snaith, *Adv. Inorg. Chem.* **1991**, 37, 47 - 142; (c) E. Weiss, *Angew. Chem. Int. Ed.* **1993**, 32, 1501 - 1523.
- [42] (a) D. Barr, W. Clegg, R. E. Mulvey, R. Snaith, K. Wade, *J. Chem. Soc., Chem. Commun.* **1986**, 295 - 297; (b) D. Barr, W. Clegg, R. E. Mulvey, R. Snaith, D. S. Wright, *J. Chem. Soc., Chem. Commun.* **1987**, 716 - 718; (c) D. Barr, R. Snaith, W. Clegg, R. E. Mulvey, K. Wade, *J. Chem. Soc. Dalton Trans.* **1987**, 2141 - 2147; (d) D. R. Armstrong, D. Barr, R. Snaith, W. Clegg, R. E. Mulvey, K. Wade, D. Reed, *J. Chem. Soc. Dalton Trans.* **1987**, 1071 - 1081.
- [43] (a) D. R. Armstrong, D. Barr, W. Clegg, R. E. Mulvey, D. Reed, R. Snaith, K. Wade, *J. Chem. Soc., Chem. Commun.* **1986**, 869 - 870; (b) D. R. Armstrong, D. Barr, W. Clegg, S. M. Hodgson, R. E. Mulvey, D. Reed, R. Snaith, D. S. Wright, *J. Am. Chem. Soc.* **1989**, 111, 4719 - 4727.
- [44] W. Clegg, K. W. Henderson, L. Horsburgh, F. M. Mackenzie, R. E. Mulvey, *Chem. Eur. J.* **1998**, 4, 53 - 56.

Chapter 6: Structural Variations of Bis(bis(trimethylsilyl)methyl)magnesium

6.1) The Quest for Direct-remote-Metallation

The final passage of this PhD thesis ends back where it all started with the metallation reaction. Previously, in Section 1.3 a hypothetical ideal proton abstractor was described and featuring high on the wish list was the ability to deprotonate at positions inaccessible via other reagents. Although, the sodium TMP-zincate [(TMEDA)Na(μ -TMP)(μ -*t*Bu)Zn(*t*Bu)] (**1**) has successfully effected *meta* and *meta/para* deprotonation of *N,N*-dimethylaniline^[1] and toluene,^[2] respectively, a general mixed-metal amide reagent that could be envisaged and developed for synthetically useful, regioselective *meta*-deprotonation of substituted aromatics would be an exciting breakthrough. From a synthetic chemist's viewpoint, two contributory factors could lead to deprotonation in the *meta* or *para* position. First of all, weak directing groups on substrates in the Directed-*ortho*-Metallation sense should be most amenable to such special deprotonations. Likewise, a finely tuned reagent of our time might unlock the door and it is upon this approach that this final chapter is composed.

In line with previous examples of Alkali-Metal-Mediated Metallation (AMMM), a co-complexation reaction represented an attractive route to our new complex metallator producing a single molecule with a well-defined structure. In the pursuit of *meta* or *para* deprotonation of substituted aromatics, our initial studies were directed towards building a bulkier, bimetallic base in an adaptation of Schlosser's concept of "steric buttressing".^[3] Encouragement came in the form of previous work within the Mulvey group where it was shown that switching the alkyl group but keeping the other components of the synergic base the same can have a profound effect on the outcome of the magnesiation reaction. For instance, the bimetallic mixture NaMg(*n*Bu)(TMP)₂ di-

magnesiates toluene at the 2,5 (*ortho*, *meta*)-positions producing a two-fold deprotonated arene that is encapsulated within an extraordinary host-guest molecule $[(\text{TMP})_6\text{Na}_4(2,5\text{-Mg}_2\text{C}_6\text{H}_3\text{CH}_3)]$ termed an inverse crown (Figure 6.1).^[4] The name inverse crown is derived from the interchange of Lewis basic (anionic; here the $\text{C}_6\text{H}_3\text{CH}_3^{2-}$ guest) and Lewis acidic [cationic; here the $(\text{Na}_4\text{Mg}_2\text{N}_6)^{2+}$ host ring] sites compared with their dispositions in conventional crown ether complexes (host rings containing O atoms, Lewis basic; core guest metal cations, Lewis acidic).^[5] However, upon switching *n*Bu for the more sterically encumbered, silyl-stabilised ligand Me_3SiCH_2 within the synergic bimetallic mixture $\text{NaMg}(\text{CH}_2\text{SiMe}_3)(\text{TMP})_2$, the orientation of the metallation shifts away from the methyl group and the *ortho* site of toluene and is manifested in the 3,5 (*meta*, *meta*) di-metallated inverse crown structure.^[6]

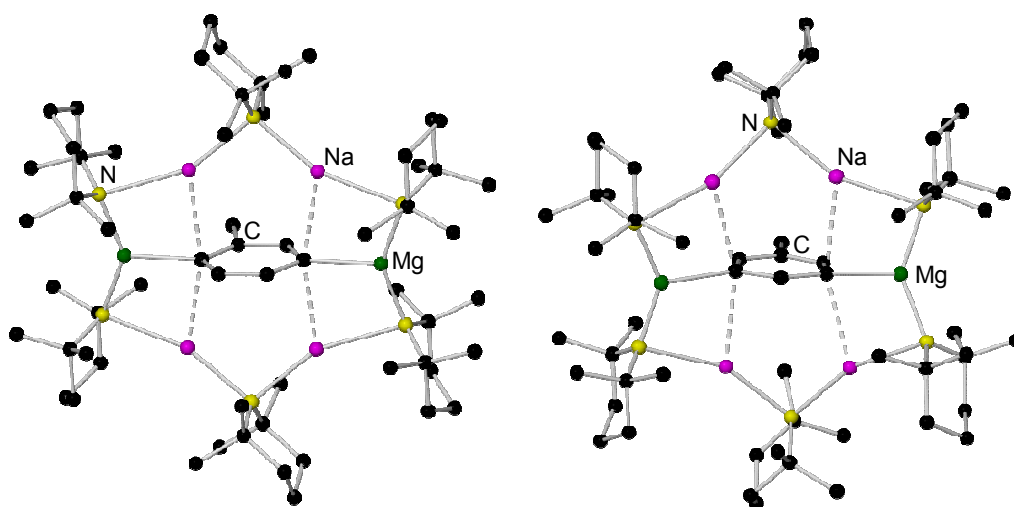


Figure 6.1: Molecular structures of the 2,5- (L.H.S) and 3,5-dideprotonated (R.H.S) toluene inverse crowns with selective atom labelling.

The heteroneopentyl ligand Me_3SiCH_2 was a key component in the sodium TMP-zincate that delivered and trapped the hypersensitive α -metallated THF fragment,^[7] while derived from the bis-alkyl starting material $\text{M}(\text{CH}_2\text{SiMe}_3)_2$ (where M is either Mg

or Mn) it has played an important role in the extension of AMMM to new metals and substrates.^[8] However, in terms of the mono-metallation regioselectivities afforded with this ligand when incorporated within bimetallic species there has been little variation from those exhibited with sodium zincate **1**. For this reason, we chose to template our new tailor-made metallating device around its bulkier, higher homologue $(\text{Me}_3\text{Si})_2\text{CH}$ in the hope that this structural modification would enhance our chances of regularly delivering direct remote metallations.

The molecular structure of the unsolvated homoleptic magnesium alkyl $[\text{Mg}\{\text{CH}(\text{SiMe}_3)_2\}_2]$ has been determined by X-ray and neutron diffraction studies (Figure 6.2).^[9] The crystalline dialkylmagnesium compound was obtained from the metathesis reaction of $\text{LiCH}(\text{SiMe}_3)_2$ and $[\text{Mg}(\text{OC}_6\text{H}_2t\text{Bu}_{2,6}\text{-Me}_4)_2]$ in hexane, and an ambient temperature X-ray crystallographic study revealed a polymeric array with a C-Mg-C primary skeleton and an unprecedented intermolecular interaction between the Mg atoms and a γ -methyl group of a neighbouring $[\text{Mg}\{\text{CH}(\text{SiMe}_3)_2\}_2]$ unit. Additionally, low temperature X-ray and neutron diffraction data were collected and the weak intermolecular interaction, attributed to an agostic $\text{Mg}\cdots\text{CH}_3$ interaction was examined. However, while the C-H bonds do not differ significantly in length from the average methyl C-H bond, the agostic interaction can be rationalised by a three-centre, two-electron bond involving the Si, C and Mg atoms with a pseudo five-coordinate trigonal bipyramidal geometry at the C resulting in a longer Si-C bond and a distortion towards sp^2 bonding for the CH_3 group with increased H-C-H angles and Si-C-H angles. $[\text{Mg}\{\text{CH}(\text{SiMe}_3)_2\}_2]$ and its reaction products with nitriles have been the subject of a couple of reports^[10] but its potential utility in metallation chemistry has remained unexplored.

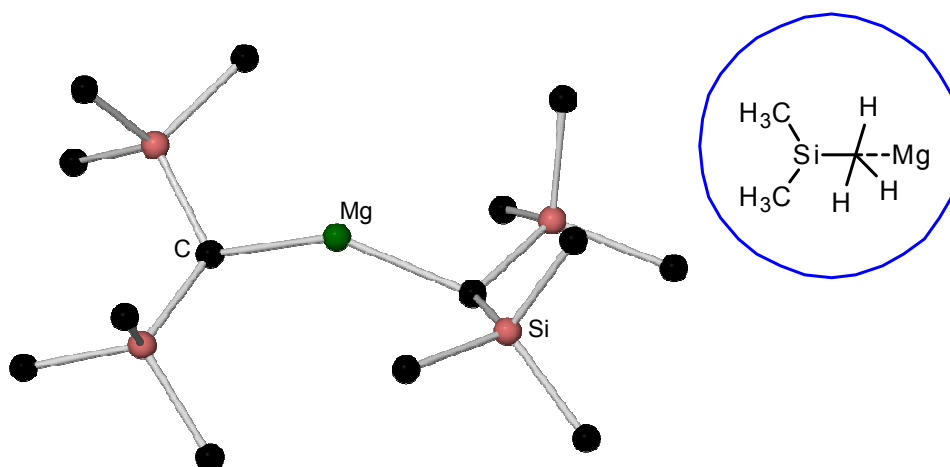


Figure 6.2: Monomeric section of the molecular structure of $[\text{Mg}\{\text{CH}(\text{SiMe}_3)_2\}_2]_\infty$ with selective atom labelling and inset, depiction of the weak, intermolecular interaction.

The monomeric monosolvated complex $[\text{Mg}\{\text{CH}(\text{SiMe}_3)_2\}_2(\text{OEt}_2)]$ is obtained upon dissolution of the parent compound in diethyl ether and its molecular structure (Figure 6.3) was obtained by Lappert as part of his investigations into the adducts formed between $[\text{Mg}\{\text{CH}(\text{SiMe}_3)_2\}_2]$ and nitriles,^[10b] but advantageously it can also be synthesised in bulk quantities as a stable white solid that can be stored in a dry box under an inert atmosphere making it an ideal starting material for our investigations.

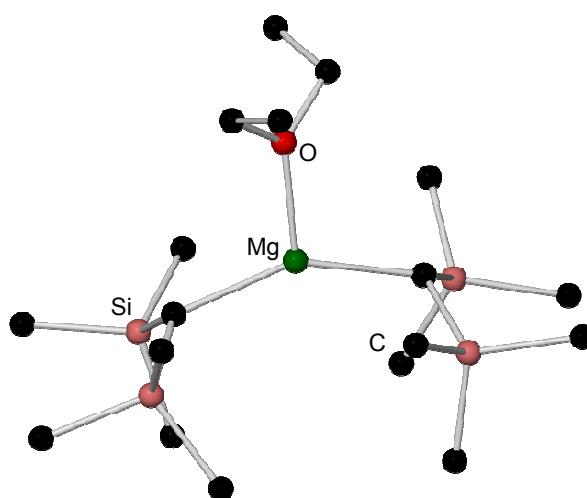
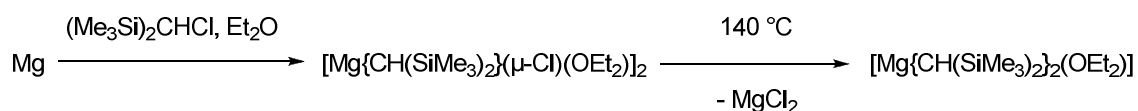


Figure 6.3: Molecular structure of $[\text{Mg}\{\text{CH}(\text{SiMe}_3)_2\}_2(\text{OEt}_2)]$ with selective atom labelling.

The ether solvate is prepared using the conventional Grignard reagent route, where a solution of $(\text{Me}_3\text{Si})_2\text{CHCl}$ in diethyl ether is added dropwise to a stirred suspension of magnesium turnings and the reaction mixture is refluxed for 2 hours (Scheme 6.1). The volatiles were then removed *in vacuo* and the white solid was purified by sublimation providing $[\text{Mg}\{\text{CH}(\text{SiMe}_3)_2\}_2(\text{OEt}_2)]$ in a yield of 82%.



Scheme 6.1: Synthesis of $[\text{Mg}\{\text{CH}(\text{SiMe}_3)_2\}_2(\text{OEt}_2)]$ via the conventional Grignard reagent route.

In the rational design of future syntheses, detailed knowledge of the intermediate chemistry taking place and information on the composition and structure of the active reagent will prove vital in ensuring maximum synthetic efficiency and the best reagent for the specific task is employed. Accumulating valuable information of this type is a key objective of this research project and in surveying the bi-silyl ligands potential future utility in mixed-metal deprotonative metallation, an important starting point was revealing the structural chemistry of any new bimetallic bases. Following the well-defined template for Alkali-Metal-Mediated Magnesiumation and the ensuing synergic element, solid ether-solvated $[\text{Mg}\{\text{CH}(\text{SiMe}_3)_2\}_2]$ was added to a hexane solution of LiTMP, both with and without an extra equivalent of TMP(H), before an equimolar quantity of TMEDA was introduced. Following gentle heating and the removal of solvent *in vacuo* after filtration, small needle crystals were deposited at ambient temperature. Surprisingly, X-ray crystallographic analysis revealed the known oxo-inverse crown ether complex $[\text{Li}_2\text{Mg}_2(\text{TMP})_4\text{O}]$ previously reported by the Mulvey group in 1998 (Figure 6.4).^[11]

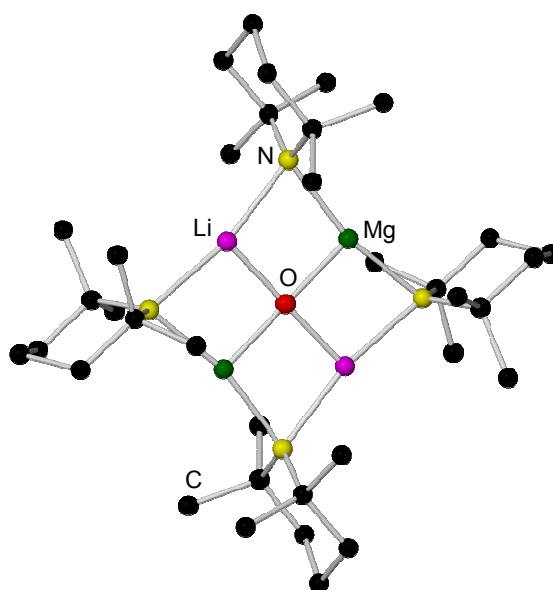
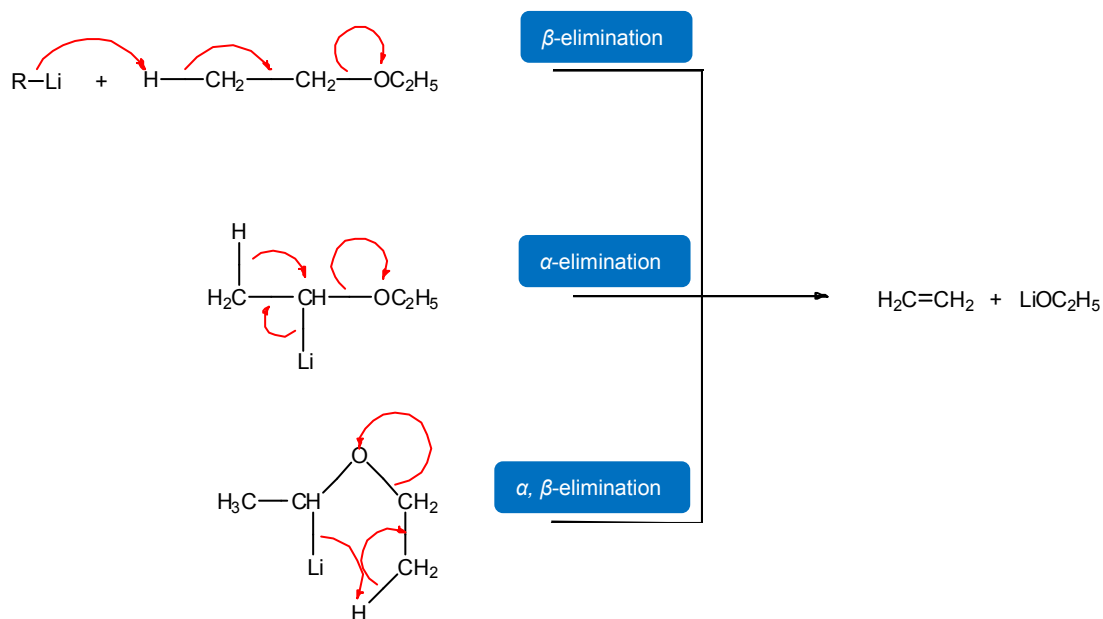


Figure 6.4: Molecular structure of the Li/Mg TMP oxo inverse crown ether.

Captured at the inversion centre of this inverse crown ether is a guest oxide (O^{2-}) ion that occupies a square planar site binding to all four metal atoms and the three coordinate geometry of both the Li and Mg atoms is completed by two amido N atoms, which bridge to the metal atoms to produce an eight-membered ring. Initial suspicion was cast on adventitious oxygen or moisture present in the reaction mixture affording the captured oxide, however, this complex was reproducibly provided several times by the above mentioned reaction mixture. Although, we cannot unequivocally rule out rogue oxygen or moisture, it appeared that an alternative oxidative or hydrolytic pathway could be responsible for the preparation of the previously reported magnesium inverse crown in this instance.

Organometallic reagents and ethers have often experienced a tumultuous relationship. In harmony, they are a perfect couple with polar ether solvents affording higher solubilities and faster kinetics in organometallic-mediated reactions than those witnessed in non-polar hydrocarbon solvents.^[12] However, hostile side-reactions that expel oxygen from ethers to produce a new metal-oxygen bonded compound have often

strained the rapport.^[13] The cleavage of ethers is commonly encountered in organometallic chemistry and the outcome of THF decomposition has been discussed elsewhere in this thesis. Furthermore, the cleavage of diethyl ether with organolithium compounds to ethylene and lithium ethoxide has been known for a long time.^[14] In the literature, three different mechanisms have been postulated (Scheme 6.2), and in an attempt to elucidate the cleavage mechanism Maercker prepared the α - and β -deuterated diethyl ethers.^[15] The two ether molecules were found to decompose by different mechanisms but in competition experiments both undeuterated and α -deuterated ethers were cleaved by β -elimination.



Scheme 6.2: Three proposed mechanisms for the decomposition of diethyl ether by organolithium reagents.

Perhaps, most pertinent to this study, sodium-magnesium or sodium-manganese bases have been found to promote cleavage of at least six bonds in THF and strikingly, the ring fragments are captured in distinct crystalline complexes.^[16] In an astounding illustration of “cleave and capture” chemistry the cleaved butyl chain was converted into a 1,4-dimetallated butadiene and entrapped in the signature manner of products of

the AMMM (Figure 6.5). Drawing parallels to the isolation of the lithium-magnesium TMP oxo-inverse crown in the $[\text{Mg}\{\text{CH}(\text{SiMe}_3)_2\}_2]$ system of this project, the oxygen atom of the decomposed THF was captured as an oxide fragment in an isostructural inverse crown $[\text{Na}_4\text{M}_2(\text{TMP})_4\text{O}]$ (where M is magnesium or manganese). These intriguing findings allude to a similar turn of events when the solvating ether molecule is liberated as $[\text{Mg}\{\text{CH}(\text{SiMe}_3)_2\}_2]$ is incorporated in the bimetallic motif. As a consequence could the resulting lithium-magnesiates promote cleavage of diethyl ether and capture of the oxide fragment in an inverse crown structure? For this reason, ether solvents were excluded and an alternative strategy was devised to investigate the proficiency of the bulky bi-silyl ligand in synergic systems.

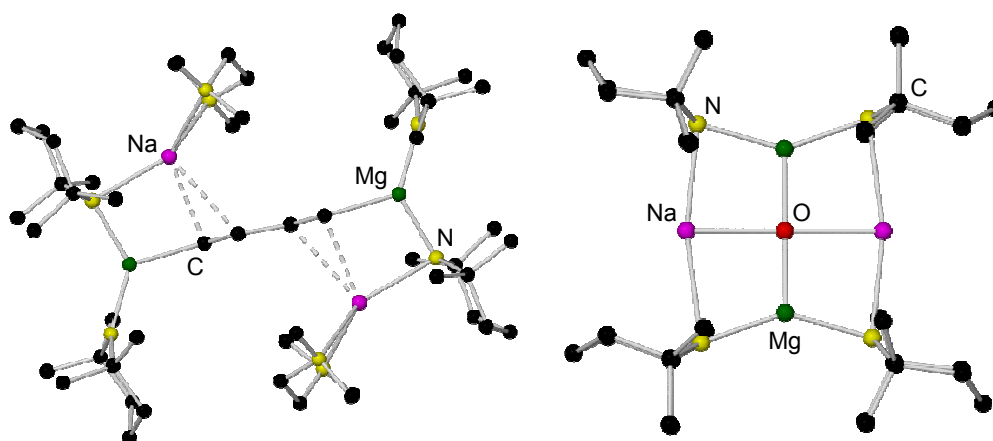


Figure 6.5: Molecular structures of the di-magnesiated butadiene (L.H.S) and oxo inverse crown ether (R.H.S) produced on bimetallic induced fragmentation of THF.

6.2) A Potential New Precursor to Heterobimetallic Complexes

In order to circumvent the perceived cleavage of the solvating ether solvent, a simple donor exchange was performed. The solid material of $[\text{Mg}\{\text{CH}(\text{SiMe}_3)_2\}_2(\text{OEt}_2)]$ was dissolved in hexane, giving a colourless solution and in light of its potential incorporation in any future bimetallic base, an equimolar quantity of the stronger donor

solvent TMEDA was introduced. Following a gentle heat to give a homogeneous solution, the mixture was stored in a freezer operating at $-28\text{ }^{\circ}\text{C}$ depositing colourless crystals in a yield of 56%. An X-ray crystallographic study revealed donor exchange had taken place as the product was the TMEDA-solvated complex $[\text{Mg}\{\text{CH}(\text{SiMe}_3)_2\}_2(\text{TMEDA})]$ (**21**).

The molecular structure of complex **21** is illustrated in Figure 6.6. The didentate TMEDA donor ligand results in Mg adopting a distorted tetrahedral (C_2N_2) geometry (mean angle around Mg is 108.9°) in comparison to the trigonal planar arrangement exhibited in the monodentate ether solvated complex $[\text{Mg}\{\text{CH}(\text{SiMe}_3)_2\}_2(\text{OEt}_2)]$ and this results in a reduced C(1)-Mg(1)-C(10) bond angle in **21** of 111.86° [compared to $148.45(10)^{\circ}$ in the diethyl ether solvated congener]. Turning to the bond distances, the greater steric demands involved at the four-coordinate Mg centre in **21** result in slightly elongated Mg-C_{sp3} bond distances of 2.2165(18) and 2.2071(17) Å for Mg(1)-C(1) and Mg(1)-C(10), respectively, in comparison to 2.141(2) Å in the two-fold symmetry molecule $[\text{Mg}\{\text{CH}(\text{SiMe}_3)_2\}_2(\text{OEt}_2)]$.

Successful isolation of TMEDA complex **21** and the lack of ethereal solvents encouraged us sufficiently enough to revisit our previous attempt to prepare a new lithium TMP-magnesiato reagent. On addition, of **21** via a solid addition tube to a solution of LiTMP containing an additional equivalent of TMP(H), a white precipitate instantly appears. Following isolation of this precipitate and removal of some solvent, the Schlenk tube was stored in a refrigerator (at $5\text{ }^{\circ}\text{C}$) producing a small crop of crystals. X-ray crystallographic analysis of these revealed the formation of $[\{(\text{TMEDA})_2\text{Li}\}^+\{\text{Mg}(\text{CH}(\text{SiMe}_3)_2)_3\}^-]$ (**22**), a new lithium magnesiato but with the absence of TMP not the kind we had ideally hoped to prepare.

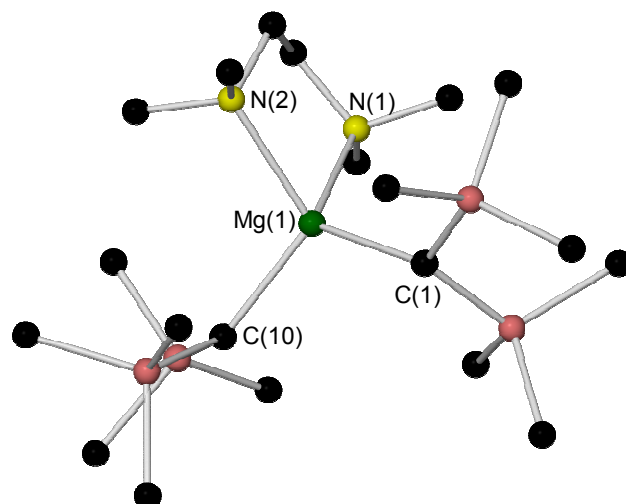


Figure 6.6: Molecular structure of **21** with selective atom labelling. Hydrogen atoms are omitted for clarity. Selected bond distances (Å) and angles (deg): Mg(1)-C(1) 2.2165(18), Mg(1)-C(10) 2.2071(17), Mg(1)-N(1) 2.3025(15), Mg(1)-N(2) 2.2874(16); C(1)-Mg(1)-C(10) 111.86(7), C(1)-Mg(1)-N(2) 117.63(6), C(10)-Mg(1)-N(2) 112.23(6), C(1)-Mg(1)-N(1) 112.98(6), C(10)-Mg(1)-N(1) 118.98(6), N(1)-Mg(1)-N(2) 79.91(6).

The structure of **22**, depicted in Figure 6.7, can be described as a solvent-separated ion-pair. The cationic moiety comprises of a distorted tetrahedral (N₄) lithium centre (mean angle of 110.03°) coordinated by two TMEDA molecules, whereas the anionic moiety consists of magnesium bonded to three of the bi-silyl ligands. The Mg-C bond distances are the same within experimental error to each other [Mg(1)-C(10) 2.183(2); Mg(1)-C(20) 2.186(2); Mg(1)-C(30) 2.183(2) Å, respectively] and are within the range found in Power's previously reported contact ion-pair [$\{\text{Li}(\text{THF})_{0.6}(\text{Et}_2\text{O})_{0.4}\}^+ \{\text{Mg}(2,4,6\text{-}i\text{PrC}_6\text{H}_2)_3\}^-$] where the three distances of the corresponding bonds are 2.147(4), 2.206(4) and 2.249(4) Å.^[17] In both complexes, reflecting the high sterics of the ligands, the Mg atoms adopt a distorted trigonal planar geometry, however, in **22** the angles at Mg do not deviate too far from the idealised trigonal values [C(10)-Mg(1)-C(20) 117.56(9); C(10)-Mg(1)-C(30) 120.63; C(20)-Mg(1)-C(30) 119.86(8)°, respectively],

while the Mg atom sits 0.1772(6) Å out of the C-C-C plane and in contrast to the parent unsolvated magnesium alkyl $[\text{Mg}\{\text{CH}(\text{SiMe}_3)_2\}_2]$, there are no intermolecular $\text{Mg}\cdots\text{CH}_3\text{Si}$ agostic type interactions in **22**.

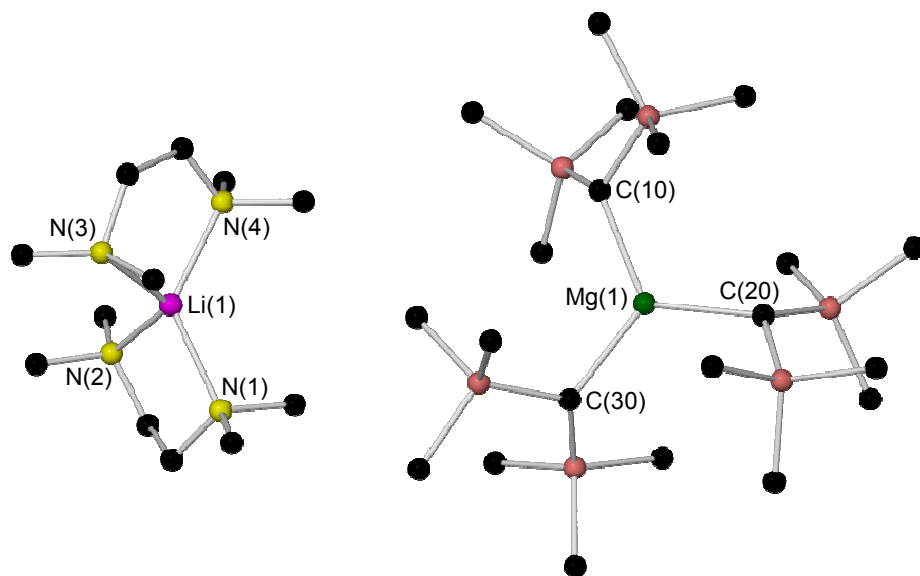


Figure 6.7: Solvent-separated ion-pair structure of **22** (cation L.H.S; anion R.H.S) with selective atom labelling. Hydrogen atoms and disordered component of TMEDA are omitted for clarity. Selected bond distances (Å) and angles (deg): Li(1)-N(1) 2.116(4), Li(1)-N(2) 2.104(4), Li(1)-N(3) 2.266(7), Li(1)-N(4) 2.079(8), Mg(1)-C(10) 2.183(2), Mg(1)-C(20) 2.186(2), Mg(1)-C(30) 2.183(2); N(1)-Li(1)-N(2) 87.58(16), N(1)-Li(1)-N(3) 119.5(2), N(1)-Li(1)-N(4) 128.2(2), N(2)-Li(1)-N(3) 116.6(2), N(2)-Li(1)-N(4) 121.0(4), N(3)-Li(1)-N(4) 87.3(3), C(10)-Mg(1)-C(20) 117.56(9), C(10)-Mg(1)-C(30) 120.63(8), C(20)-Mg(1)-C(30) 119.86(8).

Table 6.1 compares the ^1H and ^{13}C NMR chemical shifts for $[\text{Mg}\{\text{CH}(\text{SiMe}_3)_2\}_2(\text{OEt}_2)]$ and **21** in d_6 -benzene solution. The major difference between the two species is found in the ^{13}C NMR spectra and the resonance denoting the CH of the bi-silyl ligand. In the ether solvated complex the CH comes into resonance at 3.25 ppm, while as a consequence of the inductive effect, the presence of two donor atoms in **21** results in a higher electron density at the carbon causing resonance to occur at a relatively low

frequency (-0.12 ppm). Compound **22** possesses low solubility in d_6 -benzene solution, thus its ^1H and ^{13}C NMR spectra had to be recorded in the more polar solvent d_8 -THF. The solution structure of **22** in this solvent is different from that in the solid-state, as evidenced by the presence of free TMEDA in these spectra (Table 6.2). This indicates that in the presence of a strong donor solvent, such as THF, in a large excess the TMEDA ligands are replaced presumably furnishing $[\{\text{Li}(\text{THF})_x\}^+\{\text{Mg}(\text{CH}(\text{SiMe}_3)_2)_3\}^-]$. Under these ambient temperature conditions the three $\text{CH}(\text{SiMe}_3)_2$ ligands are equivalent giving rise to two singlets at -1.70 and 0.01 ppm; while in the absence of donor molecules bonding to the Mg, the bi-silyl ligand resonances appear more deshielded at 4.24 and 6.47 ppm in comparison to **21** and the related ether solvate, albeit the spectra are measured in different solvents. Searching the literature for magnesium complexes of either the mono- or bi-silyl ligands, there are very few NMR studies available for comparison with no spectra recorded in d_8 -THF solution.

Table 6.1: Comparison of ^1H NMR (400.13 MHz, 300 K) and ^{13}C NMR (100.62 MHz, 300 K) chemical shifts (δ in ppm) for $[\text{Mg}\{\text{CH}(\text{SiMe}_3)_2\}_2(\text{OEt}_2)]$ and **21 in d_6 -benzene solution.**

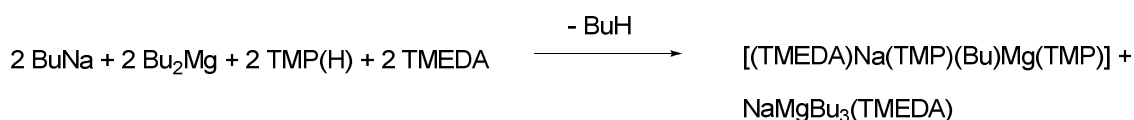
Compound	$\delta(\text{CH}(\text{SiMe}_3)_2)$	$\delta(\text{CH}(\text{SiMe}_3)_2)$	$\delta(\text{D}^*-\text{CH}_2)$	$\delta(\text{D}-\text{CH}_3)$
$[\text{Mg}\{\text{CH}(\text{SiMe}_3)_2\}_2(\text{OEt}_2)]$	-1.54	0.29	3.31	0.75
	3.6	5.5	65.2	13.9
21	-1.68	0.33	1.68	1.99
	-0.1	6.9	47.9	57.0

*Where D is donor

Table 6.2: ^1H NMR (400.13 MHz, 300 K) and ^{13}C NMR (100.62 MHz, 300 K) chemical shifts (δ in ppm) for **22 in d_8 -THF solution.**

	$\delta(\text{CH}(\text{SiMe}_3)_2)$	$\delta(\text{CH}(\text{SiMe}_3)_2)$	$\delta(\text{TMEDA-CH}_2)$	$\delta(\text{TMEDA-CH}_3)$
^1H	-1.70	0.01	2.30	2.15
^{13}C	4.2	6.5	46.0	58.8

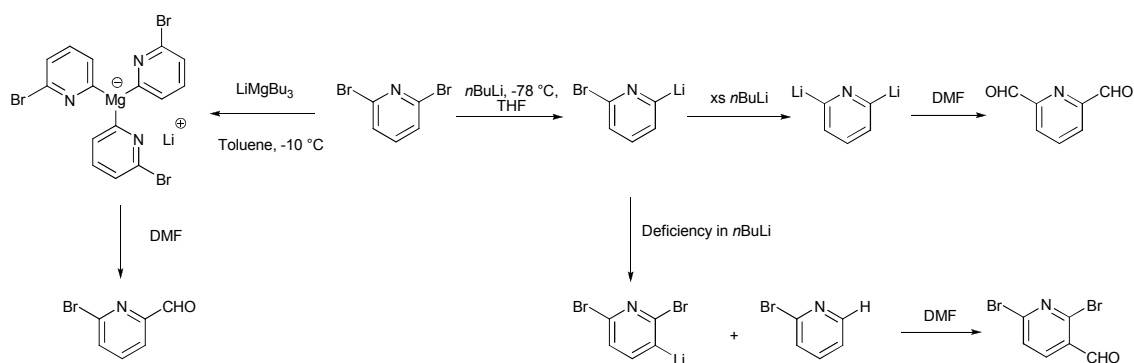
While the synthesis of **22** did not yield the mono-alkyl bis(amido) complex $[(\text{TMEDA})\text{Li}(\mu\text{-TMP})\{\mu\text{-CH}(\text{SiMe}_3)_2\}\text{Mg}(\text{TMP})]$ we desired, previous work within the Mulvey group gives reason for optimism.^[18] Investigating the synthesis of the related *n*-butyl sodium magnesiate the optimum yield was achieved using only one molar equivalent of TMP(H) meaning a maximum possible yield of 50%. NMR spectroscopic analysis of the oil left behind following isolation of the heteroleptic complex and removal of solvent indicates *n*-butyl and coordinated TMEDA resonances, thus the co-product was suspected to be the tris-alkyl $[\text{NaMg}(\text{Bu})_3(\text{TMEDA})]$ (Scheme 6.3). Unfortunately, due to time constraints further examination of the bi-silyl system has not been possible, however, with this precedent set further work should involve examining the reaction filtrates for heteroleptic magnesiate complexes in the AMMM template and the subsequent effect of stoichiometry on the potential products.



Scheme 6.3: Optimised synthesis of a mixed alkyl-amido synergic reagent, concomitantly producing the sodium tributylmagnesiate co-product.

However, complex **22** on its own is worthy of further examination. Previously, in Section 2.4, Mongin's employment of a sub-stoichiometric amount of Bu_3MgLi for the metallation of functionalised thiophenes^[19] was discussed and the methodology was

extended to fluoro-aromatics with the subsequent lithium aryl-magnesiates successfully trapped with electrophiles or involved in Pd-catalysed cross coupling reactions in one-pot procedures.^[20] Furthermore, Mase and Houpis at Banyu Pharmaceuticals have demonstrated the vast potential of lithium tri-alkyl magnesiates in synthesis.^[21] In their preparation of a novel M₃ antagonist being investigated for the treatment of chronic obstructive pulmonary diseases and urinary incontinence, a key step in the procedure is the formylation of 2,6-dibromopyridine. Lithium-bromide exchange of the pyridine can be effected with a molar equivalent of *n*BuLi in THF at -78 °C to give a mono-lithiated compound that when intercepted by DMF affords the product in excellent yield. However, cryogenic temperatures and more significantly when it came to scale up, pinpoint accuracy of the *n*BuLi charge were essential to achieve the desired outcome. For example, exposure of the mono-lithiated intermediate to excess *n*BuLi affords the di-lithiated derivative; while a deficiency in *n*BuLi results in the lithio-intermediate targeting another molecule of the pyridine starting material (Scheme 6.4). Desiring a more stable intermediate, the magnesium-bromine exchange reaction was investigated and it was found that the metal-halogen exchange of 2,6-dibromopyridine cleanly proceeded at -10 °C in toluene with 0.35 equivalents of LiMgBu₃. In addition to the ambient temperature, the exchange reaction is not sensitive to the reagent charge, proceeding well with various amounts of *n*BuMgCl and *n*BuLi illustrating a robust, scaleable procedure for the selective functionalisation of 2,6-dibromopyridine. Mase examined the applicability of the process and found LiMgBu₃ to be an efficient reagent for selective mono-formylation of dibromoarenes and dibromoheteroarenes via magnesium-bromine exchange^[22] and consequently, ensures with respect to our own work that future studies on the reactivity and applications of **22** should be carried out.



Scheme 6.4: Possible reaction pathways for 2,6-dibromopyridine upon treatment with *n*BuLi or the ate complex LiMgBu₃.

6.3) Experimental section

Synthesis of [Mg{CH(SiMe₃)₂}₂(OEt₂)]

A solution of (Me₃Si)₂CHCl (11 mL, 50 mmol) in diethyl ether (20 mL) was added dropwise to a stirred suspension of excess magnesium turnings (2.5 g, 102 mmol) in diethyl ether (100 mL). The reaction mixture was refluxed for 2 hours and then filtered. Volatiles were removed from the filtrate *in vacuo* to yield a crude solid which was then washed with diethyl ether (10 mL). Following removal of the solvent, the crude solid was sublimed at 140 °C in an oil bath. The collected white product was dried under vacuum for 2 hours and isolated in the dry box where it was stored for future reactions (typical yield: 8.57 g, 82 %). ¹H NMR (400.13 MHz, 300 K, *d*₆-benzene): δ 3.31 [br, 4H, CH₂ (Ethyl)], 0.75 [br, 6H, CH₃ (Ethyl)], 0.29 [s, 36H, CH₃ (SiMe₃)], -1.54 (s, 2H, CH). ¹³C {¹H} NMR (100.62 MHz, 300 K, *d*₆-benzene): δ 65.2 [CH₂ (Ethyl)], 13.9 [CH₃ (Ethyl)], 5.5 [CH₃ (SiMe₃)], 3.3 (CH).

Synthesis of [Mg{CH(SiMe₃)₂}₂(TMEDA)] 21

[Mg{CH(SiMe₃)₂}₂(OEt₂)] (0.34 g, 1 mmol) was dissolved in hexane (10 mL) and an equimolar quantity of TMEDA was added (0.15 mL, 1 mmol). The mixture was stirred for 2 hours and the cloudy white suspension was gently heated to obtain a transparent,

colourless solution. When cool, the Schlenk tube solution was transferred to the freezer (at -28 °C) where a white crystalline material was deposited overnight (0.26 g, 56%). ^1H NMR (400.13 MHz, 300 K, d_6 -benzene): δ 1.99 [s, 12H, NCH_3 (TMEDA)], 1.68 [s, 4H, NCH_2 (TMEDA)], 0.33 [s, 36H, CH_3 (SiMe_3)], -1.68 (s, 2H, CH). ^{13}C $\{^1\text{H}\}$ NMR (100.62 MHz, 300 K, d_6 -benzene): δ 57.0 [NCH_2 (TMEDA)], 47.9 [NCH_3 (TMEDA)], 6.9 [CH_3 (SiMe_3)], -0.1 (CH).

Crystal data for **21**: $\text{C}_{20}\text{H}_{54}\text{N}_2\text{MgSi}_4$, $M = 459.32$, monoclinic, $\text{P}2_1/\text{n}$, $a = 11.3379(18)$ Å, $b = 16.0499(14)$ Å, $c = 16.8076(14)$ Å, $\beta = 102.253(12)^\circ$, $V = 2988.8(6)$ Å³, $Z = 4$; 15140 reflections collected, 7568 were unique, $R_{\text{int}} = 0.0512$, $R = 0.0466$, $R_w = 0.1276$, $\text{GOF} = 1.073$, 268 refined parameters, max. and min. residual electron density = 0.559 and -0.351 $\text{e} \cdot \text{\AA}^{-3}$.

Synthesis of $\{[(\text{TMEDA})_2\text{Li}]^+ \{\text{Mg}(\text{CH}(\text{SiMe}_3)_2)_3\}^- \}$ **22**

Hexane (10 mL) was added to a Schlenk tube and $\text{TMP}(\text{H})$ (0.17 mL, 1 mmol) was then introduced. $n\text{BuLi}$ (0.63 mL of a 1.6 M solution in hexane, 1 mmol) was subsequently added dropwise and the pale yellow solution was allowed to stir for 1 hour. $[\text{Mg}\{\text{CH}(\text{SiMe}_3)_2\}_2(\text{TMEDA})]$ (0.46 g, 1 mmol) was then added via a solid addition tube and instantly the mixture turns cloudy, depositing a white precipitate. The solid was isolated by filtration and identified by NMR spectroscopy to be **22** [0.24 g, 37% (maximum possible yield 50% with respect to ratio of starting materials)]. The filtrate was concentrated by the removal of solvent *in vacuo* and stored in a refrigerator (at 5 °C). A very small amount of colourless crystals were deposited 72 hours later. ^1H NMR (400.13 MHz, 300 K, d_8 -THF): δ 2.30 [s, 8H, NCH_2 (TMEDA)], 2.15 [s, 24H, NCH_3 (TMEDA)], 0.01 [s, 54H, CH_3 (SiMe_3)], -1.70 (s, 3H, CH). ^{13}C $\{^1\text{H}\}$ NMR (100.62

MHz, 300 K, d_8 -THF): δ 58.8 [NCH₂ (TMEDA)], 46.0 [NCH₃ (TMEDA)], 6.5 [CH₃ (SiMe₃)], 4.2 (CH).

Crystal data for **22**: C₃₃H₈₉N₄LiMgSi₆, M = 741.87, triclinic, P-1, $a = 12.6044(15)$ Å, $b = 13.7396(14)$ Å, $c = 15.8696(14)$ Å, $\alpha = 105.095(8)^\circ$, $\beta = 104.161(9)^\circ$, $\gamma = 96.986(8)^\circ$, $V = 2521.9(5)$ Å³, $Z = 2$; 36310 reflections collected, 12151 were unique, $R_{\text{int}} = 0.0579$, $R = 0.0501$, $R_w = 0.1281$, GOF = 0.946, 433 refined parameters, max. and min. residual electron density = 0.736 and -0.436 e·Å⁻³.

Chapter 6 - References

- [1] D. R. Armstrong, W. Clegg, S. H. Dale, E. Hevia, L. M. Hogg, G. W. Honeyman, R. E. Mulvey, *Angew. Chem. Int. Ed.* **2006**, *45*, 3775 - 3778.
- [2] D. R. Armstrong, J. García-Álvarez, D. V. Graham, G. W. Honeyman, E. Hevia, A. R. Kennedy, R. E. Mulvey, *Chem. Eur. J.* **2009**, *15*, 3800 - 3807.
- [3] (a) C. Heiss, F. Leroux, M. Schlosser, *Eur. J. Org. Chem.* **2005**, 5242 - 5247; (b) C. Heiss, F. Cottet, M. Schlosser, *Eur. J. Org. Chem.* **2005**, 5236 - 5241.
- [4] R. E. Mulvey, *Organometallics* **2006**, *25*, 1060 - 1075.
- [5] R. E. Mulvey, *Chem. Commun.* **2001**, 308 - 310.
- [6] V. L. Blair, L. M. Carrella, W. Clegg, B. Conway, R. W. Harrington, L. M. Hogg, J. Klett, R. E. Mulvey, E. Rentschler, L. Russo, *Angew. Chem. Int. Ed.* **2008**, *47*, 6208 - 6211.
- [7] A. R. Kennedy, J. Klett, R. E. Mulvey, D. S. Wright, *Science* **2009**, *326*, 706 - 708.
- [8] (a) V. L. Blair, W. Clegg, B. Conway, E. Hevia, A. R. Kennedy, J. Klett, R. E. Mulvey, L. Russo, *Chem. Eur. J.* **2008**, *14*, 65 - 72; (b) V. L. Blair, L. M. Carrella, W. Clegg, J. Klett, R. E. Mulvey, E. Rentschler, L. Russo, *Chem. Eur. J.* **2009**, *15*, 856 - 863; (c) V. L. Blair, W. Clegg, R. E. Mulvey, L. Russo, *Inorg. Chem.* **2009**, *48*, 8863 - 8870; (d) V. L. Blair, A. R. Kennedy, R. E. Mulvey, C. T. O'Hara, *Chem. Eur. J.* **2010**, *16*, 8600 - 8604.
- [9] P. B. Hitchcock, J. A. K. Howard, M. F. Lappert, W. P. Leung, S. A. Mason, *J. Chem. Soc., Chem. Commun.* **1990**, 847 - 849.
- [10] (a) C. F. Caro, P. B. Hitchcock, M. F. Lappert, M. Layh, *Chem. Commun.* **1998**, 1297 - 1298; (b) A. G. Avent, C. F. Caro, P. B. Hitchcock, M. F. Lappert, Z. Li, X. H. Wei, *Dalton Trans.* **2004**, 1567 - 1577.
- [11] A. R. Kennedy, R. E. Mulvey, R. B. Rowlings, *Angew. Chem. Int. Ed.* **1998**, *37*, 3180 - 3183.
- [12] M. Schlosser, in *Organometallics in Synthesis - A Manual*, Wiley, **2002**.
- [13] H. C. Aspinall, M. R. Tillotson, *Inorg. Chem.* **1996**, *35*, 2163 - 2164.
- [14] K. Ziegler, H. G. Gellert, *Justus Liebigs Ann. Chem.* **1950**, *567*, 185 - 195.
- [15] A. Maercker, *Angew. Chem. Int. Ed.* **1987**, *26*, 972 - 989.
- [16] R. E. Mulvey, V. L. Blair, W. Clegg, A. R. Kennedy, J. Klett, L. Russo, *Nature Chem* **2010**, *2*, 588 - 591.

- [17] K. M. Waggoner, P. P. Power, *Organometallics* **1992**, *11*, 3209 - 3214.
- [18] E. Hevia, D. J. Gallagher, A. R. Kennedy, R. E. Mulvey, C. T. O'Hara, C. Talmard, *Chem. Commun.* **2004**, 2422 - 2423.
- [19] O. Bayh, H. Awad, F. Mongin, C. Hoarau, F. Trécourt, G. Quéguiner, F. Marsais, F. Blanco, A. Abarca, R. Ballesteros, *Tetrahedron* **2005**, *61*, 4779 - 4784.
- [20] H. Awad, F. Mongin, F. Trécourt, G. Quéguiner, F. Marsais, F. Blanco, A. Abarca, R. Ballesteros, *Tetrahedron Lett.* **2004**, *45*, 6697 - 6701.
- [21] T. Mase, I. N. Houpis, A. Akao, I. Dorziotis, K. Emerson, T. Hoang, T. Iida, T. Itoh, K. Kamei, S. Kato, Y. Kato, M. Kawasaki, F. Lang, J. Lee, J. Lynch, P. Maligres, A. Molina, T. Nemoto, S. Okada, R. Reamer, J. Z. Song, D. Tschäen, T. Wada, D. Zewge, R. P. Volante, P. J. Reider, K. Tomimoto, *J. Org. Chem.* **2001**, *66*, 6775 - 6786.
- [22] T. Iida, T. Wada, K. Tomimoto, T. Mase, *Tetrahedron Lett.* **2001**, *42*, 4841 - 4844.

Chapter 7: General Experimental Techniques

7.1) Schlenk Techniques

Given the air and moisture sensitivity of the organometallic reactants and products in this project, the use of a high-vacuum Schlenk line (Figure 7.1) and standard Schlenk techniques was common practice. All reactions were carried out under a protective blanket of argon on a standard vacuum/argon double manifold.



Figure 7.1: A typical Schlenk line in use.

A Schlenk line has two independent paths. The first is connected to a vacuum pump and the other provides dry, oxygen-free argon gas. Schlenk tubes are attached to the vacuum line via one of the five connections on the line, each of which has a two-way tap (coated with high vacuum grease), which can be adjusted to provide either vacuum or an argon supply. To evacuate air from the tubes we make use of the vacuum line and then reverse the tap to refill the tube with argon. It is standard practice to carry out this process three times to ensure the best possible inert atmosphere in the Schlenk tube before any reactions can be carried out. A solvent trap, which is placed in a Dewar flask of liquid nitrogen, is also present to ensure no volatile substances reach and therefore damage the

vacuum pump. To protect the argon line we also make use of an oil-filled release Dreschel flask which prevents the build up of pressure in the apparatus.

7.2) Use of a Dry Box with a Gas Recirculation and Purification System

An argon filled dry box fitted with Neoprene gloves was used to prevent decomposition during the manipulation of all solids, for example, in the determination of reactant weights or product yields and in the preparation of samples for NMR spectroscopic analysis. A typical glove box is shown Figure 7.2.



Figure 7.2: A typical research glove box.

The transfer of chemicals and required apparatus is carried out via the port on the right hand side of the box. Once such items are safely locked in the port, it is evacuated and refilled in the fashion described for the Schlenk line. The evacuation process was carried out twice, to minimise the possibility of water and oxygen leaking into the main body of the box on opening of the inner port door. Any moisture and oxygen entering the main body of the dry box is closely monitored by built in meters with the level

detected displayed on the control panel. Solid products that have been isolated can be taken into the box under vacuum. Providing all joints are well greased, the vacuum within the vessel will be maintained until it is inside the box where it can be opened to an argon atmosphere. Similarly, new reactants can be removed from the dry box by placing dry, clean and greased glassware into the port with the taps open and repeating the evacuation/argon flush procedure.

7.3) Solvent and Liquid Purification

The solvents and majority of reagents employed during this project were purchased from the Aldrich Chemical Company including *n*BuLi (1.6 M solution in hexane), *t*BuLi (1.7 M solution in pentane), ZnCl₂ (1 M solution in diethyl ether), Me₂Zn (1 M solution in heptanes) and *n*BuMgCl (2 M solution in THF). *t*BuONa and TMEDA were both purchased from Lancaster Chemicals and TMP(H) from Acros Organics.

All solvents were degassed and dried before use to minimise the oxygen and water content of the solvents. All solvents used in this investigation were distilled over nitrogen in the presence of sodium and benzophenone.^[1] Sodium reacts with benzophenone to produce a ketyl radical, which can be detected due to its intense blue colour. As it is highly reactive with both oxygen and water, the radical yields colourless or yellow products in their presence, thus, this provides a simple way of determining when the solvent is dry and oxygen free, that is when the solution remains blue. The dried solvent was then collected in an inert atmosphere in a round-bottomed flask which had been dried at 120 °C for several hours. An airtight Subaseal® was then used to seal the flask as this allows removal of solvent whilst preventing entry of oxygen. To remove solvent, a glass syringe and needle which were previously flushed three times with argon is used. The needle was pierced through the Subaseal® and a volume of

argon was injected into the flask to prevent a negative pressure on the removal of solvent thus preventing any contamination of the solvent.

NMR solvents were commonly de-gassed using the freeze-pump-thaw method,^[2] which involves freezing the solvent under argon using a Dewar flask of liquid nitrogen. When the solvent is frozen, a small vacuum is applied to remove the volatile gases that have been dissolved and the solvent is left to fully thaw under argon. In total, the freeze/thaw cycle is repeated three times.

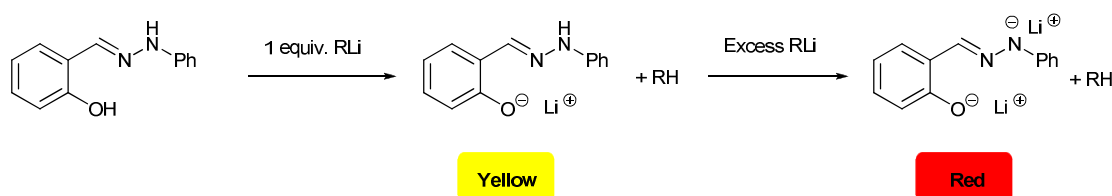
Some NMR solvents and reagents such as TMP(H) were dried using freshly oven-dried 4Å molecular sieves.

Several of the reactants in this report, particularly amines, are highly hygroscopic. Before their use, moisture contamination had to be removed from such liquids to prevent subsequent hydrolysis reactions in the organometallic solutions. This was done by distillation. A solid drying agent, typically calcium hydride, was added to the liquids before distillation for several hours. The dried liquid was then collected into an argon filled flask, which contained oven-dried 4Å molecular sieves as an extra precaution for longevity purposes and was quickly sealed with a Subaseal®.

7.4) Standardisation of Reagents

Alkyl lithium solutions decompose on reaction with air and moisture, decreasing the molarity of the bulk solution. Therefore, it is important that these reagents are standardised to establish the actual molarity and to ensure the correct stoichiometry is being applied when it comes to your reactions. Titration of the alkyl lithium with salicylaldehyde phenylhydrazone in dry THF is a convenient method for achieving this. The end point is denoted by the yellow solution turning red.^[3]

Salicylaldehyde phenylhydrazone is prepared by direct reaction of phenylhydrazine and salicylaldehyde in ethanol for 30 minutes at $-15\text{ }^{\circ}\text{C}$ and is stored in a desiccator as a powdery yellow solid. To standardise your alkyllithium reagent, salicylaldehyde phenylhydrazone (approximately 0.6 g) is weighed accurately into a Schlenk tube (X g) and dried under vacuum. This is then dissolved in dry THF (10 mL) and the solution is titrated against *t*BuLi or *n*BuLi until the yellow colour is replaced by a permanent red depicting the end-point (Y mL). The molarity of the alkyllithium solution can then be derived by the calculation outlined in Scheme 7.1.



The molarity of the solution can then be calculated:
 Moles of salicylaldehyde phenylhydrazone (Z) = (X) / 212.25

1 mole of indicator reacts with 1 mole of alkyllithium:
 Molarity of solution (mol l^{-1}) = (Z) / (Y) \times 1000

Scheme 7.1: Standardisation procedure for alkyllithium reagents and the calculation to determine their molarity.

7.5) Preparation of Common Starting Materials

The metal alkyls *n*BuNa and *t*Bu₂Zn were used frequently throughout this project. Their preparations which were repeated numerous times will be detailed in this section.

Synthesis of *n*BuNa^[4]

*t*BuONa (1.92 g, 20 mmol) was suspended in dry hexane (50 mL). Then at $0\text{ }^{\circ}\text{C}$, *n*BuLi (12.5 mL of 1.6 M hexane solution, 20 mmol) was added dropwise and the contents of the Schlenk tube were allowed to stir overnight, resulting in precipitation of a white

pyrophoric solid. The solid was collected by filtration and washed three times with 20 mL of dry hexane (Typical yield: 1.2 g, 75%).

Synthesis of $t\text{Bu}_2\text{Zn}$ ^[5]

A mixture of dry diethyl ether (10 mL) and ZnCl_2 (20 mL of 1 M diethyl ether solution, 20 mmol), was treated with $t\text{BuLi}$ (24 mL of 1.7 M pentane solution, 40 mmol) at 0 °C. The Schlenk tube was then surrounded in a black plastic bag to block out light, and its contents were stirred for 3 hours. The deposited LiCl was then removed by Schlenk filtration through Celite and glass wool. The resulting, clear solution was then transferred to the sublimation apparatus via cannula and the solvent was removed under vacuum. When all solvent had been removed, the cold finger was filled with an isopropanol/liquid nitrogen mixture. The $t\text{Bu}_2\text{Zn}$ was then allowed to sublime on the finger for approximately one hour. The coolant was then removed and the sublimation apparatus was transferred to the glove box, where the $t\text{Bu}_2\text{Zn}$ was collected from the cold finger (a white crystalline solid in consistent yields of around 70%) and weighed into a Schlenk tube.

7.6) Analytical Procedures

^1H NMR spectroscopic experiments were performed on a Bruker DPX400 spectrometer with an operating frequency of 400.13 MHz. The ^{13}C NMR spectra were recorded on the same instrument at an operating frequency of 100.62 MHz. All chemical shifts are quoted relative to TMS standard at 0.00 ppm.

The NMR abbreviations are as follows: s (singlet); d (doublet); t (triplet); q (quartet); m (multiplet) and br (broad peak). For brevity and simplicity, aromatic resonances have

been classed as d or t, when strictly they may be dd or td. The coupling constants for such peaks have been omitted due to overlap rendering precise calculation difficult.

IR spectra were recorded on a Perkin-Elmer Spectrum 100 FT-IR spectrometer and elemental analyses were carried out on a Perkin-Elmer 2400 elemental analyser. Due to the extreme air and moisture sensitivity of the compounds prepared during this project and their difficulty in burning properly (for example, formation of metal nitrides/carbides), ideal analyses were often not obtained.

Melting/decomposition points were measured on a Büchi melting point B-545 apparatus and GC-MS analysis was performed on an Agilent 7890A apparatus, GC with 5975C triple axes detector, run under CI mode (methane).

The X-ray structural data was collected at 123(2) K on an Oxford Diffraction Gemini S Diffractometer with Mo-K α radiation ($\lambda = 0.711073 \text{ \AA}$).^[6] Structures were solved using SHELXS-97, while refinements were carried out on F^2 against all independent reflections by the full-matrix least-squares method using SHELX-97 program.^[7]

Crystallographic data can be found on the disk inserted at the back of this thesis.

Chapter 7 - References

- [1] D. F. Shriver, M. A. Drezdzon, in *The Manipulation of Air-Sensitive Compounds*, 2nd ed., Wiley and Sons, New York, **1986**, pp. 88 - 89.
- [2] D. F. Shriver, M. A. Drezdzon, in *The Manipulation of Air-Sensitive Compounds*, 2nd ed., Wiley and Sons, New York, **1986**, p. 104.
- [3] B. E. Love, E. G. Jones, *J. Org. Chem.* **1999**, *64*, 3755 - 3756.
- [4] C. Schade, W. Bauer, P. v. R. Schleyer, *J. Organomet. Chem.* **1985**, *295*, c25 - c28.
- [5] P. C. Andrikopoulos, D. R. Armstrong, H. R. L. Barley, W. Clegg, S. H. Dale, E. Hevia, G. W. Honeyman, A. R. Kennedy, R. E. Mulvey, *J. Am. Chem. Soc.* **2005**, *127*, 6184 - 6185.
- [6] CrysAlisPro, Program for Integration and Absorption Correction, Oxford Diffraction Ltd., Abingdon (UK), **2008**.
- [7] (a) G. M. Sheldrick, *Acta Crystallogr. Sect. A* **2008**, *64*, 112 - 122; (b) G. M. Sheldrick, SHELXL93, *Program for the Refinement of Crystal Structures*, University of Göttingen, Göttingen (Germany), **1993**.

Chapter 8: Conclusions and Future Work

8.1) Conclusions

This investigation set out to explore and ideally extend the remarkable synergic chemistry that can be generated when pairing a high polarity group 1 metal (Li, Na, K) amide with a subordinate low polarity metal reagent (commonly Mg or Zn alkyls). Focusing on zinc-hydrogen exchange processes, reactions of the sodium TMP-zincate [(TMEDA)Na(μ -TMP)(μ -*t*Bu)Zn(*t*Bu)] (**1**) towards a series of organic substrates were investigated. Through structurally mapping these reactions (by isolation of “reactive intermediates”) and subsequent electrophilic quenches, these studies have made important contributions in establishing this reagent as an excellent chemo- and regioselective metallating agent, while offering complementary insight into the selectivity and mechanism of the bimetallic base underlining how the cooperative action of the bi-metal partnership promotes special reactions beyond the scope of traditional homometallic reagents.

A new concept within Directed-*ortho*-Metallation (*DoM*) chemistry has been developed during the course of this PhD. Conventionally, zinc reagents fail in *DoM* chemistry as a consequence of their weak basicity. However, upon treatment with the synergic sodium-zinc base **1**, three electron-rich aromatic substrates, *N*, *N*-diethyl benzamide, *N*, *N*-diethyl-3-methoxybenzamide and *N*, *N*-diethyl phenyl *O*-carbamate were cleanly zincated *ortho* to the directing substituent under ambient temperatures with no suggestion of complications in the form of the side reactions noted for the analogous organolithium-mediated deprotonations that necessitate the utilisation of expensive and energy-inefficient, subambient temperatures. Whilst, breaking with convention, reaction with benzyl methyl ether surprisingly produced an *ortho*-zincated intermediate instead

of the expected “thermodynamic” α -metallated product and this true synergic reaction that to the best of our knowledge cannot be replicated by any monometallic reagent potentially opens the door to the classic DoM reaction for a whole new class of previously discarded alkyl ether aromatic substrates.

Coupled to its supreme deprotonative ability, the synergic zincate base also exhibits a unique ability to deliver unexpected and exquisite structures more within the remit of a supramolecular chemist. Through metallation of *N,N*-diethyl thiophene-2-carboxamide in hydrocarbon solution, a novel tetrameric architecture was revealed. Sodium zincate **1** was found to display ambibasic behaviour with both the bridging TMP and *t*Bu ligands extracting two protons from each substituted thiophene molecule to fashion an “anti-crown” metallacycle consisting of four-deprotonated thiophene subunits linked by the carbanionic carbon atoms to four zinc atoms in a cyclic tetramer. The core metallacycle which displays an overall bowl appearance is a very rare example of a 16-MC-4 zinc metallacrown and to the best of our knowledge represents the first example of a complex of this size where all the organic constituents are carbon atoms for any metal. This reaction also provides a nice, illustrative example of solvent effects and their influence on structure and reactivity for when the reaction is performed in bulk, polar THF solution the solvent-separated ion-pair nature of the bimetallic base prevents any communication between the two metals and only mono-deprotonation of the thiophene derivative transpires.

Additionally, synergic base **1** and a magnesium derivative [(TMEDA)Na(μ -TMP)(μ -*n*Bu)Mg(TMP)] unpredictably provided access to a series of zwitterionic benzannulated zinc or magnesium metallacycles through reaction with chlorobenzene via a cascade sequence of four separate reactions. Sodium mediates the direct *ortho*-zincation or magnesiation of chlorobenzene and following “ate” elimination, delivers the TMEDA

ligand to nucleophilically attack the benzyne, thereby generating novel open and cyclic zwitterions. Although, not incorporated in the final isolated products the alkali-metal must be present in the mixture, and thus again it is the cooperativity between the different components that appears to be behind the construction of these novel metallacycles and hence these reactions are interpreted as further but uniquely different examples of synergic synthesis.

The distinct, special chemistry of these bimetallic reagents was driven home by a simple case study. Thus the AMMZn of *N,N*-dimethylaniline was shown to afford a mixture of *ortho*-, *meta*- and *para*-regioisomers in solution, however, the predominant *meta*-substituted derivative – a regioselectivity normally closed to synthetic aromatic chemistry – could be isolated in reasonable yields in a clean, pure crystalline form. The synergic facet of the AMMZn was illustrated by some control reactions with *N,N*-dimethylaniline where the two monometallic reagents were added sequentially. Conventional sodiation of the *N,N*-dialkylaniline substrate promotes *ortho*-deprotonation in keeping with the well established principles of DoM chemistry; and this regioselectivity is retained following subsequent co-complexation with the dialkyl zinc reagent and the introduction of the final component of bimetallic base **1**, TMP(H). Upon utilising this indirect, sequential approach the elusive *meta*-zincated product is only generated in trivial quantities under harsh reflux conditions and its formation can be traced to a retro-reaction that produces sodium TMP-zincate **1** in solution. The secret to unlocking special synergic reactivity may therefore be found in coupling both metals in the same, well-defined bimetallic reagent for only when that synergic TMP bridge is present to facilitate the metal...metal' cooperativity does the unique *meta*-regioselectivity materialise.

Accompanying, these many examples of its Brønsted basicity, when the synergic reagent was employed with the stable nitroxyl radical TEMPO, a single electron transfer (SET) reaction produced a new heterotri-anionic zincate containing an anionic TEMPO bridge. This result ascertains that **1** can also act as a SET agent, supporting the hypothesis that SET could be at play in the extended Mulvey groups previously reported 1,6-addition reactions with benzophenone, fluorenone and 2-benzoylpyridine. In an extension of this reaction, TEMPO was also treated with dialkyl zinc reagents and a group 1 metal in elemental form resulting in a single electron reduction of this important radical to the TEMPO⁻ anion. Preparation of the Na⁺TEMPO⁻ salt and its crystallisation from hexane/TMEDA produced a four-runged ladder structure which represents one of the first examples of elemental-metal reduction of the TEMPO radical.

The final topic of this investigation looked at the extension of AMMM to bulkier, more experimentally challenging ligands, namely the bi-silyl group in the form of [Mg{CH(SiMe₃)₂}₂]₂. Although, this study is yet to harvest the finely tuned reagent we desire for synthetically useful, remote metallations further research may bring it to pass; or alternatively, based on precedent in the literature the isolated lithium tri-alkyl magnesiate product may itself prove be a valuable reagent upon further examination.

Evaluating the PhD investigation as a whole, it is evident that synergic chemistry not only assembles interesting and exciting structures but that it represents a valuable addition to the arsenal of any synthetic chemist. These compounds can perform unprecedented zincations, on occasion offering new regioselectivities previously thought to be unobtainable, on aromatic substrates that are generally inert towards conventional zinc reagents at ambient temperatures and in the presence of sensitive

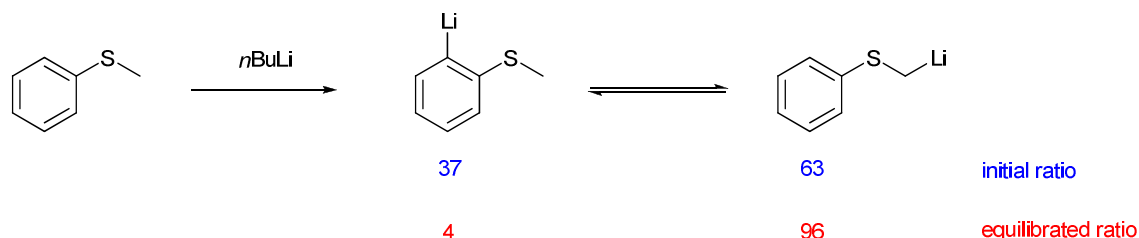
functional groups, thus illustrating that the metallation reaction is no longer the domain of a few, select high polarity metals.

8.2) Future Work

The underlying theme running throughout this PhD project has been the metallation reaction. In this project a variety of elegant and diverse structures have been successfully prepared and characterised as a precursor to, or as the outcome of, a metallation reaction. Potential applications of a few of these complexes will be discussed shortly but first of all the question must be asked, “where next for the synergic bases and their accord with the metallation reaction?”

In order to find popular acceptance it is conceivable that two criteria hold the key. Complementing the DoM of the benzamide and phenyl *O*-carbamate substrates was the *ortho*-metallation of benzyl methyl ether, a completely new metallation regioselectivity for this molecule using highly favourable reaction conditions. If sodium-mediated zincation can be further utilised to achieve previously unobtainable metallation regioselectivities, its stock may soar. To this end, the reaction of sodium TMP-zincate **1** should be pursued with a range of primary and secondary alkyl ethers which have thus far shown little or no promise in the DoM reaction and additionally the nitrogen equivalent, *N,N*-dimethylbenzylamine should be screened for even though dimethylaminomethyl groups reliably direct *ortho*-lithiation with *n*BuLi,^[1] following the unique *meta*-deprotonation of *N,N*-dimethylaniline by **1** a more remote metallation cannot be ruled out. Finally, sulfides are weak DMGs with the lithiation of thioanisole presenting a mixture of α - and *ortho*-lithiated compounds.^[2] It is found that around one third of the kinetic mixture is the *ortho*-lithiated compound before slow isomerisation to the α -lithiated sulfide follows (Scheme 8.1). Reactions of this type with zincate **1** may

also be worth considering, for *ortho*-deprotonation and consequential manifestation of the *ortho*-metallated sulfide in the bimetallic contact ion-pair motif typical of AMMZn products may prevent the ensuing equilibration and provide a smooth route to *ortho*-substituted thioanisole molecules.



Scheme 8.1: Lithiation of thioanisole with *n*BuLi leading to a mixture of α - and *ortho*-lithiated products.

The biggest challenge, however, is transforming these stoichiometric metallations into catalytic processes or at least beginning to introduce a degree of atom economy. Although unintended, the synthesis of the tri-alkyl magnesiate [$\{(\text{TMEDA})_2\text{Li}\}^+\{\text{Mg}(\text{CH}(\text{SiMe}_3)_2)_3\}^-$] (**22**) may allow that following the work of Mongin^[3] and Mase^[4] with LiMgBu_3 in metal-hydrogen (M-H) and metal-halogen (M-X) exchange reactions, respectively, and therefore **22** should be the subject of a few preliminary M-H and M-X exchange reactions. However, perhaps the salient detail here draws upon the classical relationship between structure and reactivity. For should these tri-alkyl magnesiates retain solvent separated ion-pair structures in solution it becomes far more likely that each of the active/basic alkyl arms are equivalent; within heteroleptic sodium TMP-zincate **1** and its contact ion-pair motif this is not the case. DFT calculations modelling the reaction of **1** and a number of individual organic substrates indicate that there is very little chance of the terminal *t*Bu group ever engaging in a deprotonation and this has been borne out by the structural experimental studies where it is consistently found to retain its terminal position attached strongly to

zinc. So the question to address is, “is the key to obtaining atom efficient deprotonations to be found in changing the structure of **1**?” Well as discussed earlier, the di-metallation of benzene provides an interesting case, for di-deprotonation of the arene was found only to be possible when TMEDA was initially excluded from the reaction mixture and introduced at a later stage, as it was found to exert a deactivating effect on the ability of **1** to di-deprotonate benzene to any significant extent.^[5] Although, this is likely to produce a polymeric base unit, some of the active arms may not be at such a positional disadvantage thus out of curiosity a few reactions of this mixture – minus the TMEDA – should be performed with some of the substrates utilised in this PhD programme and the results compared.

In the context of the tetrameric di-zincated thiophene complex **6** (Figure 8.1) introduced in Section 2.4, the quenching conditions require further consideration. The metallated intermediates themselves can be considered bases and deprotonation of the THF solvent introduced with the iodine is believed to be responsible for the modest yield of the di-iodinated thiophene noted. On that basis, further experiments should be performed with different electrophiles that do not depend upon prior dissolution in THF. Simple and of potential value may be D₂O with the availability of ²D NMR spectroscopy providing an additional tool to establish the yield and efficiency of the di-metallation but overall, particularly attractive and stimulating is the complexity of the structure.

Since Pecoraro and Lah reported the first metallacrown structure in 1989,^[6] the number of metallacrowns has soared with over 600 reports of metallacrown research detailing rings ranging from 8-MC-4 to 60-MC-20.^[7] Metallacrowns have been used for a variety of functions, notably as single-molecule magnets,^[8] while some metallacrowns exhibit antibacterial activity.^[9] Following the synthesis of crown ethers and the discovery of their complexing properties towards alkali-metal cations,^[10] host-guest chemistry has

advanced rapidly taking in areas such as supramolecular chemistry and materials science. Intermolecular interactions between host and guest molecules play a central role not only in self-assembling supramolecular arrays but also in biological chemistry with metallocrown container molecules composed from the 15-MC-5 structure type selectively encapsulating carboxylate anions in hydrophobic cavities.^[11] Encouragement for taking **6** in this direction is provided by the work of Hawthorne who showed a class of macrocyclic mercuracarborands are excellent Lewis acid hosts that efficiently bind anions and nucleophilic species.^[12] Particularly promising is the 12-MC-4 complex that binds a chloride anion (Figure 8.1) possesses a smaller cavity than found in **6** and like **6**, the metallacyclic core does not contain any heteroatoms [it is made up exclusively of four Hg-C-C repeating units]. Therefore, in addition to functionalising the thiophene rings via electrophilic quenching, applications of **6** to supramolecular chemistry and molecular recognition could prove exciting and well worth conducting examining different guest molecules.

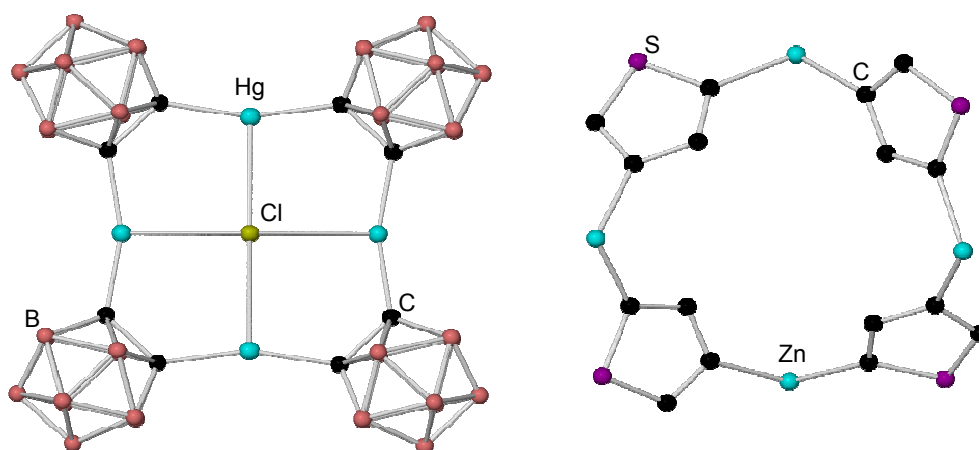


Figure 8.1: Anionic moiety of a host-guest complex comprising of carborane-supported mercury metallacycles (L.H.S) and the core of **6 (R.H.S) with selective atom labelling.**

The synthesis of the benzannulated zwitterionic complexes **12**, **14** and **15** (Figure 8.2) could be the area that is particularly pregnant with future potential. At the end of

Chapter 4, it was briefly discussed that subsequent studies geared towards creating a small library of these complexes could be undertaken, introducing appendage and scaffold diversity, starting from a number of halo-aromatics or alternatively, moving away from our traditional chelating donors and investigating DMF and other carbonyl compounds currently finding utility in multicomponent reactions.^[13] Imaginable side reactions with such molecules and your bimetallic bases may be sidestepped by *in situ* generation of benzyne via *ortho*-metallation with an alkyllithium reagent or the carbon-silicon cleavage route that has become the mainstay technique for aryne generation,^[14] followed by addition of your metal reagent (*i.e.*, $t\text{Bu}_2\text{Zn}$) and the neutral nucleophile.

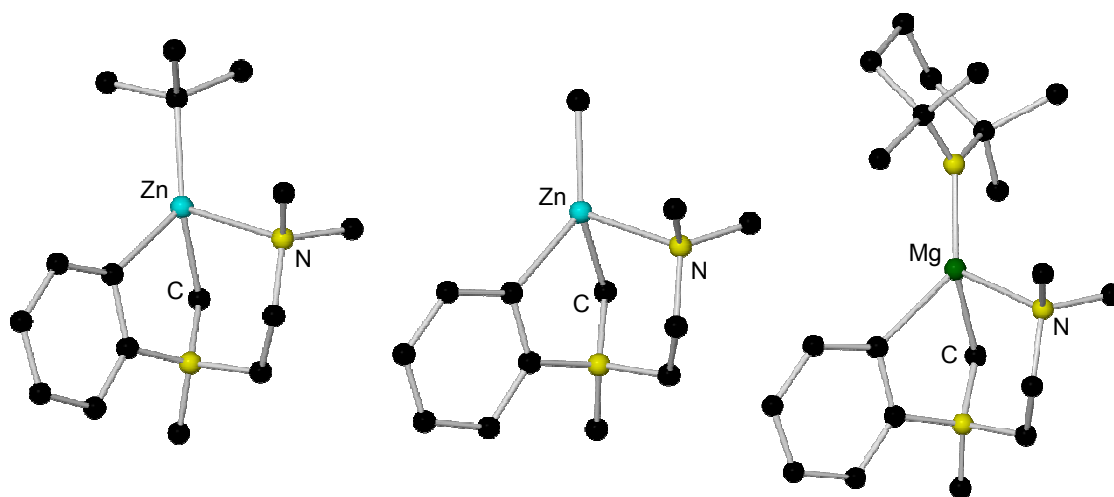
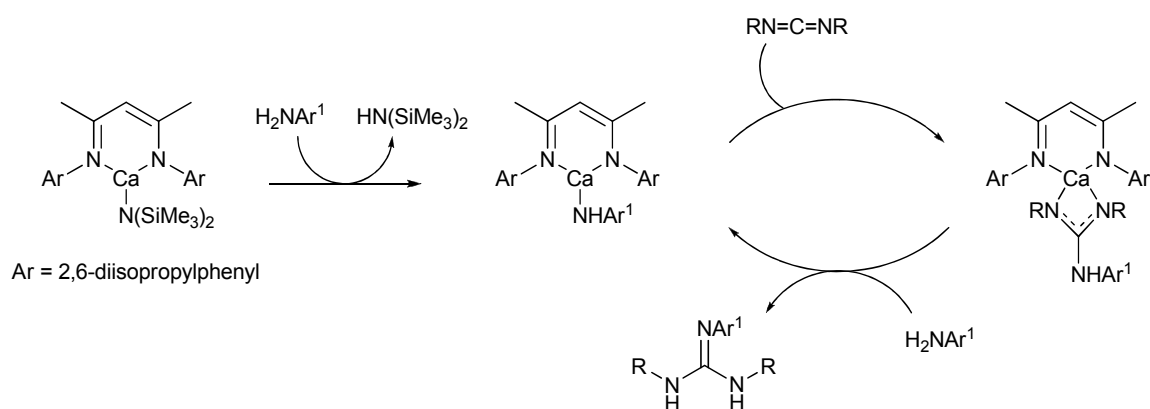


Figure 8.2: Molecular structures of 12, 14 and 15 with selective atom labelling.

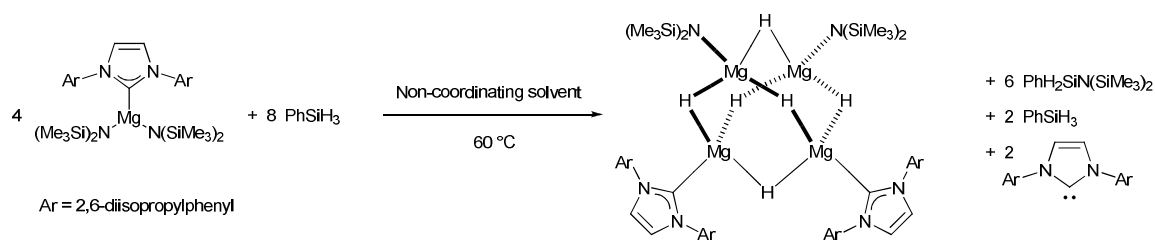
However, exploration of the reaction chemistry of the isolated metallacyclic complexes may bear greater reward. Focusing primarily on the Mg zwitterionic complex **15** for now, the insertion of unsaturated organic molecules into the metal-N bond of amido complexes is finding wide applicability in numerous catalytic processes.^[15] Foremost are the reactions of isocyanates and carbodiimides as they provide convenient routes for the preparation of the highly significant ureas and the key pharmacophore guanidines,^[16] respectively. In the context of group 2 chemistry, Hill and Barrett have revealed that inexpensive and easily prepared β -diketiminato heavy alkaline earth

amides are highly competent pre-catalysts for the catalytic hydroamination of both isocyanates^[17] and carbodiimides (Scheme 8.2).^[18]



Scheme 8.2: Proposed catalytic cycle for the hydroamination of carbodiimides using a calcium amide pre-catalyst.

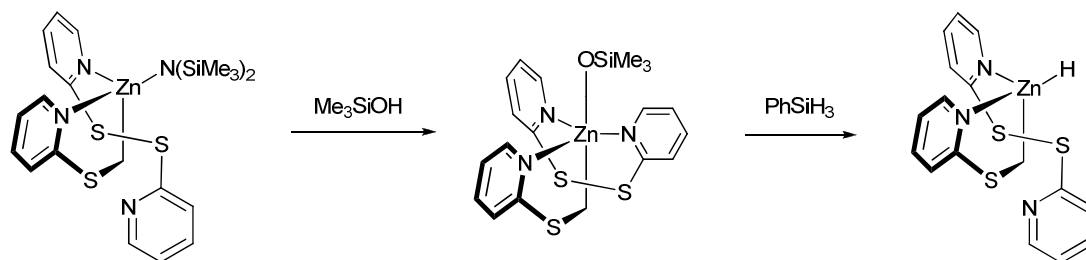
While it may be worth briefly surveying **15** in terms of catalytic hydroamination, this reaction is commonly the domain of the aforesaid heavier alkaline earth metals and the lanthanides.^[19] One area where magnesium is attracting increasing interest is hydrogen storage, in the guise of magnesium hydride clusters. Strict limitations in respect of weight and volume for mobile applications have seen solid and light-weight main group hydrides become a topic of interest in hydrogen storage.^[20] Hill has reported that treatment of the carbene adduct $[\text{Mg}\{\text{N}(\text{SiMe}_3)_2\}_2(\text{IPr})]$ [where IPr is 1,3-bis(2,6-diisopropyl-phenyl)imidazol-2-ylidene] with two molar equivalents of PhSiH_3 affords the magnesium hydride cluster $[\text{Mg}_4\text{H}_6(\text{IPr})_2\{\text{N}(\text{SiMe}_3)_2\}_2]$ (Scheme 8.3).^[21] Significantly, in relation to our benzannulated species and its bulky backbone it was found that the sterically encompassing carbene ligand was crucial to maintaining the homogeneity of the solution and therefore the creation of the remarkably specific hydride species.



Scheme 8.3: Synthesis of a hydride-rich magnesium cluster from PhSiH_3 and an $\text{Mg}(\text{HMDS})_2$ -carbene adduct.

In 2011, Harder and co-workers reported the largest known magnesium hydride cluster $[(\text{para})_3\text{Mg}_3\text{H}_{10}]$ to date where para is the bridged bis(β -diketiminate) ligand 4-(2,6-diisopropylphenylamino)pent-3-en-2-ylidene-benzene-1,4-diamine.^[22] Although, these bulky ligands utilised for stabilisation of the complex render these systems impractical for hydrogen storage, this cluster releases its H_2 completely at 200 °C providing an excellent model for future systems. Later in the same year, Parkin discussed the synthesis, structure and reactivity of a mononuclear organozinc hydride complex.^[23] A multidentate alkyl ligand derived from tris(2-pyridylthio)methane $[(\text{Tptm})\text{H}]$ grants isolation of a rare, well-defined zinc complex featuring a terminal hydride which is prepared from the HMDS derivative via the siloxide following treatment with a silanol (Scheme 8.4). The structural similarity of these compounds to the zwitterions prepared during the course of this PhD project and Hill's aforementioned studies might signal a potential application for these novel species. The reaction of both the Mg and Zn metallacycles prepared should be pursued with PhSiH_3 in search of new metal hydride complexes, if necessary going through the alkoxide route employed by Parkin for even if hydride formation does not transpire, zinc and magnesium alkoxides are active catalysts for the ring-opening polymerisation of cyclic esters^[24] presenting an another attractive potential use for these compounds. Finally, given it is the amide employed by both Hill and Parkin it might prove beneficial to attempt the synthesis of a

benzannulated metallacycle that harbours a terminal HMDS ligand if further functionalisation proves problematic.



Scheme 8.4: Parkin's synthesis of a mononuclear organozinc hydride via displacement of a siloxide ligand.

Chapter 8 - References

- [1] (a) F. N. Jones, M. F. Zinn, C. R. Hauser, *J. Org. Chem.* **1963**, *28*, 663 - 665; (b) G. W. Klumpp, *Rec. Trav. Chim. Pays-Bas* **1986**, *105*, 1 - 21; (c) D. A. Shirley, J. P. Hendrix, *J. Organomet. Chem.* **1968**, *11*, 217 - 226.
- [2] D. A. Shirley, B. J. Reeves, *J. Organomet. Chem.* **1969**, *16*, 1 - 6.
- [3] (a) H. Awad, F. Mongin, F. Trécourt, G. Quéguiner, F. Marsais, F. Blanco, B. Abarca, R. Ballesteros, *Tetrahedron Lett.* **2004**, *45*, 6697 - 6701; (b) O. Bayh, H. Awad, F. Mongin, C. Hoarau, F. Trécourt, G. Quéguiner, F. Marsais, F. Blanco, B. Abarca, R. Ballesteros, *Tetrahedron* **2005**, *61*, 4779 - 4784.
- [4] (a) T. Mase, I. N. Houpis, A. Akao, I. Dorziotis, K. Emerson, T. Hoang, T. Iida, T. Itoh, K. Kamei, S. Kato, Y. Kato, M. Kawasaki, F. Lang, J. Lee, J. Lynch, P. Maligres, A. Molina, T. Nemoto, S. Okada, R. Reamer, J. Z. Song, D. Tschäen, T. Wada, D. Zewge, R. P. Volante, P. J. Reider, K. Tomimoto, *J. Org. Chem.* **2001**, *66*, 6775 - 6786; (b) T. Iida, T. Wada, K. Tomimoto, T. Mase, *Tetrahedron Lett.* **2001**, *42*, 4841 - 4844.
- [5] D. R. Armstrong, W. Clegg, S. H. Dale, D. V. Graham, E. Hevia, L. M. Hogg, G. W. Honeyman, A. R. Kennedy, R. E. Mulvey, *Chem. Commun.* **2007**, 598 - 600.
- [6] M. S. Lah, V. L. Pecoraro, *J. Am. Chem. Soc.* **1989**, *111*, 7258 - 7259.
- [7] G. Mezei, C. M. Zaleski, V. L. Pecoraro, *Chem. Rev.* **2007**, *107*, 4933 - 5003.
- [8] C. M. Zaleski, E. C. Depperman, J. W. Kampf, M. L. Kirk, V. L. Pecoraro, *Angew. Chem. Int. Ed.* **2004**, *43*, 3912 - 3914.
- [9] C. Dendrinou-Samara, A. N. Papadopoulos, D. A. Malamataris, A. Tarushi, C. P. Raptopoulou, A. Terzis, E. Samaras, D. P. Kessissoglou, *J. Inorg. Biochem.* **2005**, *99*, 864 - 875.
- [10] (a) C. J. Pedersen, *J. Am. Chem. Soc.* **1967**, *89*, 2495 - 2496; (b) C. J. Pedersen, *J. Am. Chem. Soc.* **1967**, *89*, 7017 - 7036.
- [11] (a) C. S. Lim, J. W. Kampf, V. L. Pecoraro, *Inorg. Chem.* **2009**, *48*, 5224 - 5233; (b) J. Jankolovits, J. W. Kampf, S. Maldonado, V. L. Pecoraro, *Chem. Eur. J.* **2010**, *16*, 6786 - 6796.
- [12] X. Yang, C. B. Knobler, Z. Zheng, M. F. Hawthorne, *J. Am. Chem. Soc.* **1994**, *116*, 7142 - 7159.

- [13] (a) H. Yoshida, Y. Ito, J. Ohshita, *Chem. Commun.* **2011**, 47, 8512 - 8514; (b) K. M. Allan, C. D. Gilmore, B. M. Stoltz, *Angew. Chem. Int. Ed.* **2011**, 50, 4488 - 4491.
- [14] (a) H. Yoshida, H. Fukushima, J. Ohshita, A. Kunai, *Tetrahedron Lett.* **2004**, 45, 8659 - 8662; (b) A. M. Dyke, A. J. Hester, G. C. Lloyd-Jones, *Synthesis* **2006**, 24, 4093 - 4112.
- [15] W. X. Zhang, Z. Hou, *Org. Biomol. Chem.* **2008**, 6, 1720 - 1730.
- [16] R. G. S. Berlink, A. C. B. Burtoloso, M. H. Kossuga, *Nat. Prod. Rep.* **2008**, 25, 919 - 954.
- [17] A. G. M. Barrett, T. C. Boorman, M. R. Crimmin, M. S. Hill, G. Kociok-Köhn, P. A. Procopiu, *Chem. Commun.* **2008**, 5206 - 5208.
- [18] J. R. Lachs, A. G. M. Barrett, M. R. Crimmin, G. Kociok-Köhn, M. S. Hill, M. F. Mahon, P. A. Procopiu, *Eur. J. Inorg. Chem.* **2008**, 4173 - 4179.
- [19] (a) T. G. Ong, G. P. A. Yap, D. S. Richeson, *J. Am. Chem. Soc.* **2003**, 125, 8100 - 8101; (b) W. X. Zhang, M. Nishiura, Z. Hou, *Chem. Eur. J.* **2007**, 13, 4037 - 4051.
- [20] (a) F. Schüth, B. Bogdanović, M. Felderhoff, *Chem. Commun.* **2004**, 2249 - 2258; (b) S. A. Shevlin, Z. X. Guo, *Chem. Soc. Rev.* **2009**, 38, 211 - 225.
- [21] M. Arrowsmith, M. S. Hill, D. J. MacDougall, M. F. Mahon, *Angew. Chem. Int. Ed.* **2009**, 48, 4013 - 4016.
- [22] S. Harder, J. Spielmann, J. Intemann, H. Bandmann, *Angew. Chem. Int. Ed.* **2011**, 50, 4156 - 4160.
- [23] W. Sattler, G. Parkin, *J. Am. Chem. Soc.* **2011**, 133, 9708 - 9711.
- [24] (a) M. D. Jones, M. G. Davidson, C. G. Keir, L. M. Hughes, M. F. Mahon, D. C. Apperley, *Eur. J. Inorg. Chem.* **2009**, 635 - 642; (b) C. A. Wheaton, B. J. Ireland, P. G. Hayes, *Organometallics* **2009**, 28, 1282 - 1285; (c) J. D. Monegan, S. D. Bunge, *Inorg. Chem.* **2009**, 48, 3248 - 3256; (d) W. C. Hung, C. C. Lin, *Inorg. Chem.* **2009**, 48, 728 - 734; (e) I. L. Fedushkin, A. G. Morozov, V. A. Chudakova, G. K. Fukin, V. K. Cherkasov, *Eur. J. Inorg. Chem.* **2009**, 4996 - 5003.